Spare copy

An abstract of thesis submitted for a Ph.D. degree by A.L. Lucas.

I - A system for the acquisition and processing of seismic data for refraction studies of the Earth's crust.

The use of arrays of seismometers for seismic refraction measurements of crustal structure using explosions is reviewed, and the general factors to be considered in the design of equipment for the acquisition and processing of such data are discussed. The design and construction of a particular system using digital magnetic tape recording are described in detail. The three main modes of operation are the recording of ten channels of seismic information in the field, the replay in the laboratory of these ten channels to a multi-channel galvanometer oscillograph, and the transfer of the digital information to punched paper tape for input to a general purpose digital computer. The programmes that have been developed for handling this data on an Elliott 803 computer are described.

The system was used during a crustal experiment using depth charges in September, 1965. The performance during this test is evaluated.

II - Stress systems in an inhomogeneous crust.

The plane strain stress in an elastic half-space in which there are discrete variations in density over rectangular areas of the cross section is calculated by the double integration of the result for a point force acting within an homogeneous elastic half-space. The resulting stress system is shown to be a valid solution of the equations of elasticity, and analytical results are derived for several special cases. The application of the theory of elasticity to crustal processes is reviewed, and numerical results are used to discuss the stress systems associated with isostatic compensation and with a crust of varying density.

I A SYSTEM FOR THE ACQUISITION AND PROCESSING OF SEISMIC DATA FOR REFRACTION STUDIES OF THE EARTH'S CRUST.

II STRESS SYSTEMS IN AN INHOMOGENEOUS CRUST.

A thesis submitted for the Degree of

Doctor of Philosophy

in the

University of Durham

by

Andrew Lefevre Lucas

St. Cuthbert's Society

September 1966.

Summary

I - A system for the acquisition and processing of seismic data for refraction studies of the Earth's crust.

The use of arrays of seismometers for seismic refraction measurements of crustal structure using explosions is reviewed, and the general factors to be considered in the design of equipment for the acquisition and processing of such data are discussed. The design and construction of a particular system using digital magnetic tape recording are described in detail. The three main modes of operation are the recording of ten channels of seismic information in the field, the replay in the laboratory of these ten channels to a multi-channel galvanometer oscillograph, and the transfer of the digital information to punched paper tape for input to a general purpose digital computer. The programmes that have been developed for handling this data on an Elliott 803 computer are described.

The system was used during a crustal experiment using depth charges in September, 1965. The performance during this test is evaluated.

II - Stress systems in an inhomogeneous crust.

The plane strain stress in an elastic half-space in which there are discrete variations in density over rectangular areas of the cross section is calculated by the double integration of the result for a point force acting within an homogeneous elastic half-space. The resulting stress system is shown to be a valid solution of the equations of elasticity, and analytical results are derived for several special cases. The application of the theory of elasticity to crustal processes is reviewed, and

numerical results are used to discuss the stress systems associated with isostatic compensation and with a crust of varying density.

Contents

Preface

This thesis describes work performed during the five years commencing October, 1961. During the first two years the theoretical problem described in the second part of this thesis was solved and a design study and equipment survey were carried out on a system for investigating granite batholiths and other local variations in crustal structure by seismic refraction methods. Consequently, when a contract was signed between the University of Durham and the European office of Aerospace Research, U.S.A.F., for the construction and use of such equipment, it was possible to place orders for components immediately. This system, which was first tested in the field in September, 1965, is described in the first part of this thesis.

Acknowledgements

I wish to thank Professor K.C. Dunham for the privilege of working in the department. I am grateful to Dr. M.H.P. Bott for suggesting as topics of research both the use of seismic methods for investigating deep crustal structure and the theoretical problem of crustal stresses, and for his supervision and advice during the course of the work.

The people who have contributed to the design, construction and field testing of the seismic data system are too numerous to thank by name here, but mention must be made of Dr. H.I.S. Thirlaway and the group at Blacknest for their advice in the early stages of the project and for the loan of equipment and of Mr. C. Chaplin and his technical staff for the help without which this work would not have been possible. Further, I would like to thank Dr. F. Gray and Dr. R.E. Long for their day-to-day advice and Dr. J.S. Steinhart and Dr. S. Kaufman for the benefit of their rare visits.

Finally, I wish to thank D.S.I.R. for financial support for two years and the European Office of Aerospace Research, U.S.A.F., for both personal support for three years and finance for equipment.

I A SYSTEM FOR THE ACQUISITION AND PROCESSING OF SEISMIC DATA FOR REFRACTION STUDIES OF THE EARTH'S CRUST.

CONTENTS

FIGURES

TABLES

CHAPTER I

THE SPECIFICATION OF A SYSTEM FOR THE ACQUISITION AND PROCESSING OF SEISMIC DATA FOR REFRACTION STUDIES OF THE EARTH'S CRUST

(1) Introduction

Seismic methods for determining the variations of the elastic properties within the Earth give the most direct and least ambiguous techniques for studying the crust and upper mantle. In particular, gravity surveying is unable to resolve the structure in the lower crust of granite batholiths (Bott, Day and Masson-Smith, 1958). In 1961 the author began to consider how the techniques of seismology could be applied to the solution of this problem. The outcome of this study was the design of a multi-channel recording and data processing system for use in crustal refraction experiments with explosive sources. In July, 1963, the University of Durham was awarded a contract under the VELA-UNIFORM programme of the Advanced Research Projects Agency to construct this system and "to investigate the relatively local but fundamental variations in continental crustal structure down to and including the Mohorovičić discontinuity with particular reference in the first instance to granite batholiths, and the effects of such variations on seismic propagation paths". The first half of this thesis describes the design, construction and use of this system. The second half presents the results of a theoretical elastostatic problem that was solved in the period before the award of the VELA-UNIFORM contract.

Refraction experiments using controlled explosions have emerged as the most effective technique for studying the structure of the crust. The method was discussed in detail by Steinhart and Meyer (1961). The

advantages of this method over earthquake studies are the elimination of the three unknown spacial co-ordinates and the unknown time of the source, and the simpler nature of the source function. Experiments using quarry blasts are clearly not so versatile with respect to the shot point location as, for example shots fired at sea, and suffer from the facts that quarry blasts are intended to generate a minimum of seismic energy and that the source function is often complicated by the effects of ripple firing (Willis, 1963; Frantti, 1963).

Two refraction travel time curves for arrivals in opposite directions along the same line may be interpreted in terms of homogeneous layers bounded by planes. Such interpretations should be accompanied by amplitude studies and considerations of the possible occurrence of reflections (Steinhart and Meyer, 1961). Surveys conducted over an area are generally interpreted by assuming the travel time associated with a particular marker horizon to be influenced by "delay times" which are characteristic of the shot point and the recording location. The most important expression of this concept is the time term theory (Scheidegger and Willmore, 1957; Willmore and Bancroft, 1960). The travel time, t_{ij}, is given by

$$t_{ij} = a_i + b_j + \frac{\Delta_{ij}}{v},$$

where a_i and b_j are "time terms" characteristic of the shot point and recording location respectively, Δ_{ij} is the range, and v is the velocity of the refracting layer. An experiment with n shot points and m recording stations involves $(n + m)$ unknowns apart from v, and yields $(n + m)$ normal equations which do not have a unique solution unless one time term is known or two time terms are known to be equal. The second paper (1960) discusses the significance of this theory in planning refraction experiments. Smith,

Steinhart and Aldrich (1966) have extended the theory to the case where

$$v = v_0 + v_1 . \Delta .$$

This dependence of the velocity on the range is associated with a vertical velocity gradient in the refracting medium. Another method of interpreting seismic refraction sections is the "plus-minus" method (Hagedoorn, 1959). This technique is a development of the work of Thornburgh (1930) in which wave fronts are constructed by using the fact that all points on the minimum trajectory between two locations are points where the sum of the travel times from the two locations is constant. The 'reciprocal' method of Hawkins (1961) is similar. These methods of interpreting refraction data are reviewed by Willmore, Herrin and Meyer (1963).

The present work is concerned mainly with the application of seismometer arrays to the study of refracted arrivals and with techniques of data processing and instrumentation. In recent years methods have advanced through the increased usage of magnetic tape recording, of seismometer arrays which improve the effective signal-to-noise ratio and allow measurements of apparent phase velocities, and of digital data processing techniques which are more versatile and potentially faster than analogue methods. The reporting of the present work is complicated by the fact that while it has been proceeding, the technologies involved have undergone great advances. For example, motivated by the political need to distinguish between earthquakes and clandestine underground nuclear explosions, array systems have progressed from the temporary, experimental installation on Salisbury Plain (Whiteway, 1961) to the array currently under construction in Montana which has over five hundred buried seismometers in 21 clusters and an aperture of 200 kilometres (Frosh and Green, 1966). Similarly, changes have occurred in the

electronic modules available in the United Kingdom for the construction of data processing systems. For example, the provisional data sheets for the 2 megacycle-per-second digital logic modules, which are described in Chapter 2, appeared in 1963, and the full design data was published in 1964. Now, in 1966, integrated circuits would be used instead of these modules, and the equipment would be much smaller and dissipate less power.

In this first chapter the use of multi-channel systems in seismology is summarized with emphasis on their use in explosion studies of crustal structure, and the basic specification of a data processing system for such studies is drawn up. In subsequent chapters the implementation of this system is described in detail using block diagrams. Because of the large amount of hardware involved in the system, no attempt is made to present the complete circuit diagrams here.

(ii) Multi-channel systems in seismology

The directional properties of groups of geophones have been used in exploration seismology for many years, and ingeneous analogue devices have been devised for picking out events which correlate across the spread (Reiber, 1936; Tullos and Cummings, 1961; Jackson, 1965; Anstey and Lerwill, 1966). The use of groups of geophones also increases the effective signal-to-noise ratio. The signal-to-noise improvement for apparently random noise is reduced by any coherence (Denham, 1963), and for coherent noise may be increased by a correctly designed spread of geophones (Hales and Edwards, 1955; Smith, 1956) and by weighting the signals from a line array and summing (Holzman, 1963). A comparison between additive and multiplicative compounding was made by Dyk (1956). With the advances in data processing methods, magnetic delay line and digital filtering

techniques have been used (Jones et al, 1955; Smith, 1958; Robinson and Treitel, 1964). These methods can duplicate the operation of conventional filters, and, because both past and future values of the traces may be used, new functions may be introduced. In particular, filters without phase distortion may be designed. The types of filtering that have been developed for use with these two techniques may be broadly divided into three categories. Firstly, the velocity filtering and cross-correlation process is only a particular form of filtering (Jones and Morrison, 1954); Melton and Bailey, 1957). Combination by multiplication is, of course, not a linear process. Secondly, if the effects of the propagation paths may be represented by a linear filter, then the records may be clarified by the application of an inverse linear filter (Backus, 1959; Lindsey, 1960; Goupillaud, 1961; Rice, 1962; Watson, 1965). Thirdly, a number of filters have been designed by applying the Wiener optimum linear filter theory to multitrace seismic data processing (Wiener, 1949). According to this theory each trace is individually filtered in such a way as to minimize the root-mean-square of the difference between the summed output and the required signal which, together with the noise, makes up the input. Optimum systems for ghost suppression have been discussed by Schneider, Larner, Burg and Backus (1964), for the attenuation of multiple reflections by Schneider, Prince and Giles (1965), and for velocity filtering by Fail and Grau (1963) and Embree, Burg and Backus (1963). The design of such optimum filters is a function of the statistical properties of the signal and of the coherent and incoherent noise, and the resulting filters are difficult and costly to construct. Foster, Sengbush and Watson (1964) considered the design of sub-optimum filters to perform the functions of ghost suppression and velocity filtering using more practical filters.

They simplified the optimum theory by letting the amplitude of one of the two types of noise tend to infinity, and then applying an inverse filter to reduce the distortion of the signal due to the effect of this approximation.

The problem of detecting underground nuclear explosions has promoted a rapid development in the use of arrays of seismometers to study teleseismic signals. Many of the principles of groups of geophones used in prospecting methods are equally applicable to this problem, although the values of the parameters of the signals and therefore of the arrays are very different. In the United Kingdom arrays of seismometers with dimensions comparable to the largest apparent wavelength of the signal have been used to study the structure of teleseismic signals and to separate and identify seismic phases by a process of velocity filtering using correlation methods (Whiteway, 1961; Willmore, 1962; Thirlaway, 1963; Truscott, 1964; Carpenter, 1965; Birtill and Whiteway, 1965; Thirlaway, 1966). Birtill and Whiteway (1965) discuss in detail the ability of azimuth and velocity filtering methods to separate sinusoidal signal components, and consider all the facets of the technology of such array systems and the results of their application to teleseismic events. Somers and Manchee (1966) simply consider the response of the particular geometry of the Yellowknife array for a 1c/s sinusoidal signal.

The crustal structure in the vicinity of an array influences the noise characteristics at the site and also the waveforms and timing of arrivals. For this reason a crustal refraction experiment using depth charges at sea was carried out to study the crust in the neighbourhood of the Eskdalemuir array station (Agger and Carpenter, 1964). Whiteway (1966)

has considered the application of arrays to earthquake seismology, and the Eskdalemuir array has been used for near earthquake studies (Key, Marshall and McDowall, 1964; Agger and Key, 1965).

Initial work in the United States on the application of multi-channel systems to the detection problem tended to concentrate on optimum Wiener systems designed to greatly reduce the effective ambient noise level and thus relatively enhance the teleseismic signal. Studies have considered both experimental and theoretical noise distributions and both horizontal and vertical distributions of seismometers (Burg, 1964; Backus, Burg, Baldwin and Bryan, 1964; Roden, 1965; Backus, 1966). The dimensions of the horizontal clusters of seismometers are small compared to the apparent wavelength of the signal, but are sufficient to discriminate against coherent microseismic noise. Recently work has started in Montana on a'large aperture seismic array' which, it is hoped, will take advantage of all the developments in array technology (Frosh and Green, 1966). This array is made up of twenty-one sub-arrays and has an aperture of 200 kilometres. Each sub-array consists of a cluster of twenty-five geophones and each geophone is located in a cased borehole. An elaborate data processing system with digital telemetry is proposed with the intention of making it possible to apply an over all inverse filter to remove the effects on propagation of the crust in the vicinity of the array.

Explosion studies of crustal structure before 1961 are reviewed by Steinhart and Meyer (1961). In 1961 it seemed that the array methods, which were being developed through the research on the detection problem, could be applied with advantage to these studies. This has proved to be so. The United States Geological Survey has conducted experiments using spreads of

$2\frac{1}{2}$ kilometres (Warrick et al, 1961; Ryall, 1964) with both conventional explosives (Eaton, 1963; Healy, 1963; Jackson, Stewart and Pakiser, 1963; Roller and Healy, 1963) and nuclear explosives (Stewart and Pakiser, 1962; Pakiser and Hill, 1963; Ryall and Stewart, 1963). Eaton (1963) and Roller and Healy (1963) have reported deep reflections. The use of nuclear explosives permits the study of the mantle by refraction work at greater ranges. Other groups in the United States have also combined in experiments with conventional explosives in Maine in 1961 (Meyer et al, 1962; Steinhart et al, 1962), in North Carolina in 1962 (Shima, McCamy and Meyer, 1964), and at Lake Superior in 1963 (Steinhart, 1964; Smith, Steinhart and Aldrich, 1966), and with nuclear explosions (Weisbrich, 1965). Sander and Overton (1965) report the use of two 6.7 kilometre in-line arrays at the ends of crustal refraction profiles shot under extremely difficult conditions during 1962 and 1963 in the islands north of the Canadian mainland. Shima, McCamy and Meyer (1964) determined apparent velocities across a fixed array by measuring the differences in phase angle of Fourier spectral densities. McCamy and Meyer (1964) used a computer method with velocity filtering and correlation techniques to plot the degree of correlation as a third dimension against apparent velocity and time. They discuss the problem of 'velocity aliasing' which occurs when the phase difference between the signal at added seismometers is an integer multiple of 2π (see also Birtill and Whiteway, 1965) and point out that aliased events should be revealed by repeating the processing with different settings of the band pass filters of the original traces. This velocity aliasing is called 'quasi-aliasing' by Fox-Hulme (1965) and is of course quite distinct from the high frequency aliasing associated with the folding frequency of sampled data systems.

As previously mentioned, explosion studies were carried out in the

United Kingdom to 'calibrate' the Eskdalemuir array station (Agger and Carpenter, 1964), and this yielded data on the crustal structure in the surrounding region. In September 1965 an experiment organized by the groups at Edinburgh and Birmingham was carried out to determine the nature and thickness of the Earth's crust between Wales and Ireland. The depth charges of this experiment were used for the field testing of the system described in this thesis (see Chapter 5).

The problems of seismic array instrumentation, recording and data processing largely depend upon the number of channels to be recorded individually, the upper frequency limit of these channels, the duration of the recording time, the proportion of the recorded data that has to be processed, and the complexity of the data processing calculation. The field problems depend very largely on the dimensions of the array. In terms of these criteria, the worst cases are the large arrays required for monitoring nuclear explosions (Truscott, 1964; Birtill and Whiteway, 1965; Frosh and Green, 1966). These arrays must operate continuously. The problems of data handling and processing in slightly less demanding applications are considered by Phinney and Smith (1963), Smith (1965) and Anderson, Bennet, Parks and Willmore (1966). The specification of the seismic refraction system used for crustal studies by the United States Geological Survey is described by Warrick, Hoover, Jackson, Pakiser and Roller (1961). Electronic data processing systems for handling small amounts of data are described by Bogert (1961), Haubrich and Iyer (1962), De Bremaecker, Donoho and Michel (1962), Miller (1963), and Hinde and Gaunt (1966).

The various design possibilities occur in various combinations depending on the requirements of a particular application. Some of the basic points

will be briefly discussed below:-

(a) The signal-to-noise improvement may be maintained but the number of individually recorded channels reduced by summing the outputs from geophones before recording.

(b) The amount of cable may be reduced by using amplitude-mudulated or frequency modulated signals on a common line. The Montana array uses digital telemetry. Alternatively, radio transmission may be used. This problem is related to that of the power supplies at the dispersed head amplifiers. Power may be supplied locally by batteries or be passed along the signal lines if the line resistance is not too great and the seismic information is propagated by a carrier signal. The use of solar cells or thermal generators has been considered.

(c) On-line correlators have been developed with a view to decreasing the amount of off-line monitoring required and to producing triggered recording systems for tape economy.

(d) Magnetic tape recording is used today in most multi-channel seismic systems. The important point about this recording method is that the signal information is preserved in its electrical form so that the original event can effectively be recreated any number of times with, if required, an altered time base. Direct recording is not suitable for crustal refraction systems because of the low frequency cut-off in the record-replay response. If the data is to be processed in a digital form, the question arises as to whether to use frequency modulation recording in the field and digitize in the laboratory, or to digitize in the field and use digital recording. The digital record-replay

process does not introduce any error into the data because the dynamic range and accuracy depend only on the digitizing device. It is particularly important for array systems that the digital record-replay process cannot introduce the relative timing errors between channels which correspond to the 'skew' of a frequency modulation record-replay system. Frequency modulation recording has the advantage that, for a given information rate, the tape speed is slower than that required for digital recording by a factor of about ten. For crustal explosion studies in which the recording time is limited, the arguments for and against digital recording are well balanced. The principal point in favour is the fidelity of the recording method and the principal point against is the complexity of the field equipment. It is the writer's opinion that the decisive factor is the number of array systems involved. If one is concerned with only one array, it is realistic to put the digitizing equipment in the field and avoid the need for frequency modulation hardware; if one is concerned with a series of array stations, it is more economical to keep the digitizing equipment in the laboratory and to use frequency modulation recording in the field. It is interesting to note that in the last few years there has been a strong trend in commercial exploration seismology towards digital recording; here high sampling rates and tape speeds are required, but the duration of recordings is short.

The possibility of using different recording methods should always be considered in specialist applications. The pulse

duration modulation recording process, which comes between the frequency modulation and digital processes with respect to efficiency of tape utilization and which permits time-division multiplexing, is applicable to systems with a multiplicity of signal channels having relatively low frequency content. Thompson (1965) advocates the use of 'delta-modulation' recording systems for crustal seismology.

(e) The initial work of the U.K.A.E.A. group was performed using an analogue computing system. However, for greater versatility, accuracy and potential speed, digital systems are now generally used (or, are being constructed). If general purpose computers are used, the main problems are editing the field data and transferring the continuous seismic data onto computer-compatible magnetic tapes which usually store information in blocks with gaps between blocks. Consequently, the hardware for writing computer-compatible tapes has to include extensive memory facilities, and is generally complex and expensive. For this reason systems which need to handle smaller quantities of data have tended to use punched paper tape (produced either on-line or off-line), even although this method of transfer is very slow.

(f) The further development of large-scale seismic data processing lies in the completion of special-purpose, hybrid analogue-digital computers (Birtill and Whiteway, 1965; Smith, 1965; Hutchins, 1966) and of hardware for writing magnetic tapes, which are compatible with fast general-purpose computers, from field tapes (Anderson, Bennet, Parks, and Willmore, 1966; Parks, 1966).

In the next section the instrumentation required for crustal refraction experiments is considered.

(iii) The specification of a system for crustal refraction studies

Consider the specification of a system designed to apply the advantages (described in section (ii)) of array techniques and data processing on a general purpose digital computer to crustal refraction studies . Figure 1 shows a schematic diagram of such an experiment using depth charges at sea. Travel times are here determined by recording a radio time signal at both the shot point and the array station. The construction of shot point hardware will not be discussed in this thesis, but the implementation of the array station will be described in Chapter 3.

In order to reject coherent signal or noise components, the in-line dimensions of the array should be equal to at least one wavelength of these components. The dominant frequency components of the signal for ranges from, say, 50 kilometres to 200 kilometres will be from about 3 c.p.s. to about 20 c.p.s., and 3 c.p.s. geophones may be used with advantage. If one takes the maximum apparent velocity to be 8 km/sec and the corresponding minimum frequency to be 3 c.p.s., then the dimension of the array should be about 2.7 kilometres. The advantages of increasing the number of geophones in the array are to increase the rejection of random noise and to reduce the problem of velocity aliasing. However, the data handling problems and the cost of the instrumentation increase with the number of independently recorded channels. The system adopted here uses ten geophones, and each geophone output is recorded individually.

The limiting factor in crustal refraction experiments at large ranges is the background level of seismic noise at a selected quiet site (Brune and Oliver

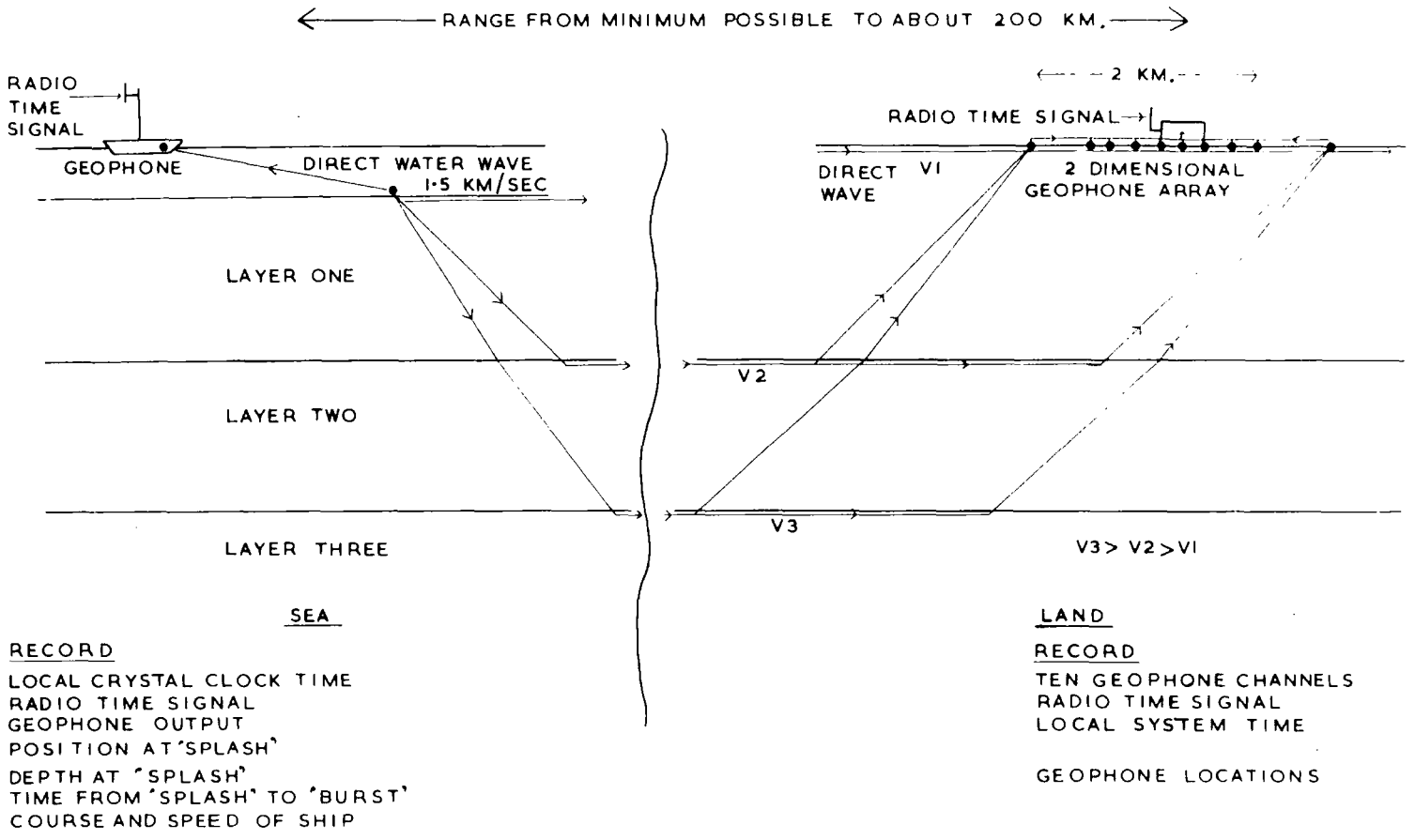

SCHEMATIC DIAGRAM OF A SEISMIC EXPERIMENT USING DEPTH CHARGES TO INVESTIGATE CRUSTAL STRUCTURE.

FIGURE 1

1959; Frantti, Willis and Wilson, 1962). On a world-wide basis, a vertical component noise level of about 1 millimicron peak-to peak at 1 c.p.s. (0.63×10^{-6} cm/sec at 1 c.p.s.) is about the minimum attainable. Britain is on a continental margin and the corresponding minimum is greater. The noise at Eskdalemuir in the 1 to 3 c.p.s. band is very low for the British Isles and varies between 3 and 20 millimicrons r.m.s. (Birtill and Whiteway, 1965). The noise velocity tends to be lower at higher frequencies.

It is necessary to ensure that the pre-amplifier noise, referred to input, is less than the geophone output due to the microseismic noise. The array will be used with 3 c.p.s. refraction swamp geophones (B.P. design), which have a sensitivity of about 1.0 volts/cm/sec at 5 c.p.s. for damping 0.56 critical, and pre-amplifiers (also to a B.P. design) which have a quoted noise level referred to input of about 0.7 microvolts (p-p) for a bandwidth from 0.1 c.p.s. to 80 c.p.s. The pre-amplifiers have, in fact, been used with a level response from 2 c.p.s. to 18 c.p.s., and 3 db down at 45 c.p.s. Assuming that the reduction in bandwidth reduces the pre-amplifier noise to 0.5 microvolts (p-p), this is equivalent with this geophone to a ground velocity of 0.5×10^{-6} cm/sec or to a displacement of 0.8 millimicrons (p-p) at 1 c.p.s. This combination of geophone and pre-amplifier is clearly satisfactory for the present system.

The most important decision about the array instrumentation is that digital magnetic tape recording should be used. In this respect the advice of Whiteway (private communication, May, 1962) is followed. The frequency band of seismic energy at the ranges used in crustal experiments extends no higher than 20 c/s, so that a channel sampling rate of 100 samples/second and a folding frequency of 50 c/s is adequate. In order that the computer programmes used for processing the data should not be too slow, signals will

not be interpolated between samples, but instead the sample which is nearest in time to the required value will be used. This means that, for a 100 samples/second rate, there is a possible time misalignment on each channel of $\pm$ 5 milliseconds in the data processing. For a 10 c.p.s. signal component this time error corresponds to a maximum amplitude error of $\pm$ 0.16 of the peak-to-peak amplitude, and this error is considered acceptable. Since there are ten channels of seismic data, the system sampling rate is a thousand samples per second.

Assume that an analogue-to-digital converter is used which gives a ten bit pure binary output, so that the full-scale output range is from zero to 1023. Suppose that the output value changes by 120 for a change of 1 volt in the analogue input voltage, and consider the maximum signal gain that should exist between the geophone and the input to the analogue-to-digital converter (A.D.C.). If the system was designed so that at maximum gain the pre-amplifier noise corresponds approximately in magnitude to the truncation (or quantization) error, then there would be no possibility of recovering signal lost in this noise. It has been seen that such considerations would only be realistic for very quiet sites selected on a world-wide basis. However, it will be supposed that the peak-to-peak pre-amplifier noise is to correspond to a converter input voltage of 0.1 volts or an output of 12 units. The corresponding gain required between the geophone and the A.D.C. is therefore 200,000. Since, in the present system, the seismic signal will be passed directly along the cables (i.e. no frequency or amplitude modulation), this gain corresponds to the product of the pre-amplifier gain and the maximum channel gain occurring at the array recording system.

The significance of this gain may alternatively be considered by anticipating the existence of a galvanometer replay facility such that,

at maximum gain, the full-scale output range of the A.D.C. corresponds to a full-scale trace deflection of 16 cm. Consequently, one microvolt of geophone output recorded at maximum gain can correspond to a galvanometer deflection of about 4 mm. This figure could be increased (with sacrifice of linearity) by simple modifications to the replay hardware. The corresponding figure in the specification drawn up by Warrick, Hoover, Jackson, Pakiser and Roller (1961) is one inch.

The second important decision concerns the method of transferring data into the general purpose digital computer. The ideal method is to use off-line equipment for writing computer-compatible magnetic tapes. As has been discussed earlier, this is expensive and complicated because magnetic tapes for general purpose computers have a block format. Also, unfortunately, there is no standardization of formats between different computer manufacturers in the United Kingdom, so that such off-line equipment has to be tied to a particular make of computer. However, since the present project requires the processing of relatively few events, it is just feasible to use punched paper tape for computer input. One sample of the A.D.C. and timing and control information will occupy two paper tape characters, so that one second of recorded data generates 2,000 characters, or over 16 feet of paper tape. However, the fastest tapepunches operate at 300 characters per second (The European Computer Users Handbook, 1964, Computer Consultants Limited), and such punches would be less reliable and considerably more expensive than punches operating at 100 ch.p.s. The solution adopted is to use a well-known synchronous punch operating at 100 ch.p.s., and to slow the replay by a factor of 32, so that the average rate of punching is 62.5 ch.p.s. The

decision to use punched paper tape fundamentally effects all the digital instrumentation, which is designed with the ultimate paper tape format in mind.

The above paragraphs have described the basic concepts of a system for the acquisition and processing of seismic data for crustal refraction studies, and the two fundamental decisions relating to the instrumentation have been discussed. The effects of these decisions on the hardware and data handling facilities will now be considered in general terms.

A simple functional diagram of the entire system is given in figure 2. The 'system time' is defined to be the output of a local crystal clock, and differs from 'absolute time' represented by a radio time signal. With reference to the array recording system in the field, the first point is that with digital recording it is particularly important to be able to check that the recorded data is recoverable. For this reason the recorded data is read by a read head adjacent to the write head, and the extensive monitoring facilities utilize this replayed data. Secondly, because each second of recorded data can produce over 16 feet of paper tape and because it is intended that there should be a close correspondence between the magnetic tape and paper tape formats, the system time (in seconds, minutes and hours (12)) is written on the magnetic tape every second. A third point is that the form of the digital write logic in the recording system is controlled by the needs of the flux-sensitive replay equipment required for the slow replay to the punch. Even although digital processing techniques are to be used, the first step in the laboratory data handling system must be to obtain a multi-channel

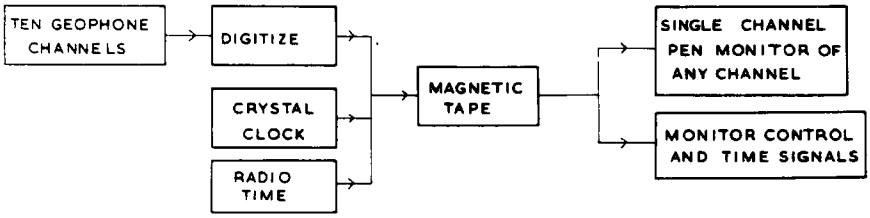

ARRAY FIELD SYSTEM

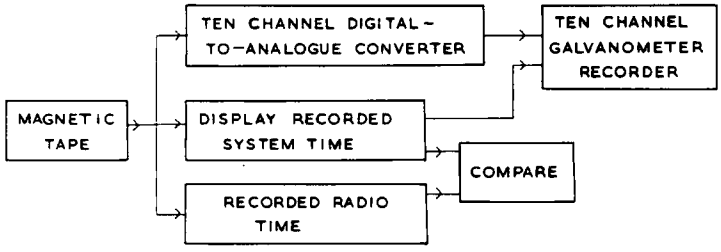

LABORATORY REPLAY SYSTEM

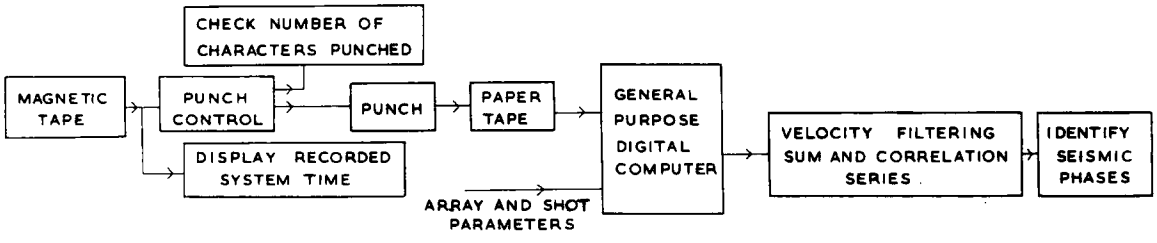

DATA PROCESSING SYSTEM

A SIMPLIFIED FUNCTIONAL DIAGRAM OF THE SEISMIC DATA SYSTEM

FIGURE 2

analogue record of the geophone channels. The laboratory replay system shown in figure 2 also displays the recorded system time, and allows time markers to be written on the multi-channel visual record. Facilities must also exist for determining the difference between 'system time' and 'absolute time'. The next step in the data processing sequence is to determine from the visual record the interval of system time which is to be transferred to punched paper tape. The paper tape punch control hardware includes facilities for automatically starting or ceasing to punch at a specified system time, and for checking the number of characters punched per recorded second. This last function could be left to be performed by the computer itself, but in practice it is very desirable to have an off-line check that the punched data tapes are correct in this fundamental respect. The basic computer programmes are concerned with reading and checking the data in the punched tape format, which is peculiar to this system, and with carrying out basic velocity filtering calculations with a view to identifying seismic phases.

When considering the implementation of a system such as that shown in figure 2, one must remember the vital practical principle that as much of the hardware as possible should be common to all modes of operation. The most important example in the present system stems from the need to use a commercially-available flux-sensitive magnetic tape replay head and electronics in the paper tape punch system. The outputs of these electronics are squared and differentiated in order to simulate the conventional replay process, and consequently the replay logic and subsequent hardware are common to both types of replay.

The construction of the system summarized in figure 2 is described in detail in the chapters that follow.

CHAPTER 2

METHODS OF SYSTEM DESIGN AND CONSTRUCTION

(i) General considerations

The purpose of this chapter is to introduce the concepts of digital system design used in the present work so that the subsequent descriptions of particular systems can be free from general comments. Digital design will here be considered in terms of logic modules, and the circuit diagrams required to implement these functions will not be discussed.

In an analogue system information is represented by a signal which may have any value within thefull-scale range; in a digital system such information is represented by a number (or sequence of numbers) which can only take a finite number of values, and the information is therefore subject to a truncation error. Rational numbers or information coded in an integer form may be represented exactly in a digital system, and the important point is that once the information is in a digital form, it may be manipulated without introducing further inaccuracy. Because transistor devices are most conveniently designed with two possible states, electronic counting is generally carried out with a base of 2. That is, the binary system is used, and each digit of a binary number is either a 0 or a 1. The binary digit is commonly referred to as a bit. A pure binary word of N bits may represent the integer numbers from zero to $2^N - 1$. Whilst such a code is ideal for the internal workings of a machine, the machine operators are more familiar with numbers with a base of ten. Each decimal digit can be represented by a four bit binary word, but since there is considerable wastage in this representation, different forms of the binary decimal code exist.

The binary digit with its possible values of 0 or 1 may be represented

by any two-state system which may be real, such as a circuit with two discrete ranges of output voltage or a relay which is either open or shut, or abstract, such as the concepts of true and false or yes and no. Two simple logical functions are the AND gate, where the output is 1 if all the inputs are 1, and the OR gate, where the output is 1 if any of the inputs are 1. The output of the logical NOT is 1 if the input is 0, so that this is the logical equivalent of an inverting amplifier. In these types of logic the output is dependent only on the input, and complex functions may be studied by using the methods of Boolean algebra. The operation of simple systems of this type may be represented by 'truth tables', which display the logical output for all possible combinations of logical input. The design of parity bit generators using truth tables is illustrated in figure 7.

The logical functions discussed in the above paragraph are not concerned with the effects of the passage of time. In a synchronous system the timing of events is determined by a regular set of pulses, but in asynchronous systems the timing is controlled by the logic units themselves. Consideration of time introduces the notion of transferring information by voltage steps as well as voltage levels, and suggests the development of a range of logical elements which may exist in two states and which are capable of a memory function in that their outputs are not instantaneously related to their inputs. Positive voltage steps are generally used to perform A.C. input operations. Circuits which can only exist in one state for a certain time after activation and then revert to their stable state are variously called delay units, monostable vibrators, univibrators, or one shot multivibrators. They may be used for delaying

a voltage change, for forming a D.C. pulse, or for altering the duration of a D.C. pulse. The circuit which may exist indefinitely in either state is called the bistable or Eccles-Jordan circuit, and performs a memory function. The third member of this family which has no input and acts as a pulse train generator is the multivibrator or astable circuit in which both states are unstable, and the circuit oscillates from one to the other. The nature of this family of circuits is such that the logic output and its conjugate are both available.

The bistable circuit will occur in the present system performing three types of function. Firstly, a single unit may be used to store the result of some simple decision. Secondly, if the two A.C. inputs are tied together in such a way that one positive-going input pulse simply changes the state of the circuit, then it requires two positive voltage steps at the input to generate one at the output, and a number of these units in series may form a binary pulse rate divider or pulse counter. The base of the counter or divider may be changed by using a voltage edge generated at a late stage to alter the state of an earlier stage. This feedback by-passes some of the 2^N possible states of a counter with N stages, and reduces the number of states occurring in one complete cycle. The third type of use is the shift register which may be regarded as a synchronous memory device. A shift register bistable is usually driven by two conjugate outputs, and on the application of a pulse to its shift input, it adopts the logic state of the driving unit. These gate inputs to the shift register bistable have a built-in delay so that if a number of shift register bistables are connected in series, and a pulse is applied to their common shift line, then the information is safely moved one location along this series shift register.

A new bit is entered at one end of the shift register and the oldest bit is lost at the other. If the contents of a series shift register is interpreted as a pure binary number, then a shift corresponds to multiplication or division by two. Alternatively, if a number of shift register bistables with a common shift line are driven from different sources, this will be called a parallel shift register. The use of bistable circuits (as used in the present system) is not the only available method of performing memory functions, which are distinct from long-term recording methods. A capacitance can store for a limited time either a binary digit or, with some inaccuracy, an analogue signal. Magnetic core storage is widely used for the main stores of digital computers. Delay lines may also be used for some storage applications (Richards, 1957).

In the present text the functions of switches and gates are such that information is transmitted by a closed switch or an open gate and, conversely, is blocked by an open switch or a closed gate.

There are two principal methods of converting a voltage to a digital form. Mechanical methods which may be used for ultra-low frequency signals are here excluded. The direct method employs a series of switches, each of which contributes to a sum a voltage which is weighted according to a binary scale. The switches are tested inorder of decreasing significance to see whether their contribution makes the sum voltage greater than the signal voltage, and if this is so, the switch is released. Consequently, when all the switches have been tested, the condition of the switches represents the largest quantized voltage that is less than the signal voltage. The principle of a digital-to-analogue converter is similar but the operation is reversed in that the switch

settings are specified and it is the sum voltage that is the output signal. The second method of digitizing is to convert the signal voltage to a time interval by generating a linear ramp voltage, and to measure the ramp duration by counting a standard frequency. This second method is simpler than the first, but is not capable of such accuracy.

(ii) Practical considerations

The equipment described in this thesis uses transistors as opposed to valves throughout, and the only H.T. line is an unstabilised + 50 volt line required for the DM 160 tubes which give a visual output of binary registers. The digital logic is performed using commercially available encapsulated logic modules. The advantage of using such modules is that it should be possible by studying the manufacturer's loading data to go straight from a design on paper to working hardware with known operating tolerances and reliability. This section is concerned with the factors which influenced the selection of the two types of logic used and with various practical considerations related to the hardware.

Many problems face the manufacturers of a range of digital modules; two will be discussed here. The first is to know how many different types of module to make. For some types of application it is feasible and convenient to standardize on just one logical function such as the NOR element which may be easily implemented. The Elliott MINILOG is such an element. Other logical functions may be produced by standard configurations of NOR units, and when these configurations are combined into a system, a significant number of NOR elements may be redundant.

A practical snag is that the different drive requirements of, say, other NOR units and computer peripheral equipment tend to result in the manufacture of more than one basic module anyway. However, NOR logic is inefficient for systems using a significant number of counter stages (3 NOR elements) or shift registers (4 NOR elements). It is more economical to use packaged bistable modules. Here again, one manufacturer (Ferranti) provides a bistable with sufficient methods of input to allow its use as a counter or as a shift register, while another (Mullard) provides separate modules for these two functions. This difference also relates to the question of how many leads a standard module package should have. The second problem concerns the maximum speed of the module. The bone of contention here is whether, excluding the direct financial factor, a module can be too fast for a particular application. Ferranti dismiss the suggestion that it can as 'misguided' (Pucknell, 1964). The writer's opinion is that, employing standard methods of construction, it is unwise to use modules with a maximum pulse repetition rate greater than 100 kc/s unless it is essential, for, referring to faster modules, it does seem rather pointless to give detailed and liberal specifications for the modules themselves and then say that for correct operation of an entire system a power supply line must be decoupled by capacitors 'wired in at strategic intervals' (Pucknell, 1964). This introduces a subjective factor into the design.

The solution adopted in the present work is to use both 2 mc/s modules (Ferranti 200 series) and 100 kc/s modules (Mullard-Phillips) which have common nominal D.C. logic levels of zero and -6 volts. The faster

modules satisfactorily drive the slower ones. The 2 mc/s modules are used for all circuits with a pulse repetition rate greater than 100 kc/s and for all modules which have to supply an A.C. drive to other 2 mc/s units. All ten stages of the A.D.C. counter and the ten associated storage registers are fast modules, but, otherwise, 100 kc/s modules are used where possible. Both these series of logic modules include a full range of logic gates, flip-flops and amplifiers. The Ferranti range also includes a module (LCA 1 G) containing six capacitor-diode-resistor digital feedback circuits. A list of the types of modules used is given in Appendix 1.

Consider the terminology used in the digital logic circuits. The principle output, denoted by Q (Mullard) or I (Ferranti), is at 0 (nominal earth voltage) in the RESET state of a bistable and at $\underline{I}$ (nominal - 6 volts) in the SET state. The quasi-stable state of a monostable is the set state and the stable state is the reset state. In the 2 mc/s modules the logical set or reset function is performed by a positive voltage at the base of the appropriate transistor, and the direct SET and RESET inputs are labelled accordingly. A gated A.C. input passes a signal if the gate input is at 0. The notation of the gate inputs of the 2 mc/s units is such that, if the 1 gate is connected to the 1 O/P of some driving bistable and the 0 gate is connected to the 0 O/P of the same driving bistable, then a clock pulse causes the module to take up the state of the driving bistable. The construction of a shift register is immediately apparent. A counter stage is formed by cross-coupling the gate inputs to the outputs of the same stage. Although the operation of the 100 kc/s logic is similar, the notation is different because it is assumed that information is carried by a '1' signal level of -6 volts. Consequently, the RESET function, for example, is commonly carried out by a positive voltage on the SET input.

A negative voltage on the RESET input could of course be used. Similarly, a clock input will cause a set function if the gate input G_S is at 1 and the gate G_R at 0, but it is the 0 at G_R which actually permits the set function to occur. A shift register may be completely blocked by putting both gate inputs to 1. This fact is used in the design of the time code bit generator (see Chapter 3).

The impedance levels of the 100 kc/s AND and OR diode gates are such that an OR gate cannot drive an AND gate. If the inverted outputs are available the requirement for this sequence of logic can be overcome by using the fact that an AND gate acts as an OR gate for '0's and an OR gate acts as an AND gate for '0's. In the present work this principle was used in the design of the double shift pulse generator in the punch control logic (see figure 16).

When logical design has been transformed into the corresponding hardware by careful application of the loading data it is often found that incorrect operation occurs due to 'kick-back' or 'kick-through' effects. For example, if the 100 kc/s FF2 shift register is driven by a bistable, the state of this driving module is often altered by the application of a shift pulse to the FF2 circuit. Such effects due to spurious pulses can often be suppressed by the use of diodes. In fact, in critical applications the 100 kc/s FF1 (counter stage) and FF2 (shift register stage) are replaced by FF3 and FF4 modules respectively, which are designed to avoid these effects. Another common cause of mal-operation is the noise on the power supply lines generated by the logic modules themselves. The -6 volt diode clamping line of the 2 mc/s modules is the most vulnerable line. The most critical module in both ranges of logic is the monostable, and a R-C filter should be used on the -6 volt supply input. Marginal timing errors can

also cause incorrect operation. This is most likely to occur if a waveform which drives several modules has a relatively slow rise or fall time. A waveform originating from the Q output of a 100 kc/s OS1 is particularly vulnerable to this form of error. In fact, this 'de-bugging' of digital hardware may require considerable electronic engineering 'know-how'. This was particularly true of the 2 mc/s logic, although the writer was unfortunate in having to do this the hard way before there was adequate manufacturer's data available.

Analogue circuits and digital logic circuits have all been constructed on 'veroboard' circuit board (Winter, 1962). The construction of the pre-amplifiers was contracted out and they are built on specially designed printed circuit boards. The system is built as a number of separate 19 inch chassis, and these are then placed into 19 inch cabinets. The inter-chassis connections are made when possible at the front panels; the exceptions are units such as the tape decks which are manufactured with rear connectors. Questions arise about the size and method of interconnection of circuit boards. The problem is that if one uses small plug-in boards for complex logic functions, one tends to be limited not by the number of modules that one may get onto the board, but by the number of pins on the circuit board connectors. It is expensive to standardize on plug-in boards with a large number of pins in the printed circuit board connectors. The alternative approach is to put an entire complex logic system on one large board carrying, say, fifty modules. This is clearly advantageous if the complex function has relatively few input and output lines. This is the method adopted for the construction of the array recording chassis (see figure 18) which consists of three small boards (a 2 mc/s oscillator, the ramp comparator circuit, and a

ten bit parity generator) and four large horizontal boards each 18" x 16.6". The first of these boards carries all the 2 mc/s logic for the A.D.C. and control; the second board carries the clock chain which divides down to 1 pulse every 12 hours; the third board carries the time code bit, parity and channel identity bit generators; the fourth board carries the digital tape write logic and amplifiers. The front panel can tilt forwards and lie flat and the four large boards are each connected to the basic chassis by leads to connectors at one of the four corners of the chassis, so that, for fault finding, it is possible to run the equipment with these boards not in a stack but with each one rotated upwards from a corner of the chassis. Nevertheless, it is true that, with this method of construction, the correction of faults under field conditions will be slow, although there are sufficient outputs available at the front panel for the nature of faults to be rapidly diagnosed. The conventional plug-in printed circuit board approach is used in the other chassis of the field and laboratory systems (see figure 19). This is advantageous when the logic is simple and is frequently duplicated, so that a number of identical boards may be constructed.

Finally in this review of practical considerations, the power supplies will be briefly discussed. Since the field equipment is not intended to run for periods of more than, say, twelve hours, no attempt has been made to reduce the power consumption of the tape decks with a view to using accumulators to drive the system in the field. Instead the equipment is run from an A.C. mains supply or from a mains generator fitted to a Land Rover, and the minimization of power consumption is not a primary consideration. Mullard low voltage power supply units (YL 6101 to YL 6104) are used because these modules offer the opportunity of separating the

rectification and stabilisation functions. This facility is used, and the chassis containing the stabiliser units for the array recording logic supplies is located immediately below the chassis containing this logic (see figure 21) while the larger chassis (see figures 20 and 23) containing the unstabilised power supply modules may be situated some distance away. It was over-heating in this compact stabiliser chassis that necessitated the introduction of forced ventilation. It should be noted that these stabiliser modules are not suitable for driving directly from accumulators because they each require a second floating supply.

CHAPTER 3

THE ARRAY SYSTEM IN THE FIELD

(i) Further design considerations

The general concepts of the array instrumentation have been discussed in section (iii) of Chapter 1, and, from considerations of the entire data acquisition and processing system, the following points were made:

(a) The maximum analogue system gain between the geophone and the analogue-to-digital converter should be about 200,000.

(b) The form of the digital tape write logic is controlled by the requirements of the flux-sensitive replay system.

(c) The complete system time should be written on to the magnetic tape every second.

(d) Since it is essential to ensure that the recorded digital information is recoverable, it is replayed and monitored.

(e) The magnetic tape format should be such that the information can be directly transferred to paper tape.

The consequences of these points will now be considered in turn.

(a) The gain of each channel is divided between the pre-amplifier and the recording system. A large pre-amplifier gain reduces the problem of noise pick-up on the lines but increases the remote power consumption and, for a given maximum undistorted output (or, effectively, a given pre-amplifier supply voltage), diminishes the dynamic range of the system under manual control, since the gain of a remote pre-amplifier is not usually manually variable. The adopted solution is a pre-amplifier (B.P. design) with a gain of 200 and a maximum

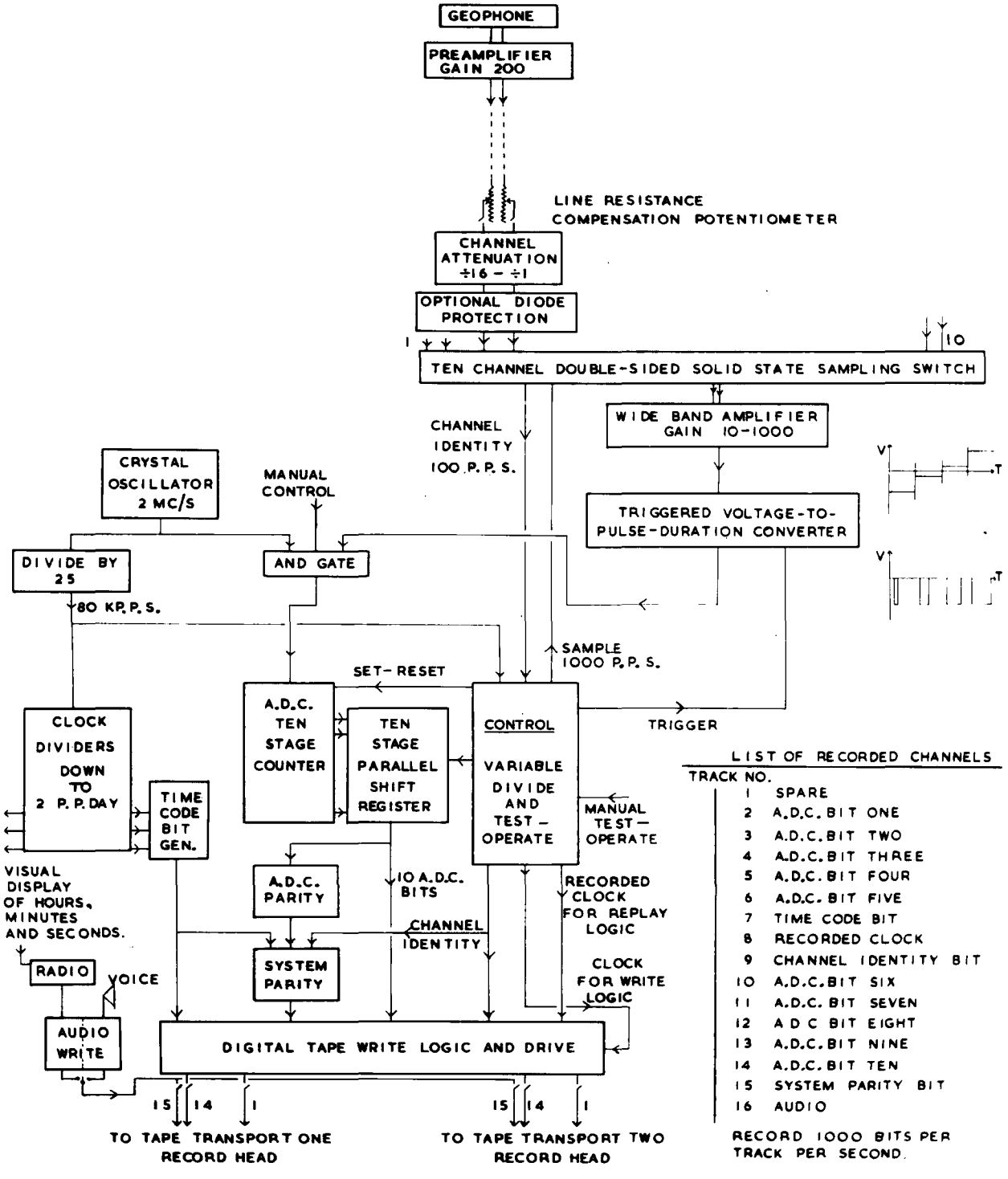

SCHEMATIC DIAGRAMS OF SEISMIC DATA PROCESSING SYSTEM

I - ARRAY FIELD RECORDING SYSTEM

FIGURE 3

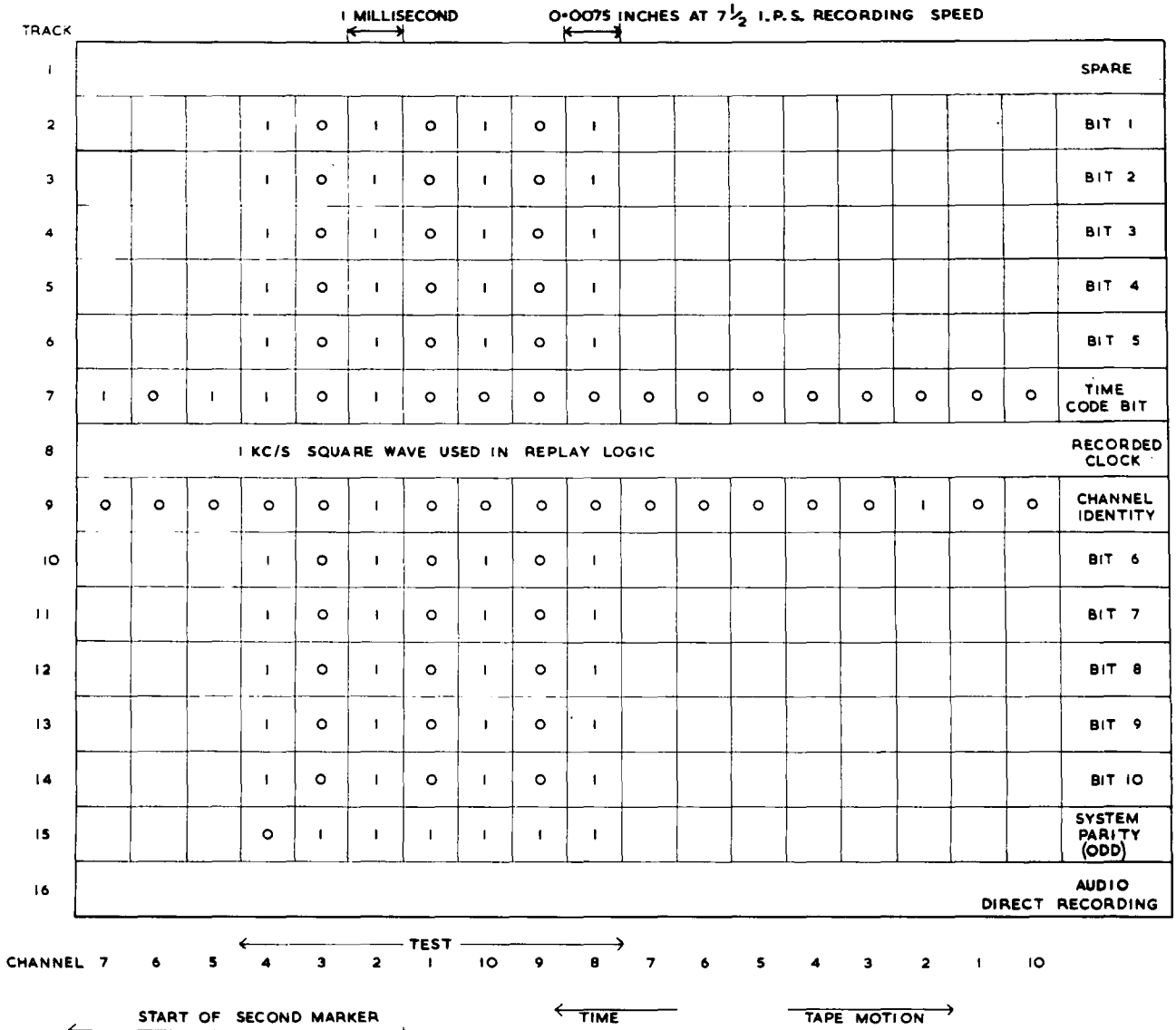

23 BIT TIME CODE WORD (SERIES)

1-3	OPENING PHRASE "101"
4-5	TWO BIT TIME CODE
6-11	SECONDS COUNTER
12-17	MINUTES COUNTER
18-21	HOURS COUNTER (12)
22-23	CLOSING PHRASE "01"

THE OTHER 977 T.C.B. BITS IN EACH SECOND ARE "0".

TWO BIT TIME CODE

	4	5
SECOND	1	0
MINUTE	0	1
QUARTER HOUR	1	1

NOTE

THERE IS NO FIXED RELATIONSHIP BETWEEN THE CHANNEL IDENTITY BIT AND THE TIME CODE BIT.

MAGNETIC TAPE FORMAT

FIGURE 4

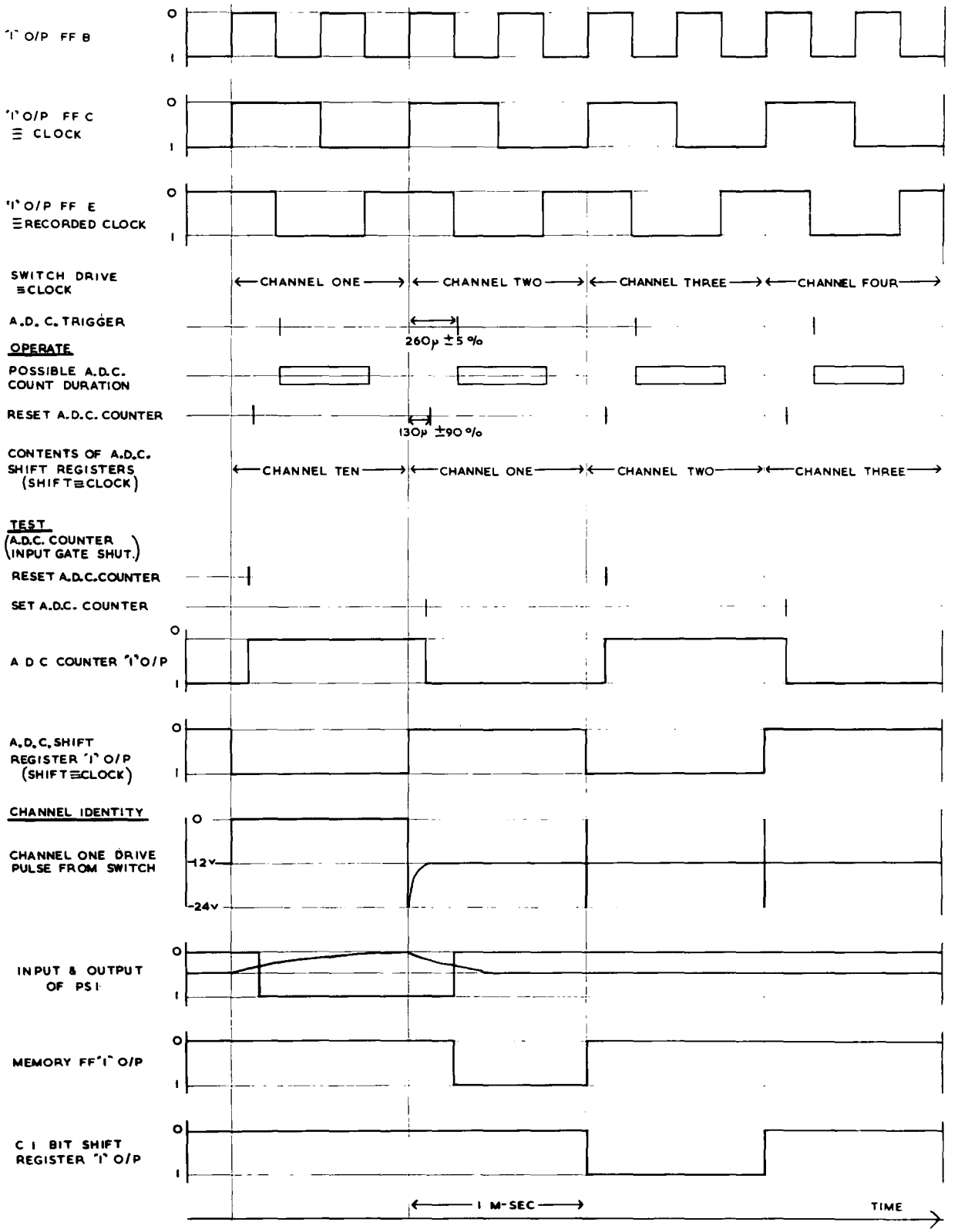

THE RECORDING SYSTEM CONTROL WAVEFORMS AND TIMING

FIGURE 5

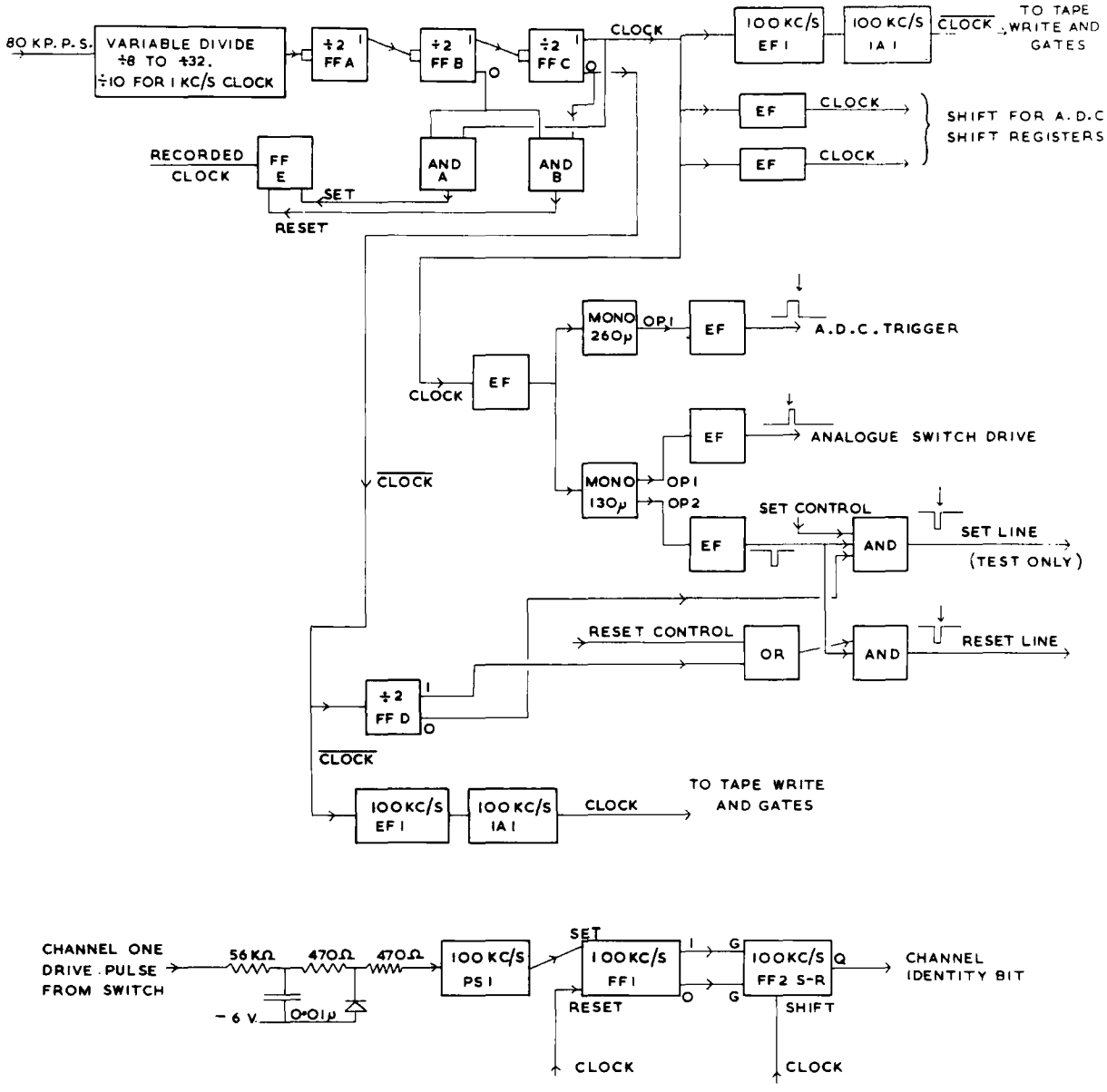

KEY:-

FF	BISTABLE
EF	EMITTER FOLLOWER
IA1	INVERTING AMPLIFIER
AND	AND LOGIC GATE
OR	OR LOGIC GATE
MONO	MONOSTABLE
PS1	PULSE SHAPER

SWITCHING OF D.C. CONTROL LEVELS

	OPERATE	TEST
RESET CONTROL	1	0 (FLOATING)
SET CONTROL	0	1
A.D.C. INPUT AND	1	0

A BLOCK DIAGRAM OF THE RECORDING SYSTEM CONTROL LOGIC

FIGURE 6

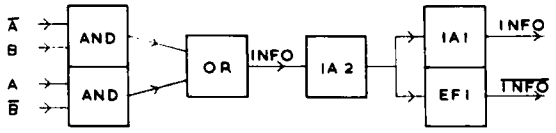

TRUTH TABLE			GATE	
A	B	INFO		
0	0	0		
0	1	1	$\bar{A}$	B
1	0	1	A	$\bar{B}$
1	1	0		

INFO HAS EVEN PARITY

TWO BIT MODULE

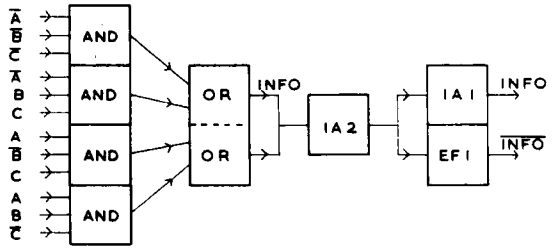

TRUTH TABLE				GATE		
A	B	C	INFO			
0	0	0	1	$\bar{A}$	$\bar{B}$	$\bar{C}$
0	0	1	0			
0	1	0	0			
0	1	1	1	$\bar{A}$	B	C
1	0	0	0			
1	0	1	1	A	$\bar{B}$	C
1	1	0	1	A	B	$\bar{C}$
1	1	1	0			

INFO HAS ODD PARITY

THREE BIT MODULE

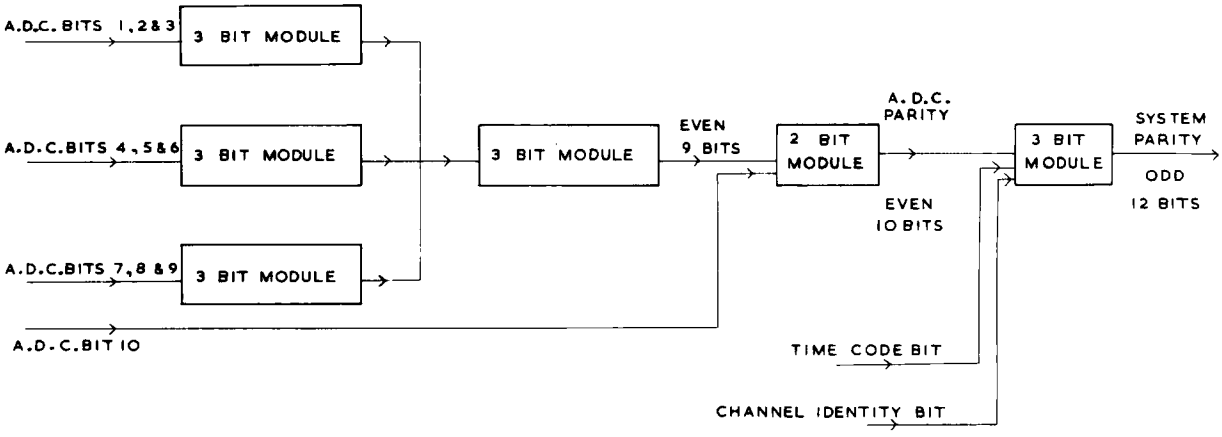

RECORD SYSTEM PARITY GENERATION

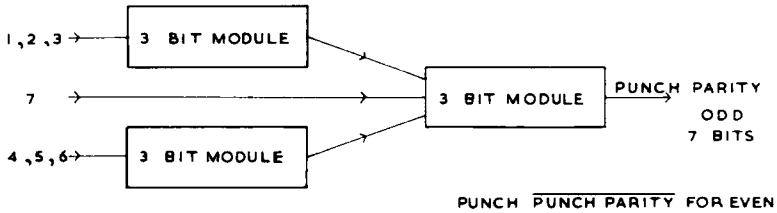

PUNCH $\overline{\text{PUNCH PARITY}}$ FOR EVEN COMPUTER PARITY

PAPER TAPE PUNCH PARITY GENERATION

THE GENERATION OF PARITY BITS

FIGURE 7

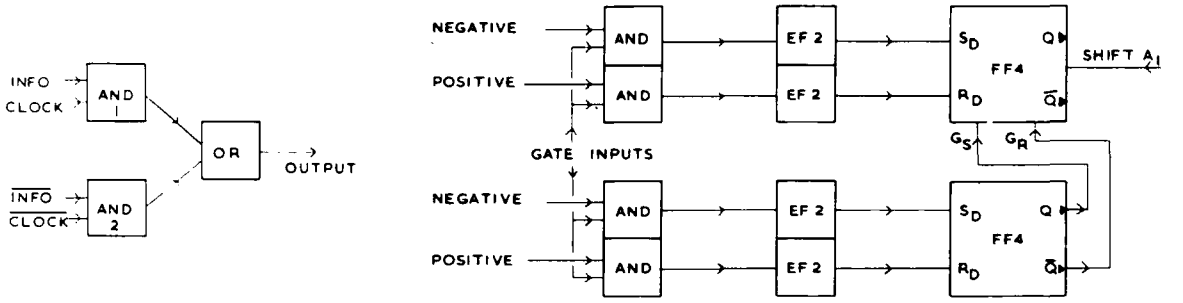

PHASE MODULATION RECORD LOGIC

REPLAY LOGIC BOARD (TWO CHANNELS)

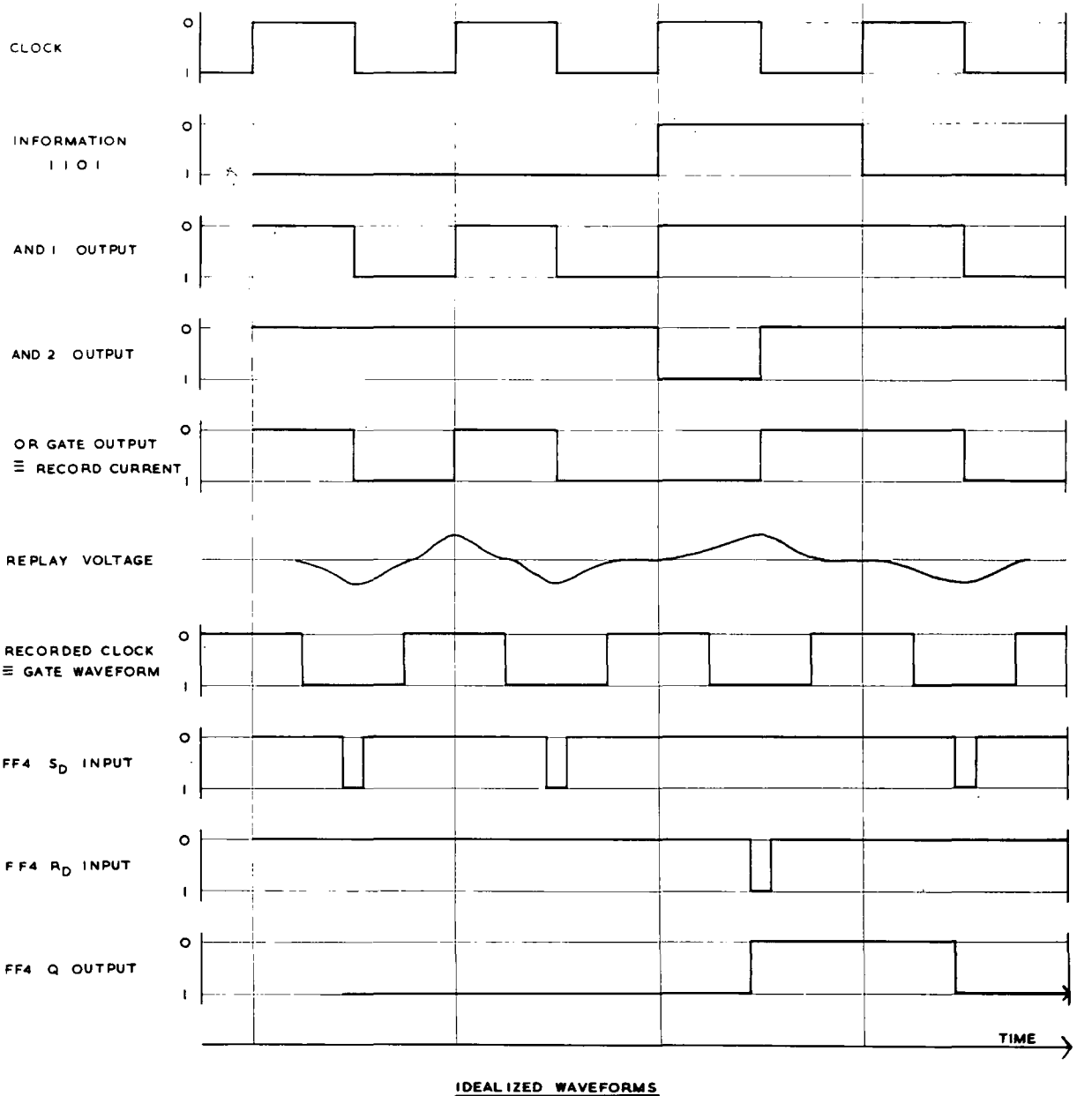

IDEALIZED WAVEFORMS

THE DIGITAL RECORD-REPLAY PROCESS

FIGURE 8

undistorted output of 4 volts peak-to-peak, and a maximum nominal channel gain at the recording system of 1000.

(b) The flux-sensitive replay process (Noble, 1963) is such that a digital write logic is required which gives frequent changes of magnetic flux whatever the sequence of recorded numerical information. This eliminates the use of the standard non-return-to-zero methods, and suggests phase modulation recording as one possible alternative (Hunter and Ridler, 1957). In this method a bit is written either in phase or out of phase with a clock square waveform, and at least one flux change is ensured per bit (see figure 8). A clock track, which corresponds to this clock waveform advanced by a quarter of a bit, is recorded ('record clock') and provides a waveform on replay for gating the significant flux-change at the centre of a bit.

(c) One digital track of the magnetic tape is devoted exclusively to recording system time, which is the output of the internal crystal clock. Every second a 23 bit serial word is written on to this track, and then (for a 1 kc/s system rate) 977 logical zeros are written before the next second marker. This 23 bit serial word is made up as follows:-

opening identity, 101	3 bits
coarse time code	2 bits
seconds	6 bits
minutes	6 bits
hours (12)	4 bits
closure identity, 01	2 bits.

The coarse 2 bit time code is as follows:-

second marker	1	0
minute marker	0	1
15 minute marker	1	1

(d) The necessity of replaying the digital information from the magnetic tape and re-constituting before monitoring means that the conventional replay electronics (as opposed to the flux-sensitive electronics) are included in the field system. Three monitoring facilities are provided in this field replay system:-

(1) The analogue signal from each channel may, in turn, be re-constituted from the digital information and be displayed on a single-channel hot-wire pen recorder.

(2) The coarse two-bit time code is extracted from the time code information, and a green lamp may be caused to flash when the selected type of marker occurs.

(3) The information which supplies the channel identity data is made to cause a red lamp to flicker visibly. The origin of this information is such that this flickering also indicates that the analogue switch is cycling correctly.

In addition to these arrangements for monitoring, two other test facilities exist. One, which is of use in the field and is vital for fault finding, is a function whereby the analogue-to-digital converter 10 bit counter is alternately set and reset.

Because there are an even number of channels and they are sampled in sequence, this digital process simulates inputs of either zero on channels 1, 3, 5, 7 and 9 and 1023 on the even channels, or vice versa. This known signal can be used to test the system from the A.D.C. counters onwards. In particular, in the field replay system, a square wave should be seen on the pen record when the channel selector is rotated through the channels from one to ten. The second check facility which is only of practical use in data processing is the generation of a 'system parity bit' before the magnetic recording and of a 'computer parity bit' before paper tape punching. These parity bits are checked when the data is read into the computer.

(e) Each sample is written as one parallel word across the multi-track magnetic tape, and a recorded clock waveform is used to gate the information on replay. The point being made here is that all the information which is to be transferred to the punched paper tape should be recorded in a common format and be replayed in time synchronization with this gate waveform. Thus a system in which there is a fixed time relationship between the sampling and the system clock is to be preferred. It will be seen later that the channel identity information becomes available at a time near the middle of a bit interval, and consequently, because of the above principle, is stored outside the tape write registers, and is written during the following bit interval.

Two fundamental decisions remain with regard to the recording instrumentation. The first is to select a method of rejecting the common

mode pick-up on the input lines. This is particularly important in a transportable system such as this because the use of lightweight, unscreened cable is essential for practical as well as economic reasons, and because some lines should be over a kilometre in length. Differential noise, caused for example by magnetic induction in an untwisted cable, is logically indistinguishable from signal of the same frequency, and therefore can only be rejected if it differs in frequency from the signal. In general one cannot filter or attenuate common mode noise which is much larger than the differential signal because this can only be done with reference to earth voltage, and any unbalance in the filter or attenuator at any frequency will convert a proportion of the common mode signal at this frequency to a differential component. One method of rejecting common mode noise is to use the differential property of transformers. In the present system where the signal is carried in its direct low frequency form (as opposed to a.m. or f.m. transmission), special low frequency transformers, such as those made by Geo Space in the United States, would be necessary. An alternative method is to use a high quality differential D.C. amplifier, but such amplifiers are expensive. In the present system the channels have to be multiplexed into one line before the analogue-to-digital converter anyway, so the system adopted is to multiplex the double-sided low level inputs, which carry both signal and common mode noise, to just one wideband, differential amplifier which is followed by the A.D.C. . The advantages of this unusual system are that it should give good common mode rejection and that the use of an input amplifier for each channel is avoided; the principal disadvantage is that because of the high frequency components in the multiplexer output, one cannot apply a low pass filter to the

signals after the rejection of common mode so that any line pick-up above the folding frequency and less than, say, 10 kc/s which does pass through to the A.D.C. will cause aliasing of the sampled data. Such a system depends on the use of a double-sided multiplexer switch with a noise level comparable to the pre-amplifier noise referred to output, with a large dynamic range in order to pass the common mode signals, and with a good overall transfer accuracy so that unbalance on the two sides of the switch does not generate differential signal from common mode noise. A 1 kc/s system rate is too fast for the multiplexer to be implemented by relays. The multiplexer may be either a solid state switch or a mechanical rotary switch with precision flush bonded switch plates (as manufactured by S. Davall and Sons Ltd.). The choice between these two forms of multiplexer is regarded to be the second fundamental decision because the solid state multiplexer and the digitization may be controlled externally but the rotary switch has to generate the pulses that control the timing of the A.D.C. This is true for such a mechanical device even if it is driven by a synchronous motor governed by the system clock. The solid state multiplexer is selected because of its greater reliability and life, assuming adequate protection against high level transient signals, and because it greatly simplifies the system logic since one can fix an exact relationship between the sampling rate and system time (see paragraph (e) above).

Some further design features relating to the field instrumentation will now be discussed. Firstly, there is the choice of the method of operation of the analogue-to-digital converter. The simple ramp converter, which transforms a voltage into a time interval, seems suitable since, as

has been discussed, there will be a timing error of $\pm$ 5 milliseconds in practical data processing programmes. However, in considering the design of the converter, it will be assumed that the converter output is an approximation to the signal value at the equi-spaced moments in time when the ramp voltage passes through the zero input level. The pulse frequency that is counted in order to measure a time interval in a digital form is limited to 2 mc/s by hardware considerations. The number of useful stages in the counter can clearly be optimized since if there are too few, the truncation error of $\pm \frac{1}{2}$ bit is relatively large, but if there are too many, the timing error in the above approximation is also large. If this timing error is transformed to a maximum equivalent amplitude error for a sinusoidal signal component of frequency f c/s and output amplitude $\pm$ pN units ($0 < p \leqslant 1$), where the converter full-scale output is $\pm$ N units, then, for a perfectly linear comparator and a 2 mc/s counter, the total maximum amplitude error, referred to the amplitude pN, is

$$\pm \left(\pi \, f \, p \, N. \; 10^{-4} + \frac{50}{pN} \right) \%, \quad \ldots\ldots\ldots (1)$$

and the optimum value of N for given f and p is equal to $400. \, p^{-1} \, f^{-\frac{1}{2}}$. The corresponding minimum amplitude error is equal to $\pm$ $0.25 \, f^{\frac{1}{2}}$ %, (e.g. $\pm$ 1% at 16 c/s). For a ten stage counter the magnitude of the error given by equation (1) for a range of values of f and p is shown in table I.

		p		
		$\frac{1}{20}$	$\frac{1}{4}$	1
f in c/s	4	2.0	0.6	0.7
	8	2.1	0.7	1.4
	20	2.2	1.2	3.3

TABLE I - The A.D.C. percentage error for N equal to 512.

The results presented in table I represent the theoretical basis for the initial assumption in Chapter 1 of a ten bit A.D.C.. Clearly a sample-and-hold device is not necessary in the present application.

It has already been pointed out that it is desirable to have a fixed timing relationship between the sampled data and system time. It is also necessary to have a fixed relationship between the triggering of the ramp comparator and the 2 mc/s pulse train which is counted, so as to avoid a count uncertainty of $\pm \frac{1}{2}$ unit at the start of the count. Consequently, the timing of the entire system is derived from one 2 mc/s oscillator. A further advantage of this system over a system with, for example, a separate 10 kc/s oscillator controlling the digitization and driving the clock chain, is that the sampling rate may easily be altered by changing the base of the counters which divide down the 2 mc/s signal.

It is necessary to write channel identity information on to the magnetic tape. It would simplify the data processing if each sample contained a unique label giving the channel number, but this is not essential since the sampling sequence is cyclic. The introduction of a four bit channel identity code is clearly unacceptable since it would destroy the present arrangement where one sample corresponds to one parallel word on magnetic tape and two characters on paper tape. Instead, one digital track is devoted to channel identity information, and a '1' is written in the words containing a sample from channel 2, but otherwise a '0' is written. The disadvantage of this system is that if an error occurs on this track due to tape drop-out for example, then correct channel identity cannot definitely be re-established until the next sample of channel two.

The format of the digital information on the magnetic tape is shown

schematically in figure 4. The track allocation is designed to minimize the possible effects of tape 'skew' in that the replay gate waveform is recorded on a central track and the two important control tracks are recorded immediately on either side. The ten A.D.C. bits are recorded on the next five tracks on either side of the recorded gate waveform. The simple allocation of these ten bits does not minimize the possible effects of skew in that the least significant and the most significant bits are the most vulnerable. However, it can be argued that in one case an error has a minimal effect while in the other the effect of an error is so large as to be relatively easily detected and corrected. The system parity bit, which is a parity bit for the other twelve bits of the word, is located in the extreme unsymmetrical digital track, since if a parity error is to occur, the least damaging circumstance is that it should be due to an error in the parity bit itself. The two outside tracks are not used for digital information. In the present system one is used for the direct recording of an audio channel (either microphone or radio) and the other is not used.

Figure 4 also shows the pattern of data occurring during the test function, the form of the channel identity track, and the start of a second marker on the time code track. An important point in the data processing programmes is that there are no set or reset inputs to the analogue switch internal decade counter as supplied, so that the relationship between the second markers and the channel identity after the system clock has been reset is arbitrary. However, for a system sampling rate of 1 kc/s, the channel corresponding to the onset of any second marker should be constant so long as the system clock is not reset. An alternative design would have been to tie the switch more directly to the system clock

and combine the channel identity and time code tracks. Such a system would suffer relative to the present one in that it would be more difficult to change the sampling rate from 1 kc/s without breaking the sampling sequence each second and that of course the system logic and data processing would be more complicated.

The fundamental requirement of the magnetic tape recording system is that the recording speed should be as slow as possible for tape economy, and that the size of the tape spools should be as large as possible to minimize the danger of losing important information while tapes are being changed. At the standard sampling rate the digital information is written a 1 kc/s per track, so recording speeds of $3\frac{3}{4}$ i.p.s. and $7\frac{1}{2}$ i.p.s. correspond to packing densities of 267 and 133 bits/inch respectively. The approach adopted during the design of the present system was that it should be possible to operate even under field conditions at $3\frac{3}{4}$ i.p.s., and that it would certainly be possible to do so at $7\frac{1}{2}$ i.p.s. At the time when the construction of the system was started, the tape deck which appeared to be the best technical and economical buy had 8 inch reels giving 48 minutes recording time at $7\frac{1}{2}$ i.p.s., so that the reload time would be quite significant. It was at that time an economically justifiable solution to use two such decks, thus giving an unlimited continuous recording facility, rather than one large deck with 14 inch spools. In fact it has transpired that the conventional record-replay process will operate at a recording speed of $3\frac{3}{4}$ i.p.s., but that such data cannot at present be replayed to the paper tape punch because of the apparent random static skew of the flux-sensitive replay system. This skew is much greater than the specified skew for the replay head

itself, but experiments suggest that it is not caused by variations in the operating conditions of the flux-sensitive replay electronics. Anyhow, this apparent skew is independent of time, and it would be possible to overcome this problem by modifying the replay logic gate input waveforms. However, during the field tests of September, 1965, a recording speed of $7\frac{1}{2}$ i.p.s. was used.

(ii) A description of the array recording instrumentation

A schematic diagram of the array recording system is shown in figure 3. Firstly, consider briefly the following units of this diagram which were purchased (or borrowed) as complete units.

(a) Ten B.P. swamp geophones (3 c/s).

The damping of these geophones, which were discussed in section (iii) of Chapter 1, is calculated from the value of the parallel damping resistor and the pre-amplifier input impedance to be about 0.58 critical.

(b) Ten channel double-sided solid state sampling switch. This module includes the ring counter logic and series-pair transistor switches. The drive to the pairs of these switches is through transformers so that if no drive pulses are supplied, all ten switch channels are open. The drive pulse to the channel one switch is bought out and used for channel identity. The most important features in the specification are:-

Full-scale input range $\pm$ 2.5 volts

Over all transfer accuracy $\pm$ 75 volts.

(c) A wide band amplifier (Redcor 371-022).

This is a wideband, low level differential d.c. amplifier.

An important point is that the overload recovery time is fast so that a disturbance at one geophone does not block the whole array. In practice the important features are that the noise with a finite source resistance (100 mv p-p for gain 1000, bandwidth 50 kc/s and 1000 ohm source resistance) is rather larger than one might expect from a study of the specification sheet, and that the process whereby common mode rejection is achieved in the present type of application is complex since the input line and source are included in a feedback loop. Because the common mode rejection is reduced at high frequencies and because it is necessary to attenuate high frequency differential pick-up, the system is run in the field with the lowest permitable bandwidth of 3 kc/s, corresponding to a settling time of 600 μ-secs to 0.01% of full-scale.

The important points from the specification of this amplifier are:-

gain 10, 20, 50, 100, 200, 500, 1000.

bandwidth D.C. - 100 c/s to D.C. - 50 kc/s.

input impedance 1000 meg.

common mode rejection 1000 x gain, D.C. to 150 c/s.

overload recovery time 80 μ-secs.

(d) Tape transports.

The two mains-operated tape transports used are the T.D.R. 4 model of Thermionic Products (Electronics) Ltd., with speeds from $1\frac{7}{8}$ i.p.s. to 15 i.p.s. and fitted with 16 track record and replay heads to S.B.A.C. spacing for 1" tape.

(e) Radio.

Two Eddystone 960 communications receivers are used for receiving time signals and for communication purposes. If one radio is not required at the shot point, both are included in the array system, although only the output of one may be recorded.

The function and operation of the other units of the block diagram (figure 3) will now be discussed in turn, starting with the analogue input circuitry.

Pre-amplifier.

The pre-amplifier has a gain of 200 and is powered by mercury cells. Four such batteries give a life of three weeks at a cost of six pounds per pre-amplifier. There is a battery on-off switch on the pre-amplifier board. The pre-amplifier is cased in a P.V.C. tube which is permanently sealed at one end. Both input and output lines pass through the other end which is sealed by compressing a rubber disc between two brass plates (figure 17). Large reversible electrolytic capacitors are used on the output low pass filter with the intention that they could not be damaged by control signals passed down the line to activate a calibration circuit. However, the calibration circuits have not yet been added.

Channel attenuation.

This function enables an attenuation of from + 1 to + 16 to be applied individually to the differential signals on the different channels. This is necessary since different channels may require different gains. The important point about this attenuation is its impedance which is about 2.6 kΩ . A low impedance helps reduce the

noise pick-up on the input lines, reduces the effective source resistance of the wideband amplifier and hence improves its performance, and improves the linearity of the attenuator. On the other hand it also makes the line resistance of about 120 Ω per line per 800 yards contribute significantly to the attenuation of the signal. For this reason a double-ganged 'line resistance compensation' potentiometer is included in the input circuit so that all channels can be adjusted to have the same effective line length.

Optional diode protection.

Since the input lines go through the attenuators to the solid state switch, an optional protection facility on the switch inputs is provided by diode clipping at ± 4 volts using OA200 silicon diodes and voltage levels from mercury cells. The attenuation due to the current limiting resistor of this protection circuit (whether in or out) and the effective line resistance, R per line (i.e. one side), is

$$X \quad \frac{1200}{1325 + R} \quad .$$

Ten channel double-sided sampling switch.

This unit has been described already. The point to be made here is that the high input impedance of the differential amplifier is shunted by a resistor of about 100 kΩ across the switch output. The purpose of this is to reduce the effect of any leakage currents through 'open' switches.

Triggered voltage-to-pulse duration converter.

The ramp comparator circuit is basically that published by Rakovich (1963) which is a collector-coupled monostable with a 'bootstrap'

integrator in the timing circuit (Nambiar and Boothroyd, 1957; Nambiar, 1958). Compensation for the second order time term may be introduced to this circuit by adding resistance-capacitance feedback. Nambiar and Boothroyd (1957) suggest that such compensation in a 'bootstrap' circuit with a single transistor emitter follower can reduce the error at the end of the sweep due to non-linearity to about 0.15%. Such linearity is more than adequate for the present application. The circuit is modified to trigger off a negative-going edge from a 2 mc/s module and the rectangular pulse at one of the collectors drives a 211 G/A trigger/amplifier module to give a '1' output to open the A.D.C. input AND gate during the quasi-stable state.

Before discussing the digital functions on the block diagram, the timing control of the digital system will be considered. The standard system rate of 1 kc/s will be assumed. The control waveforms of the digital system and the corresponding hardware are given in fugures 5 and 6 respectively. The second waveform, which is described as '1 O/P FFC ≡ CLOCK ', is the 1 kc/s square waveform used for the phase modulation tape logic, so that the interval during which a parallel word is written on to the magnetic tape starts at the positive-going edge of this clock waveform. Consequently, this clock waveform is also used to shift information into the registers which drive the write logic. The logic of the phase modulation record-replay process is shown in figure 8. The 'recorded clock' waveform is used to gate the significant flux changes which occur on replay at the centre of a bit.

At the start of a bit interval the switch moves on one channel and the previous count in the A.D.C. is shifted into the registers which drive

the write logic. After an arbitrary delay (130 p-secs ± 90%), the A.D.C. counters are reset to zero in readiness for starting the next count. The switch output is allowed 260 p-secs (± 5 %) to settle, and then the ramp comparator is triggered and the count starts. The maximum count duration is 512 p-secs, so that the count will be completed after 800 p-secs, at the latest. This permits operation at system rates up to 1250 samples per second. At the completion of the bit interval, the count number is shifted into the registers where it is written on to the tape during the next bit interval, and the sequence is repeated.

The test signal in the A.D.C. counter is generated by manually closing the input AND gate of the counter and switching the circuit so that every alternate reset pulse is suppressed and a pulse is applied on the set line instead. The hardware for doing this is shown in figure 6. A point to notice is that control is exercised from the front panel by switching D.C. levels.

The drive pulse to channel one of the analogue switch, which is brought out to provide the channel identity information, is shown in figure 5. This output has large amplitude noise transients at the start of each clock interval, and the signal has to be filtered and squared as shown in figures 5 and 6. The load presented to the switch drive pulse by this circuit has to be minimal in order to prevent the switch opening prematurely (i.e. before 1 millisecond) on channel one. Because of this filtering the output of the pulse shaper does not coincide with a bit interval, so the channel identity information has to be stored and recorded in the word corresponding to the next sample. An examination of figure 5 shows why, during recording, the channel identity bit corresponds in time to the switch

on channel three, and why, on replay, it corresponds to a sample on channel two.

The logic for the generation of the system parity bit is shown in figure 7. In this application a static parity generator of this type is simpler than a dynamic one in which, for example, the different stages of the counter are reset in turn, and the number of stages which change state is counted.

The digital units of the block diagram (figure 3) will now be briefly described in turn.

2 mc/s crystal oscillator.

This circuit employs a Marconi quartz crystal 1655 E, operating in the open air (see figure 18) and located not far from a fan at the top of a cabinet, and a circuit provided by the manufacturer (see 'notes on circuit and equipment No. 30'). The performance of this oscillator under field conditions is considered in Chapter 5.

Divide by 25.

A five stage counter using 2 mc/s modules with feedback from the last stage to the first, second and third stages appeared, from the manufacturer's provisional loading data, to incur some danger of overloading. Consequently, six modules are used to give two divide-by-five counters in series.

Clock dividers down to 2 p.p. day.

The sequence of counters in this chain is

divide by 8 (2 mc/s modules)	3 stages
divide by 10,000 (100 kc/s modules)	
divide by 2	1 stage
divide by 5	3 stages
divide by 8	3 stages

divide by 125	7 stages
seconds counter	
divide by 15	4 stages
divide by 4	2 stages
minutes counter	
divide by 15	4 stages
divide by 4	2 stages
hours counter (12)	
divide by 4	2 stages
divide by 3	2 stages

Note that since 2^{13} equals 8192, fourteen is the minimum number of stages for a divide by 10^4. The positive manual reset voltage is applied (through resistors and diodes) to the SD input of the 100 kc/s modules and the reset inputs of the 2 mc/s modules. The stages of the last sixteen stages, which represent system time in hours, minutes and seconds, are displayed on the front panel using Mullard DM 160 tubes which are driven directly by the bistables through a 100 kΩ resistor. These tubes are lit up when the logic drive is '0' (i.e. reset). Tables for interpreting the time code are given in appendix 2, where the bits are numbered according to their position in the 23 bit serial time code bit word.

Time code bit generator.

It is required to generate a 23 bit serial code in the format already discussed. The main problem is the construction of a triggered 24 bit ring counter which has one stable state and, on triggering, cycles once through the 23 other states. One possibility is to use a five stage counter (with feedback) in which both outputs of each stage drive 12 inputs of different

5-input AND gates. This heavy loading would necessitate the use of FF3 modules rather than FF1 counter units. The alternative is to use a twelve stage shift register counter so that each ring counter output is obtained by AND gating only two outputs. Such a counter consists of a 12 stage series shift register with the output of the final stage cross coupled to the input gates of the first stage, so that an inversion of information occurs between stages twelve and one. The contents of the registers and the outputs used to drive the AND gates to generate the ring counter outputs are shown in table 2.

Since it is required to modulate the ring counter outputs with information, the first design generally requires a six-input gate for each bit, while the second requires a three-input AND gate. The two bit coarse code is set up on two bistables using the positive-going edges available on the completion of a second, a minute or a quarter hour. The outputs of the twenty-one AND gates (corresponding to the 21 bits which may take the value '1') drive one OR gate, and the output of this gate is amplified and its inverse made available for driving write logic and parity generators. This is the time code bit. There is little difference between the two methods economically because the difference in the number of bistables is offset by the difference in AND gates. The shift register counter is adopted because of the greater logical simplicity of the ring counter. It is necessary that the ring counter should block at the completion of a cycle. This may be achieved either by suppressing the shift input, which is equivalent to CLOCK, or by breaking the cross coupling between the last and first stages of the

COUNT NUMBER	NUMBER OF STAGE												AND GATE INPUTS	
	1	2	3	4	5	6	7	8	9	10	11	12		
0*	0	0	0	0	0	0	0	0	0	0	0	0	$\overline{12}$	$\overline{1}$
1	1	0	0	0	0	0	0	0	0	0	0	0	1	$\overline{2}$
2	1	1	0	0	0	0	0	0	0	0	0	0	2	$\overline{3}$
3	1	1	1	0	0	0	0	0	0	0	0	0	3	$\overline{4}$
4	1	1	1	1	0	0	0	0	0	0	0	0	4	$\overline{5}$
5	1	1	1	1	1	0	0	0	0	0	0	0	5	$\overline{6}$
6	1	1	1	1	1	1	0	0	0	0	0	0	6	$\overline{7}$
7	1	1	1	1	1	1	1	0	0	0	0	0	7	$\overline{8}$
8	1	1	1	1	1	1	1	1	0	0	0	0	8	$\overline{9}$
9	1	1	1	1	1	1	1	1	1	0	0	0	9	$\overline{10}$
10	1	1	1	1	1	1	1	1	1	1	0	0	10	$\overline{11}$
11	1	1	1	1	1	1	1	1	1	1	1	0	11	$\overline{12}$
12	1	1	1	1	1	1	1	1	1	1	1	1	12	1
13	0	1	1	1	1	1	1	1	1	1	1	1	$\overline{1}$	2
14	0	0	1	1	1	1	1	1	1	1	1	1	$\overline{2}$	3
15	0	0	0	1	1	1	1	1	1	1	1	1	$\overline{3}$	4
16	0	0	0	0	1	1	1	1	1	1	1	1	$\overline{4}$	5
17	0	0	0	0	0	1	1	1	1	1	1	1	$\overline{5}$	6
18	0	0	0	0	0	0	1	1	1	1	1	1	$\overline{6}$	7
19	0	0	0	0	0	0	0	1	1	1	1	1	$\overline{7}$	8
20	0	0	0	0	0	0	0	0	1	1	1	1	$\overline{8}$	9
21	0	0	0	0	0	0	0	0	0	1	1	1	$\overline{9}$	10
22	0	0	0	0	0	0	0	0	0	0	1	1	$\overline{10}$	11
23	0	0	0	0	0	0	0	0	0	0	0	1	$\overline{11}$	12
24 ≡ 0*	0	0	0	0	0	0	0	0	0	0	0	0	$\overline{12}$	$\overline{1}$

* stable state.

TABLE 2 - Outputs of the time code bit generator shift register.

shift register. Also, since the detection of the stable state is not dependent on the states of all the registers, it is a necessary precaution to reset the register to the correct stable state after every cycle. This may be done either by using a direct reset or by breaking the cross coupling between stages number 12 and 1 in such a way that the first stage remains in the reset state as shift input pulses continue to be applied. The system whereby the register is controlled through the cross coupling is adopted. At the start of the stable count interval (i.e. number 24) when the first and last stages must be in the reset state for the ring counter output to occur, the G_R gate input of the first stage is forced to '1', thus preventing a SET operation. The ring counter is triggered by simply re-establishing the cross coupling.

AND gate (A.D.C. input).

During normal operation the output of this gate consists of intervals of 2 mc/s signal, commencing whenever the ramp comparator is triggered and ending when the ramp voltage equals the input voltage to the A.D.C. The gate may be closed manually by a D.C. control voltage (earth), and this is done during the generation of the test signal.

A.D.C. ten stage counter.

Ten 2 mc/s binaries form a 'divide by 1024' counter.

The ten stages have common set and common reset lines.

Ten stage parallel shift registers.

Ten 2 mc/s binaries form a parallel shift register, and, on application of a pulse to their shift inputs, adopt the states of the

ten A.D.C. counter stages. Each of the two outputs of each register is able to drive directly the three 100 kc/s AND gate inputs required for the digital write logic (1) and the generation of a parity bit (2).

Control - variable divide and test-operate.

The operation of this unit has already been discussed. The hardware is shown in figure 6 and the corresponding waveforms in figure 5. The operation of the 2 mc/s variable divide unit is controlled by modifying the counter cycle using an appropriately wired 15 pin printed circuit board connector located immediately adjacent to the counter modules (see figure 18). The maximum number of stages is five, denoted by A, B, C, D and E in order of increasing significance or decreasing frequency, and some possible values of the divisor N, the corresponding channel sampling rates, and methods of their implementation (assuming feedback from the final stage) are shown in table 3. The case N equals nine where there are three feedback paths from the last stage can be treated by two divide-by-three stages. The inputs and outputs corresponding to the fifteen pins are given in table 4. For example, for the standard divide-by-ten using stages A to D inclusive, the following pins are joined together:-

1 and 2

5, 6 and 7

10 and 11

12 and 13.

A.D.C. parity.

The generation of a parity bit for the ten bits of the A.D.C. output shift register is shown in figure 7. A practical point is that this bit is constant during the test function (alternately zero and 1023).

DIVISOR N	CHANNEL SAMPLING RATE IN S/S	NUMBER OF STAGES	STAGES WITH FEEDBACK
8	125	3	-
9	111·1	4	A,B,C
10	100	4	B,C
11	90·9	4	A, C,
12	83·3	4	C
14	71·4	4	B
16	62·5	4	-
20	50	5	C, D
32	31·2	5	-

TABLE 3 - The operation of the variable divide.

PIN NO.	FUNCTION
1	Input to divider
2	Input to stage A
3	Inverse output of stage B
4	Feedback in to stage A
5	Feedback in to stage B
6	Inverse output of stage D
7	Feedback in to stage C
8	Inverse output of stage E
9	Feedback in to stage D
10	Output of stage C
11	Input to stage D
12	Output of stage D
13	OUTPUT OF DIVIDER
14	Output of stage E
15	Input to stage E

TABLE 4 - Connector pins of variable divide control

System parity bit.

The generation of a parity bit for all twelve recorded digital channels from the A.D.C. parity bit, the time code bit and the channel identity bit is also shown in figure 7.

Digital tape write logic and drive.

The logic of the phase modulation recording process and the use of the special clock waveform recorded in order to control the replay are shown in figure 8. Each track of the write heads is centre-tapped and has an inductance of 12 MH, a resistance of 16 ohms and a specified record current for saturation of 10 milliamps. A standard 100 kc/s amplifier consisting of an EF2 and EF1 (operated with grounded emitter) is used to amplify the OR gate output and drive one track of heads on either one or both tape transports. The drive on each track is through a 560 ohm resistor to a -6 volt line, and protection against inductive transients is provided by OA85 diodes. Using this circuit the two states of the tape are 'unmagnetized' and 'saturated', and the replay waveform is severely distorted because of the non-linearity of the magnetic recording process. This distortion increases any problems due to 'skew'. At the present time (July, 1966) a simple modification, whereby a reverse 5 milliamp bias current is supplied to the low impedance head giving recording currents of +5 milliamps and -5 milliamps, has been tested and yields a symmetric replay waveform. A current of 5 milliamps through both sides of the centre-tapped record winding is equivalent in terms of magnetization produced to a 10 milliamp current in one side only, as in a more usual digital tape write circuit. When this modification is made to the record system,

the reduction of the recording speed to $3\frac{3}{4}$ i.p.s., which is prevented by the 'skew' of the slow speed replay system, will be aided.

Audio write.

The amplified output of a microphone or the output of the radio receiver (600 ohm output) may be written on to the audio track of either one or both tape decks. Direct current bias is used.

(iii) A description of the field replay system

The purpose of the replay system in the field, using read heads adjacent to the write heads on the tape transports, is to monitor the geophone channels and the recorded control information at the time of recording. A block diagram of the replay system is shown in figure 9, and the units of the block diagram will be considered in turn.

Head amplifiers.

Each track of the replay head drives a two-stage capacitance-coupled amplifier through a capacitance and a 1 kΩ resistance.

Positive and negative peak detectors.

The outputs of the head amplifiers undergo one more stage of amplification and then the positive and negative peaks are detected by diode clipping at threshold voltages controlled by potentiometer circuits (i.e. amplitude sensing rather than peak sensing). The positive peaks pass through one more capacitance-coupled common emitter switching stage to give -6 volt logic outputs, and the negative peaks pass through a degenerate common emitter stage and a common emitter switch stage to again give logic outputs. This last combination of two common emitter stages was found preferable to one non-inverting

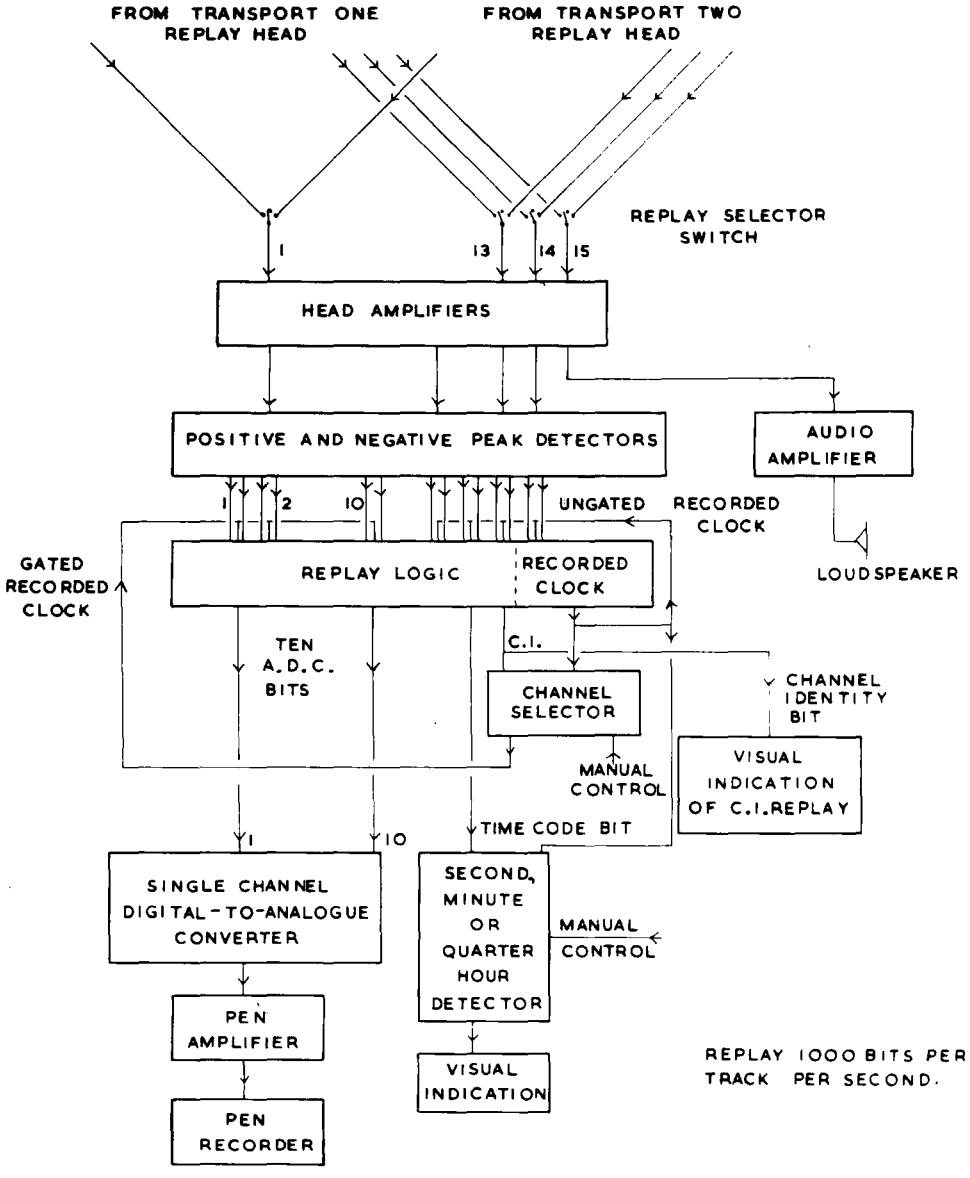

SCHEMATIC DIAGRAMS OF SEISMIC DATA PROCESSING SYSTEM

2-ARRAY FIELD REPLAY SYSTEM

FIGURE 9

common base stage which overloaded the diode clipping circuit.

Replay logic.

The logic outputs from the peak detector boards drive the replay logic boards (see figure 8). The recorded clock replay channel has no gate input signal, and so the corresponding FF4 is alternately set and reset and the recorded clock waveform is regenerated. The ten replay channels corresponding to the ten A.D.C. bits have common gate inputs ('gated recorded clock') which are distinct from the gate inputs of the other channels. This is because the channel selector for the single channel digital-to-analogue converter modifies the gate input waveform so that nine out of ten A.D.C. samples are suppressed. The modified gate waveform only permits the peaks corresponding to samples of the selected channel to pass through the replay logic AND gates. An unmodified gate waveform is needed for the time code and channel identity replay channels. The cross coupling of figure 8 between the two channels on each logic board is not used here, but is used for replay to the paper tape punch.

Channel selector.

A ten state counter, which is driven by the replayed recorded clock waveform and which is constructed from five shift register stages, is reset to the state corresponding to a count of two by the channel identity replay logic, so that the state of this register during the 'OPEN' interval of the gate waveform corresponds to the channel number of the A.D.C. sample passing into the replay logic registers during the same 'OPEN' interval. A logic output coincident

with the information of any one channel may be obtained by passing two appropriate outputs from the counter to an AND gate, and, if the recorded clock gate waveform is passed to a third input of this gate, then the output of this AND gate is the 'gated recorded clock' which is required in order to select digital output corresponding only to the chosen channel. A two-pole, eleven-way rotary switch is used to select any one of the ten analogue channels or to leave the gate waveform unmodified.

Audio amplifier.

A $1\frac{1}{2}$ watt amplifier (Henry's Radio) is used to drive the loudspeaker located within the radio. The loudspeaker may be switched either to the audio replay or to the radio output, but the radio must be turned off at the time of switching.

Visual indication of channel identity replay.

The state of the channel identity replay logic should be a '1' for one millisecond in every ten. This output waveform is used to trigger a monostable which drives a red lamp through an amplifier. The stable state of the lamp is on, but the duration of the unstable state and of the recovery time of the monostable are such that correct replay produces a clearly visible flicker of the red lamp. Also, correct operation of the channel selector generally indicates that the channel identity information is correct.

Second, minute or quarter hour detector.

The contents of the time code bit replay logic FF4 is fed to a five bit serial shift register. A second marker is detected by the 101 opening phrase of the time code and a minute, second or quarter hour coarse code message is simultaneously sought, and, if it is found,

a green lamp is caused to flash onfor about a quarter of a second. The choice of the coarse code message which is sought is controlled by two two-way switches on the front panel. After each opening phrase is detected, the detector has to be blocked for at least 22 milliseconds so that some chance combination of bits in the time code word cannot trigger the detector. If this coarse time code detector is used with the flux-sensitive replay system, a longer blocking interval is required.

Single channel digital-to-analogue converter.

This unit provides a low performance digital-to-analogue converter which ultimately drives a pen recorder. This system has low gain (1023 units correspond to a pen deflection of about 2 cm.) and poor accuracy, but is adequate for field monitoring purposes. The ten replay logic registers, which contain the A.D.C. outputs associated with only one channel because of the modification of the gate inputs by the channel selector, drive ten current switches each of which controls the same nominal current of 4.5 milliamps. The voltage developed across each 250 ohm collector load is used to tap off very small currents to a common line through high resistances which have values weighted according to the binary scale. The current through a low resistance (250 Ω), which is connected from this common 'sum' line to the collector supply voltage line, is the 'zero order hold' analogue output. This type of circuit will be discussed in more detail when the laboratory replay facilities are considered. One important difference between this system and the laboratory system is that, in the laboratory system, all ten bits change simultaneously

to their new value, but here the relative timing of the changes is controlled by the skew and may legitimately occur any time during the interval when the gate waveform is 'OPEN'. Consequently, incorrect transient values of significant duration can occur. The signal across the 250 ohm summing resistor is applied to a double-sided balanced direct-coupled amplifier with a single-sided output about earth voltage.

Pen amplifier.

The pen is driven from the D.A.C. output amplifier through a direct-coupled common collector class B amplifier with complementary transistors and supply lines of ± 6 volts. The cross-over distortion is not significant in this application.

Pen recorder.

The single channel pen recorder (Cambridge Instrument Company Limited, type no. 72127) has a coil resistance of 100 ohms and a sensitivity of 50 ma/cm. A 12 volt supply is required for the motor, which has speeds from 0.2 to 1.5 cm/sec, and a 1.5 volt supply for the heated stylus.

This field system may be run from a 50 c/s (1 phase), nominal 240 volt, one kilowatt supply. A mains supply is preferable, but a well-regulated mains generator can be used. Great care must be taken with the earthing arrangements of mains equipment under field conditions.

CHAPTER 4

DATA PROCESSING SYSTEMS

(i) The ten channel galvanometer replay facility

The first steps in the data processing system must be to obtain an analogue record of the ten geophone channels and to relate this record to the recorded system time. This output is needed for indicating the quality of the record, for initial interpretations and for determining which sections of the record should be subject to detailed analysis. It also gives an indication of the coherence of the signals across the array, and hence of the likely effectiveness of velocity filtering techniques. The output of the coarse time code marker is replayed on the same multi-channel record, and the complete replayed system time is indicated on DM160 tubes, so that the interval of system time which it is required to transfer to punched paper tape may easily be determined. A schematic diagram of this replay facility is shown in figure 10. It is desirable that the analogue system should have a large range of gain, even with loss of linearity, so that signals recorded at low levels may be examined. This also requires that the accuracy, referred to the full-scale signal, should be high. Provision should also be made for calibrating each D.A.C. channel individually by simulating inputs of 0 and 1023, for if all channels are so calibrated simultaneously, then it would be difficult to sort out which traces correspond to which channels.

The digital output corresponding to each channel is definitely available in the replay logic registers for about 0.5 milliseconds in every 10 milliseconds, and could, if one ten bit parallel shift register were used, be available for one millisecond in every ten. However, an analogue recorder generally requires a continuous input signal, and the

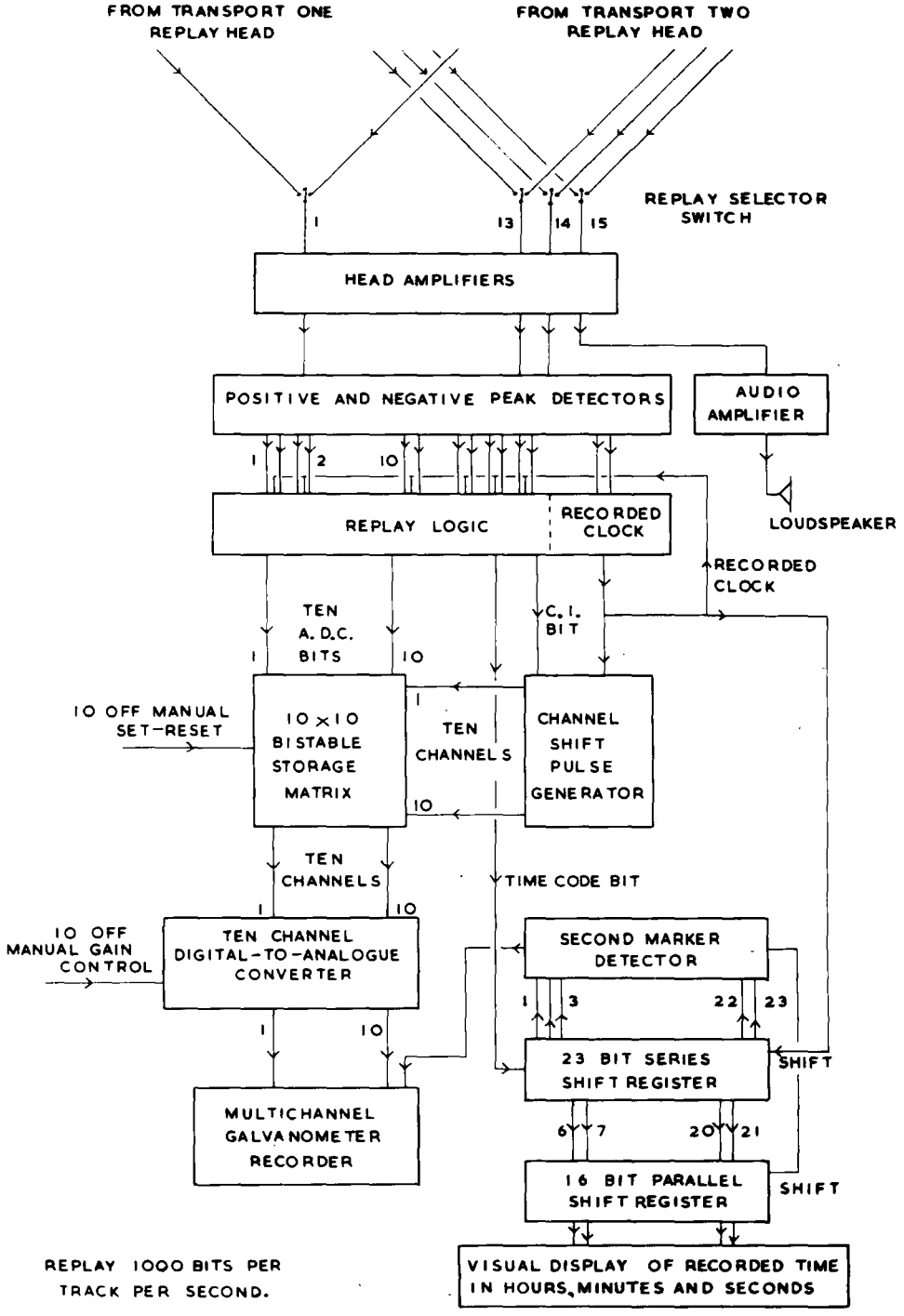

SCHEMATIC DIAGRAMS OF SEISMIC DATA PROCESSING SYSTEM

3-LABORATORY REPLAY SYSTEM

FIGURE 10

important design questions concern the methods of de-multiplexing the information and of memorizing the signal during the nine millisecond gap. If the D.A.C. output is capable of providing a large current and the load impedance is high, capacitance storage of the analogue output voltage would be possible, and one D.A.C. circuit and an analogue de-multiplexer would be required. Such a system demands that the set and reset inputs, which are needed for the individual calibration functions, be gated to the bistables by a channel counter. An alternative system is to use ten different ten-bit parallel digital storage elements so that the signal from each channel may be stored continuously in its digital form. This is equivalent logically to moving the de-multiplexer from the analogue signals to the earlier digital information, and has the advantages that digital de-multiplexing does not affect the accuracy and that the set and reset drives for the calibration of individual channels may be continuous.

The method selected, in which one hundred shift register modules are used for digital de-multiplexing, has the important virtues of great simplicity and maximum dynamic range, but these are achieved at the cost of involving a large quantity of hardware.

The head amplifiers, peak detectors, replay logic and audio channel of figure 10 use the same hardware as the field replay system, although the channel selector switch must be in its eleventh non-operative position so that all the recorded information passes through to the replay logic registers. The remaining elements of the schematic diagram are concerned either with the ten channel D.A.C. or the visual display of the recorded system time, and will be discussed in turn.

23 bit series shift register.

The contents of the time code bit replay logic FF4 is continuously passed into a 23 bit series shift register.

Second marker detector.

Any second marker is detected by an AND gate which examines the three oldest bits in the series shift register for the 101 opening phrase and the two newest bits for the 01 closure phrase.

16 bit parallel shift register.

When a second marker is detected, the contents of the sixteen stages of the series shift register, which correspond to the bits of the time word from 6 to 21 inclusive, are shifted out into a 16 bit parallel shift register.

Visual display of recorded time in hours, minutes and seconds.

The contents of the above 16 bit parallel shift register are displayed using 16 DM160 tubes. The stage of these tubes during replay is exactly the same as that of those tubes in the recording system during the corresponding second of recording, and so the system time may be determined using the tables of Appendix 2.

Channel shift pulse generator.

The field replay system includes a ten stage counter which is made up of five shift register stages and which is synchronized with the identity of the replayed channels. In the present application the same counter is used to drive ten AND gates and provide ring counter outputs which drive shift line amplifiers.

10 x 10 bistable storage matrix.

The hundred shift register storage elements represent the ten bits

of samples from each of the ten channels. The logical operation is that of a digital de-multiplexer. Each of the ten replayed A.D.C. bits drives the gate inputs of the ten registers corresponding to the particular bit in each of the ten channels, and each of the ten outputs of the channel shift pulse generator drives the common shift inputs of the ten registers corresponding to the particular channel. Thus, there are ten ten-bit parallel shift registers, and each one contains samples exclusively from one particular channel and changes its state every 10 milliseconds (for a 1 kc/s system rate).

The logical operation of the storage matrix is as described, but in fact a considerable amount of hardware is required in order to drive the hundred shift register modules. In particular, the solution to the problem of driving the gate inputs using 100 kc/s modules is expensive. Each parallel ten-bit shift register is supplied with its own manual D.C. set and reset lines for calibration purposes.

Multi-channel galvanometer recorder (Consolidated Electrodynamics).

An ultra-violet recording oscillograph with an 18 trace capacity is used. The paper width is 7 inches. The recorder runs from a 12 volt supply so that, if ever required, it could be used in the field with an accumulator. However, the power consumption is so great (up to 500 watts during switch-on) that such use would be limited. It has a range of recording speeds from 0.2 to 52 inches per minute.

The drive current to the galvanometers from the digital-to-analogue converters has a zero-order hold form (i.e. a staircase) which changes every ten milliseconds. A galvanometer always acts as a low pass filter, but it is necessary to select a natural frequency

and a degree of damping which will give a smooth response to this form of input. The problem is one of optimizing the step function response to give an approximately linear rise, which is completed in about 10 milliseconds, and a minimum of overshoot. The selected galvanometers (type 7-339) have an undamped natural frequency of 50 c/s, a terminal resistance of 30 ohms, an undamped direct current sensitivity of 4.6 amp/inch, and require a 350 ohm external damping resistance for 64% critical damping. The parallel damping circuit used (see figure 12) consists of a 250 ohm potentiometer (gain control), a 0 - 100 ohm variable resistor (damping control) and a 50 ohm fixed resistor in series. The resistance presented to earth through the galvanometer and chain of damping resistors has a minimum value of 30 ohms at maximum gain and has a maximum possible value of about 100 ohms.

Ten channel digital-to-analogue converter.

It is required to generate an analogue output to drive the galvanometer recorder from the ten bistables in each of the ten parallel shift registers. The low effective impedance ($<$ 100 ohms) and the high current sensitivity suggest the direct use of the galvanometer in a passive adder circuit as shown in figure 11.

If each bit of each ten-bit parallel shift register controls an ideal switch, then

$$i = \sum_{s=1}^{s=10} \delta_s \frac{E - ir}{Rs} ,$$

where δ_s (s = 1, 2 ... 10) equals one or zero.

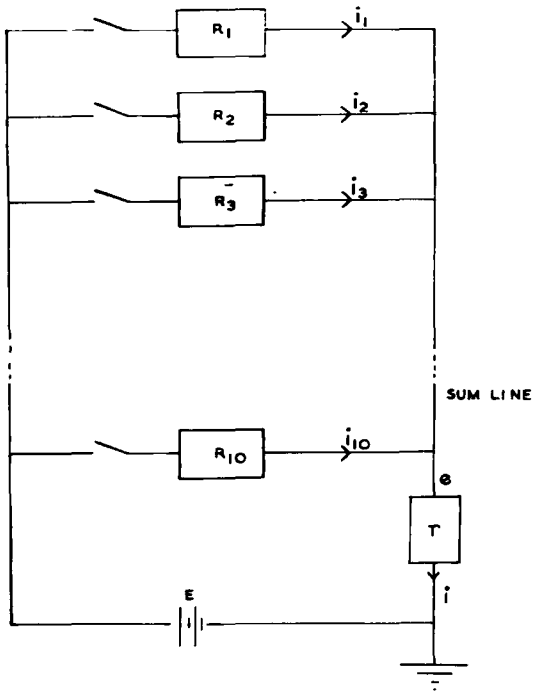

SCHEMATIC DIAGRAM OF DIGITAL-TO-ANALOGUE CONVERTER

FIGURE 11

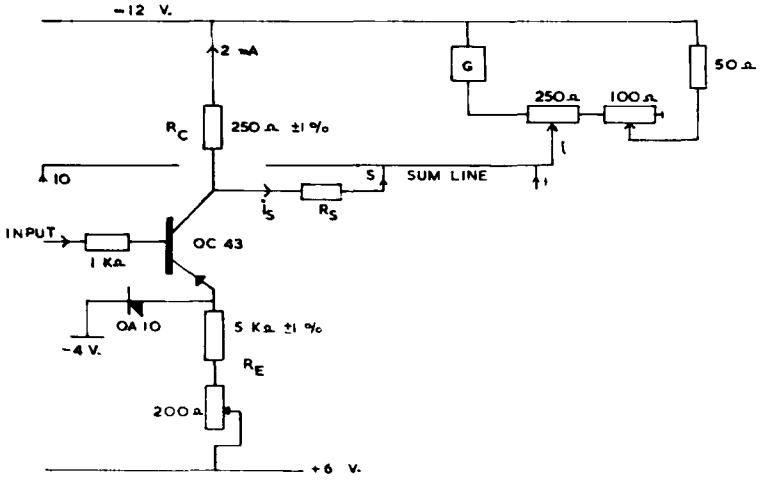

CURRENT SWITCH AND GALVANOMETER DRIVE

FIGURE 12

Therefore

$$i = \frac{E \sum_{s=1}^{s=10} \frac{\delta_s}{Rs}}{1 + r \sum_{s=1}^{s=10} \frac{\delta_s}{Rs}},$$

where, for a binary converter, $Rs = R_1 . 2^{s-1}$. The variation of the denominator from unity to about $(1 + \frac{2r}{R1})$ represents a non-linear term in the adder circuit, and it is a necessary design criterion that $R1 \gg r$. The selected values of $r \leq 100$ ohms and R1 equal to 39 KΩ give a maximum distortional error of $\pm$ 0.25 % due to this effect. This value of R1 is chosen since 20 megohms is the largest convenient value for R_{10}.

The current switch circuit, as driven by each of the matrix bistables, is shown in figure 12. In fact, the transistors each switch a constant current, which is regulated by the large emitter resistance R_E, and the switch is effectively transformed to a voltage switch by the collector load resistance, R_C. The standard switching current of a nominal 2 milliamps is a thousand times greater than the quoted typical collector current with reversed bias at the base at 25° C and 200 times the maximum figure. The setting-up procedure is to adjust the variable resistances in the emitter legs so that the voltages (as measured with a digital voltmeter) across the collector loads when the current switch is on is the same for all ten bits. The accuracy of the conversion is then controlled by the accuracy of the weighted resistors R_1 to R_{10}. Table 5 shows the values of the resistors used and the associated

Theoretical resistance in kΩ	Actual* resistance/s	Numerical error (full-scale 0-1023)
39	39 K ± 0.1%	.51
78	78 K ± 0.25%	.64
156	156 K ± 0.5%	.64
312	300 K, 12 K	.64
624	620 K, 3.9 K	.32
1,248	1.2 M, 50 K	.16
2,496	1.5 M, 1.0 M	.08
4,992	1.5 M, 3.5 M	.04
9,984	10 M	.02
19,968	20 M	.01
		± 3.06

* Tolerances ± 1% unless stated otherwise.

TABLE 5 - Digital-to-analogue converter resistors.

inaccuracy. This type of inaccuracy is important because it can produce a false discontinuity in the analogue output. However, the maximum discontinuity on passing from, say, 511 to 512 is 3 units which, for a full-scale range of 6 inches, corresponds to a deflection of only 0.02 inches.

The full-scale deflection, D_{max}, of the galvanometer, which corresponds to 1023 units, is given for a 2 milliamp switch current and R1 equal to 39 KΩ by

$$D_{max} = R_c S_{max} 10^{-7} \text{ inches,}$$

where S_{max} is the maximum galvanometer sensitivity in inches/amp.

Putting $S_{max} = 0.22 . 10^6$ and $D_{max} = 6$ inches gives a value of R_c equal to 270 ohms. In practice R_c is equal to 250Ω (± 1%).

The greatest non-linearity in the D.A.C. system will be the non-linearity of the oscillograph itself, which is said to be equivalent to an error of only 2% for a six inch deflection because of the 'square' pole piece design of the galvanometers. This error could be reduced by supplying a D.C. bias current to each galvanometer from a supply line more negative than -12 volts so that symmetrical deflections would be obtained.

Finally, a vital practical point when using the equipment is to appreciate that the galvanometer inputs are at about -12 volts and that consequently, when the D.A.C. is being set up, the insulation of the signal input side from earth must be tested before switching on, and when the galvanometer drives are to be connected or disconnected, the system must be switched off.

(ii) The paper tape replay facility.

When the galvanometer replay records have been examined, it will be decided which portions of data are to be transferred to punched paper tape for input to the digital computer. A schematic diagram of the transfer system is shown in figure 13. The speed of operation of the synchronous punch is 100 characters per second so that, for a recording system rate of 1 kc/s, a time scale expansion of 32 is required in order to supply 13-bit samples at a rate of $31\frac{1}{4}$ per second and characters for punching at $62\frac{1}{2}$ ch.p.s. This leaves an adequate margin for high instantaneous replay rates due to the distortion of replay waveforms or, for example, anomalously slow recording speeds when the recording system is run from a generator. The lowest recording speed anticipated during the design was $3\frac{3}{4}$ i.p.s. so that the lowest replay speed required on the tape transport with flux-sensitive replay is $\frac{15}{128}$ i.p.s. The paper tape format is shown in figure 15, and it represents a direct transfer of the thirteen bits of digital information recorded on the magnetic tape. The ten A.D.C. bits are numbered from one to ten in order of increasing significance. The method of changing one 13 bit word into two 7 bit words uses the coupling between the replay logic channels shown in figure 8. The first character of each sample always has a '1' in the outer track 0 and, of course, the second character has a '0' on this track except during a time code marker. This alternating sequence, which is only broken up by a second marker and which is on an outside track, helps in the handling of the paper tape since second markers can easily be seen and, if necessary, be interpreted.

The tedious task of replaying information to the tape punch is minimized by providing facilities for pre-selecting the system time at

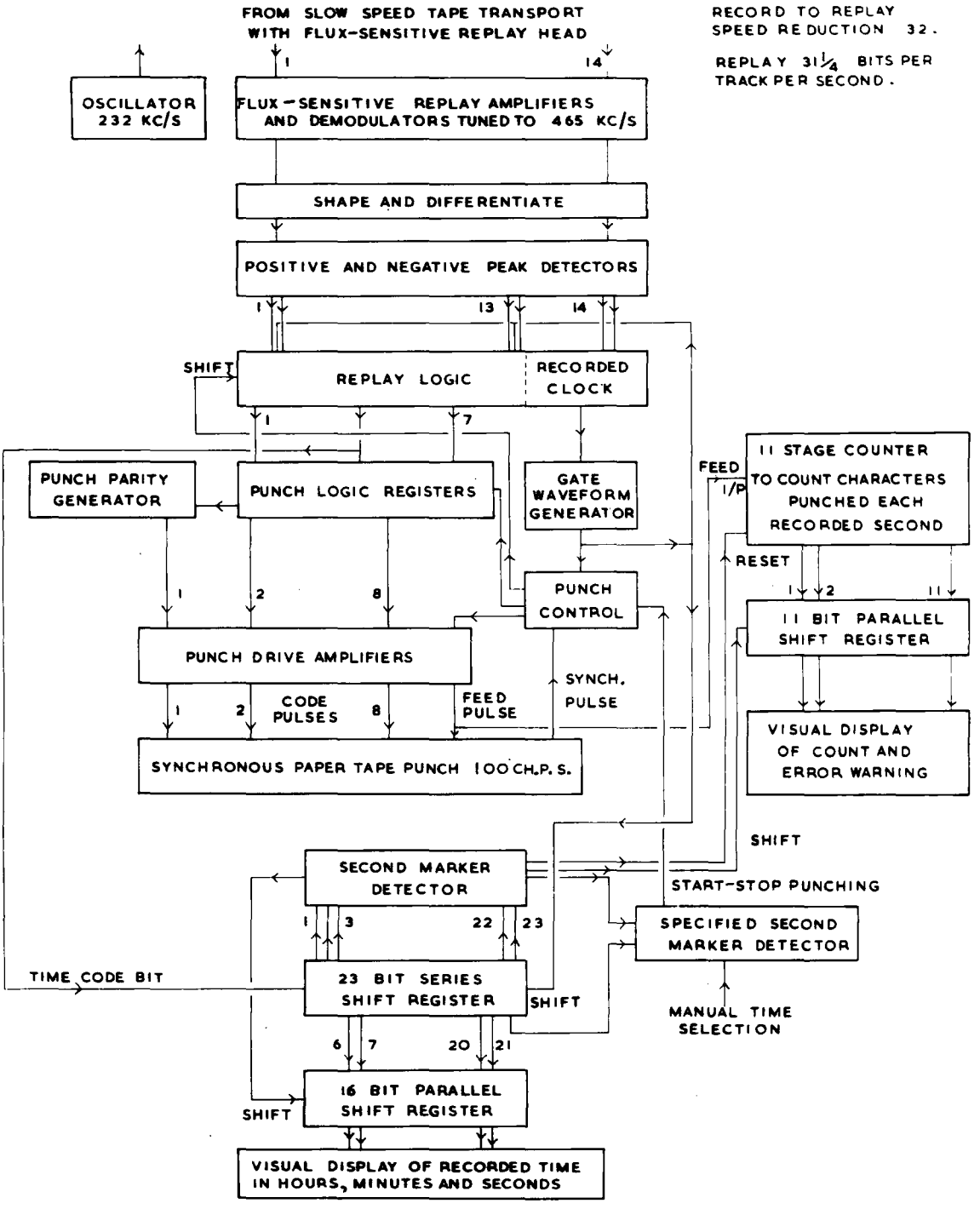

SCHEMATIC DIAGRAMS OF SEISMIC DATA PROCESSING SYSTEM

4 – PUNCH REPLAY SYSTEM

FIGURE 13

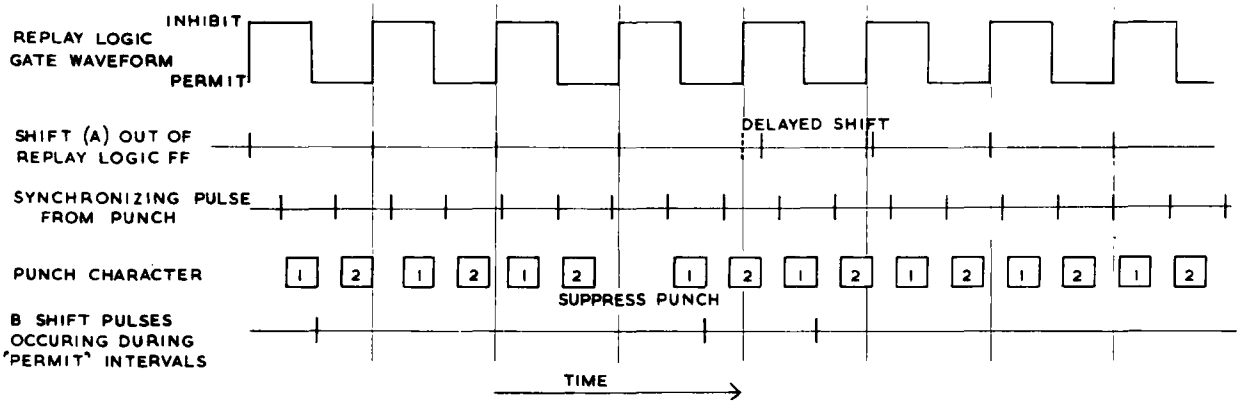

PAPER TAPE PUNCH TIMING

FIGURE 14

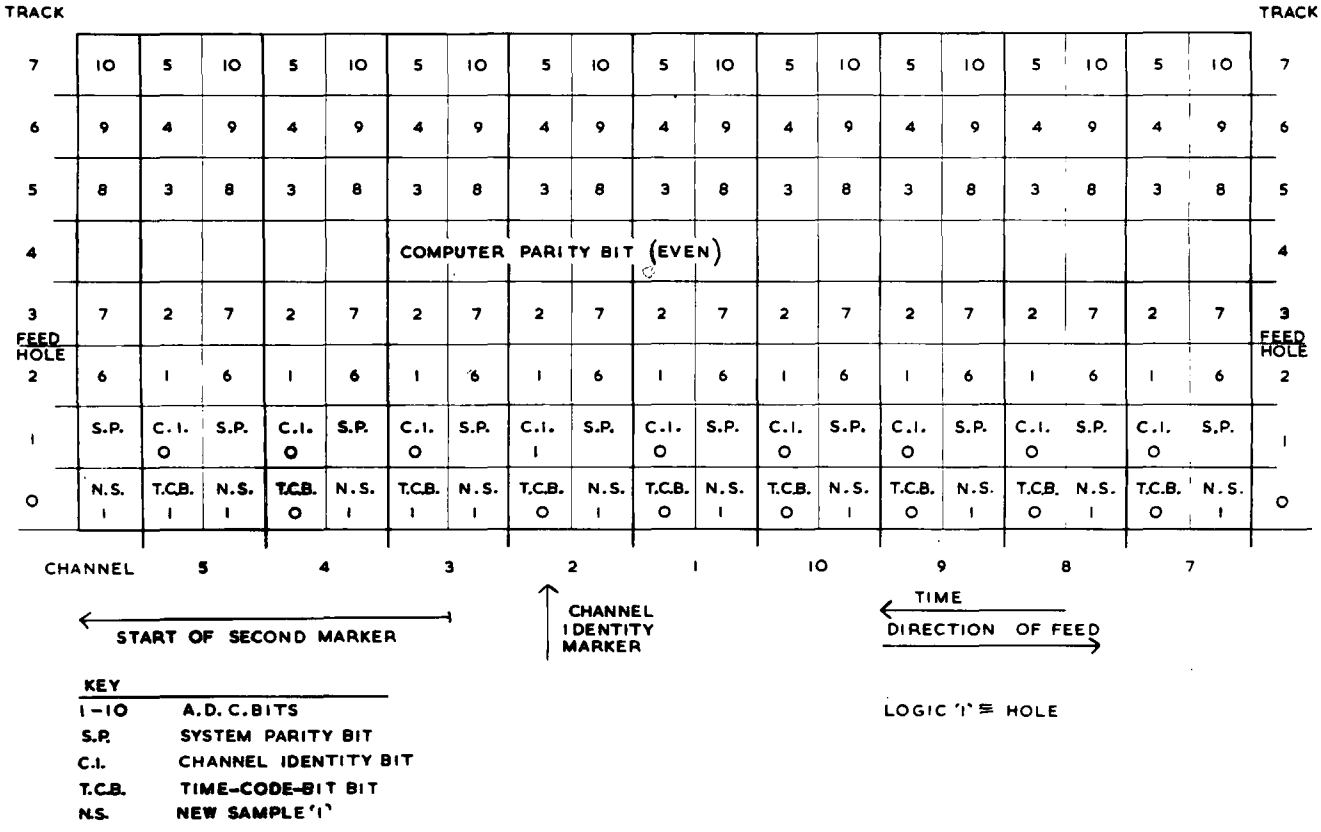

PAPER TAPE FORMAT

FIGURE 15

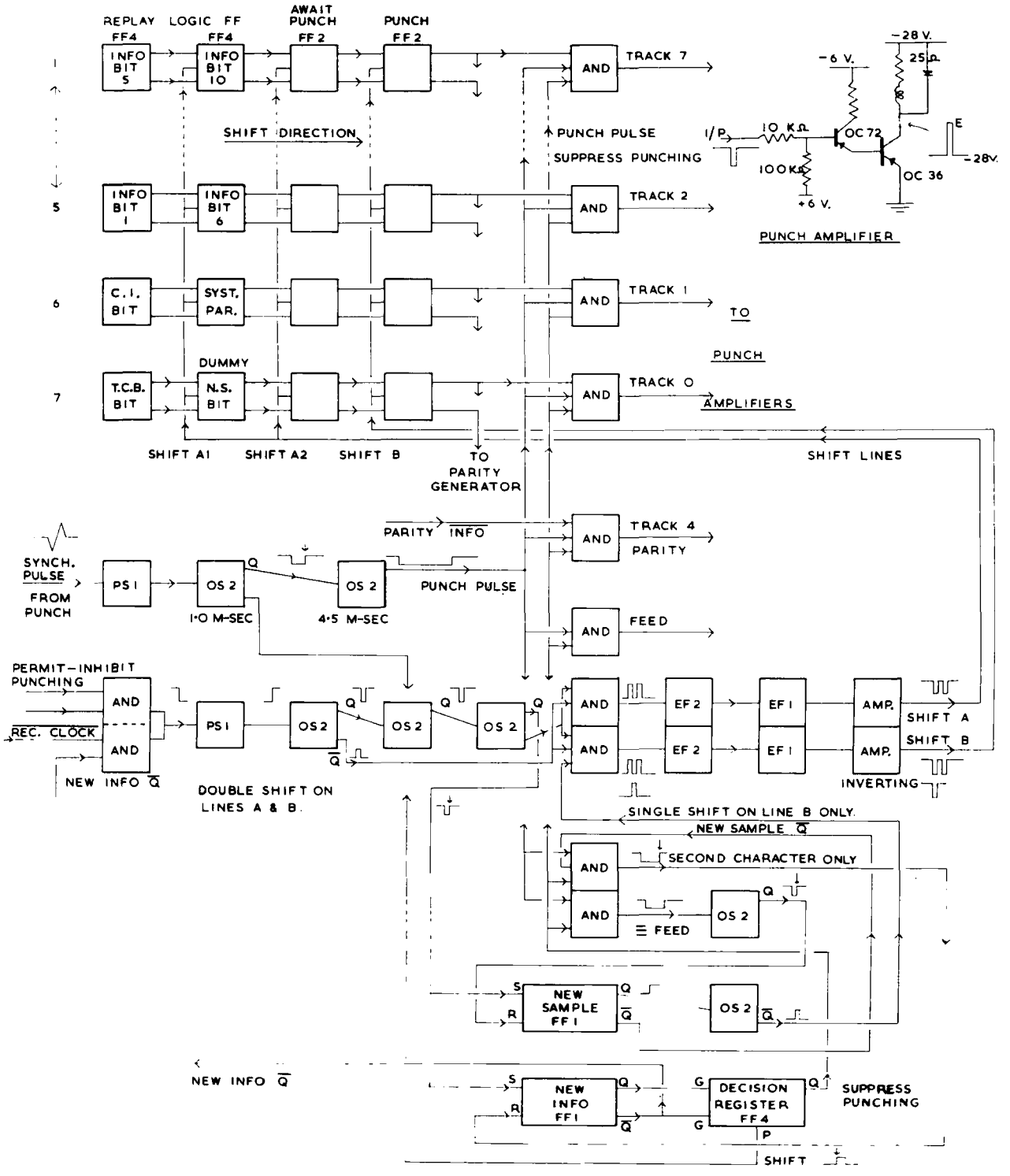

THE PAPER TAPE PUNCH DRIVE LOGIC

FIGURE 16

which it is required to start or stop punching. Since it could waste a great deal of time if tapes with serious errors are produced and taken to the digital computer, a check is provided by counting the number of characters punched per recorded second, and if this number is incorrect, a warning light comes on and the punching can, if required, be stopped automatically.

Consider the problem of supplying information from the digital replay logic to a synchronous punch which generates synchronizing pulses at 100 p.p.s. Assume that pairs of replay logic registers, which correspond to two tracks on the digital magnetic tape, form parts of 4 bit series shift registers as shown in figure 16. Information may be shifted up two bits from the replay logic registers to the 'await punch' and 'punch' registers by applying two shift pulses to lines A1, A2 and B, and may be shifted from the 'await punch' registers to the 'punch' registers by one shift pulse on line B. When it is required to punch the second character of the sample, a shift pulse is applied to line B only, because it is possible that by this time the replay logic AND gates will be open again (see figure 14) and the replay logic registers may have already assumed the states associated with the next sample. If a shift pulse is applied to lines A1 and A2 in these circumstances, this information would be shifted prematurely and would be lost. A second point is that the contents of the replay logic registers should not be shifted into the 'await punch' and 'punch' registers as soon as the replay logic gates close because it is possible that the second punch cycle may still be taking place and that the information in the 'punch' register is still required (see figure 14). The solution is to shift

this information either when the replay logic AND gates close or at the end of the second punch cycle, whichever is latest.

Consider the elements of the schematic diagram (figure 13) in turn. The peak detectors and the replay logic use the same hardware as the field replay system; the second marker detector, the 23 bit series shift register, the 16 bit parallel shift register and the visual display of system time use the same hardware as the galvanometer replay system. The new elements of the block diagram are as follows:-

Slow speed tape transport.

This deck, which has speeds from $\frac{15}{128}$ i.p.s. to 15 i.p.s., is fitted with a special head for flux-sensitive replay and with a record head since it is intended that the deck could be used in the field shot point system if necessary. Both heads have 16 tracks on 1 inch tape to SBAC spacing.

Flux-sensitive replay amplifiers and demodulators tuned to 465 kc/s.

Oscillator 232 kc/s.

The type of flux-sensitive head made by M.S.S. (Noble, 1963) uses a gapped-ring modified so as to permit the reluctance of the ring to be switched between a high and a low value at a high frequency. The flux being driven round a ring by the magneto-motive force of the recorded signal is therefore 'chopped' at the switching rate, and the signal flux is converted to a fixed frequency alternating flux whose amplitude is proportional to that of the recorded signal. The two windings on each track are an oscillator winding and a 'read' winding giving an amplitude modulated output at twice the oscillator frequency. The output of the read winding is amplified and demodulated to give the

flux-sensitive signal output.

Shape and differentiate.

Gate waveform generator.

The outputs from the commercial replay electronics are passed through single stage amplifiers to 100 kc/s pulse shaper modules, whose outputs are differentiated, thus simulating the conventional replay process. This hardware occupies the same printed circuit rack locations as are otherwise occupied by the conventional replay head amplifiers, and these boards drive the same peak detector and replay logic boards, although, because of the problem of the significant apparent skew, the recorded clock waveform does not drive the logic gate inputs directly, but is used to generate a delayed gate input of controlled duration using two monostables in series. This gate waveform generator has to be modified if the time scale expansion factor is altered.

Synchronous paper tape punch 100 ch.p.s.

The Teletype high speed tape punch for transistor operation requires code and feed pulses of 1 amp, 28 volts and 4.5 millisecond duration, and it is able to operate with simultaneous feed and code pulses. The synchronizing output pulse is generated by a magnetic pick-up, and the timing of this pulse relative to the mechanical operation of the punch is fully adjustable.

Punch drive amplifiers.

The circuit used to supply the feed and code pulses from logic AND gate outputs is shown in figure 16.

Punch parity generator.

The generation of parity bits for the 7 information bits of each

punched character is shown in figure 7.

Punch logic registers.

Punch control.

The problem of supplying information to a synchronous punch has already been considered. The paper tape punch drive logic is shown in figure 16. Three control bistables are used to detect the end of the second punch cycle (new information FF1), to distinguish the first and second punch cycles of a sample (new sample FF1), and to store the decision concerning the availability of new information at the time of the synchronization pulse (decision register FF4). The arrival of each synchronization pulse initiates the same chain of logic (the logic punch cycle), but the action is different depending on whether there is no new information available for punching, or whether the available information is the first or second character of a sample. The action of this 'logic punch cycle' and of the entire punch control system is considered in appendix 3.

Specified second marker detector.

The system time at which it is required to start or stop punching may be set up on 18 two-way centre-off switches which represent the time code bits from number 4 to number 21 inclusive. The specified time is detected by an 18 input OR gate driving a bistable which is connected to a permit-inhibit punching input of the double shift pulse generator (see figure 16).

11 stage counter to count characters punched each recorded second.

An eleven stage 'divide-by-2000' counter with feedback from the final stage to the fifth and sixth stages is reset when a second marker is detected and counts the number of punch feed pulses. The

reset state of this counter is

1 0 1 1 1 1 1 1 1 1 1 .

11 bit parallel shift register.

The contents of the above counter is moved into an eleven bit parallel shift register on the completion of each recorded second.

Visual display of count and error warning.

The outputs of the eleven bit parallel shift register and the output of the permit-inhibit punching register are displayed on DM160 tubes, so that the value of each count is displayed for about 32 seconds. Because of the nature of the coupling between the magnetic tape replay and the punch (see figure 14), it is permitable for 1999, 2000 or 2001 characters to be punched between successive outputs of the second detector, although the average over a number of consecutive seconds must tend to 2000. Hence the three acceptable states of the parallel shift register are

0 0 1 1 1 1 1 1 1 1 1 ,

1 0 1 1 1 1 1 1 1 1 1 ,

and 0 1 1 1 1 1 1 1 1 1 1 .

The occurrence of these three states is detected with AND gates, and is used to suppress the output of a red error-warning lamp.

The final points to be made about this mode of replay are that a 930 foot reel of tape costs about six shillings and can store 55 seconds of recorded data.

(iii) Some further remarks about the hardware

The descriptions of hardware in this thesis have been given in general terms and have not considered the practical day-to-day problems

that occur during the design, construction and testing of such systems. The purpose of this section is to present a few photographs which show the end products of this work. A pre-amplifier board and its case are shown in figure 17. Figure 18 shows a rear view, with the dust covers removed, of the digital recording system. The three small boards carry the ramp comparator circuit, the 2 mc/s oscillator, and the A.D.C. parity generator. The large boards carry, in descending order, the A.D.C. logic and control, the crystal clock divider chain, the generators for the time code, parity and channel identity bits, and, fourthly, the tape write logic and drive amplifiers. The more usual method of construction with a rack holding 28 printed circuit boards is illustrated in figure 19. In the foreground are shown a 2 mc/s module (cylindrical), a 100 kc/s module, a printed circuit board and a penny. In fact, the right hand half of this rack holds the replay logic and field monitoring boards, while, in the laboratory, the left hand half holds the punch drive and control logic.

The field system, which is installed in a caravan, is shown in figures 20, 21 and 22. The right hand cabinet of figure 21 contains, from top to bottom, the main digital recording chassis of figure 18, the chassis containing the D.C. voltage stabilizers, the line input chassis with gain controls and the wideband amplifier, and the analogue switch. The lowest chassis of the left hand cabinet contains the replay head amplifiers and peak discriminators, and additional power supplies are located in the bottom of this cabinet. Figure 22 gives a rear view of these two cabinets with the rear doors removed. Figure 20 shows the unstabilized power supply chassis, situated beneath the left hand cabinet, and a further case containing two radios and the rack which contains the replay logic and the field

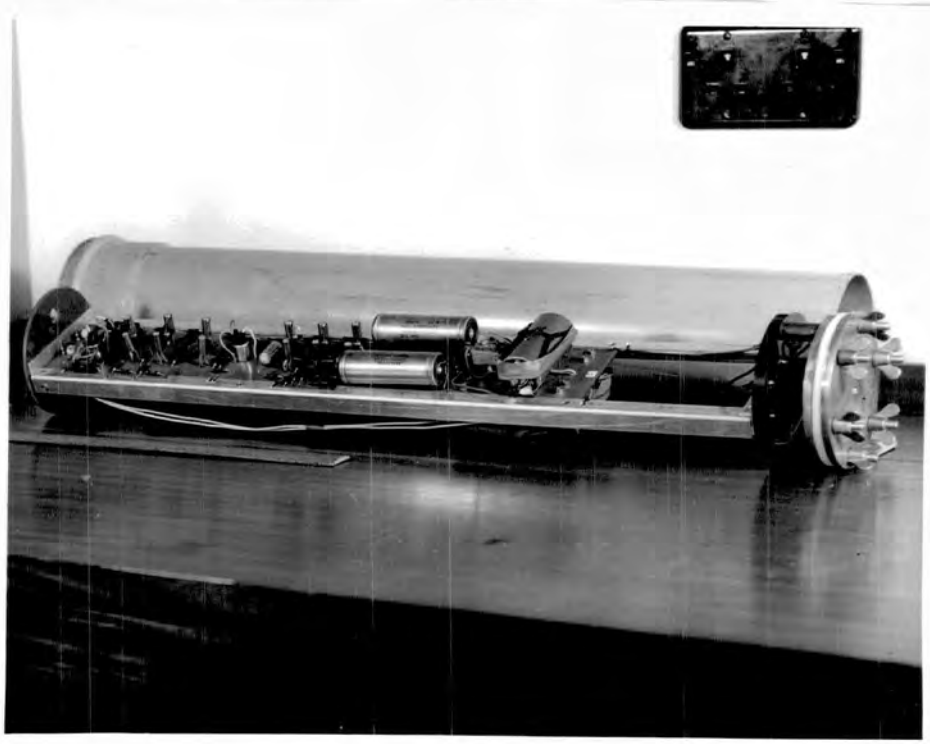

Figure 17 A pre-amplifier and case

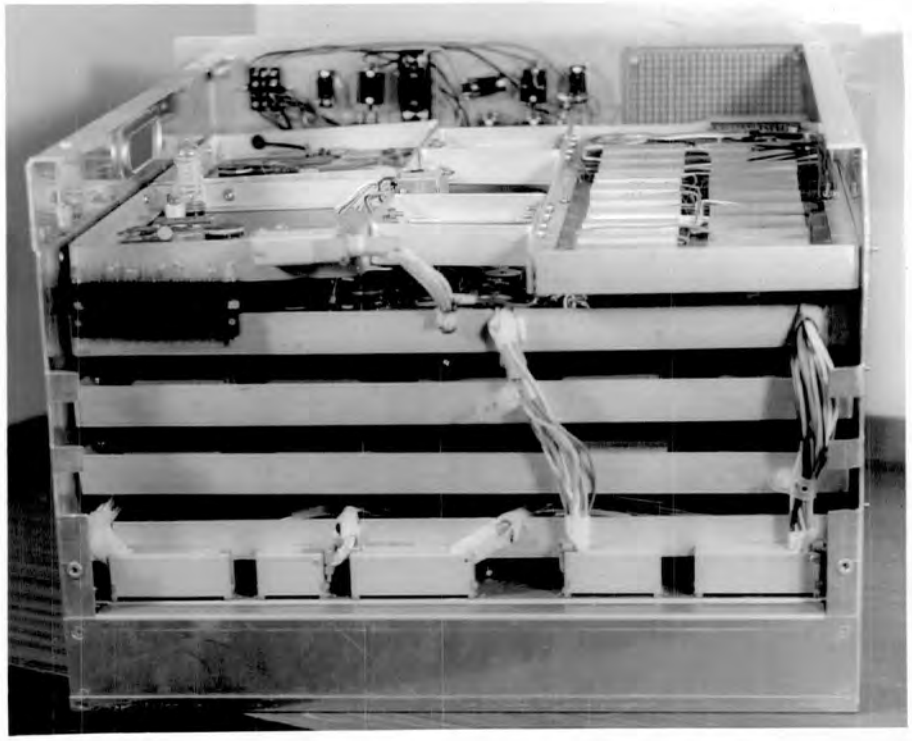

Figure 18 A rear view of the digital recording chassis

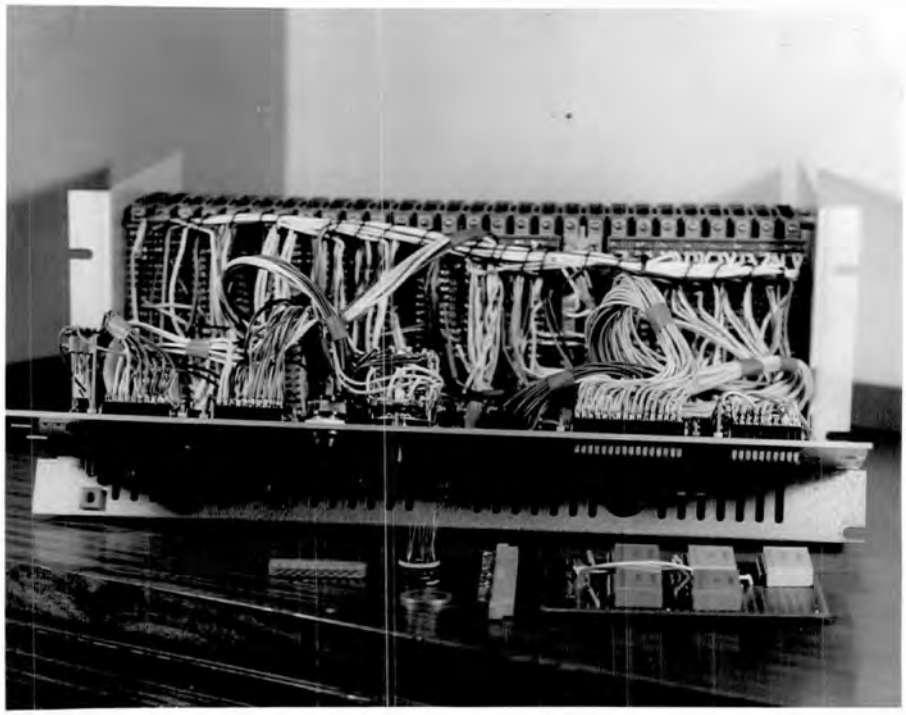

Figure 19 Construction using printed circuit boards

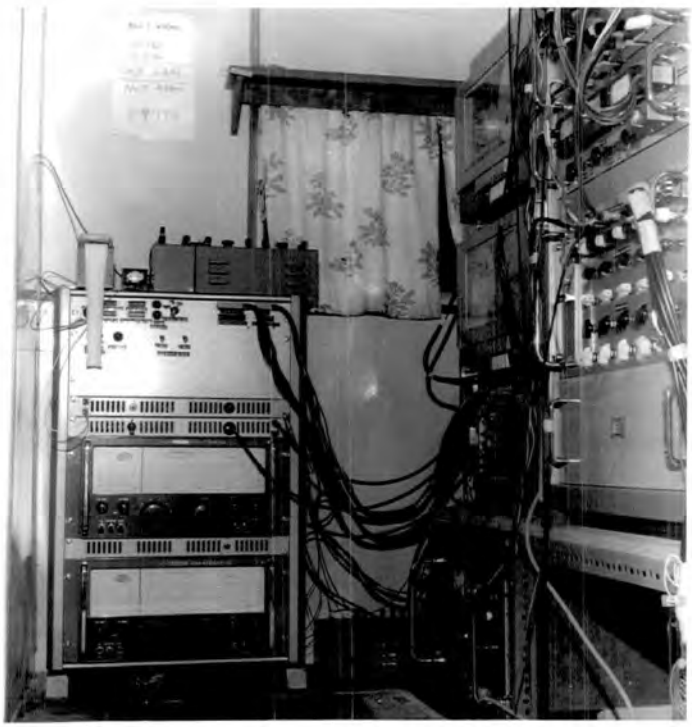

Figure 20 The field system

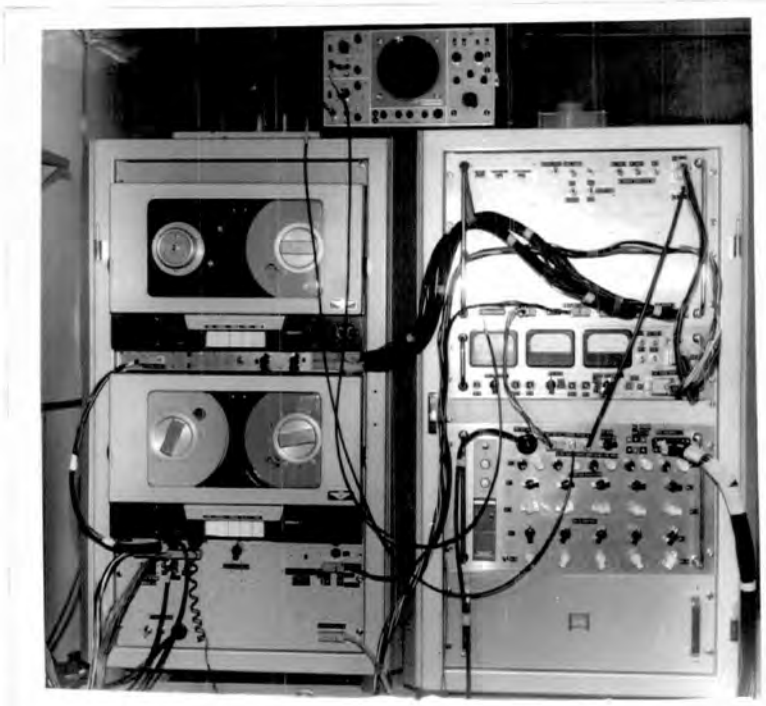

Figure 21 The two main cabinets of the field system

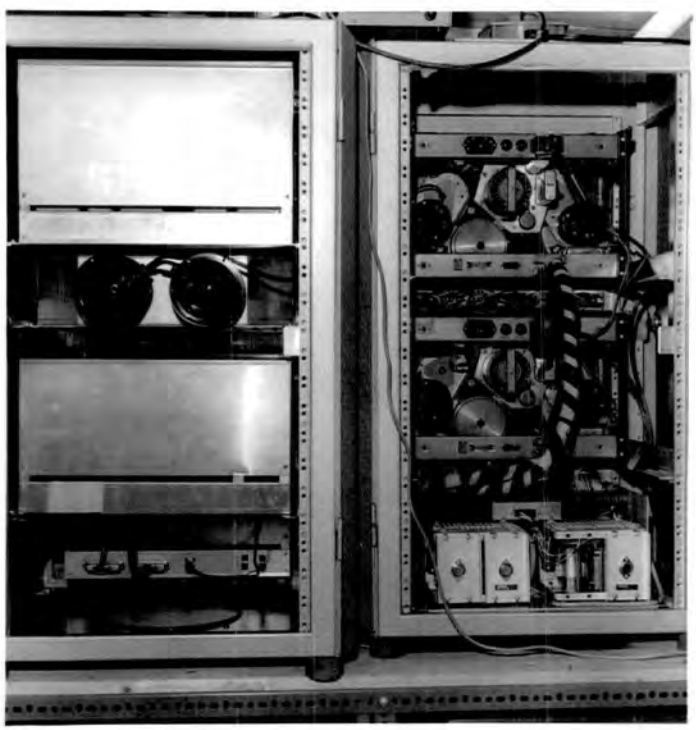

Figure 22 A rear view of the main cabinets

Additional hardware for laboratory replay - 1

Figure 23

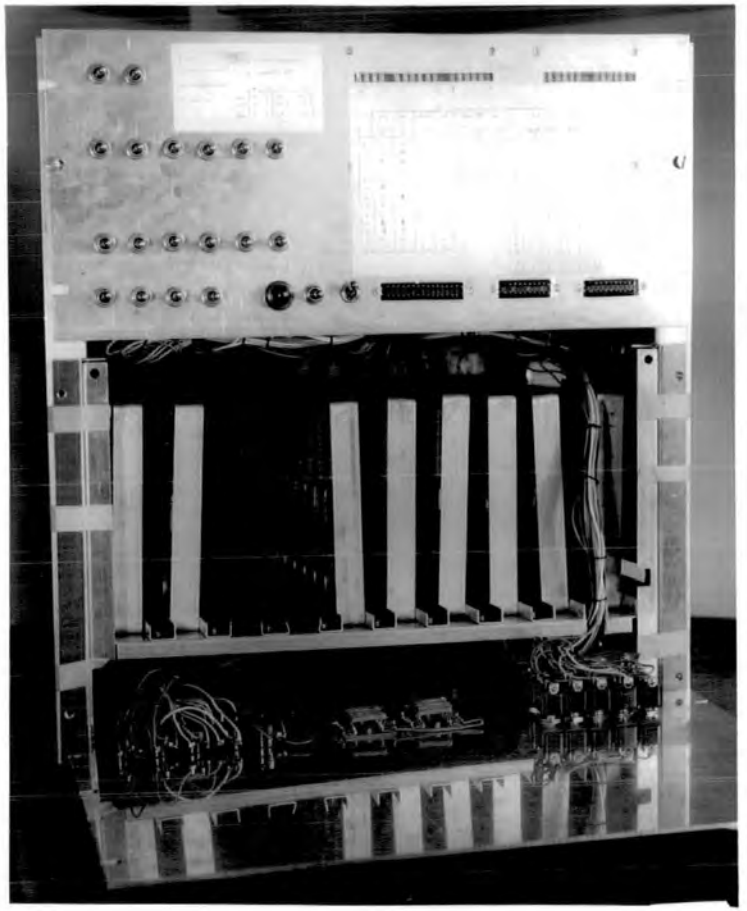

Additional hardware for laboratory replay - 2

Figure 24

monitoring system (see also figure 19).

Figure 23 shows the same rectifier chassis as figure 20, the chassis which contains the flux-sensitive replay electronics and the tape punch power amplifiers and the -28 volt power supply, the low speed tape deck, and, on top of the cabinet, the galvanometer recorder. The lower part of the chassis shown in figure 24 shows eight of the ten D.A.C. channels and the ten gain controls and set-reset switches on the front panel, which is lying flat in the photograph. The damping controls and the outputs to the galvanometers are located on a rear member. The front panel of the upper part shows the tubes which display the replayed system time and the number of characters punched per recorded second, and also the switches for setting up the time when punching is to start or stop.

(iv) The velocity filtering calculation

Assuming a recording system sampling rate of 1 kc/s, each channel, p, is sampled a hundred times each recorded second at nominal times

$$s_o + p + 10n \text{ milliseconds},$$

where s_o is a fixed integer and n is a variable integer. Define a 'second block' of data to be a sequence of a thousand consecutive samples of the digital system commencing at the completion of a twenty-three bit serial time code word. Such a block should contain a hundred samples from each of the ten channels, and the recorded data may be considered to be a sequence of such blocks. The first sample of a 'second block' corresponds to a time of 23 milliseconds relative to the start of the time code word or to the state of the system crystal clock dividers corresponding to an integer number of seconds.

Let s be the channel of this first sample, and define a (p) such that

$$a(p) = 1 \text{ if } p < s$$
$$= 0 \text{ if } p \geqslant s \ .$$

Then, within a 'second block' of data, channel p is sampled at times (relative to the onset of the time code word) of

$$23 - s + 10 \times a(p) + p + 10 \times n \text{ milliseconds}$$
$$\text{where } 0 \leqslant n \leqslant 99 \ ,$$

and this sample will be stored in the computer in an array element

$$AA\ (k + a(p) + n,\ p)$$

where k is an arbitrary integer constant.

During the velocity filtering programme it is required to determine the value of n corresponding to the sample of channel p nearest in time to some time $(t_{GRID} + t_p)$, where t_{GRID} is one of a regular set of time ordinates and t_p is the delay corresponding to the particular channel p for a particular array configuration, tuning velocity and azimuth. Define the corresponding value of n by

$$n = n_{GRID} + n_p \ .$$

The term n_{GRID} is not necessarily an integer, but, if it is an integer, then each value of n_p is a constant and there is a considerable saving of computation. Also, increments of n_{GRID} will be restricted to factors of a hundred, so that computation times within different 'second blocks' are identical. Thus calculations will only be performed at intervals of 10, 20, 40, 50 milliseconds.

In order to find a required sample it is necessary to minimize the function

$$t_{GRID} + t_p - 23 + s - 10.a(p) - p - 10\,(n_{GRID} + n_p)\,,$$

where n_{GRID} and n_p are integers.

Since the time of onset of a time code word is to be a grid point, find n_p for $n_{GRID} = t_{GRID} = 0$ by minimizing

$$t_p - 23 + s - 10.a(p) - p - 10.n_p$$

for an integer value of n_p .

Thus,

$$n_p = (\text{entier}\,\tfrac{1}{10}\,(s - 18 - p + t_p)) - a(p)$$

where t_p is the delay time of channel p in milliseconds and the function entier (x) is defined to be the greatest integer less than x. The required minimization is obtained by adding a half to the expression within the entier function. If a calculation is carried out at a grid time T defined by

$T = 10\ ml$ milliseconds, for an integer value of m, where 101 is the time, in milliseconds, between adjacent grid points, then the required sample of channel p will be stored within the 'second block' in the location

$$AA\ (k + (\text{entier}\,\tfrac{1}{10}\,(s - 18 - p + t_p)) + ml,\ p)$$

provided that $0 \leq ml - a(p) + \text{entier}\,\tfrac{1}{10}\,(s - 18 - p + t_p) \leq 99$.

In the velocity filtering calculation the ten channels are divided in some specified manner into two groups of five, and the following two functions are formed at each grid point denoted by ml :-

$$RED\ (ml) = \sum_{j=1}^{j=5} \text{gain}\ (p).\ AA\ (k + m_p + ml,\ p)$$

and

$$BLUE\ (ml) = \sum_{k=1}^{k=5} \text{gain}\ (p).\ AA\ (k + m_p + ml,\ p)\,,$$

where $m_p = \text{entier}\,\tfrac{1}{10}\,(s - 18 - p + t_p)$.

The two output functions used are

$$\text{ADD (ml)} = \text{RED (ml)} + \text{BLUE (ml)}$$

and $$\text{MULTIPLY (ml)} = (\text{sign of FF})\ (\text{square root of } |\text{FF}|)$$

$$\text{where FF} = \text{RED (ml)} \times \text{BLUE (ml)}.$$

The function MULTIPLY (ml) is therefore an un-normalized, unsmoothed cross correlation function between the two sums RED and BLUE. Denote the maximum and minimum algebraic values of n_p or $(m_p - a(p))$ by the identifiers MAX and MIN. Then, given one 'second block' of data, the functions ADD and MULTIPLY can only be completed for values of ml such that

$$\text{ml} + \text{MAX} \leq 99 \quad (\text{MAX} \geqslant 0)$$

and $$\text{ml} + \text{MIN} \geqslant 0 \quad (\text{MIN} \leqslant 0).$$

Introduce the following notation;

let m_0 be the first grid point to depend on data in this 'second block',

let m_3, equal to $m_0 + \frac{100}{1}$, be the first grid point to depend on data in the next 'second block',

let m_2 be the last grid point to depend on data from the previous 'second block',

and let m_1, equal to $m_2 + \frac{100}{1}$, be the last grid point to depend on data from this 'second block'.

Then, the velocity filtering calculation for each 'second block' of data is divided into three sections as follows:-

from m_0 to m_2 - complete calculations started with data from the previous 'second block',

from m_{2+1} to $m_3 - 1$ - perform complete calculations,

and from m_3 to m_1 - start calculations which will be completed when data from next 'second block' is available.

The computer programme used for carrying out these calculations will be described in the next section.

(v) The digital computer programmes.

The sequence of programmes used for processing the seismic data on an Elliott 803 computer with film handlers is shown schematically in figure 25. The data on the punched paper tape is read in and checked a recorded 'second block' at a time. It is stored within the computer in the array shown diagramatically at the top of figure 26, and is then transferred to the film store.

The velocity filtering programme for each 'second block' of data has to be divided into three parts in the manner described in the previous section. The problem may be handled on the computer either by testing each sample for availability and inhibiting the calculation if the sample is unavailable or, since the combination of samples is additive, by setting unavailable samples to zero and carrying out an unmodified calculation. The method of processing adopted here is to place the 'second block' of data in the middle of three consecutive 'second blocks' with the two end 'second blocks' set to zero (see figure 26), and to carry out unmodified calculations. Such a system avoids testing the availability of each required sample but of course involves extra additions of dummy samples.

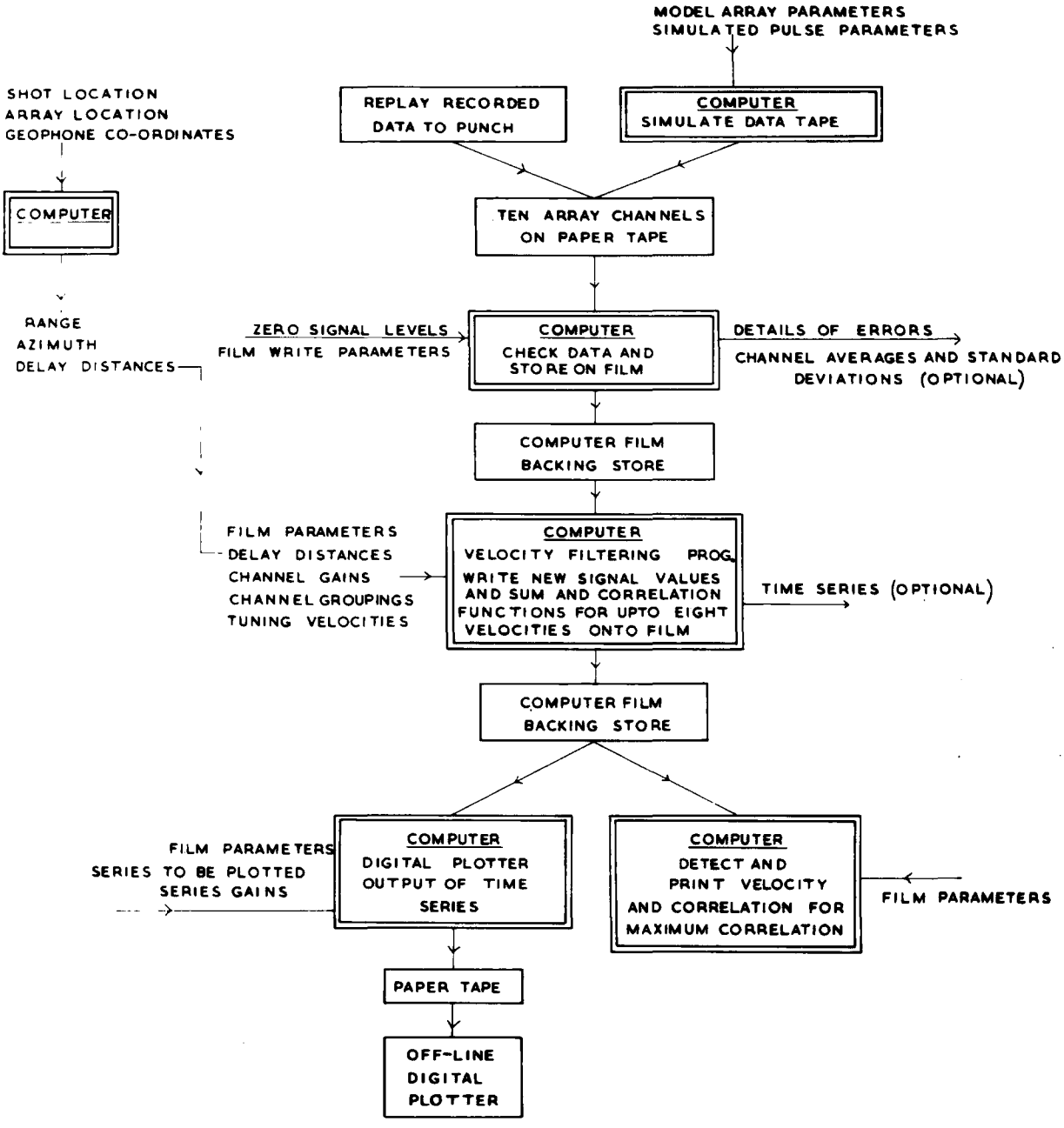

SCHEMATIC DIAGRAMS OF SEISMIC DATA PROCESSING SYSTEM

5 – PROCESSING THE DATA USING A DIGITAL COMPUTER

FIGURE 25

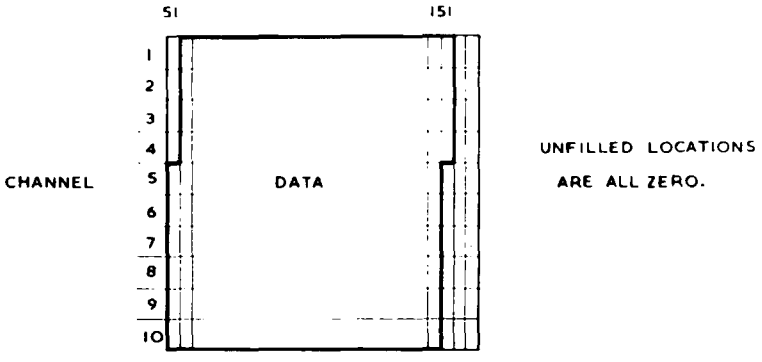

PROGRAMME ONE – THE STORAGE ARRAY AA[51:153,1:10]

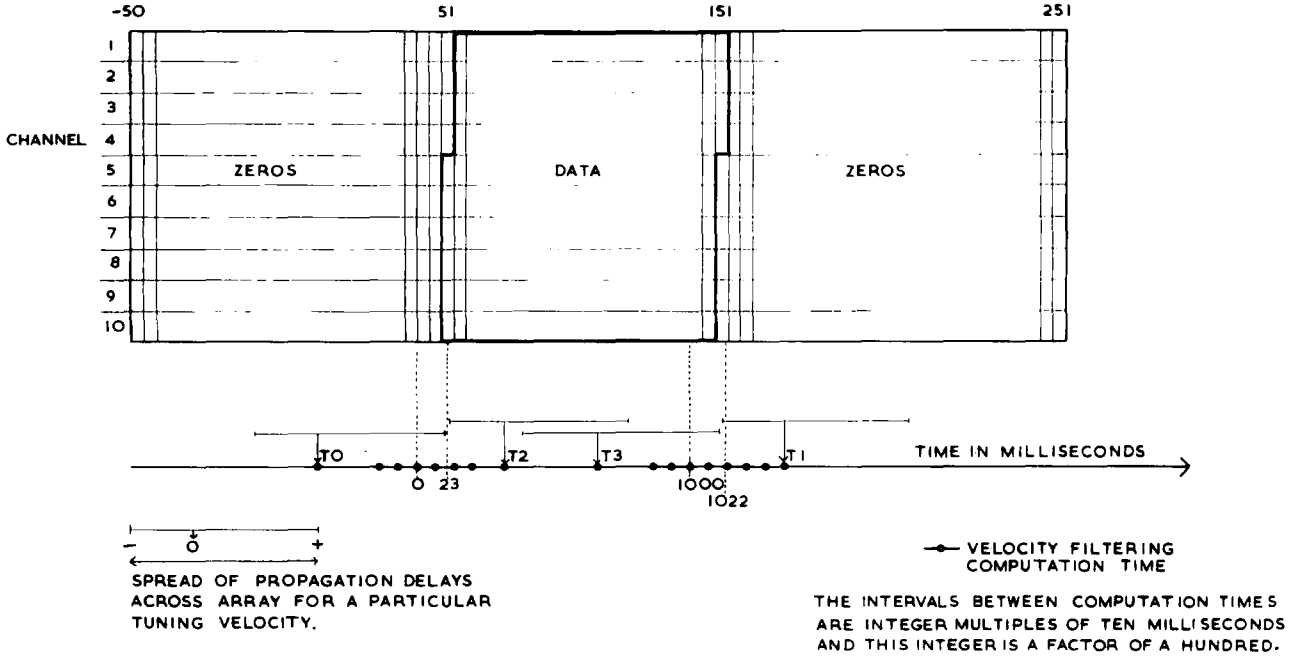

PROGRAMME TWO – THE PROCESSING ARRAY AA[-50:251,1:10]

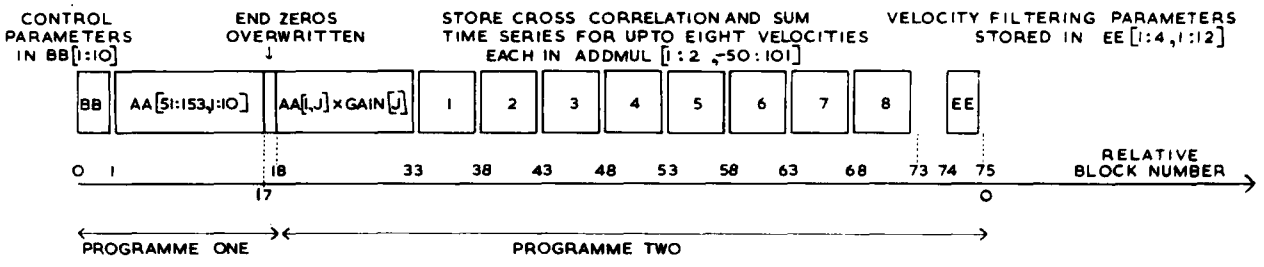

COMPUTER FILM STORAGE FORMAT

THE STORAGE OF ONE SECOND OF RECORDED DATA IN THE COMPUTER

FIGURE 26

It is increasingly efficient for smaller seismic array spreads and for higher tuning velocities when the proportion of dummy samples used is low. The values for m_0 and m_2 are calculated simply and in such a way that they err on the safe side, in the sense that an error will occur if a calculation, which is supposed to be completed within the 'second block' of data, is not completed, but an error will not occur if one, which is supposed not to be completed, is in fact finished.

The velocity filtering programme reads a 'second block' from the film, carries out the channel gain multiplication and writes the result on to film, and then performs calculations for up to eight tuning velocities with the other parameters constant. The results for each tuning velocity are written on to film. The film storage format is also shown in figure 26. The arrays BB and EE store the necessary control data such as the system time, the channel identity of the first sample, the tuning velocities, or the values of T_0 and T_2 .

The delay distance of each channel, for a given array location and configuration and a given shot location, is calculated by assuming a plane incident wave at the array site. This approximation can introduce errors for short range shots and large out-of-line arrays.

A programme entitled 'graph plotter output' has been written to display elegantly the results of the velocity filtering calculation on an off-line Benson-Lehner digital plotter. This output displays the ADD or MULTIPLY functions for the different tuning velocities against time, but, although it is an attractive output to use, it does not constitute a practical system because a paper tape character has to be punched for each increment of pen movement and the output of the considerable quantity of paper tape from the computer takes too long.

Consequently, programmes ('miniature graph plotter output' and 'miniature frame') have been written to give a smaller plotter output of the MULTIPLY function only.

An alternative programme ('maximum correlation') selects the velocity at each grid point for which the function MULTIPLY is greatest. The interpretation of this function of the unsmoothed, un-normalized time series obviously requires great care, and it is really intended that this programme be just the first step in the development of programmes for the numerical detection of correlations.

Finally, in order to test this data handling system, a programme is used to produce punched paper tape which simulates that generated by the array system for the case of a square pulse crossing a model array.

The above programmes together with specimen data tapes and flow diagrams are included in the appendices. They are written in the Elliott Algol programming language, but contain machine code orders for the manipulation of bits of information. Also machine code instructions are used in some of the inner loops for inserting and extracting elements of arrays in the manner indicated in appendix 4. This is worthwhile because the addressing facility in Elliott Algol is particularly slow. However, the use of machine code in Algol does mean that one has not got the test facilities that are usually regarded as essential for pure machine code programmes, and also one loses the built-in safeguards of Algol. Even so, in this type of application, machine code in Algol is certainly preferable to trying to use pure machine code. The two precompiled packages used with these programmes are briefly described in appendix 5.

The programme for reading the punched paper tape has an optional

facility for finding the averages and standard deviations of each channel during a second block. The output obtained, with channel zero levels of 100p, using test data generated in the A.D.C. of the field recording system is shown in figure 27. Error messages are usually produced at the start of a reel of punched paper tape before channel identity is established. In order to test the computing system, a paper tape was produced to simulate a square pulse of 50 millisecond duration crossing an in-line array with geophone spacings of 300 metres at a velocity of 6 km/sec. The graph plotter outputs of the signal inputs and the sum and cross correlation functions for velocities of 4, 5, 6, 7, 8 and 9 km/sec. are shown in figures 28, 29 and 30. The interval between adjacent computation points is 20 milliseconds. The form of the output correlation functions is complicated by the high frequency component of the signal inputs and by the fact that the duration of the pulse is not an integer number of computation intervals, but it can be seen that the maximum correlation amplitude occurs for the third tuning velocity. These graph plotter outputs demonstrate the successful combination of data from two 'second blocks' and illustrate the fact that as the tuning velocity increases, so the number of calculations that can be completed within a 'second block' also increases. The corresponding output produced by the 'miniature graph plotter output' and 'miniature frame' programmes is shown in figure 31, and figure 32 shows the equivalent output of the 'maximum correlation' programme. Figure 33 shows the cross correlation function for a computation interval of 10 milliseconds, using a slightly different velocity filtering programme from that used in producing figure 30.

```
Second marker found
TCB shift register =      00000000000000010110001111000000000001
M =       100CIRING =         2      DELTA CI =         0
Second error register =          0
CI error register =         0
TCC =      2086
ISC =      2000
Perfect second
```

		n	Mean	Standard Deviation
Channel	1	100	923.00	0.00
Channel	2	100	-200.00	0.00
Channel	3	100	723.00	0.00
Channel	4	100	-400.00	0.00
Channel	5	100	523.00	0.00
Channel	6	100	-600.00	0.00
Channel	7	100	323.00	0.00
Channel	8	100	-800.00	0.00
Channel	9	100	123.00	0.00
Channel	10	100	-1000.00	0.00
	325	342		

PROGRAMME ONE OUTPUT WITH TEST DATA.

```
Second marker found
TCB shift register =      00000000000000001010000000000000000001
M =       100CIRING =         4      DELTA CI =         0
Second error register =          0
CI error register =         0
TCC =      2076
ISC =      2000
Perfect second
```

		n	Mean	Standard Deviation
Channel	1	100	21.35	97.42
Channel	2	100	21.45	97.86
Channel	3	100	21.35	97.42
Channel	4	100	21.30	97.20
Channel	5	100	21.20	96.77
Channel	6	100	21.00	95.90
Channel	7	100	22.90	108.54
Channel	8	100	20.25	92.63
Channel	9	100	22.20	101.13
Channel	10	100	23.45	106.58
	100	117		

PROGRAMME ONE OUTPUT WITH SIMULATED DATA.

Figure 27 Programme One output

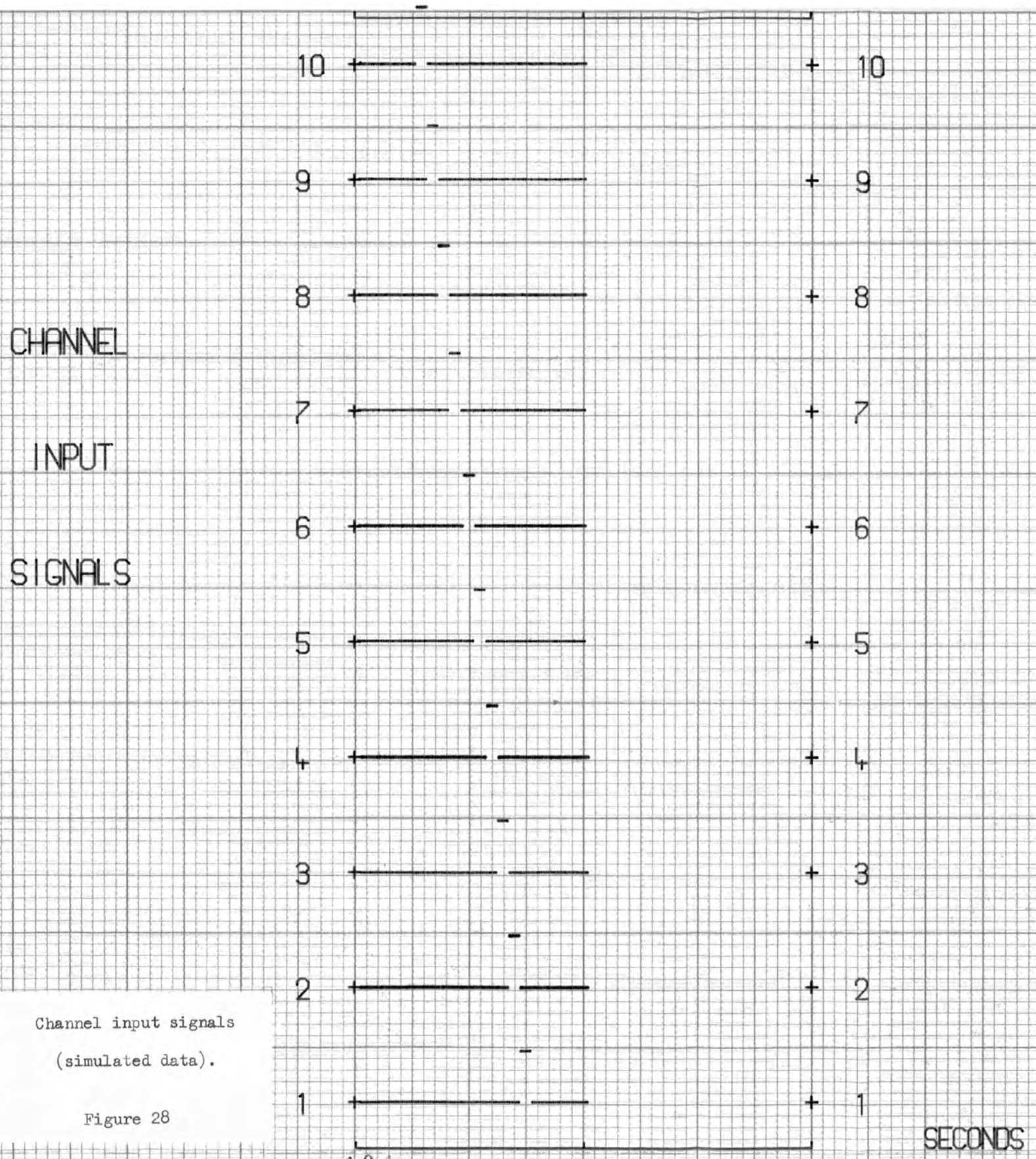

Channel input signals

(simulated data).

Figure 28

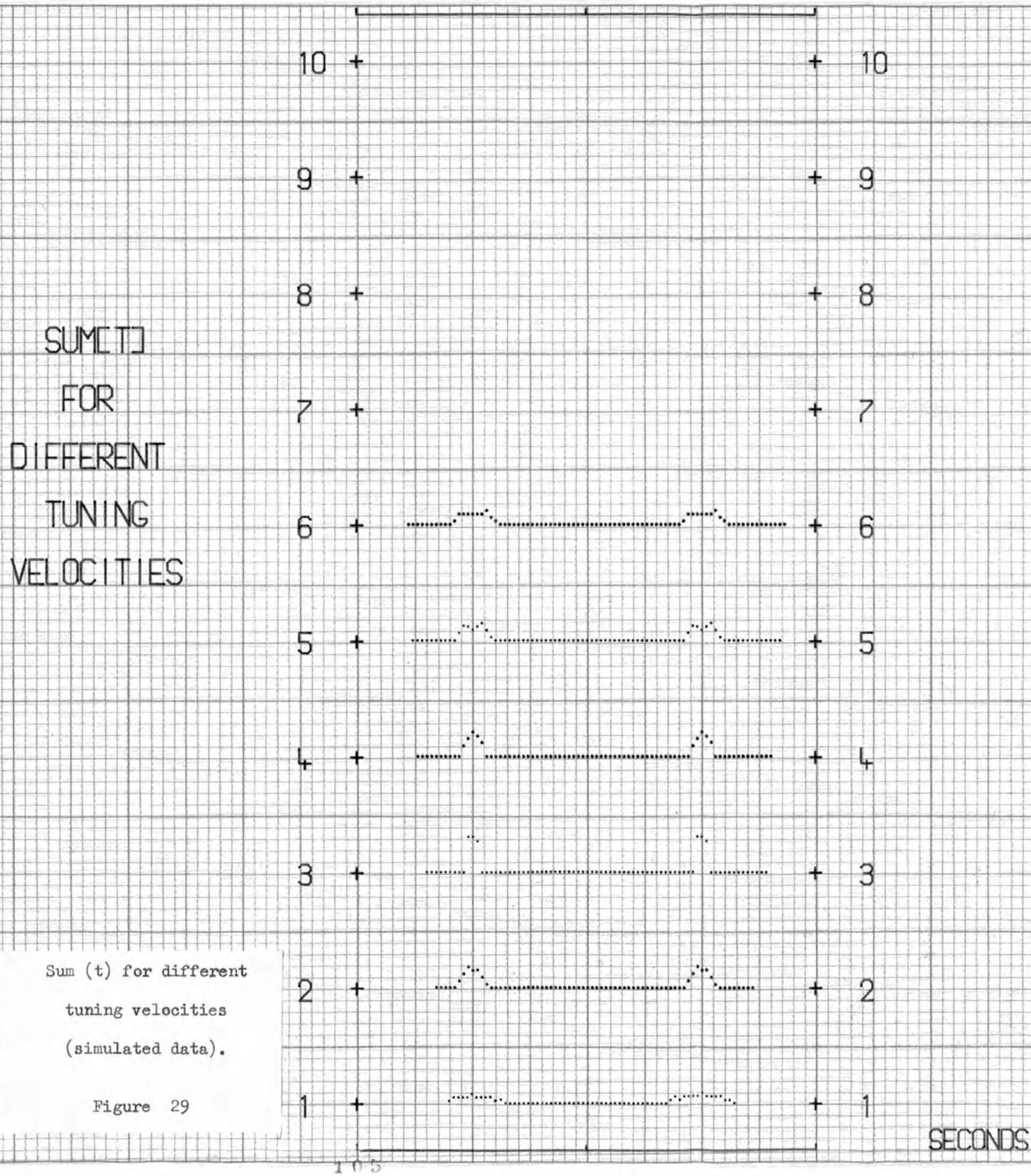

Sum (t) for different tuning velocities (simulated data).

Figure 29

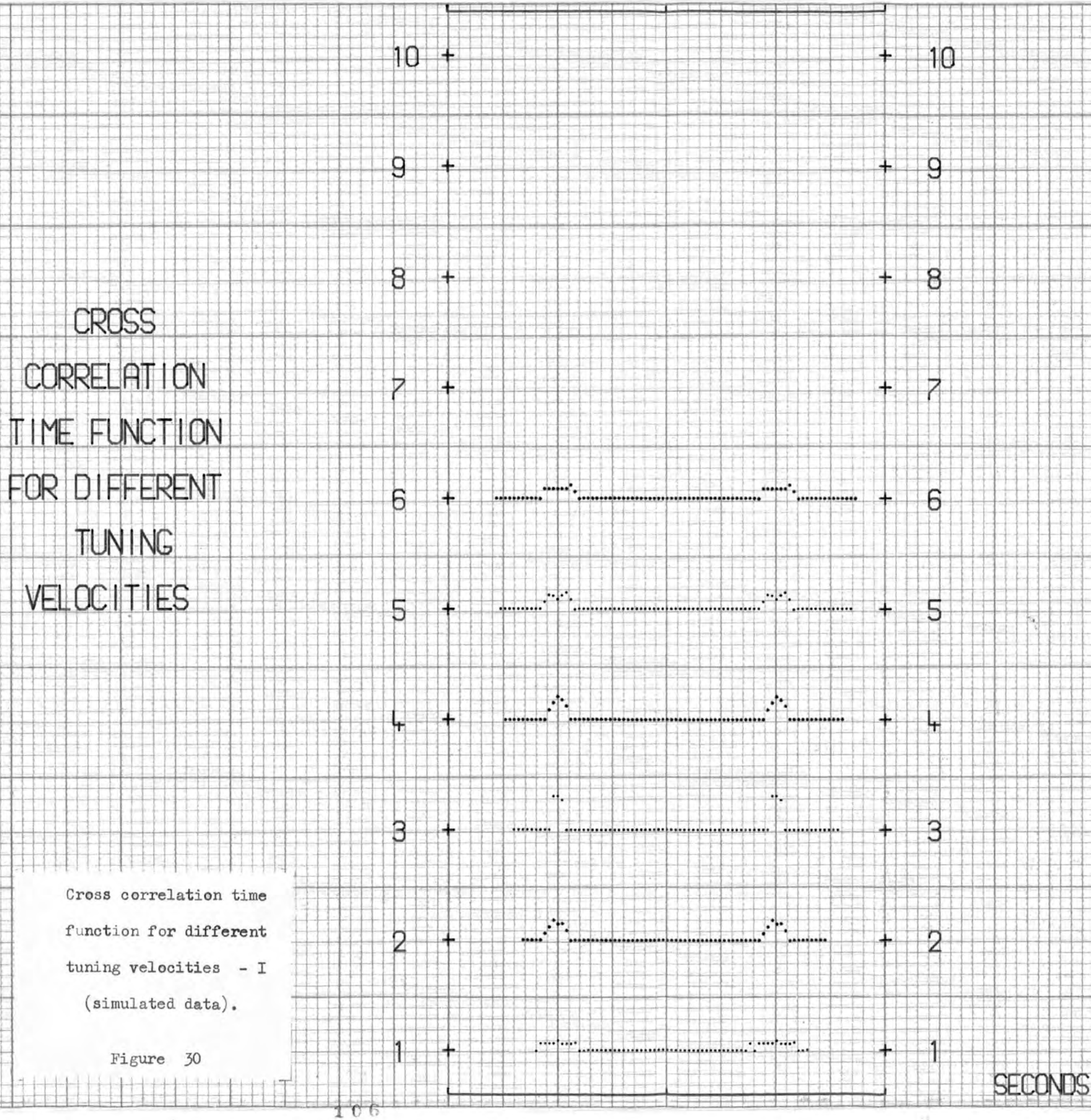

Cross correlation time function for different tuning velocities - I (simulated data).

Figure 30

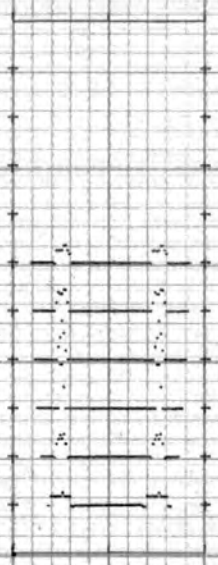

Figure 31 - Miniature graph plotter output.

```
velocities
  4.00
  5.00
  6.00
  7.00
  8.00
  9.00

  2    5   2    5   1  442   1  442
  1  441   6  645   5  932   3 2269   3 2269
  4 1331   5 1089   6  628   1  471   2    5
  2    5   1    5   1    5   1    5   1    5
  1    5   1    5   1    5   1    5   1    5
  1    5   1    5   1    5   1    5   1    5
  1    5   1    5   1    5   1    5

second marker1010000000000000000001   1    5
  1    5   1    5   1    5   1    5   1    5
  1    5   1    5   1    5   1    5   1    5
  1    5   1    5   1    5   1    5   1    5
  1    5   2    5   2    5   1  442   1  442
  1  441   6  645   5  932   3 2269   3 2269
  4 1331   5 1089   6  628   1  471   2    5
  2    5

End of program

Reinput tapes 1 and 2
```

Figure 32 Maximum correlation output for simulated data.

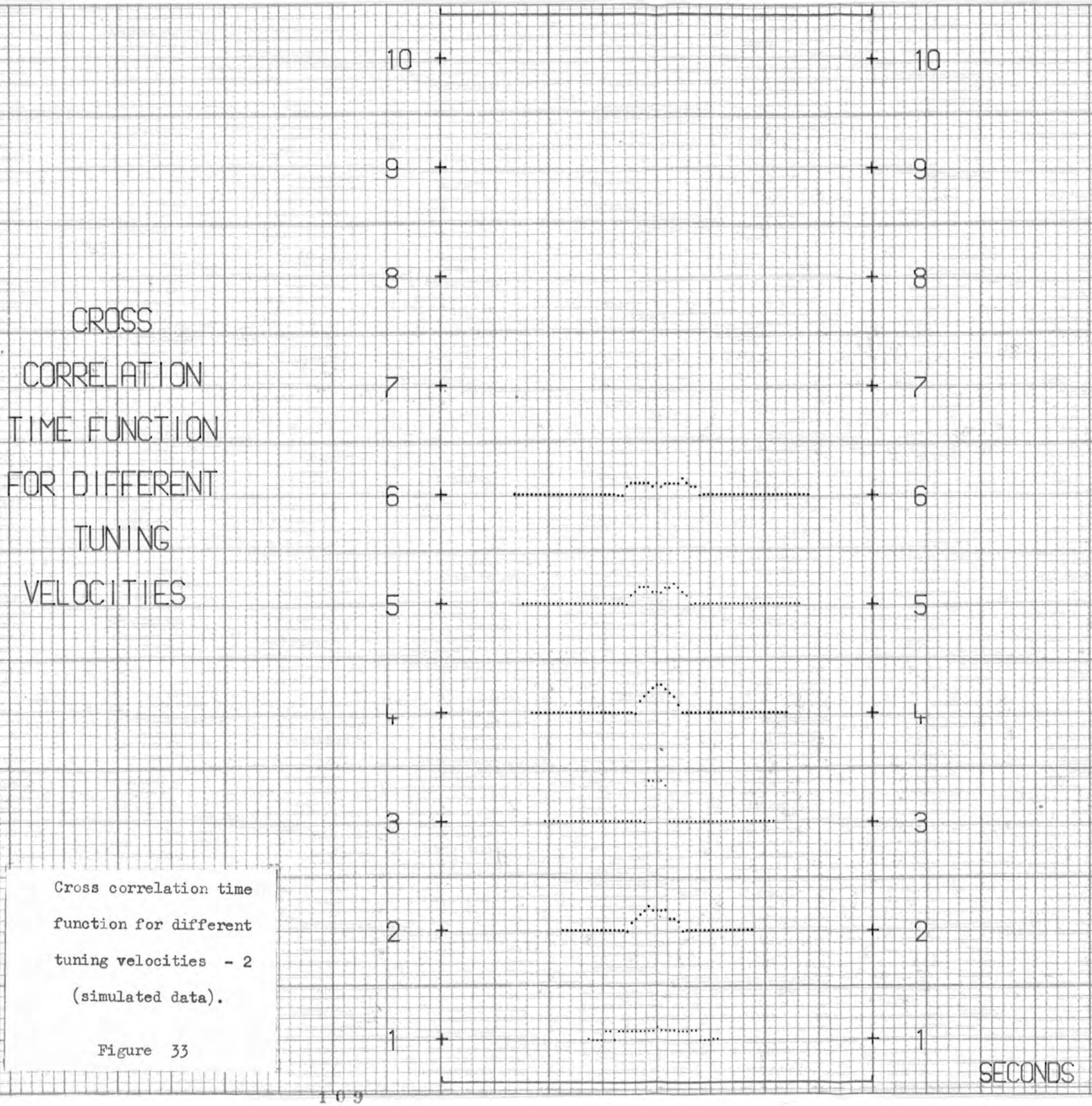

Cross correlation time function for different tuning velocities - 2 (simulated data).

Figure 33

The programmes include various optional facilities so that the running times can vary considerably. The time taken by 'programme one' to read and check a 'second block' of data and calculate the channel averages and standard deviations is nine minutes. The time taken by the velocity filtering programme depends on the computation interval and, for the first or last 'second blocks' of a continuous sequence, on the extreme delay times which are a function of the tuning velocity. For a computation interval of 20 milliseconds the programme takes about four minutes per second per velocity. It took a total of 75 minutes to produce the paper tape to plot figures 28, 29 and 30.

CHAPTER 5

THE PERFORMANCE OF THE SYSTEM

(i) Introduction

The purpose of this chapter is to review the performance of the system described in the previous chapters. The present limitations of the system will be indicated and future developments will be suggested. Thus, although the hardware for the three basic functions is fully operational, the equipment is not presented as forming a perfect or a completed system.

(ii) The operation of the data systems in the laboratory

The correct operation of equipment is frequently verified by the normal day-to-day tests that are carried out during the development of a system. The occurrence of a fault condition should be immediately obvious provided that sufficient monitoring facilities have been built into the system. The purpose of this section is to present evidence to show the correct operation in the laboratory of the three basic systems, which will be considered in turn:-

(a) The recording system.

An important factor in the recording system is the performance of the ramp comparator analogue-to-digital converter. Mention will be made of a particular series of measurements in which the analogue switch was removed and a variable D.C. voltage was applied to the input of the wide band amplifier. The applied voltage was adjusted so that the digital A.D.C. output was stable and the input voltage to the A.D.C. was noted on a digital voltmeter. A series of twelve such readings

for input voltages over the range from +3 volts to -3 volts were obtained. Since it was possible to get a constant digital output, this experiment indicates that the inherent noise level of the converter is something less than the truncation error of $\pm \frac{1}{2}$ bit. Also, it gives an indication of the possible combined effects of non-linearity and drift, because the measurements took about forty minutes to complete and when the first measurement was repeated at the end, there was a difference of 2 bits. A 'least squares' analysis of the form

$$(\text{input voltage}) = A \cdot (\text{output count}) + B$$

gave A equal to 0.008882 volts with a standard error of 0.000013 volts and B equal to -4.003 volts with a standard error of 0.006 volts.

In general the correct operation of the recording system is demonstrated by the corresponding correct output of the two replay systems.

(b) The galvanometer replay system.

Figure 34 shows the galvanometer record for a sine wave recorded on all ten seismic channels and replayed at minimum D.A.C. gain. Figure 35 shows one of the same channels replayed at maximum D.A.C. gain and also the RESET and SET levels corresponding to 0 and 1023. The time code trace is the output of the coarse code detector which is set to identify 'second' markers.

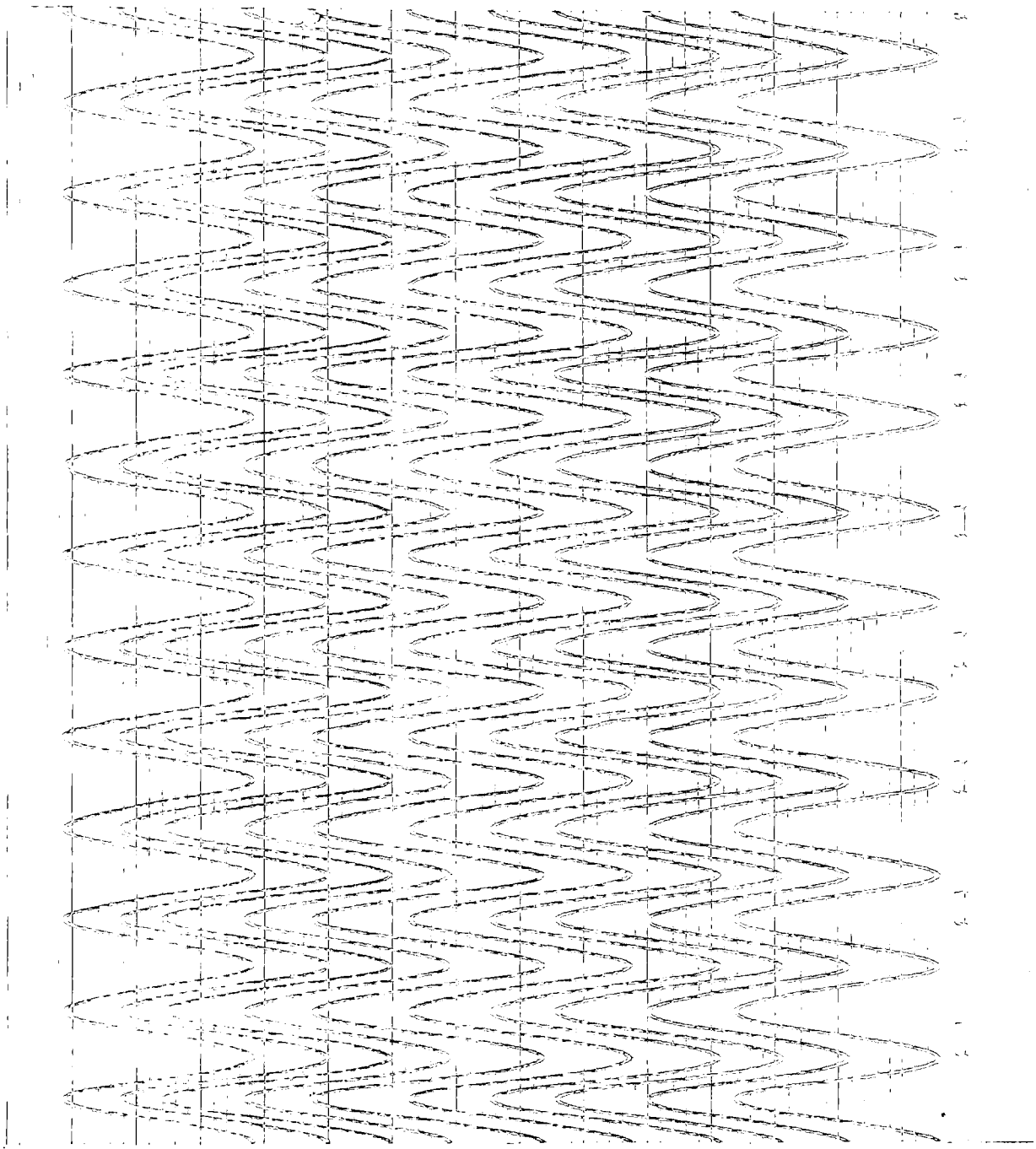

Figure 34 Galvanometer replay at minimum D.A.C. gain.

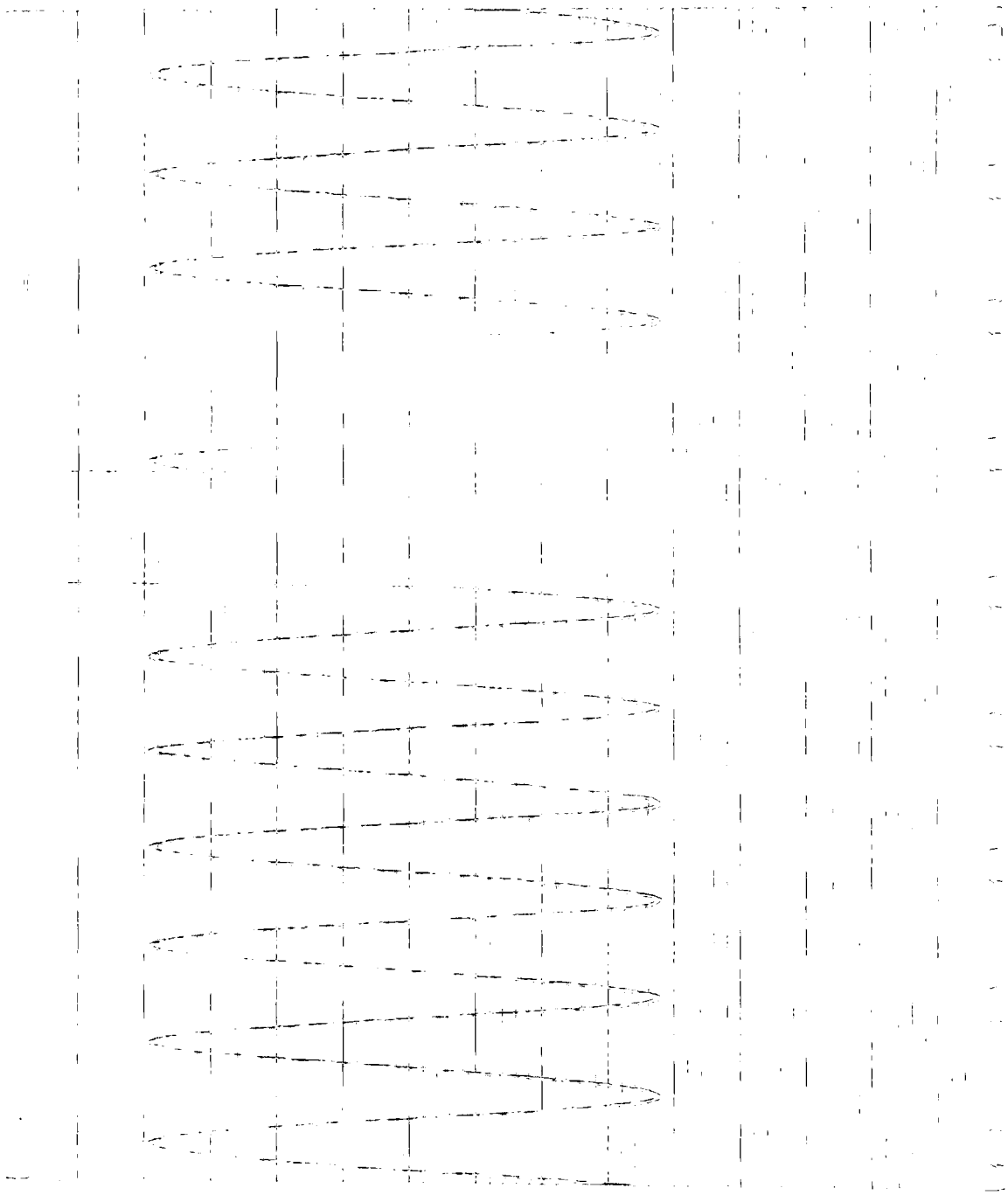

Figure 35 Galvanometer replay at maximum D.A.C. gain.

(c) The paper tape system and computer programmes.

The successful operation of the punch replay system is demonstrated by the 'programme one output with test data' (figure 27) which uses data originally formed in the output registers of the A.D.C. The operation of the velocity filtering programme is shown with simulated data in figures 28, 29 and 30 and also in figure 33 for which a slightly different version of the programme was used.

The limiting factor in the use of these systems at the present time is the speed of the data processing on the Elliott 803 which, as has been indicated, is so slow that even for the most elementary velocity filtering calculations, the use of the system is severely inhibited. It is the basic speed of this particular general purpose machine for relatively simple operations that is the trouble, and not the use of paper tape.

(iii) The recording system in the field

The recording system was set up in September, 1965, at Feldon Range, near Richmond, Yorkshire, during a depth charge experiment organized by the seismological groups at Edinburgh and Birmingham to determine the nature and thickness of the Earth's crust between Wales and Ireland. A map of the array is shown in figure 36. The central reference point of the array is taken to be located at 54° 26.40' N, 1° 49.55' W. The equipment was powered by a mains generator fitted to a Land Rover. The system was recording for a total of 23 hours and at the times of twenty-one of the twenty-five shots fired. The ranges and azimuths of these twenty-one shot points from the array varied from 260 kilometres to 370 kilometres and from 219° to 245° respectively.

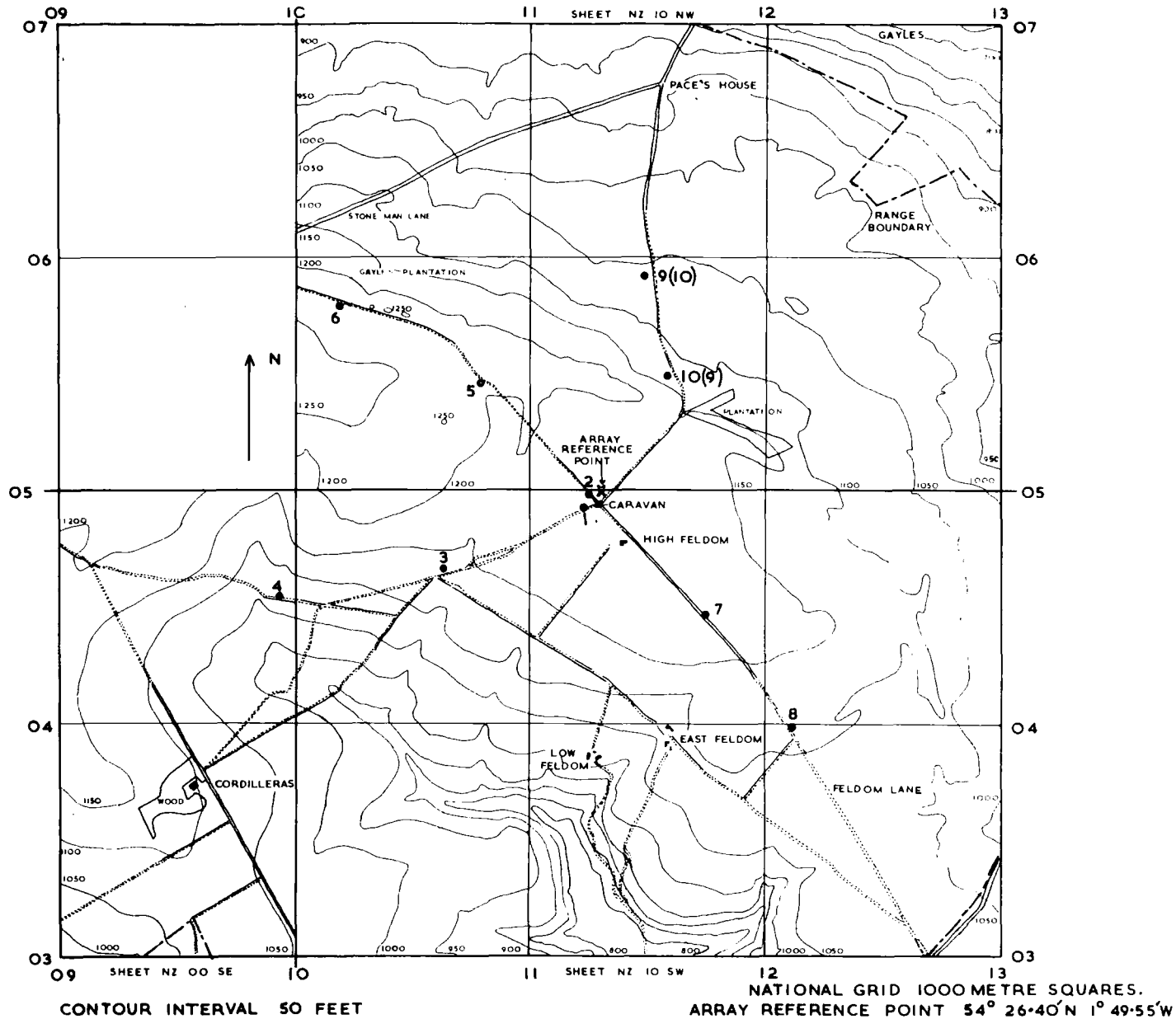

CONTOUR INTERVAL 50 FEET

NATIONAL GRID 1000 METRE SQUARES.
ARRAY REFERENCE POINT 54° 26·40′N 1° 49·55′W

Figure 36 THE FELDOM RANGE ARRAY SITE

During this test the equipment within the caravan worked satisfactorily without any fault conditions developing. The main difficulty that occurred was the extensive damage to the lines by livestock. It was only possible to keep many channels operating most of the time because there were enough people available to trace and repair the damage as soon as it occurred. The main amplifier gain was at different times either five hundred or a thousand. The high frequency common mode noise on the input lines had a maximum measured value of about 1.0 volts (peak-to-peak). Under these conditions some high frequency noise was apparent in the switch output waveform. It was noticed that high common mode pick-up on one line can cause such noise on several channels because of the slight 'cross-talk' occurring in the analogue switch and the high gain.

(iv) The results from the field test

The first stage in handling the field data was to relate the 'system time' to absolute time as represented by the M.S.F. radio signal. The replayed audio track was passed through a 1 kc/s band pass filter and mixed with the output of the coarse time code second detector. The relationship between system time and absolute time was determined at intervals of about 45 minutes by producing a pen record of the mixed signal and by comparing the two signals on a double beam oscilloscope. A computer programme was used to find the best straight line fit of system time against absolute time in the form

$$(\text{SYSTEM TIME}) = (1 + a) \cdot (\text{ABSOLUTE TIME}) + b \quad \text{seconds}$$

for each of the three periods of recording and to calculate the known shot times in terms of system time. The deviation of the two time scales during the travel time is negligible so that if the travel time is measured on the

system time scale, no correction is necessary. The three values of a obtained were $-32{\cdot}3 \cdot 10^{-6}$, $-31{\cdot}4 \cdot 10^{-6}$ and $-31{\cdot}7 \cdot 10^{-6}$ with standard errors of $0{\cdot}4 \cdot 10^{-6}$, $0{\cdot}3 \cdot 10^{-6}$ and $0{\cdot}1 \cdot 10^{-6}$ respectively. The greatest standard error of any calculated shot time was six milliseconds and the average value was three milliseconds.

The next stage in the data handling was to replay the recorded events to the ten channel oscillograph using the visual display of the replayed system time. When this was done it was found that there was considerable noise on many of the records with a principal alias frequency of about 33 c/s. This is attributed to the high frequency noise that was noticed on the switch waveform during the recording. Its effect was removed from the galvanometer records, but not from the recorded digital data, by providing an optional facility for shunting the galvanometers with a capacitance to give low pass filters with cut-offs at about 10 c/s. An example of the type of record then obtained is shown in figure 37 (see inside back cover). This record is for shot 11 at a range of 283·5 kilometres. With the present system the calibration of such a record is calculated rather than measured. An example of this calculation is given in Appendix 13. The delay distances in metres and the attenuator settings of channels one to ten for shot 11 are -107, -45, -703, -1250, -2, -154, -102, -224, 806, 551 and $\frac{1}{2}$, $\frac{1}{2}$, $\frac{1}{2}$, 1, $\frac{1}{2}$, $\frac{1}{4}$, 1, $\frac{1}{4}$, 1, 1 respectively. It was noted in the field log book that the condition of the lines of channels 6 and 8 was suspect.

An examination of the twenty-one records obtained shows that the coherence of waveforms across the array is poor. In fact it is difficult to determine from the records which channels are inverted throughout the experiment relative to some standard channel because of the reverse polarity

of the line connections. No attempt has been made to apply the present velocity filtering programme to the field data because the noise pick-up would necessitate the modification of the already critically slow programme to include a low pass digital filter and because the apparent lack of coherence suggests that the exercise would be unrewarding. The selection of first arrivals from a scrutiny of the multi-channel records is highly subjective. Nevertheless, an exercise was carried out to try to detect the first arrival at ranges of about 280 kilometres. Each record was read just once without reference to the shot time or to other records. This procedure suffers from the fact that it gives no chance to reconsider genuine errors, but has the virtue that the subjective element is minimized. The results are shown in Appendix 14, and are surprisingly consistent in view of the uncertainty of mind at the time of reading some of the records. This phase would have been quite unreadable from only one or two traces. This example demonstrates the advantages of multi-channel systems for 'eye-ball' interpretation even when the formal coherence upon which machine processing depends is poor. The most likely causes of low coherence are the poor coupling of geophones and the variations of topography and sub-surface structure across the spread.

(v) Modifications to the system after the field test

The most important problem was to eliminate the high frequency noise found on the field records. In a laboratory simulation this noise was attributed to the common mode pick-up on the input lines. Whilst care had been taken to ensure that the impedance across the lines was relatively low (2·7 kΩ), the impedance to earth at the input to the recording system was high. In fact, if a nominally balanced path to earth is provided and,

ideally, the line impedance onwards from the point of input of the common mode signal is zero, then the unit does not constitute a filter in the normal sense as used in chapter three. However, it can act as an attenuator in the sense that the voltage pick-up is reduced because of this path to earth. The system has been extended so that A.C. and D.C. impedances to earth with potentiometers for balancing may be easily added to any channel.

The second important series of changes were made to enable the system to operate at a recording speed of $3\frac{3}{4}$ i.p.s. They included the modification of the record current bias to give a symmetrical digital replay waveform, the adjustment of the replay discriminator levels, and the modification of the flux-sensitive replay logic in order to select the optimum gate waveform for each recorded track.

(vi) The future development of the system

The most important development of the system in the future must be the provision of faster methods of carrying out the data processing. A processor could be several orders of magnitude faster than the Elliot 803 general purpose machine with the described programmes and still the actual time required for the mechanical operation of reading the paper tape would be much less than the computation time. Thus, although paper tape is a poor method of data transfer, it is not the cause of the limitation of the present system. An on-line device to replace the off-line incremental digital plotter would also greatly ease the problem.

Two useful additions to the hardware would be facilities for introducing a calibration voltage step at the pre-amplifier input and for transcribing

digital information from one magnetic tape to another so that the results of one series of experiments could be transferred to a 'library tape'. As it is, the results obtained in September, 1965, will have to be erased for the experiment of November, 1966.

(vii) Summary

The methods of design and construction of a multi-channel system for recording crustal refraction data with a view to applying digital processing techniques have been described in detail. An attempt has been made in this thesis to balance fairly the achievements, such as the completion of the hardware for the three basic modes of operation and the encouraging field test, and the limitations of the system in its present form. The principal limitation is that the data processing programmes on the present computer are too slow to be a useful method of research.

An Acknowledgement

The research reported in this document has been sponsored in part by the

Air Force Office of Scientific Research, OAR

under Contract AF 61 (052) - 733 with the European Office of Aerospace Research, United States Air Force.

REFERENCES

Agger, H.E. and Carpenter, E.W. 1964. A crustal study in the vicinity of the Eskdalemuir seismological array station. Geophys. J.R. astr. Soc., 9, 69-93.

Agger, H.E. and Key, F.A. 1965. The Glasgow area earthquake recorded at the UKAEA seismometer array at Eskdalemuir. Geophys. J.R. astr. Soc., 9, 537-539.

Anderson, G.C., Bennett, A.S., Parks, R. and Willmore, P.L. 1966. Advances in instrumentation. Proc. R. Soc. A, 290, 323-327.

Anstey, N.A. and Lerwill, W.E. 1966. Correlation in real time. Proc. R. Soc. A, 290, 430-447.

Backus, M.M. 1959. Water reverberations - Their nature and elimination. Geophysics, 24, 233-261.

Backus, M.M. 1966. Teleseismic signal extraction. Proc. R. Soc. A, 290, 343-367.

Backus, M.M., Burg, J.P., Baldwin, R.G. and Bryan, E. 1964. Extraction of mantle P waves from ambient noise. Geophysics, 29, 672-692.

Birtill, J.W. and Whiteway, F.E. 1965. The application of phased arrays to the analysis of seismic body waves. Phil. Trans. R. Soc. A, 258, 421-493.

Bogert, B.P. 1961. Seismic data collection, reduction and digitization. Bull. Seism. Soc. Am., 51, 515-525.

Bott, M.H.P., Day, A.A. and Masson-Smith, D. 1958. The geological interpretation of gravity and magnetic surveys in Devon and Cornwall. Phil. Trans. R. Soc. A, 251, 161-191.

Brune, J.N. and Oliver, J. 1959. The seismic noise of the Earth's surface. Bull. Seism. Soc. Am., 49, 349-353.

Burg, J.P. 1964. Three dimensional filtering with an array of seismometers. Geophysics, 29, 693-713.

Carpenter, E.W. 1965. Explosion seismology. Science, N.Y., 147, 363-373.

De Bremaecker, J. Cl., Donoho, P. and Michel, J.G. 1962. A direct digitizing seismograph. Bull. Seism. Soc. Am., 52, 661-672.

Denham, D. 1963. The use of geophone groups to improve the signal-to-noise ratio of the first arrival in refraction shooting. Geophys. Prospect., 11, 389-408.

Dyk, K. 1956. A comparison of additive and multiplicative compounding. Geophysics, 21, 361-367.

Eaton, J.R. 1963. Crustal structure from San Francisco, California, to Eureka, Nevada, from seismic-refraction measurements. J. Geophys. Res., 68, 5789-5806.

Embree, P., Burg, J.P. and Backus, M.M. 1963. Wide-band velocity filtering - the pie slice process. Geophysics, 28, 948-974.

Fail, J.P. and Grau, G. 1963. Les filtres en eventail (Fan filters). Geophys. Prospect., 11, 131-163.

Foster, M.R., Sengbush, R.L. and Watson, R.J. 1964. Design of sub-optimum filter systems for multitrace seismic data processing. Geophys. Prospect., 12, 173-191.

Fox-Hulme, G. 1965. Velocity filtering of linear seismic arrays. M.Sc. dissertation, University of Durham.

Frantti, G.E. 1963. Spectral energy density for quarry explosions. Bull. Seism. Soc. Am., 53, 989-996.

Frantti, G.E., Willis, D.E. and Wilson, J.T. 1962. The spectrum of seismic noise. Bull. Seism. Soc. Am., 52, 113-121.

Frosh, R.A. and Green, P.E. 1966. The concept of a large aperture seismic array. Proc. R. Soc. A, 290, 368-384.

Goupillaud, P.L. 1961. An approach to inverse filtering of near-source layer effects from seismic records. Geophysics, 26, 754-760.

Hagedoorn, J.G. 1959. The plus-minus method of interpreting seismic refraction sections. Geophys. Prospect., 7, 158-182.

Hales, F.W. and Edwards, T.E. 1955. Some theoretical considerations on the use of multiple geophones arranged linearly along the line of traverse. Geophys. Prospect., 3, 65-73.

Haubrich, R.A. and Iyer, H.M. 1962. Digital seismograph system for measuring Earth noise. Bull. Seism. Soc. Am., 52, 87-93.

Hawkins, L.V. 1961. The reciprocal method of routine shallow seismic refraction investigations. Geophysics, 26, 806-819.

Healy, J.H. 1963. Crustal structure along the coast of California from seismic-refraction measurements. J. geophys. Res., 68, 5777-5787.

Hinde, B.J. and Gaunt, D.I. 1966. Some new techniques for recording and analysing microseisms. Proc. R. Soc. A, 290, 297-322.

Holzman, M. 1963. Chebyshev optimized geophone arrays. Geophysics, 28, 145-155.

Hunter, D.G.N. and Ridler, D.S. 1957. The recording of digital information on magnetic drums. Electron. Engng., 29, 490-496.

Hutchins, W.H. 1966. A real time seismic array data analyser and its associated event selector. J. Br. Instn Radio Engrs, 31, 293-308.

Jackson, P.L. 1965. Analysis of variable density seismograms by means of optical diffraction. Geophysics, 30, 5-23.

Jackson, W.H., Stewart, S.W. and Pakiser, L.C. 1963. Crustal structure in Eastern Colorado from seismic-refraction measurements. J. geophys. Res., 68, 5767-5776.

Jones, H.J. and Morrison, J.A. 1954. Cross-correlation filtering. Geophysics, 19, 660-683.

Jones, H.J., Morrison, J.A., Sarrafian, G.P. and Spieker, L.J. 1955. Magnetic delay line filtering techniques. Geophysics, 20, 745-765.

Key, F.A., Marshall, P.D. and McDowall, A.J. 1964. Two recent British earthquakes recorded at the U.K. Atomic Energy Authority seismometer array at Eskdalemuir. Nature, Lond., 201, 484-485.

Lindsey, J.P. 1960. Elimination of seismic ghost reflections by means of a linear filter. Geophysics, 25, 130-140.

McCamy, K. and Meyer, R.P. 1964. A correlation method of apparent velocity measurement. J. geophys. Res., 69, 691-700.

Melton, B.S. and Bailey, L.F. 1957. Multiple signal correlators. Geophysics, 22, 565-588.

Meyer, R.P., Steinhart, J.S., Howell, B.F., Bonini, W.E., Fahlquist, D.A. and Aldrich, L.T. 1962. Cooperative Maine experiment in crustal seismology. Methods and applications of fixed linear recording arrays to crustal measurements (Abstract). J. geophys. Res., 67, 3580.

Miller, W.F. 1963. The Caltech digital seismograph. J. geophys. Res., 68, 841-847.

Nambiar, K.P.P. 1958. Junction transistor sawtooth waveform generators. Electron. Engng., 30, 61-65.

Nambiar, K.P.P. and Boothroyd, A.R. 1957. Junction transistor bootstrap linear sweep circuits. Proc. Instn. Elect. Engrs., 104B, 293-306.

Noble, R. 1963. Flux-sensitive replay heads. Electron. Engng., 35, 372-374

Pakiser, L.C. and Hill, D.P. 1963. Crustal structure in Nevada and Southern Idaho from Nuclear Explosions. J. geophys. Res., 68, 5757-5766.

Parks, R. 1966. Seismic data acquisition and processing equipment for the Edinburgh Royal Observatory. J. Br. Instn Radio Engrs, 31, 171-180.

Phinney, R.A. and Smith, S.W. 1963. Processing of seismic data from an automatic digital recorder. Bull. Seism. Soc. Am., 53, 549-562.

Pucknell, D.A. 1964. User considerations. Ferranti Limited symposium on the application of Logical Circuit Elements.

Rakovich, B.D. 1963. A Linear delay circuit with stabilized pulse duration. Electron. Engng., 35, 112-114.

Rice, R.B. 1962. Inverse convolution filters. Geophysics, 27, 4-18.

Richards, R.K. 1957. Digital computer components and circuits, 511 pp. D. Van Nostrand.

Rieber, F. 1936. A new reflection system with controlled directional sensitivity. Geophysics, 1, 97-106.

Robinson, E.A. and Treitel, S. 1964. Principles of digital filtering. Geophysics, 29, 395-404.

Roden, R.B. 1965. Horizontal and vertical arrays for teleseismic signal enhancement. Geophysics, 30, 597-608.

Roller, J.C. and Healy, J.H. 1963. Seismic-refraction measurements of crustal structure between Santa Monica Bay and Lake Mead. J. geophys. Res., 68, 5837-5849.

Ryall, A. 1964. Improvement of array seismic recordings by digital processing. Bull. Seis. Soc. Am., 54, 277-294.

Ryall, A. and Stewart, D.J. 1963. Travel times and amplitudes from nuclear explosions, Nevada Test Site to Ordway, Colorado. J. geophys. Res., 68, 5821-5835.

Sander, G.W. and Overton, A. 1965. Deep seismic refraction investigation in the Canadian Arctic Archipelago. Geophysics, 30, 87-96.

Scheidegger, A.E. and Willmore, P.L. 1957. The use of a least squares method for the interpretation of data from seismic surveys. Geophysics, 22, 9-22.

Schneider, W.A., Larner, K.L., Burg, J.P. and Backus, M.M. 1964. A new data processing technique for the elimination of ghost arrivals on reflection seismograms. Geophysics, 29, 783-805.

Schneider, W.A., Prince, E.R. and Giles, B.F. 1965. A new data processing technique for multiple attenuation exploiting differential normal move out. Geophysics, 30, 348-362.

Shima, E., McCamy, K. and Meyer, R.P. 1964. A Fourier transform method of apparent velocity measurement. Bull. Seism. Soc. Am., 54, 1843-1854.

Smith, M.K. 1956. Noise analysis and multiple seismometer theory. Geophysics, 21, 337-360.

Smith, M.K. 1958. A review of methods of filtering seismic data. Geophysics, 23, 44-57.

Smith, S.W. 1965. Seismic digital data acquisition systems. Rev. Geophysics, 3, 151-156.

Smith, T.J., Steinhart, J.S. and Aldrich, L.T. 1966. Lake Superior crustal structure. J. geophys. Res., 71, 1141-1172.

Somers, H. and Manchee, E.B. 1966. Selectivity of the Yellowknife Seismic Array. Geophys. J.R. astr. Soc., 10, 401-412.

Steinhart, J.S. 1964. Lake Superior seismic experiment : shots and travel times. J. geophys. Res., 69, 5335-5352.

Steinhart, J.S. and Meyer, R.P. 1961. Explosion studies of continental structure, 409 pp. Carnegie Institution of Washington Publication 622.

Steinhart, J.S., Meyer, R.P., Howell, B.F., Fahlquist, D.A., Bonini, W.E. and Asada, T. 1962. Maine seismic experiment : general crustal results (Abstract). J. geophys. Res., 67, 3601.

Stewart, S.W. and Pakiser, L.C. 1962. Crustal structure in eastern New Mexico interpreted from the GNOME explosion. Bull. Seism. Soc. Am., 52, 1017-1030.

Thirlaway, H.I.S. 1963. Earthquake or explosion? New Scient., 18, 311-316.

Thirlaway, H.I.S. 1966. Interpreting array records : explosion and earthquake P wavetrains that have traversed the deep mantle. Proc. R. Soc. A, 290, 385-395.

Thompson, N.J. 1965. A delta-modulation recording system for seismic use. Geophysics, 30, 51-53.

Thornburgh, H.R. 1930. Wave-front diagrams in seismic interpretation. Bull. Am. Ass. Petrol. Geol., 14, 185-200.

Truscott, J.R. 1964. The Eskdalemuir seismological station. Geophys. J.R. astr. Soc., 9, 59-67.

Tullos, F.N. and Cummings, L.C. 1961. An analogue seismic correlator. Geophysics, 26, 298-308.

Warrick, R.E., Hoover, D.B., Jackson, W.H., Pakiser, L.C. and Roller, J.C. 1961. The specification and testing of a seismic-refraction system for crustal studies. Geophysics, 26, 820-824.

Watson, R.J. 1965. Decomposition and suppression of multiple reflections. Geophysics, 30, 54-71.

Weisbrich, R.A. 1965. Project SHOAL volunteer team programme. Geophysics, 30, 262-278.

Whiteway, F.E. 1961. Tuned seismometer arrays. United Kingdom Atomic Energy Authority Field Experiments Division Note No. V5.

Whiteway, F.E. 1966. The use of arrays for earthquake seismology. Proc. R. Soc. A, 290, 328-342.

Wiener, N. 1949. Extrapolation, interpolation and smoothing of stationary time series with engineering applications. New York : John Wiley and Sons Inc. (also 1964, 160 pp., The M.I.T. Press, Cambridge, Massachusetts).

Willis, D.E. 1963. A note on the effect of ripple firing on the spectra of quarry shots. Bull. Seism. Soc. Am., 53, 79-85.

Willmore, P.L. 1962. A new seismic research group for Edinburgh. Nature, Lond., 195, 1250-1252.

Willmore, P.L. and Bancroft, A.M. 1960. The time term approach to refraction seismology. Geophys. J.R. astr. Soc., 3, 419-432.

Willmore, P.L., Herrin, E. and Meyer, R.P. 1963. Examination of irregular sub-surface structures by seismic refraction methods. Nature, Lond., 197, 1094-1095.

Winter, P.H. 1962. Modular circuit construction. Electron. Engng., 34, 173-175.

APPENDIX I

Digital logic modules

The types of Ferranti 2 mc/s logical circuit elements used in the system are

L C E. 2 0 1 G	Germanium flip-flop
L C E. 2 0 6 G	Variable period monostable unit
L C E. 2 0 7 G	Quadruple emitter follower unit
L C E. 2 0 8 G	Five input AND block
L C E. 2 0 9 G	Five input OR block
L C E. 2 1 1 G/A	Trigger/amplifier circuit
L C A 1 G	Adaptor module

The types of Mullard 100 kc/s circuit blocks used in the system are

B8 920 00	Flip flop one	FF1
B8 920 01	Flip flop two	FF2
B8 920 03	Flip flop four	FF4
B8 930 00	Twin 3 input AND gate	2.3A1
B8 930 01	Twin 2 input AND gate	2.2A1
B8 930 01	Twin 3 input OR gate	2.301
B8 930 03	Twin 2 input OR gate	2.201
B8 940 01	Twin emitter follower	2EF1
B8 940 02	Twin inverter amplifier	2IA1
B8 940 03	Twin emitter follower	2EF2
B8 940 05	Twin inverter amplifier	2IA2
B8 940 00	Emitter follower/inverter amplifier	EF1/IA1
B8 950 00	Pulse shaper	PS1
B8 950 01	One shot multivibrator one	OS1
B8 950 03	One shot multivibrator two	OS2

APPENDIX 2

The time code bit word

Bits 1 to 3;

opening identity 1 0 1

Bits 4 and 5;

coarse time code

	4	5
seconds	1	0
minutes	0	1
quarter hours	1	1

Bits 6 to 21;

system time.

(a) Unit second or minute counter

BIT NO.	9/15	8/14	7/13	6/12
0	0	0	0	0
1	0	0	0	1
2	0	0	1	0
3	0	0	1	1
4	0	1	0	0
5	0	1	0	1
6	0	1	1	0
7	0	1	1	1
8	1	0	0	1
9	1	0	1	0
10	1	0	1	1
11	1	1	0	0
12	1	1	0	1
13	1	1	1	0
14	1	1	1	1
15 ≡ 0	0	0	0	0

(b) Fifteen second or minute counter

BIT NO.	11/17	10/16
0	0	0
1	0	1
2	1	0
3	1	1
4 ≡ 0	0	0

(c) Twelve hour counter

BIT NO.	21	20	19	18
0	0	0	0	0
1	0	0	0	1
2	0	0	1	0
3	0	0	1	1
4	0	1	0	0
5	0	1	0	1
6	0	1	1	0
7	0	1	1	1
8	1	1	0	0
9	1	1	0	1
10	1	1	1	0
11	1	1	1	1
12 ≡ 0	0	0	0	0

Bits 22 and 23;

closure identity 0 1

Note that the reset state '0' corresponds to a lit tube or the absence of a hole on punched paper tape.

APPENDIX 3

The punch control logic

(a) The logic punch cycle

The arrival of a synchronizing pulse from the punch triggers the following sequence of logic:-

A decision is made as to the state of the 'new information' register, and this decision is made and held at one point (the decision register) to avoid mixed operation.

EITHER No new information available for punching ('new information' register is RESET), so suppress code and feed pulses and suppress any changes of the control bistables.

OR New information available for punching ('new information register is SET), so generate feed and code pulses.

If at the end of the feed pulse the 'new sample' register is already RESET, then RESET the 'new information' register.

After delay, RESET 'new sample' register. If this register was not already in the RESET state, apply single shift pulse to line B.

(b) The punching of one sample.

When the replay logic AND gates close, the replay logic registers contain information bits. After a short nominal delay OR at the end of the second punch cycle of the previous sample (as indicated by the RESET of the 'new information' register), whichever comes later, apply two shift pulses to lines A1, A2 and B, thus transferring the information into the 'await punch' and 'punch' registers. Then SET both the

'new sample' register and the 'new information' register.

After some time a synchronizing pulse from the punch triggers a 'logic punch cycle', with the following action:-

Punch first character

RESET 'new sample' register

Shift character from 'await punch' register into 'punch' register.

After a further ten milliseconds, a second synchronizing pulse triggers a 'logic punch cycle', with the following action:-

Punch second character

RESET 'new information' register.

It is possible that after a further ten milliseconds a third synchronizing pulse will occur before the replay logic AND gates close and before the next sample is available. This pulse (any any subsequent similar pulses) trigger a 'logic punch cycle' during which the code and feed pulses are suppressed and the 'new information' and 'new sample' registers remain in the RESET state.

APPENDIX 4

The addressing of subscripted Algol variables using Machine Code

The addresses of subscripted variables may be calculated using the following standard functions:-

address (A) - the address of the first element of the array A.

lowbound (A, I)- the declared lower subscript bound for the Ith subscript position from the left in the array A.

range (A, I) - the number of values in the range of the Ith subscript position from the left in the array A.

Then the address of the variable A(I) is

I - lowbound (A, 1) + address (A),

and the address of the variable A (I, J) is

(I - lowbound (A, 1)) x range (A, 2) + J - lowbound (A, 2) + address (A)

The values of lowbounds and range are known numerically from the array declarations, so a numerical formula in terms of I, J and address (A) can be derived.

The machine code instructions to extract an element from an address x and give its value to the identifier y are

```
0 0 x 1 3 0 0
2 0 y 0 0 0 0 ,
```

and to replace such an identifier within an array are

```
3 0 y 0 0 0 0
0 0 x 1 2 0 0 .
```

APPENDIX 5

Precompiled packages

Two precompiled packages for Elliott 803 Algol are used in the data processing programmes, and the functions of the procedure calls used will be briefly described here.

(a) 803 ALGOL FILM PACKAGE, which is designed to facilitate the use of the film backing store.

procedure locate (n, h)	-	searches for block n on film handler h.
procedure filmread (a, h)	-	reads an array a from the film on handler h.
procedure filmwrite (a,h)	-	writes an array a on to the film on handler h.
procedure in block (a,i,h)	-	reads one block of 64 elements from the film on handler h into store, where i is the position of the first element of the block in the array.
procedure outblock (a,i,h)	-	writes one block on to film as above.
procedure blocknumber	-	assigns the address of the last block read or written to the integer block number.

(b) GRAPH PLOTTER PACKAGE - D P 1 - this is an early version of an unpublished programme by J. Roper (University of Durham) for producing output for the Benson-Lehner digital plotter.

The identifiers PENX and PENY contain the co-ordinates of the pen in plotter increments of 0.005 inches.

The procedures used in the data processing programmes are:-

procedure origin (X_o, Y_o) - sets the origin for all further procedure calls at the point X_o, Y_o, where X_o and Y_o are in inches, relative to the position of the pen at the time of the origin call.

procedure plot (A, B, N, scale, SR) - the first N points given by the arrays A(x) and B(y) are plotted using the symbol specified by the string SR and scaled up by the factor 'scale'. There are three possible symbols; the decimal point, which cannot be scaled; the plus sign which is .01" wide for scale 1; the multiply sign which has arms 0.005" long for scale 1.

procedures x axis (X, Y, step, N) and y axis (X, Y, step, N) - starting at the point X, Y, an axis is drawn which is made up of N stepped intervals each 'step' inches long.

procedures write x (X, Y, scale, SR) and write y (X, Y, scale, SR) - starting at the point X, Y, the message inside the string SR will be drawn in the horizontal or vertical direction with each character scaled up by the factor 'scale'.

APPENDIX 6

Range and delay distance programme

Purpose

Given an array configuration defined by an array reference point and ten geophone locations on a local rectilinear x - y grid, where y corresponds approximately to North, the latitude and longtitude of the array reference point and of a series of shot points, then calculate for each shot point the range R (kilometres), the azimuth Z (degrees) from the array, and the delay distances (in the units of the local grid) relative to reference point of the ten geophone locations. The wavefront at the array is assumed to be plane. Denote the eastward deviation in minutes of the y direction from North by X, and give all latitudes North and longtitudes West.

Flow diagram

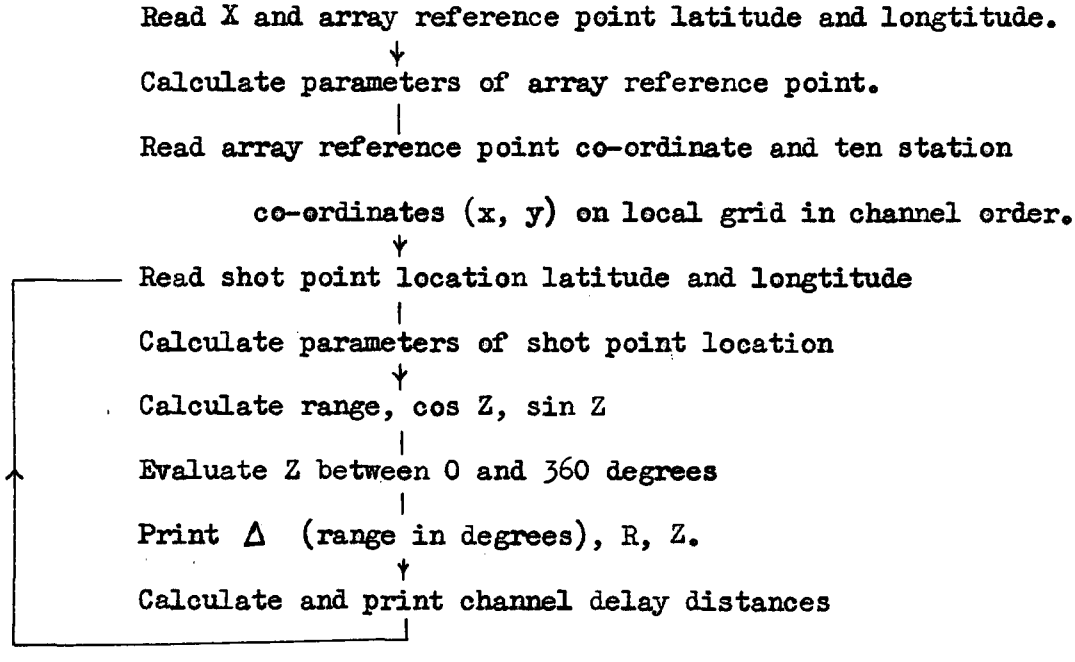

Data type

		X (minutes)			
array ref.	:	degrees	minutes (Lat N)	degrees	minutes (Long W)
array ref.	:	x_o	y_o		
Channel 1	:	x_1	y_1		
		"	"		
		"	"		
		"	"		
		"	"		
		"	"		
Channel 10	:	x_{10}	y_{10}		
shot points	:	degrees	minutes (Lat N)	degrees	minutes (Long W)
		"	"	"	"
		"	"	"	"
		"	"	"	"
		"	"	"	"
		"	"	"	"
		degrees	minutes	degrees	minutes

```
A. Lucas  Range and array delay distance calculation;

begin real degree, mins, lat, long, A,B,C,D,E,G,H,K,AD,BD,CD,x, y,xb,yb,angle,
          cangle,sangle,dangle,X,Z,m,n,t,R,cZ,sZ;
     integer k;
     array AA[1:2,1:10];
     switch ss:=L1,L2,L3;
     read X,degree,mins;
     lat:=(degree+mins/60)/57.29578;
     lat:=arctan(0.993277*tan(lat));
     read degree,mins;
     long:=(degree+mins/60)/57.29578;
     A:=cos(lat)*cos(long);
     B:=-cos(lat)*sin(long);
     C:=sin(lat);
     D:=-sin(long);
     E:=-cos(long);
     G:=sin(lat)*cos(long);
     H:=-sin(lat)*sin(long);
     K:=-cos(lat);
     read x,y;
     for k:=1 step 1 until 10 do read AA[1,k], AA[2,k];
     L1:read degree,mins;
     lat:=(degree+mins/60)/57.29578;
     lat:=arctan(0.993277*tan(lat));
     read degree,mins;
     long:=(degree+mins/60)/57.29578;
     AD:=cos(lat)*cos(long);
     BD:=-cos(lat)*sin(long);
     CD:=sin(lat);
 cangle:=A*AD+B*BD+C*CD;
       angle:=arccos(cangle);
     R:=angle*6371.22;
     sangle:=sin(angle);
     angle:=angle*57.28578;
     sZ:=((AD-D)↑2+(BD-E)↑2+CD↑2-2)/(2*sangle);
     cZ:=((AD-G)↑2+(BD-H)↑2+(CD-K)↑2-2)/(2*sangle);
     Z:=arcsin(sZ);
     if sZ≥0 and cZ≥ 0 then Z:=Z else
     if sZ≥ 0 and cZ<0 then Z:=3.14159-Z else
     if sZ<0 and cZ<0 then Z:=3.14159-Z else
     if sZ<0 and cZ≥0 then Z:=6.28318+Z;
     t:=Z*57.29578;
     print angle,sameline,R,t;
     m:=4.712389-Z+X*2.9089₁₀-4;
     if abs(m)<5₁₀-5 or abs(3.14159-m)<5₁₀-5 then goto L2;
     if abs(m-1.57079)<5₁₀-5 or abs(m+1.57079)<5₁₀-5
       or abs(4.71238-m)<5₁₀-5 then goto L3;
```

```
m:=tan(m);
n:=m+1/m;
sZ:=sin(Z-X*2.9089_10-4);
for k:=1 step 1 until 10 do
begin xb:=(m*x+AA[1,k]/m+AA[2,k]-y)/n;
      yb:=(m*AA[2,k]+y/m+AA[1,k]-x)/n;
      t:=sqrt((x-xb)↑2+(y-yb)↑2);
           if abs(sZ-(xb-x)/t)<1_10-5 then t:=-t;
           print aligned(6,1),t;
end;
goto L1;
L2:for k:=1 step 1 until 10 do
   begin t:=sZ*(x-AA[1,k]);
         print aligned(6,1),t;
   end;
   goto L1;
L3:for k:=1 step 1 until 10 do
   begin t:=cZ*(y-AA[2,k]);
         print aligned(6,1),t;
   end;
   goto L1;
end;
```

APPENDIX 7

Programme I - paper tape input

Purpose

The function of this programme is to read in punched paper tape generated by the seismic replay system, check for single errors, and, optionally, calculate the average and standard deviation of each channel and write the 'second blocks' of data on to film starting at block (nn0 + 75. nnS).

Control

The action of the programme during a 'second block' is controlled by the state of the keyboard at the start of the 'second block'. These controls are:-

4096 DOWN to suppress time code bit zero test.

2048 DOWN to suppress system parity check.

1024 DOWN to by-pass channel identity shift register.

512 DOWN to suppress calculations of means and standard deviations.

256 DOWN to suppress film output.

With all the functions in, it takes ten minutes to process a second of data. The options are provided to give speedier operation at the cost of less checks.

Data tape

(a) zero signal levels for channels 1 to 10.

(b) If 256 UP, nn0 and nnS

(c) Seismic data tapes.

Specimen data tape used for simulation

514 513 517 521 519 545 512 551 527 535

100 0

then simulated seismic data tape.

Flow diagram of programme I

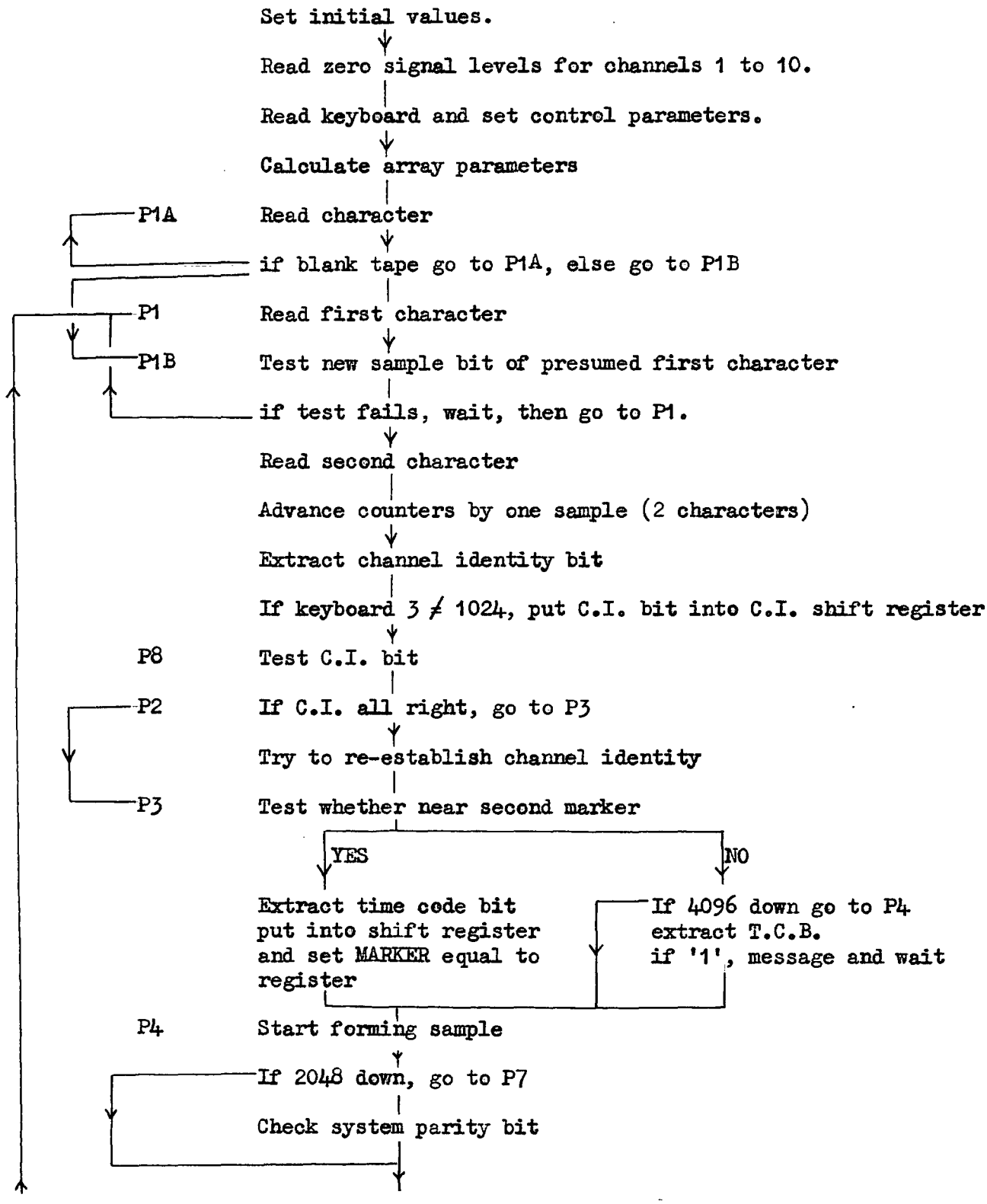

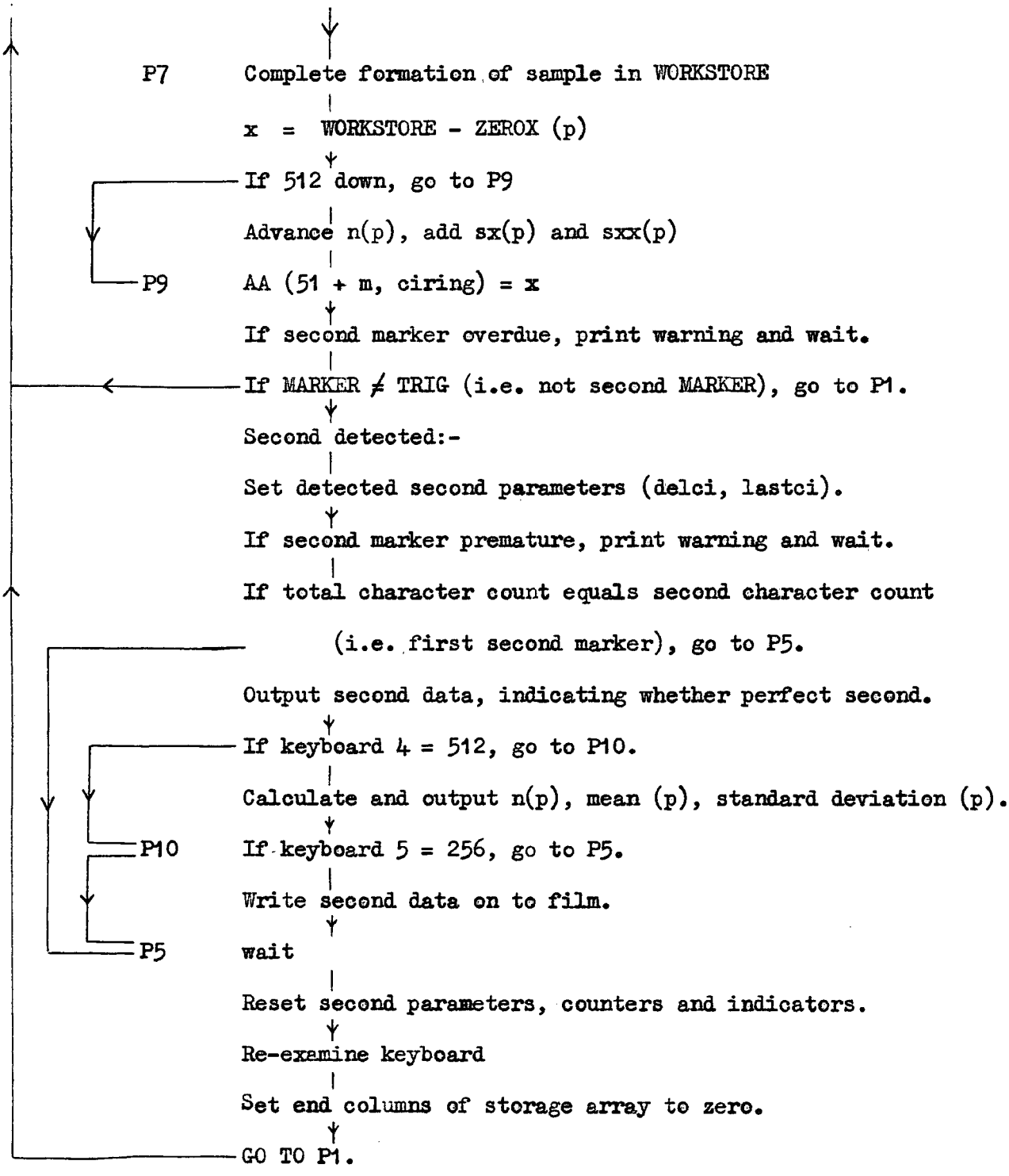
P7
Complete formation of sample in WORKSTORE
x = WORKSTORE - ZEROX (p)
If 512 down, go to P9
Advance n(p), add sx(p) and sxx(p)
P9
AA (51 + m, ciring) = x
If second marker overdue, print warning and wait.
If MARKER ≠ TRIG (i.e. not second MARKER), go to P1.
Second detected:-
Set detected second parameters (delci, lastci).
If second marker premature, print warning and wait.
If total character count equals second character count
(i.e. first second marker), go to P5.
Output second data, indicating whether perfect second.
If keyboard 4 = 512, go to P10.
Calculate and output n(p), mean (p), standard deviation (p).
P10
If keyboard 5 = 256, go to P5.
Write second data on to film.
P5
wait
Reset second parameters, counters and indicators.
Re-examine keyboard
Set end columns of storage array to zero.
GO TO P1.

```
a 1 lucas  programme one ;

begin integer tcc,isc,secerr,ciring,cishift,cierr,tcbshift,
   parrity,m,delci,lastci,perfect,char1,char2,mask,endbit,workstor,
   pcheck,time,trig,marker,p,x,r,aa0,zerx0,sx0,sxx0,n0,y,z,
   keybd1,keybd2,keybd3,keybd4,keybd5,cokey1,cokey2,cokey3,cokey4,
cokey5,nn0,nns,nnf;

real a,b;


integer array zerox,bb,sx,sxx,n[1:10];
array mean,deviation[1:10],aa[51:153,1:10];

switch ss:=p1,p1a,p1b,p2,p3,p4,p5,p6,p7,p8,p9,p10;


procedure parity(word,result);   comment checks to see that
       information in word has even parity. result=0 for even
       parity and 1 for odd;

integer word,result;
begin integer n,store,count,mask;


   store:=word;
   count:=0;
   for n:=0 step 1 until 6 do
   begin mask:=1;
      elliott(3,0,store,0,2,3,mask);
      elliott(5,1,1,0,2,0,store);
      count:=count+mask;
   end;

   mask:=1;
   elliott(3,0,mask,0,3,3,count);
   result:=count;

end of procedure parity;
```

```
procedure pattern(word,n);  comment prints least significnt n bits
         of word as pattern of 1 and 0;
value n;   integer word,n;
begin integer mask,m,store1,store2;
   mask:=1;
   for m:=n-1 step -1 until 0 do
   begin store1:=word;
      elliott(3,0,store1,0,0,0,0);   elliott(0,0,m,1,5,1,0);
      elliott(0,3,mask,0,2,0,store2);  elliott(0,0,store2,1,7,4,16);
   end;
end of procedure pattern;


procedure channelerror;
begin print ££1?Channel Identity error, TCC =?,tcc,keybd3,
   ££1?CISHIFT register =     ?;
   pattern(cishift,20);
   secerr:=cierr:=1;
   wait
end of channelerror;

sameline;
endbit:=137438953471;   comment =2↑37-1;
time:=7340035;   trig:=5242881;
tcc:=isc:=secerr:=ciring:=cishift:=cierr:=tcbshift:=m:=delci:=
   lastci:=perfect:=0;
for p:=1 step 1 until 10 do
  begin sx[p]:=sxx[p]:=n[p]:=0;
       read zerox[p];
   end;
wait;
keybd1:=4096;  keybd2:=2048;  keybd3:=1024;  keybd4:=512;  keybd5:=256;
elliott(0,6,0,0,7,0,0);
elliott(2,3,keybd1,0,2,3,keybd2);
elliott(2,3,keybd3,0,2,3,keybd4);
elliott(2,3,keybd5,0,0,0,0);
aa0:=address(aa);
aa0:=aa0-511;
zerx0:=address(zerox);
zerx0:=zerx0-1;
sx0:=address(sx);
sx0:=sx0-1;
sxx0:=address(sxx);
sxx0:=sxx0-1;
n0:=address(n);
n0:=n0-1;
if keybd5=256 then goto p1a;
read nn0,nns;
wait;
```

```
p1a: elliott(0,6,0,0,7,1,0);   elliott(2,0,char1,0,0,0,0);
     if char1=0 then goto p1a else goto p1b;

p1:  elliott(0,6,0,0,7,1,0);   elliott(2,0,char1,0,0,0,0);

p1b: mask:=1;
     elliott(3,0,char1,0,2,3,mask);   comment mask=n.s. bit;
     if mask≠1 then
     begin print ££1? New sample error, TCC =?,tcc+1;
        secerr:=1;
        wait;
        goto p1
     end;

elliott(0,6,0,0,7,1,0);  elliott(2,0,char2,0,0,0,0);
tcc:=tcc+2;
isc:=isc+2;
ciring:=ciring+1;
if ciring=11 then begin ciring:=1;  m:=m+1 end;
if m=101 then m:=100;
mask:=2;
elliott(3,0,mask,0,0,3,char2);
elliott(5,1,1,0,2,0,mask);  comment mask=ci bit;
if keybd3=1024 then goto p8;
elliott(3,0,cishift,0,0,3,endbit);
elliott(5,5,1,0,2,0,cishift);  comment put ci bit in cishift;
cishift:=cishift+mask;


p8:if ciring=2 then begin if mask=1 then goto p2 else
   channelerror end;

p2: if cierr=0 then goto p3;
    if mask≠1 then begin print ££1?CIERROR set,TCC =?,tcc;
       goto p3
    end;

    print ££1?Channel now re-established, TCC =?,tcc,
       ££s5?CIRING =?,ciring, ££1?CISHIFT =     ?;
    pattern(cishift,39);
    cierr:=0;
    ciring:=2;

p3: if isc=tcc or isc>1940 then goto p6;
  if keybd1=4096 then goto p4;
mask:=1;
    elliott(3,0,mask,0,0,3,char2);
    elliott(2,0,mask,0,0,0,0); comment mask=tc bit;
if mask=0 then goto p4;
print ££1?Time code error, TCC=  ?,tcc;
wait;
goto p4;
p6:  mask:=1;
    elliott(3,0,mask,0,0,3,char2);
    elliott(2,0,mask,0,0,0,0); comment mask=tc bit;
```

```
    elliott(3,0,tcbshift,0,0,3,endbit); elliott(5,5,1,0,2,0,tcbshift);
    tcbshift:=tcbshift+mask; comment put tc bit in tcbshift;
    elliott(3,0,tcbshift,0,0,3,time);
    elliott(2,0,marker,0,0,0,0);

p4: elliott(3,0,char1,0,5,1,1);   elliott(2,0,char1,0,5,1,1);
    elliott(5,5,5,0,2,0,workstor);
  if keybd2=2048 then goto p7;
      parity(char1,pcheck);   parity(char2,parrity);
    if pcheck+parrity=1 then
       print ££1?System pa~rity error, TCC=?,tcc;
p7:      elliott(3,0,char2,0,5,1,2);   elliott(2,4,workstor,0,0,0,0);
y:=zerx0+ciring;
elliott(0,0,y,1,3,0,0);
elliott(2,0,z,0,0,0,0);
x:=workstor-z;
if keybd4=512 then goto p9;
y:=n0+ciring;
elliott(0,0,y,1,2,2,0);
y:=sx0+ciring;
elliott(0,0,y,1,3,0,0);
elliott(2,0,z,0,0,0,0);
z:=z+x;
elliott(3,0,z,0,0,0,0);
elliott(0,0,y,1,2,0,0);
y:=sxx0+ciring;
elliott(0,0,y,1,3,0,0);
elliott(2,0,z,0,0,0,0);
z:=z+x*x;
elliott(3,0,z,0,0,0,0);
elliott(0,0,y,1,2,0,0);
p9: a:=x;
y:=10*(51+m)+ciring+aa0;
elliott(3,0,a,0,0,0,0);
elliott(0,0,y,1,2,0,0);
if isc>2010 then
  begin print ££1?No second marker, isc=  ?,isc;
    wait
  end;
if marker≠trig then goto p1;
bb[3]:=lastci;
delci:=ciring-lastci;
lastci:=ciring;
bb[5]:=delci;
if isc<1990 then
begin if tcc=isc then goto p5 else
   begin print ££1?Early second marker,ISC =?,isc;wait end
end;
print ££12?Second marker found£1?TCB shift register =     ?;
pattern(tcbshift,39);
print ££1?M =?,m,£CIRING =?,ciring,££s5?DELTA CI =?,delci,
   ££1?Second error register =?,secerr,££1?CI error register =?,
   cierr,££1?TCC =?,tcc,££1?ISC =?,isc;
```

```
if secerr=0 and isc=2000 and delci=0 then
  begin print ££1?Perfect second£13??;
    perfect:=1;
  end
  else begin print ££1? Not a perfect second£13??;
  perfect:=0;
end;
bb[4]:=perfect;
if keybd4=512 then goto p10;
print ££14s15?n£s6?Mean£s4?Standard Deviation£1??;
for p:=1 step 1 until 10 do
   begin mean[p]:=sx[p]/n[p];
deviation[p]:=sqrt(sxx[p]/n[p]-mean[p]*mean[p]);
  print ££1?Channel?,digits(3),p,digits(4),n[p],
           aligned(8,2),mean[p],aligned(13,2),deviation[p];
end;

p10:  bb[2]:=tcbshift;
if keybd5=256 then goto p5;
 nnf:=nn0+75*nns;
 print ££11??,nnf;
 locate(nnf,2);
 filmwrite(bb,2);
 filmwrite(aa,2);
 print blocknumber;
 nns:=nns+1;
p5: wait;
bb[1]:=tcbshift;
isc:=m:=secerr:=marker:=tcbshift:=perfect:=0;

keybd1:=4096; keybd2:=2048; keybd3:=1024; keybd4:=512; keybd5:=256;
elliott(0,6,0,0,7,0,0);
elliott(2,3,keybd1,0,2,3,keybd2);
elliott(2,3,keybd3,0,2,3,keybd4);
elliott(2,3,keybd5,0,0,0,0);
for p:=1 step 1 until 10 do
  begin y:=510+p+aa0;
     elliott(0,0,y,1,2,6,0);
        y:=1510+p+aa0;
      elliott(0,0,y,1,2,6,0);
      y:=1520+p+aa0;
      elliott(0,0,y,1,2,6,0);
      y:=1530+p+aa0;
      elliott(0,0,y,1,2,6,0);
      sx[p]:=sxx[p]:=n[p]:=0;
  end;
  goto p1
end of programme;
end for film package;
```

APPENDIX 8

Programme 2 - velocity filtering

Purpose

Given (ENDN - STARTN + 1) seconds of data stored on film, carry out velocity filtering calculations for nv1(≤ 8) velocities for given channel delay distances DD, given channel gains GG, and a given grouping of 5 RED channels and 5 BLUE channels. The computation interval is 10 nn0 milliseconds, and the result is written back on to film.

Control

The following functions are controlled from the keyboard:-

4096 DOWN suppresses optional printing of each completed ADD and MULTIPLY

2048 DOWN by-passes the velocity filtering calculation.

The second function is necessary if it is required to use programme three to plot the channel inputs only.

Data tape

TNN STARTN ENDN nno

DD(1) - DD(10)

GG(1) - GG(10)

RED(1) BLUE(1) RED(2) BLUE(2) RED(3) BLUE(3) RED(4) BLUE(4) RED(5) BLUE(5)

nv1

VV(1) - VV(nv1).

Specimen data tape used for simulation

```
100    0    1    2
1500   1200  900  600  300   0   -300  -600  -900  -1200
1   1   1   1   1   1   1   1   1   1
1   2   3   4   5   6   7   8   9  10
6
4   5   6   7   8   9
```

Flow diagram of Programme 2

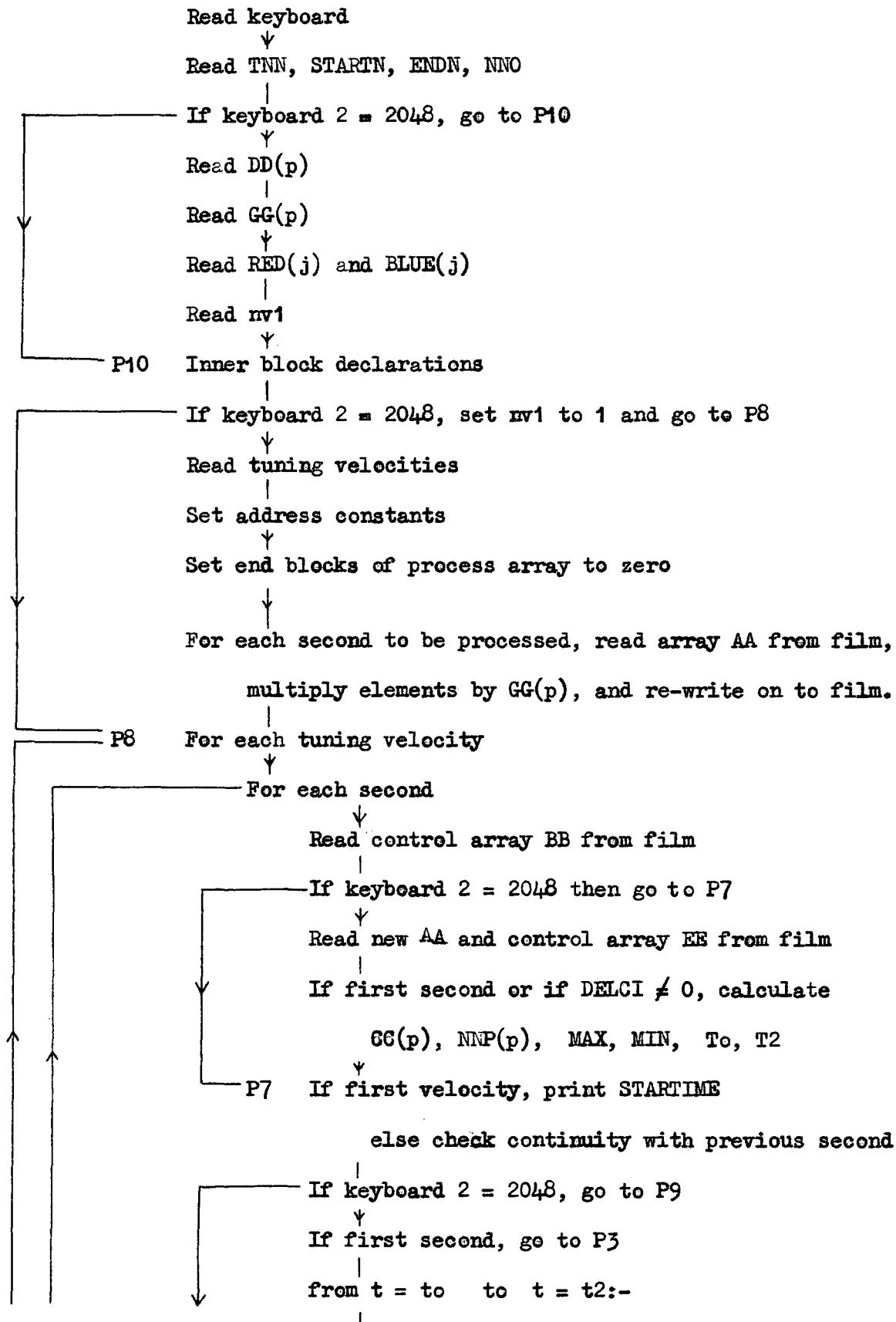

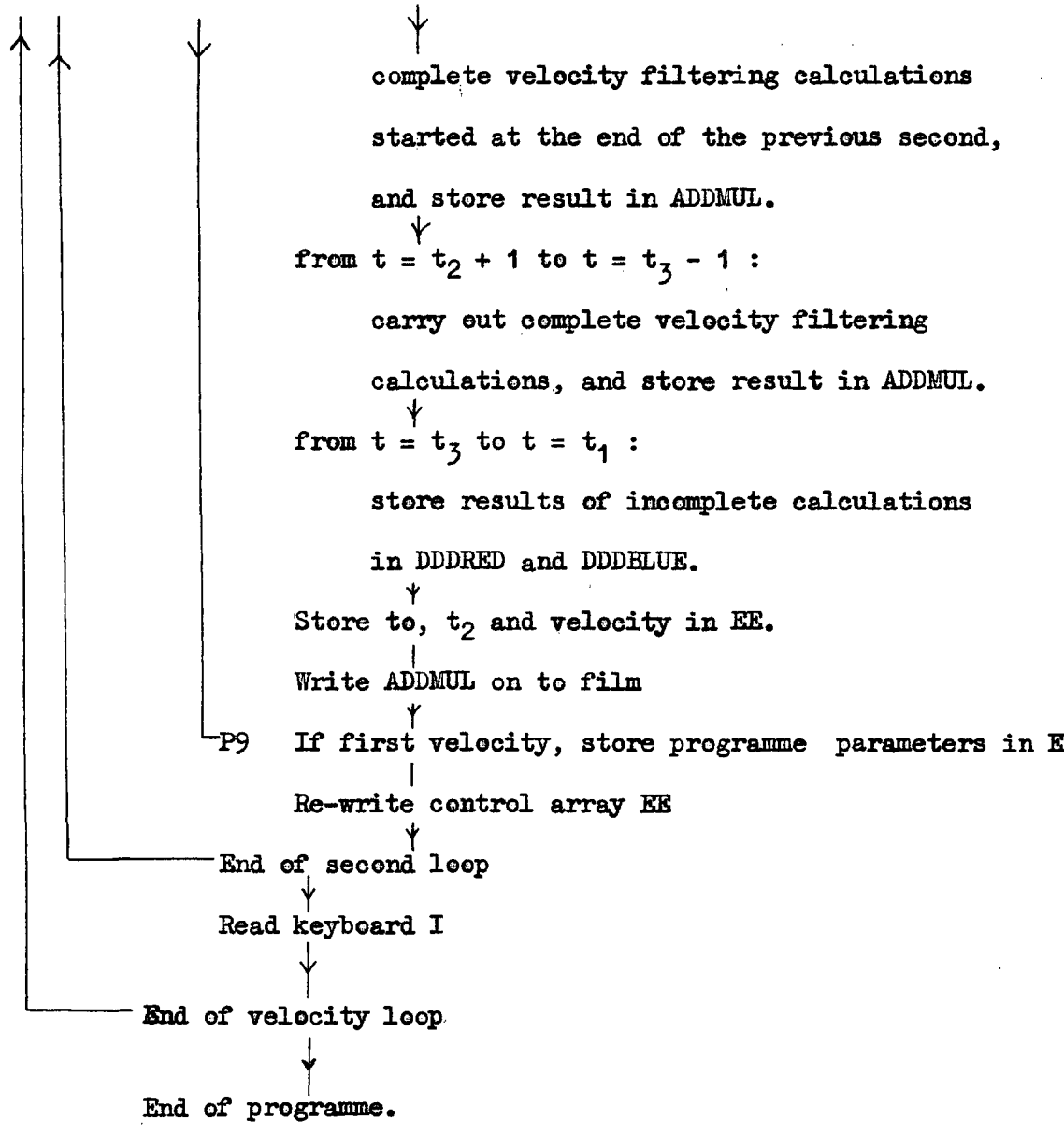
complete velocity filtering calculations
started at the end of the previous second,
and store result in ADDMUL.
from t = t2 + 1 to t = t3 - 1 :
carry out complete velocity filtering
calculations, and store result in ADDMUL.
from t = t3 to t = t1 :
store results of incomplete calculations
in DDDRED and DDDBLUE.
Store to, t2 and velocity in EE.
Write ADDMUL on to film
P9
If first velocity, store programme parameters in EE
Re-write control array EE
End of second loop
Read keyboard I
End of velocity loop
End of programme.

```
A. Lucas  Programme 2;

begin real ggg,ff,fff,xred,xblue,zzz,ddred,ddblue,redaa,blueaa;
      integer cokey1,keybd1,keybd2,keybd3,
            tnnf,ttnnf,tnn,startn,endn,nn0,nv1,nvv,nvvv,
            p,i,j,y,r,s,z,t,q,ll,rr,mm,nn,tt,jj,kk,nb,max,
            min,admul0,sectotal,vc,t0,t1,t2,t3,endtime,
            inred,inblue,redcc,bluecc,rednnp,bluennp,aa0,
            nnp0,cc0,red0,blue0,red00,blue00;
      real array aa[-50:251,1:10],dddred,dddblue[0:150],
               addmul[1:2,-50:101],dd,gg[1:10];
      integer array red,blue[1:5],nnp,bb,cc[1:10],ee[1:4,1:12];
     switch sss:=p10;
      procedure pattern(word,n); value n; integer word,n;
            begin integer mask,m,store1,store2;
                  mask:=1;
                  for m:=n-1 step -1 until 0 do
                  begin store1:=word;
                  elliott(3,0,store1,0,0,0,0);
                  elliott(0,0,m,1,5,1,0);
                  elliott(0,3,mask,0,2,0,store2);
                  elliott(0,0,store2,1,7,4,16);
                  end;
            end;

cokey1:=4096;
keybd1:=4096;
keybd2:=2048;
keybd3:=1024;
wait;
elliott(0,6,0,0,7,0,0);
elliott(2,3,keybd1,0,2,3,keybd2);
elliott(2,3,keybd3,0,0,0,0);
read tnn,startn,endn,nn0;
sectotal:=endn-startn+1;
if keybd2=2048 then goto  p10;
wait;
for p:=1 step 1 until 10 do read dd[p];
wait;
for p:=1 step 1 until 10 do read gg[p];
wait;
for p:=1 step 1 until 5 do read red[p],blue[p];
wait;
read nv1;
ll:=100/nn0;
```

```
if 11*nn0≠100 then begin print££14?nn0 invalid?;
                    wait;
                    end;
p10: begin real array vv[1:nv1];
 witch ss:=p1,p2,p3,p4,p5,p6,p7,p8,p9;
procedure sum;
      begin ddred:=ddblue:=0;
         tt:=t*nn0+51;
            for p:=1 step 1 until 5 do
begin y:=p+red0;
      elliott(0,0,y,1,3,0,0);
      elliott(2,0,inred,0,0,0,0);
      y:=p+blue0;
      elliott(0,0,y,1,3,0,0);
      elliott(2,0,inblue,0,0,0,0);
      y:=nnp0+inred;
      elliott(0,0,y,1,3,0,0);
      elliott(2,0,rednnp,0,0,0,0);
      y:=nnp0+inblue;
      elliott(0,0,y,1,3,0,0);
      elliott(2,0,bluennp,0,0,0,0);
      y:=checki(10*(rednnp+tt)+inred+aa0);
      elliott(0,0,y,1,3,0,0);
      elliott(2,0,redaa,0,0,0,0);
      y:=checki(10*(bluennp+tt)+inblue+aa0);
      elliott(0,0,y,1,3,0,0);
      elliott(2,0,blueaa,0,0,0,0);
      ddred:=ddred+checkr(redaa);
      ddblue:=ddblue+checkr(blueaa);
      end;
end;

procedure add and multiply;
begin y:=jj+t;
      fff:=ddred+ddblue;
      elliott(3,0,fff,0,0,0,0);
      elliott(0,0,y,1,2,0,0);
      ff:=ddred*ddblue;
      ff:=sqrt(abs(ff))*sign(ff);
     if keybd1=0 then print ££11??,vc,nb,t,fff,ff;
      y:=kk+t;
      elliott(3,0,ff,0,0,0,0);
      elliott(0,0,y,1,2,0,0);
end;
sameline; digits(4); freepoint(4);
if keybd2=2048 then begin nv1:=1;
                          goto p8;
                    end;
for p:=1 step 1 until nv1 do read vv[p];
aa0:=address(aa)+499;
aa0:=checki(aa0);
nnp0:=address(nnp)-1;
cc0:=address(cc)-1;
```

```
admul0:=address(addmul)-102;
jj:=152+admul0;
kk:=304+admul0;
red0:=address(red)-1;
blue0:=address(blue)-1;
red00:=address(dddred);
blue00:=address(dddblue);
for i:=-500 step 10 until 500 do
      begin for j:=1 step 1 until 10 do
            begin y:=i+j+aa0;
                  elliott(0,0,y,1,2,6,0);
            end;
      end;
for i:=1510  step 10 until 2510 do
      begin for j:=1 step 1 until 10 do
            begin y:=i+j+aa0;
                  elliott(0,0,y,1,2,6,0);
            end;
      end;

tnnf:=tnn+75*startn+1;
for i:=1 step 1 until sectotal do begin
locate(tnnf,2);
r:=1011;
for p:=1 step 1 until 16 do
      begin inblock(aa,r,2);
            r:=r+64;
     end;
for p:=1 step 1 until 10 do
      begin ggg:=gg[p];
            for q:=510 step 10 until 1520 do
            begin y:=q+p+aa0;
                  elliott(0,0,y,1,3,0,0);
                  elliott(2,0,zzz,0,0,0,0);
                  zzz:=zzz*ggg;
                  elliott(3,0,zzz,0,0,0,0);
                  elliott(0,0,y,1,2,0,0);
            end;
      end;
r:=1011;
for p:=1 step 1 until 16 do
      begin outblock(aa,r,2);
            r:=r+64;
       end;
print ££12? blocknumber?,blocknumber;
tnnf:=tnnf+75;
                        end;

p8: for vc:=1 step 1 until nv1 do begin
   tnnf:=tnn+75*startn-75;
 for nb:=1 step 1 until sectotal do begin
tnnf:=tnnf+75;
   locate(tnnf,2);
   filmread(bb,2);
  if keybd2=2048 then goto p7;
```

```
    ttnnf:=tnnf+17;
locate(ttnnf,2);
r:=1011;
for p:=1 step 1 until 16 do
      begin inblock(aa,r,2);
            r:=r+64;
      end;
  ttnnf:=tnnf+73;
  locate(ttnnf,2);
   filmread(ee,2);
if keybd1=0 then print ££11?testee?,blocknumber;

if nb=1 or bb[5]≠0 then begin
if bb[3]=10 then s:=1 else s:=bb[3]+1;
for p:=1 step 1 until 10 do
      if s>p then cc[p]:=1 else cc[p]:=0;
      max:=min:=0;
      for j:=1 step 1 until 10 do
      begin rr:=entier(0.1*(dd[j]/vv[vc]-18+s-j));
            if rr-cc[j]>max then max:=rr-cc[j];
            if rr-cc[j]<min then min:=rr-cc[j];
            nnp[j]:=rr;
      end;
    print££11?max?,max,£min?,min;
      if max>45 or min<-45 then
            begin print ££13? delay overflow?;
                  wait;
            end;
t0:=entier((-max-1)/nn0)+1;
    t2:=entier((-min)/nn0);
     end of compound statement;
checks(£t set?);
p7: if vc=1 then begin if  nb=1 then begin print ££12?starttime?;
                                          pattern(bb[1],23);
                                    end
else  if endtime≠bb[1]then
            begin print ££13?time continuity error £s4?endtime?;
                  pattern(endtime,23);
                  wait;
            end;
end of statement;
if keybd2=2048 then goto p9;
      t1:=t2+11;
      t3:=t0+11;
      mm:=11+red00;
      nn:=11+blue00;
      if nb=1 then goto p3;
    checks(£stage 1?);
      for t:=t0 step 1 until t2 do
            begin sum;
                  y:=mm+t;
                  elliott(0,0,y,1,3,0,0);
                  elliott(2,0,xred,0,0,0,0);
                  y:=nn+t;
                  elliott(0,0,y,1,3,0,0);
                  elliott(2,0,xblue,0,0,0,0);
```

```
                ddred:=ddred+checkr(xred);
                ddblue:=ddblue+checkr(xblue);
                add and multiply;
            end;
p3:    for t:=t2+1 step 1 until t3-1 do
       begin sum;
             add and multiply;
       end;
     checks(£stage 2 complete ?);
       for t:=t3 step 1 until t1 do
       begin sum;
             y:=red00+t;
             elliott(3,0,ddred,0,0,0,0);
             elliott(0,0,y,1,2,0,0);
             y:=blue00+t;
             elliott(3,0,ddblue,0,0,0,0);
             elliott(0,0,y,1,2,0,0);
       end;
    checks(£stage 3 complete ?);

ee[1,vc]:=t0;
ee[2,vc]:=t2;
ee[3,vc]:=vv[vc]*1000;
ttnnf:=tnnf+vc*5+28;
locate(ttnnf,2);
filmwrite(addmul,2);
if keybd1=0 then print £test 4?,blocknumber;
p9:  if vc=1 then begin
 endtime:=bb[2];
       ee[4,1]:=nb-1;
       ee[4,2]:=bb[1];
       ee[4,3]:=bb[2];
 checks(£vc one ?);
       ee[4,4]:=bb[4];
ee[4,5]:=nv1;
ee[4,6]:=nn0;
ee[4,7]:=11;
ee[4,8]:=tnn;
ee[4,9]:=startn;
ee[4,10]:=endn;
ee[4,11]:=bb[3];  end;
ttnnf:=tnnf+73;
locate(ttnnf,2);
       filmwrite(ee,2);
       print ££12?ee blocknumber?, blocknumber;
checks(£end of nb loop?);
end of nb loop;
     elliott(0,6,0,0,7,0,0);
       elliott(0,3,cokey1,0,2,0,keybd1);
checks(£end of vc  loop?);

end of vc loop;
end of inner block;
end of programme;
end for film;
```

APPENDIX 9

Programme 3 - graph plotter output

Purpose

The function of the programme is to produce digital plotter output of the input signals, sum functions and/or cross-correlation functions for the processed data stored on film in second blocks starting at (TNN + 75. NSTART). The last second block starts at block (TNN + 75. NEND). One second corresponds to OURSTEP inches of the x - axis of the graph. The parameters GAINADD and GAINMULT for each velocity and GAINCHANNEL for each of the ten channels are used to scale the plotter output.

Control

The following control is exercised by the keyboard.

4096 DOWN to suppress plot of ADD function

2048 DOWN to suppress plot of MULTIPLY function

1024 DOWN to suppress plot of CHANNEL INPUT functions

Precompiled package

Precompiled packages have a limited size and a special precompiled unit containing the standard graph plotter package and as many procedures as possible from the film package has to be used. The remaining film procedures are included in the programme and are translated after the programme declarations.

Output

This early version of the graph plotter package gives 5 hole plotter output on channel one. The programme is written to give all other output on channel three (eight hole).

Scaling

The internal scaling (for unity gain parameters) is such that

for ADD, $\pm$ 6,000 gives $\pm$ 0.4 inches,

for MULTIPLY $\pm$ 3,000 gives $\pm$ 0.4 inches,

and for CHANNEL INPUTS $\pm$ 600 gives $\pm$ 0.6 inches.

Timing

It takes an hour and a quarter to produce the paper tape required to plot figures 28, 29 and 30.

Data tape

	TNN	NSTART	NEND	OURSTEP
if 4096 UP	GAINADD(1)	GAINADD(2)	.....	GAINADD(nv1)
if 2048 UP	GAINMULT(1)	GAINMULT(2)	.....	GAINMULT(nv1)
if 1024 UP	CHANNEL GAIN(1)	CHANNEL GAIN(2)	...	CHANNEL GAIN(10).

Specimen data tape used for simulation (figures 28, 29, 30).

```
100    0    1    2
 1     1    1    1    1    1
 1     1    1    1    1    1
 1     1    1    1    1    1    1    1    1    1
```

Flow diagram of programme 3

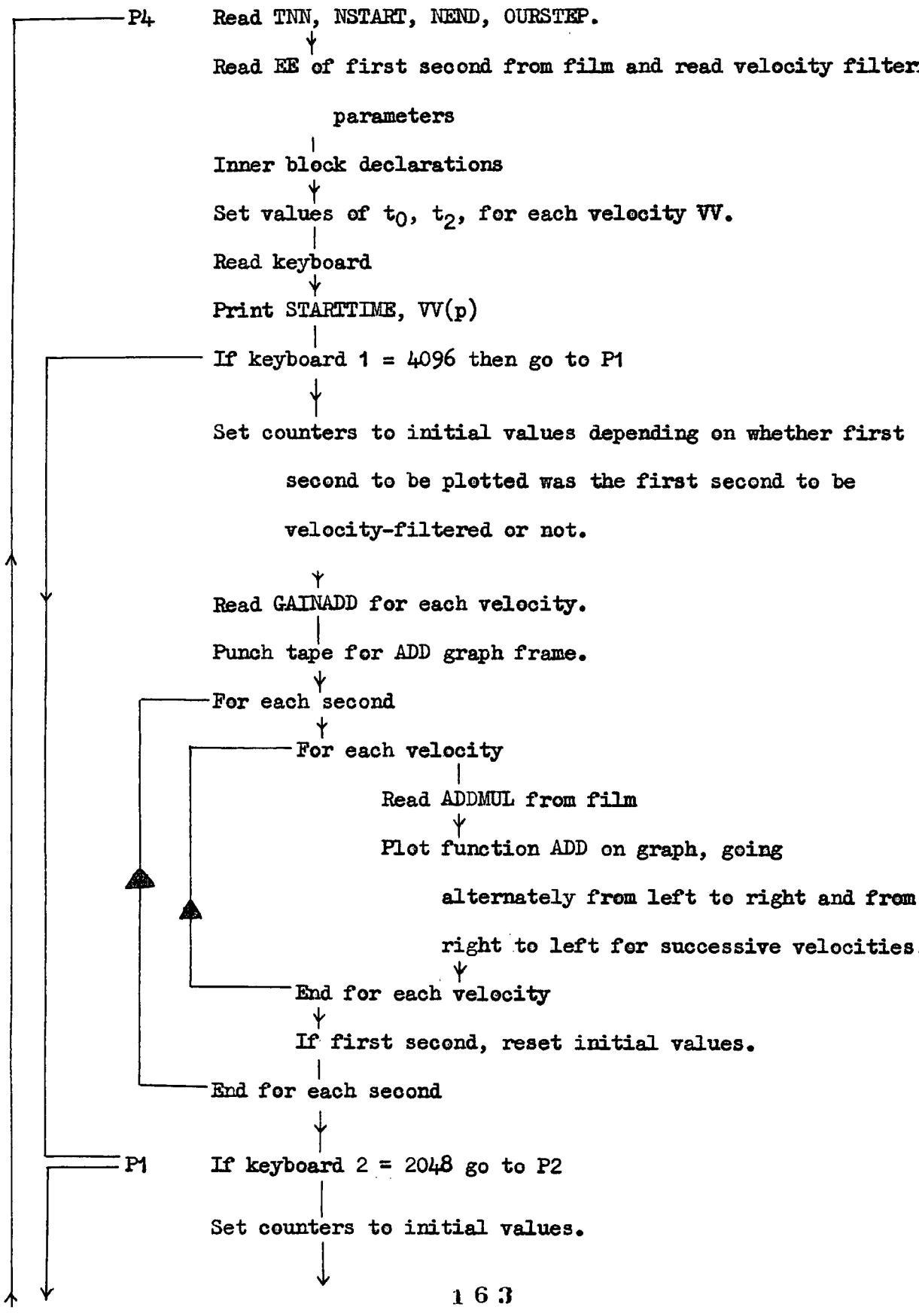

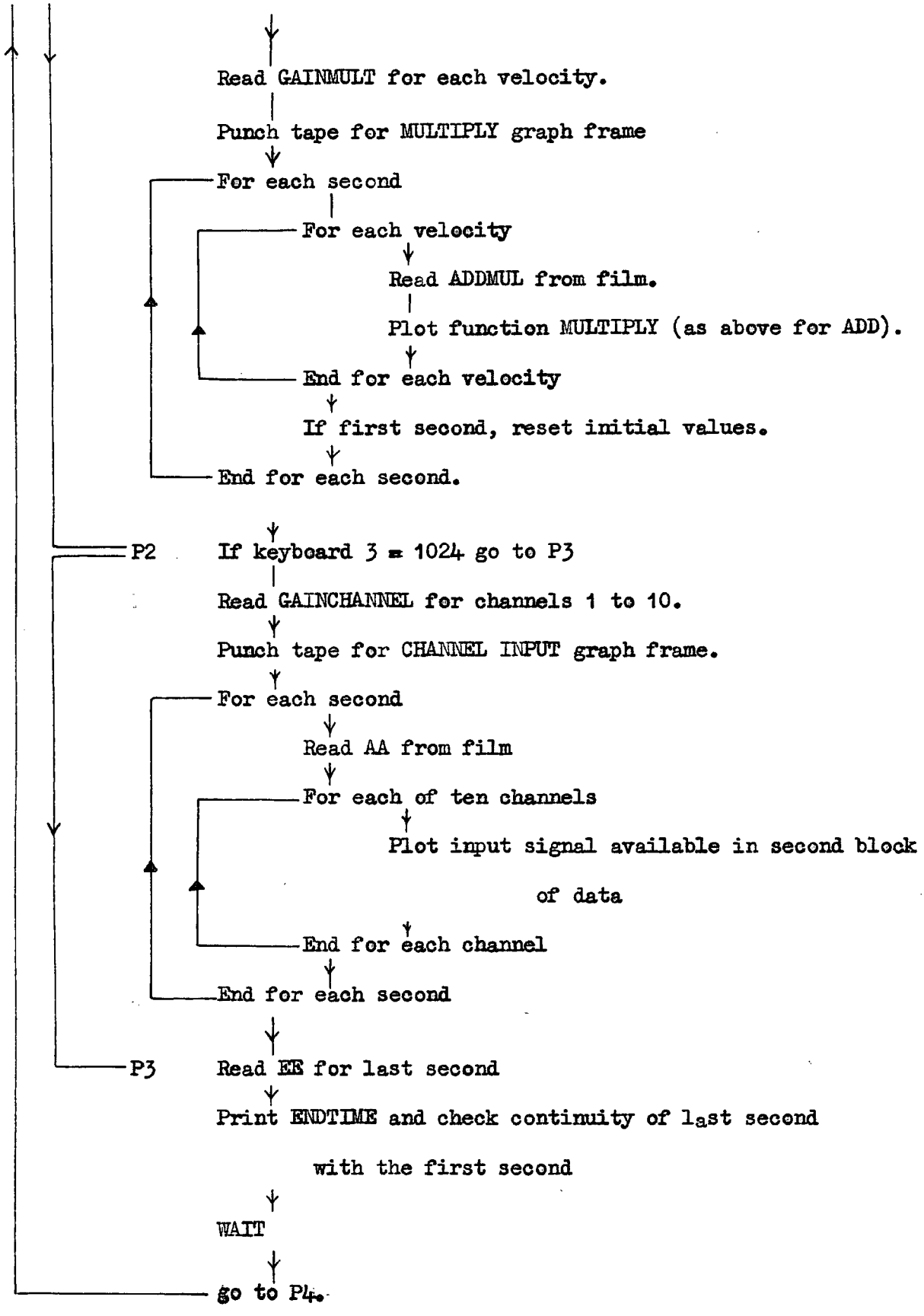
Read GAINMULT for each velocity.
Punch tape for MULTIPLY graph frame
For each second
For each velocity
Read ADDMUL from film.
Plot function MULTIPLY (as above for ADD).
End for each velocity
If first second, reset initial values.
End for each second.
P2
If keyboard 3 = 1024 go to P3
Read GAINCHANNEL for channels 1 to 10.
Punch tape for CHANNEL INPUT graph frame.
For each second
Read AA from film
For each of ten channels
Plot input signal available in second block of data
End for each channel
End for each second
P3
Read EE for last second
Print ENDTIME and check continuity of last second with the first second
WAIT
go to P4.

```
A.L.Lucas.  Programme 3 - Graph plotter output;

begin real x,y,step,ourstep,tend,xx,interval,zeroy,gain,signal;
      integer x0,y0,n,scale,nn,nnn,p,qq,tnn,nstart,nend,tnnf,
            starttime,nv1,nn0,ll,oldtnn,startn,endn,q,pp,cokey1,
            cokey2,cokey3,cokey4,keybd1,keybd2,keybd3,keybd4,xx0,
            ww,s,t,r,v,add0,mult0,u,z,j,aa0,lastci,first,endtime;
      real array b,a[1:101],gainchannel[1:10],aa[51:153,1:10];
      integer array ee[1:4,1:12],aaa[1:10];
      switch sssss:=p4;
      procedure pattern(word,n); value n; integer word,n;
            begin integer mask,m,store1,store2;
                  mask:=1;
            for m:=n-1 step -1 until 0 do
                  begin store1:=word;
                        elliott(3,0,store1,0,0,0,0);
                        elliott(0,0,m,1,5,1,0);
                        elliott(0,3,mask,0,2,0,store2);
                        elliott(0,0,store2,1,7,4,4112);
                  end;
      end;

INSERT  REMAINING  FILM  PROCEDURES

punch(3);sameline;
p4:  read tnn,nstart,nend,ourstep;
      nn:=nend-nstart+1;
      tnnf:=tnn+75*nstart+73;
      locate(tnnf,2);
      filmread(ee,2); print ££11? blocknumber?, blocknumber;
      starttime:=ee[4,2];
      nv1:=ee[4,5];
      nn0:=ee[4,6];
      ll:=ee[4,7];
      oldtnn:=ee[4,8];
      startn:=ee[4,9];
      endn:=ee[4,10];
      if oldtnn≠ tnn then
      begin print ££13? tnn error?, tnn,oldtnn;
            wait;
      end;
if endn<nend then
      begin print ££13? future time continuity error £11??, endn,nend;
            wait;
      end;
      begin real array vv[1:nv1],addmul[1:2,-50:101],
            gainadd,gainmult[1:nv1];
            integer array tt0,tt2,tt5,ttt[1:nv1];
            switch ss:=p1,p2,p3;
```

```
procedure frame1(nn,ourstep,nnn,x0);
      real ourstep; integer nn,nnn,x0;
      begin switch sss:=p11,p12;
            origin(x0-penx/200,-peny/200);
            xaxis(2,.1,ourstep,nn);
            tend:=2+ourstep*nn;
            xx:=tend+1;
            writex(xx,0.1,5,£seconds?);
            for pp:=1 step 1 until 10 do begin a[pp]:=tend;
                  b[pp]:=-.5+pp;
                  end;
            plot(a,b,10,10,£+?);
            xx:=tend+0.4; qq:=1;
p12:     writex(xx,9.4,5,£10?);
      writex(xx,8.4,5,£9?);
      writex(xx,7.4,5,£8?);
      writex(xx,6.4,5,£7?);
      writex(xx,5.4,5,£6?);
      writex(xx,4.4,5,£5?);
      writex(xx,3.4,5,£4?);
      writex(xx,2.4,5,£3?);
      writex(xx,1.4,5,£2?);
      writex(xx,0.4,5,£1?);
      if qq=0 then goto p11;
            step:=-ourstep;
            xaxis(tend,9.9,step,nn);
            qq:=0; xx:=1.5;
            goto p12;
p11:  for pp:=1 step 1 until 10 do a[pp]:=2;
      plot(a,b,10,10,£+?);
      if nnn=0 then
      begin writex(-1,7,6,£  sum(t)?);
            writex(-1,6.5,6,£   for?);
            writex(-1,6,6,£different?);
            writex(-1,5.5,6,£  tuning?);
            writex(-1,5,6,£velocities?);
      end;
      if nnn=1 then
      begin writex(-2,7,6,£    cross?);
            writex(-2,6.5,6,£ correlation?);
            writex(-2,6,6,£time function?);
            writex(-2,5.5,6,£for different?);
            writex(-2,5,6,£    tuning?);
            writex(-2,4.5,6,£ velocities?);
      end;
     if nnn=2 then
begin writex(-1,7,6,£channel?);
      writex(-1,6,6,£ input?);
      writex(-1,5,6,£signals?);
end;
end of procedure;
```

```
for p:=1 step 1 until nv1 do
begin tt0[p]:=ee[1,p];
      tt2[p]:=ee[2,p];
      vv[p]:=ee[3,p]/1000;
end;
keybd1:=4096;  keybd2:=2048;
keybd3:=1024;  keybd4:=512;
penx:=peny:=0;
wait;
elliott(0,6,0,0,7,0,0);
elliott(2,3,keybd1,0,2,3,keybd2);
elliott(2,3,keybd3,0,2,3,keybd4);

print££13? starttime?; pattern(starttime,23);
for p:=1 step 1 until nv1 do print ££11??,vv[p];
x0:=3; tend:=0;
      lastci:=ee[4,11];
if lastci=10 then first:=1 else first:=lastci+1;
for p:=1 step 1 until 10 do
if p<first then aaa[p]:=10 else aaa[p]:=0;
interval:=ourstep/11;
for p:=1 step 1 until nv1 do tt5[p]:=tt0[p]+11-1;
if keybd1=4096 then goto p1;
if nstart=startn then for p:=1 step 1 until nv1 do ttt[p]:=tt2[p]
                        +1
      else for p:=1 step 1 until nv1 do ttt[p]:=0;
add0:=address(addmul)+50;
for p:=1 step 1 until nv1 do
begin read gainadd[p];
      gainadd[p]:=gainadd[p]*2↑10-4/3;
end;
frame1(nn,ourstep,0,x0);
for q:=1 step 1 until nn do
begin xx0:=2-ourstep+q*ourstep;
     tnnf:=tnn+75*(nstart-1+q)+33;
      locate(tnnf,2);
      ww:=+1;
for p:=1 step 1 until nv1 do
begin gain:=gainadd[p]; r:=ttt[p];
      zeroy:=-.5+p; v:=tt5[p];
s:=1;
filmread(addmul,2);
if ww=+1 then
begin for t:=r step 1 until v do
      begin a[s]:=t*interval+xx0;
            z:=t+add0;
            elliott(0,0,z,1,3,0,0);
            elliott(2,0,signal,0,0,0,0);
            b[s]:=signal*gain+zeroy;
            s:=s+1;
      end;
      s:=s-1;
      plot(a,b,s,1,2.?);
end;
```

```
if ww=-1 then
begin for t:=v step -1 until r do
      begin a[s]:=t*interval+xx0;
            z:=t+add0;
            elliott(0,0,z,1,3,0,0);
            elliott(2,0,signal,0,0,0,0);
            b[s]:=signal*gain+zeroy;
            s:=s+1;
      end;
      s:=s-1;
      plot(a,b,s,1,£+?);
end;
ww:=-1*ww;
end;
if q=1 then for j:=1 step 1 until nv1 do ttt[j]:=tt0[j];
end;

p1:  if keybd2=2048 then goto p2;
      if nstart=startn then for p:=1 step 1 until nv1 do
            ttt[p]:=tt2[p]+1
      else for p:=1 step 1 until nv1 do ttt[p]:=0;
      mult0:=address(addmul)+202;
      for p:=1 step 1 until nv1 do
      begin read gainmult[p];
            gainmult[p]:=gainmult[p]*4₁₀-4/3;
      end;
      x0:=tend+8;
      frame1(nn,ourstep,1,x0);
      for q:=1 step 1 until nn do
      begin xx0:=2-ourstep+q*ourstep;
     tnnf:=tnn+75*(nstart-1+q)+33;
      locate(tnnf,2);
      ww:=+1;
      for p:=1 step 1 until nv1 do
      begin gain:=gainmult[p]; r:=ttt[p];
            zeroy:=-.5+p; v:=tt5[p];
            s:=1;     filmread(addmul,2);
      if ww=+1 then
            begin for t:=r step 1 until v do
                  begin a[s]:=t*interval+xx0;
                        z:=t+mult0;
                  elliott(0,0,z,1,3,0,0);
                  elliott(2,0,signal,0,0,0,0);
                  b[s]:=signal*gain+zeroy;
                  s:=s+1;
            end;
            s:=s-1;
            plot(a,b,s,1,£.?);
      end;
```

```
if ww=-1 then
      begin for t:=v step -1 until r do
            begin a[s]:=t*interval+xx0;
                  z:=t+mult0;
                  elliott(0,0,z,1,3,0,0);
                  elliott(2,0,signal,0,0,0,0);
                  b[s]:=signal*gain+zeroy;
                  s:=s+1;
            end;
            s:=s-1;
            plot(a,b,s,1,£+?);
      end;
      ww:=ww*(-1);
end;
if q=1 then for j:=1 step 1 until nv1 do ttt[j]:=tt0[j];
end;
p2:  if keybd3=1024 then goto p3;
      aa0:=address(aa)-1;
      interval:=ourstep/1000;
      for p:=1 step 1 until 10 do
      begin read gainchannel[p];
            gainchannel[p]:=gainchannel[p]*1_10-3;
      end;
      x0:=tend+8;
      frame1(nn,ourstep,2,x0);
      for q:=1 step 1 until nn do
      begin xx0:=2-ourstep+q*ourstep;
       tnnf:=tnn+75*(nstart-1+q)+1;
      locate(tnnf,2);
      filmread(aa,2);
      ww:=+1;
      for p:=1 step 1 until 10 do
      begin gain:=gainchannel[p];
            zeroy:=-0.5+p;
      s:=1;
      r:=aaa[p];
      if ww=+1 then
      begin for t:=0 step 10 until 990 do
      begin a[s]:=(23-first+r+p+t)*interval+xx0;
            z:=aa0+r+t+p;
            elliott(0,0,z,1,3,0,0);
            elliott(2,0,signal,0,0,0,0);
            b[s]:=signal*gain+zeroy;
            s:=s+1;
      end;
      s:=s-1;
      plot(a,b,s,1,£.?);
end;
```

```
if ww=-1 then
      begin for t:=990 step -10 until 0 do
      begin a[s]:=(23-first+r+p+t)*interval+xx0;
            z:=aa0+r+t+p;
            elliott(0,0,z,1,3,0,0);
            elliott(2,0,signal,0,0,0,0);
            b[s]:=signal*gain+zeroy;
            s:=s+1;
      end;
      s:=s-1;
      plot(a,b,s,1,£+?);
end;
ww:=ww*(-1);
end;
end;
p3:    tnnf:=tnn+75*nend+73;
      locate(tnnf,2);
      filmread(ee,2);
      print££11?blocknumber?,blocknumber;
      endtime:=ee[4,3];
      print ££13? endtime?;
      pattern(endtime,23);
      if lastci≠ee[4,11]then print ££13? lastci not continuous?;
      print £end of run?;
      wait;
      goto p4;
      end of inner block;
      end of programme;
      end for precompiled package;
       end also for precompiled package which  contains  both
             plotter and film  packages;
```

APPENDIX 10

Miniature frame and miniature graph plotter output programmes

Purpose

The object of these programmes is to produce a quicker plotter output of the MULTIPLY functions only in the form shown in figure 31. The routine 'frame' function is separated from the graph plot function, which is a degenerate form of programme 3. The extent to which the size of the graph may be reduced is limited by the plotter increments of 0.005 inches.

MINIATURE FRAME PROGRAMME

This programme uses the final form of the graph plotter package DP301, in which the plotter output is on channel 2 (5 hole).

XSTEP is the x distance in inches per second,

YSTEP is the y distance in inches per plot,

(XZERO, YZERO) is the origin of the graph in inches,

and NN is the number of seconds.

Data tape

XSTEP YSTEP XZERO YZERO NN

Specimen data tape (frame of figure 31)

0.5 0.25 0 0 2

MINIATURE GRAPH PLOTTER OUTPUT

This is a degenerate form of programme three giving the cross-correlation functions only. Consequently, the arrangements of the precompiled input packages and of the output channels are the same as programme 3.

Data tape

TNN NSTART NEND

OURSTEP YSTEP XZERO YZERO

GAINMULT(1) GAINMULT(2) ..... GAINMULT(nv1)

Specimen data tape (figure 31)

100 0 1

0.5 0.25 0 0

1 1 1 1 1 1

```
miniature frame  a.lucas;

begin real xstep,ystep,xzero,tend,yzero,xend,ytop;
      integer nn,p;
      array a,b[1:10];
      read xstep,ystep,xzero,yzero,nn;
      origin(xzero,yzero);
      xaxis(0,0,xstep,nn);
      tend:=xstep*nn;
      for p:=1 step 1 until 10 do begin a[p]:=tend;
                                        b[p]:=p*ystep;
                                  end;
      plot(a,b,1,10,5,£+?);
      ytop:=11*ystep;
      xaxis(tend,ytop,-xstep,nn);
      for p:=1 step 1 until 10 do begin a[p]:=0;
                                        b[p]:=(11-p)*ystep;
                                  end;
      plot(a,b,1,10,5,£+?);
      a[1]:=b[1]:=0;
      plot(a,b,1,1,1,£.?);
      end;
      end;
```

```
A.L.Lucas. miniature graph plotter o.p. cross  correlation;

begin real x,y,step,ourstep,tend,xx,interval,ystep,xzero,yzero,
            zeroy,gain,signal;
      integer x0,y0,n,scale,nn,nnn,p,qq,tnn,nstart,nend,tnnf,
    a0,b0,        starttime,nv1,nn0,l1,oldtnn,startn,endn,q,pp,cokey1,
          cokey2,cokey3,cokey4,keybd1,keybd2,keybd3,keybd4,xx0,
          ww,s,t,r,v,add0,mult0,u,z,j,aa0,lastci,first,endtime;
      real array b,a[1:101],gainchannel[1:10],aa[51:153,1:10];
      integer array ee[1:4,1:12],aaa[1:10];
      switch sssss:=p4;
      procedure pattern(word,n); value n; integer word,n;
            begin integer mask,m,store1,store2;
                  mask:=1;
            for m:=n-1 step -1 until 0 do
                  begin store1:=word;
                        elliott(3,0,store1,0,0,0,0);
                        elliott(0,0,m,1,5,1,0);
                        elliott(0,3,mask,0,2,0,store2);
                        elliott(0,0,store2,1,7,4,4112);
                  end;
      end;

INSERT  REMAINING  FILM  PROCEDURES

punch(3);sameline;

p4:  read tnn,nstart,nend,ourstep,ystep,xzero,yzero;
      nn:=nend-nstart+1;
      tnnf:=tnn+75*nstart+73;
      locate(tnnf,2);
      filmread(ee,2); print ££11? blocknumber?, blocknumber;
      starttime:=ee[4,2];
      nv1:=ee[4,5];
      nn0:=ee[4,6];
      l1:=ee[4,7];
      oldtnn:=ee[4,8];
      startn:=ee[4,9];
      endn:=ee[4,10];
      if oldtnn≠ tnn then
      begin print ££13? tnn error?, tnn,oldtnn;
            wait;
      end;
if endn<nend then
      begin print ££13? future time continuity error £11??, endn,nend;
            wait;
      end;
      begin real array vv[1:nv1],addmul[1:2,-50:101],
            gainadd,gainmult[1:nv1];
            integer array tt0,tt2,tt5,ttt[1:nv1];
            switch ss:=p1,p2,p3;
```

```
for p:=1 step 1 until nv1 do
begin tt0[p]:=ee[1,p];
      tt2[p]:=ee[2,p];
      vv[p]:=ee[3,p]/1000;
end;
keybd1:=4096;  keybd2:=2048;
keybd3:=1024;  keybd4:=512;
penx:=peny:=0;
wait;
elliott(0,6,0,0,7,0,0);
elliott(2,3,keybd1,0,2,3,keybd2);
elliott(2,3,keybd3,0,2,3,keybd4);

print££13? starttime?; pattern(starttime,23);
for p:=1 step 1 until nv1 do print ££11??,vv[p];
x0:=3; tend:=0;
      lastci:=ee[4,11];
if lastci=10 then first:=1 else first:=lastci+1;
for p:=1 step 1 until 10 do
if p<first then aaa[p]:=10 else aaa[p]:=0;
interval:=ourstep/11;
for p:=1 step 1 until nv1 do tt5[p]:=tt0[p]+11-1;

      if nstart=startn then for p:=1 step 1 until nv1 do
            ttt[p]:=tt2[p]+1
      else for p:=1 step 1 until nv1 do ttt[p]:=0;
      mult0:=address(addmul)+202;
      for p:=1 step 1 until nv1 do
      begin read gainmult[p];
            gainmult[p]:=gainmult[p]*ystep/2500;
      end;

origin(xzero,yzero);
a0:=address(a)-1;
b0:=address(b)-1;
for q:=1 step 1 until nn do begin
tnnf:=tnn+75*(nstart-1+q)+33;
locate(tnnf,2);  ww:=+1;
for p:=1 step 1 until nv1 do begin
gain:=gainmult[p];  s:=1;
filmread(addmul,2);
origin(-penx/200,ystep-peny/200);
if ww=+1 then begin r:=ttt[p];  v:=tt5[p];  end
          else begin r:=tt5[p];  v:=ttt[p];  end;
for t:=r step ww until v do begin
      signal:=t*interval;
      z:=a0+s;
      elliott(3,0,signal,0,0,0,0);~
      elliott(0,0,z,1,2,0,0);
```

```
        z:=t+mult0;
        elliott(0,0,z,1,3,0,0);
        elliott(2,0,signal,0,0,0,0);
        signal:=signal*gain;
        z:=b0+s;
        elliott(3,0,signal,0,0,0,0);
        elliott(0,0,z,1,2,0,0);
        s:=s+1;
        end;
        s:=s-1;
        plot(a,b,s,1,£.?);
        ww:=ww*(-1);
        end;
        signal:=nv1*ystep;
        origin(ourstep-penx/200,-signal-peny/200);
if q=1 then for j:=1 step 1 until nv1 do ttt[j]:=tt0[j];
        end;  a[1]:=-nn*ourstep;  b[1]:=0;
        plot(a,b,1,1,£.?);

     tnnf:=tnn+75*nend+73;
        locate(tnnf,2);
        filmread(ee,2);
        print££11?blocknumber?,blocknumber;
        endtime:=ee[4,3];
        print ££13? endtime?;
        pattern(endtime,23);
        if lastci≠ee[4,11]then print ££13? lastci not continuous?;
        print £end of run?;
        wait;
        goto p4;
        end of inner block;
        end of programme;
        end for precompiled package;
         end also for precompiled package which  contains  both
                plotter and film  packages;
```

APPENDIX 11

Maximum Correlation Programme

Purpose

This programme examines the results of the velocity filtering calculation on the film and, at each computation point, picks out the velocity with the maximum value of the MULTIPLY function, and prints out the number of the velocity and the corresponding value of the MULTIPLY function.

The results for the simulated data are shown in figure 32. These results, which have been fully checked, indicate the difficulty of using this type of programme for interpretation.

Data tape

TNN	NSTART	NEND

Specimen data tape for simulated data (figure 32)

100	0	1

```
maximum correlation programme A.Lucas;


begin real vv,element,mulmax;
      integer tnn,nstart,nend,tnnf,starttime,nv1,l1,tsec,endn,oldtnn,
      startn,p,q,t,maxstart,ttt,tttt,ttnnf,low,high,z,y,pp,mul0,
      cross0,mint3,minend,seccount,tt0,pmax;
      array addmul[1:2,-50:101],cross[1:8,-50:101];
      integer array ee[1:4,1:12],tt,t0,t2,t3,count[1:8];

    procedure pattern(word,n); value n; integer word,n;
            begin integer mask,m,store1,store2;
                  mask:=1;
                  for m:=n-1 step -1 until 0 do
                  begin store1:=word;
                  elliott(3,0,store1,0,0,0,0);
                  elliott(0,0,m,1,5,1,0);
                  elliott(0,3,mask,0,2,0,store2);
                  elliott(0,0,store2,1,7,4,16);
                  end;
            end;

sameline; aligned(2,2);
read tnn,nstart,nend;
mul0:=address(addmul)+202;cross0:=address(cross)-102;
tnnf:=tnn+75*nstart+73; tt0:=address(tt)-1;
locate(tnnf,2);filmread(ee,2);tnnf:=tnn+75*nstart;
starttime:=ee[4,2];
nv1:=ee[4,5];l1:=ee[4,7]; startn:=ee[4,9];
oldtnn:=ee[4,8]; endn:=ee[4,10];
if tnn≠oldtnn then begin print ££12?tnn error?;
                                wait; end;
if nstart<startn or nend>endn
          then begin print ££12? processing time discontinuity?;
                           wait;end;
maxstart:=-50;mint3:=100;
print ££12?velocities?;
      checks(£enter p loop?);


for p:=1 step 1 until nv1 do begin
     t0[p]:=ee[1,p]; t2[p]:=ee[2,p];
    vv:=ee[3,p]/1000; print ££11??,vv;
    t3[p]:=t0[p]+l1;
    if nstart>startn then begin
       if t0[p]>maxstart then maxstart:=t0[p]; end
    else if t2[p]>maxstart-1 then maxstart:=t2[p]+1;
if t3[p]<mint3 then mint3:=t3[p];
    ttnnf:=tnnf+28+5*p;
    locate(ttnnf,2); filmread(addmul,2);
    high:=t3[p]-1;pp:=p*152+cross0;
    count[p]:=0;
```

```
    for ttt:=maxstart step 1 until high do begin
        z:=ttt+mul0; y:=pp+ttt;
        elliott(0,0,z,1,3,0,0);
        elliott(0,0,y,1,2,0,0); end;
end of p loop;
checks(£exit p loop?);
minend:=(nend-nstart)*11+checki(mint3)-1;
tsec:=checki(maxstart); seccount:=0;

print ££12??;
aligned(4,0);


for p:=1 step 1 until nv1 do tt[p]:=maxstart;
digits(2);
for t:=maxstart step 1 until minend do begin


if tsec=11 then begin
    tsec:=0; seccount:=checki(seccount)+1;
    ttnnf:=tnnf+75*seccount+73;
    locate(ttnnf,2);filmread(ee,2);
    print ££12?second marker?; pattern(ee[4,2],23);
   end;
for p:=1 step 1 until nv1 do begin
     if tt[p]>t3[p] then begin
       count[p]:=checki(count[p])+1;
       tt[p]:=t0[p];
       ttnnf:=tnnf+75*count[p]+28+5*checki(p);
       locate(ttnnf,2);filmread(addmul,2);
       low:=t0[p];high:=t3[p]-1;pp:=p*152+cross0;
       for ttt:=low step 1 until high do begin
           z:=ttt+mul0;y:=pp+ttt;
           elliott(0,0,z,1,3,0,0);
           elliott(0,0,y,1,2,0,0); end;
       end;
       tttt:=tt[p];
       z:=p*152+tttt+cross0;
       elliott(0,0,z,1,3,0,0);
       elliott(2,0,element,0,0,0,0);
       if p≠1 then begin if element>mulmax then begin
           mulmax:=element;pmax:=p;end;end
       else begin pmax:=1;mulmax:=element;end;
       tt[p]:=tttt+1;
       end of p loop;
       print pmax,mulmax;
       if tsec=5*entier(tsec/5) then print ££11??;
       tsec:=tsec+1;
       end;end;end;
```

APPENDIX 12

Programme 4 - data tape simulation

Purpose

The object of this programme is to simulate NBO seconds of seismic array paper tape corresponding to a square pulse crossing the array each second. There is no system parity generator in the programme, so that if a full simulation is required, it is necessary to select both signal levels of all channels except number two to have an even number of '1' in the ten A.D.C. bits, and to select both levels of channel two to have an odd number of '1'. Alternatively, the parity check in programme I could be suppressed.

Notation

AA(p), BB(p), (p = 1, 2, ... 10), are the two signal levels of channel p, and DD(p) is the delay distance of channel p in metres.
V is the assumed velocity of the pulse in km/sec.
CITO is the channel of the first sample of the second.
TSTART is the starting time, in milliseconds, referred to the array reference point of the pulse with signal levels BB(p).
TEND is the end time, in milliseconds, referred to the array reference point of the above pulse.

Data tape

AA(1)	BB(1)
AA(2)	BB(2)
"	"
"	"
"	"
AA(10)	BB(10)

DD(1) DD(2) DD(3) DD(4) DD(5) ..... DD(10)

V CITO TSTART TEND NBO

Specimen data tape used for simulation

513	960	512	961
516	963	520	966
528	972	544	984
510	1008	550	975
526	990	534	1023

1500	1200	900	600	300
0	-300	-600	-900	-1200

6	2	475	525	2

```
A.L.Lucas  Programme 4  Data tape simulation;
begin integer array aa,bb,ttstart,ttend,dd,fca,fcb,sca,scb[1:10];
      integer col1,col2,word1,word2,word3,char1,p,char2,v,t,cit0,
            tstart,tend,nb0,ciring,nb,cibit,tcbit,parity;
      switch ss:=p1,p2,p3;
      col1:=992;
      col2:=31;
      for p:=1 step 1 until 10 do read aa[p],bb[p];
      for p:=1 step 1 until 10 do read dd[p];
      wait;
      read v,cit0,tstart,tend,nb0;
      for p:=1 step 1 until 10 do
            begin ttstart[p]:=entier(tstart+dd[p]/v+0.5);
                  ttend[p]:=entier(tend+dd[p]/v+0.5);
                  end;
      for p:=1 step 1 until 10 do
      begin word1:=aa[p];
            elliott(0,6,0,0,3,0,word1);
            elliott(0,3,col1,0,5,1,3);
            elliott(2,0,word3,0,0,0,0);
            fca[p]:=word3+1;
                  word2:=bb[p];
            elliott(0,6,0,0,3,0,word2);
            elliott(0,3,col1,0,5,1,3);
            elliott(2,0,word3,0,0,0,0);
                  fcb[p]:=word3+1;
            elliott(0,6,0,0,3,0,word1);
            elliott(0,3,col2,0,5,5,2);
            elliott(2,0,word3,0,0,0,0);
                  sca[p]:=word3;
            elliott(0,6,0,0,3,0,word2);
            elliott(0,3,col2,0,5,5,2);
            elliott(2,0,word3,0,0,0,0);
                  scb[p]:=word3;
      end;
      t:=950;
      ciring:=cit0;
      nb:=-1;
p3:   if ciring=2 then cibit:=2 else cibit:=0;
      if t=0 or t=2 or t=22 then tcbit:=1
            else tcbit:=0;
      if tcbit=1 then parity:=2 else parity:=0;
if t>ttstart[ciring] and t<ttend[ciring] then goto p1;
      char1:=fca[ciring]+parity;
      char2:=sca[ciring]+cibit+tcbit;
      goto p2;
p1:   char1:=fcb[ciring]+parity;
      char2:=scb[ciring]+cibit+tcbit;
p2:   elliott(0,0,char1,1,7,4,0);
      if t=999 then t:=0 else t:=t+1;
      if ciring=10 then ciring:=1 else ciring:=ciring+1;
      if t=0 then nb:=nb+1;
      elliott(0,0,char2,1,7,4,0);
      if nb=nb0 and t=30 then stop;
      goto p3;
end of programme;
```

APPENDIX 13

Example of calibration (calculated)

Nominal geophone sensitivity for damping 0·56 critical :-

0·70 volts/cm/sec at 3 c/s

0·96 volts/cm/sec at 6 c/s

0·78 volts/cm/sec at 20 c/s .

A.D.C. sensitivity :- 1 volt input ≡ 113 units output.

Standard effective line length of Feldom array :- 1600 yards.

Calculate nominal sensitivity of channel one for shot 11 at 6 c/s :-

Main amplifier gain 1000

Channel attenuator x 8 (i.e. ÷ 2)

D.A.C. channel calibration :- 102 3 units ≡ 4·8 cm.

Then 1 cm. of D.A.C. deflection is equivalent to 1·90 volts at the A.D.C. input,

and the nominal analogue channel gain = $200 \cdot 1000 \cdot \frac{1}{2} \cdot \frac{1200}{1565}$

= 77,000,

so 1 cm. deflection is equivalent to a ground velocity of $2{\cdot}6\ 10^{-5}$ cm/sec. This is equivalent to a displacement of $0{\cdot}7\ 10^{-6}$ cm. at 6 c/s.

Similarly, at 3 c/s, a deflection of 1 cm. is equivalent to a ground velocity of $3{\cdot}6\ 10^{-5}$ cm/sec and a displacement of $1{\cdot}9\ 10^{-6}$ cm. The microseismic noise level on this channel is about 0.5 cm. peak-to-peak at about 4 c/s, which corresponds to approximately 10 millimicrons (p-to-p). When considering this figure it must be remembered that the geophones were selected to attenuate frequencies below 3 c/s.

APPENDIX 14

Results at Feldom for first arrivals at ranges of about 280 kilometres

Shot No.	Range in kilometres	Azimuth in degrees	Travel time in seconds
9 A			A
9 B	265.9	228.8	40.35
8	281.9	227.2	42.75
7	295.0	227.4	B
6	308.1	227.8	B
1	322.2	228.2	B
5	332.4	228.5	B
4	346.1	228.8	B
3	359.6	229.0	B
2	373.4	229.4	B
10	284.7	219.4	42.6
11	283.5	222.0	42.5
12	282.3	224.6	42.0
13	282.5	229.7	42.0
17	282.2	232.6	42.3
14	283.0	235.1	42.4
15	284.6	237.6	45.7
16	287.6	240.1	42.5
18	288.0	243.2	44.0
19	276.2	242.3	40.8
20	268.5	244.1	40.3
21	260.4	246.0	38.9
22			A
23			A
24			A

A - system not running at the time of the shot.

B - not possible to read this phase.

II STRESS SYSTEMS IN AN INHOMOGENEOUS CRUST.

CONTENTS

FIGURES

TABLE

CHAPTER I

THE APPLICATION OF THE MATHEMATICAL THEORY OF ELASTICITY TO CRUSTAL PROCESSES

(1) Introduction

Field observations of the faulting and folding of originally horizontal strata are the most obvious indication that large stress differences must at some time occur in the crust of the Earth. Many workers have studied the mechanisms of failure under conditions of stress. The simplest theoretical treatment of the deformation of matter is the mathematical theory of elasticity for the infinitesimal strain of perfectly elastic isotropic materials. This theory is built up from the initial assumption that the components of strain are homogeneous linear functions of the components of stress and vice versa. These simple assumptions allow a great number of static and dynamic problems to be considered. Other theories consider finite strains or anisotropic materials, but as the complexity of the model increases so the mathematical difficulties limit the range of successful applications. The behaviour of actual materials depart in different ways and to different extents from the elastic model, and crustal processes clearly involve finite strains, but nevertheless the elastic theory may be applied as a first approximation in order to study the onset of deformation in the crust.

Two models that have been used for the crust and upper mantle as opposed to the whole Earth are the plane strain solutions for the semi-infinite half-space with various surface loads and the solid crust resting on a substratum of negligible strength (Jeffreys, 1962). An alternative approach used by Hafner (1951) is to consider stress systems within crustal blocks due to various

boundary stresses. The location of likely failure and the probable mode of failure can be determined from the stress distribution by the application of an appropriate criterion. Further data on crustal stress systems has been derived from direct measurements of stress in mine shafts and from well fracture data. Also there have been model experiments to support the theoretical investigations of the relationships between the stress distributions supposed to exist in the crust, the criteria for failure and the mechanisms of non-elastic geological processes. Indeed, much of the great volume of work currently being carried out under the international Upper Mantle Project is of some relevance to the particular problem of crustal processes.

The purpose of the present work is to extend the plane strain half-space model to include the case of a half-space in which there are discrete variations in density over rectangular areas of the cross section and in which there is therefore a stress distribution due to variable gravitational body forces. Thus in this work an inhomogeneous crust is isotropic and is homogeneous with respect to the two elastic parameters which therefore fully describe its elasticity, but is inhomogeneous as regards density. This independence of the density and the elastic constants follows from the equations of the plane theory of elasticity (Muskhelishvili, 1953, § 28). Recently Durney (1965) has published a paper concerned with the same problem in which he considers generalized harmonic variations of density and topographical surface irregularities. The approach used in the present work only permits static models to be considered and does not allow the sequence of deformation of one structural situation to be traced with time. A subjective study of this type of sequence might be made by considering a series of different models. The results will be used to calculate the stress distributions caused by isolated density anomalies such as granite batholiths and by surface loads with isostatic compensation at depth.

(ii) The mathematical theory of elasticity

The aim of this section is to introduce without proof the equations of the mathematical theory of elasticity for an isotropic, elastic solid. A comprehensive account of this theory is given by Love (1927). Finally, a brief review is given of the results for concentrated forces acting within a semi-infinite, elastic half-space.

The six independent components of the symmetrical stress tensor are $\hat{xx}$, $\hat{yy}$, $\hat{zz}$, $\hat{yz}$, $\hat{zx}$ and $\hat{xy}$. The components $\hat{yz}$, $\hat{zx}$ and $\hat{xy}$ are called "shear components of stress". At any point within an elastic body it is always possible to define a set of mutually perpendicular directions, called "principal directions" such that the shear components referred to these directions are zero. The corresponding normal stress components are the "principal stresses" $\hat{pp}_{11}$, $\hat{pp}_{22}$ and $\hat{pp}_{33}$. Throughout this work positive normal stresses are tensile stresses, and negative normal stresses are compressive stresses. The greatest shear stress occurring at a point is equal to half the difference between the greatest and least principal stress and occurs across a plane whose normal bisects the angle between the directions of greatest and least principal stress. The most elegant representation of the variation of normal and shear stress at a point is Mohr's circle diagram, described for example by Jaeger (1962).

In a body in equilibrium under body forces equal to (X,Y,Z) per unit of volume and under surface tractions, the components of stress satisfy the following equations at every point in the body:

$$\frac{\partial \hat{xx}}{\partial x} + \frac{\partial \hat{xy}}{\partial y} + \frac{\partial \hat{zx}}{\partial z} + X = 0 \quad ,$$

$$\frac{\partial \hat{xy}}{\partial x} + \frac{\partial \hat{yy}}{\partial y} + \frac{\partial \hat{yz}}{\partial z} + Y = 0 \quad ,$$

$$\frac{\partial \hat{zx}}{\partial x} + \frac{\partial \hat{yz}}{\partial y} + \frac{\partial \hat{zz}}{\partial z} + Z = 0 \quad .$$

These are the "equations of equilibrium".

The relative displacement (U, V, W) at a point may be represented as the sum of a rigid body anti-symmetric component and of a pure strain component associated with some internal deformation of the material. The six components of the symmetrical strain tensor are denoted by e_{xx}, e_{yy}, e_{zz}, e_{yz}, e_{zx} and e_{xy}. The components of the strain tensor are defined by

$$e_{xx} = \frac{\partial u}{\partial x} \quad , \quad e_{yy} = \frac{\partial v}{\partial y} \quad , \quad e_{zz} = \frac{\partial w}{\partial z} \quad ,$$

$$2e_{yz} = \frac{\partial w}{\partial y} + \frac{\partial v}{\partial z} \quad , \quad 2e_{zx} = \frac{\partial u}{\partial z} + \frac{\partial w}{\partial x} \quad \text{and} \quad 2e_{xy} = \frac{\partial v}{\partial x} + \frac{\partial u}{\partial y} \quad .$$

Love (1927) omits the half in the expressions for the shearing strains and consequently his components of strain do not constitute a second order tensor. The quantity Δ which is defined by the equation

$$\Delta = e_{xx} + e_{yy} + e_{zz} = \frac{\partial u}{\partial x} + \frac{\partial v}{\partial y} + \frac{\partial w}{\partial z}$$

is invariant for changes in the directions of the axes and is often called the "dilation" and represents the increment of volume per unit volume.

The six components of strain are not arbitrary functions since they are all related to the partial differentials of the displacement (U, V, W) through their defining equations. These equations yield a set of six "equations of compatibility" which the strain components must identically satisfy. It will be useful here to assume the relationship between stress and strain discussed in the next paragraph, and give the equations of compatibility in terms of stresses rather than strains. By using the

equilibrium equations, the equations of compatibility may be expressed as

$$\nabla^2 \hat{xx} + \frac{1}{1+\sigma} \frac{\partial^2}{\partial x^2} \left(\hat{xx} + \hat{yy} + \hat{zz} \right) = - \frac{\sigma}{1-\sigma} \left[\frac{\partial X}{\partial x} + \frac{\partial Y}{\partial y} + \frac{\partial Z}{\partial z} \right] - 2 \frac{\partial X}{\partial x}$$

$$\text{and} \quad \nabla^2 \hat{yz} + \frac{1}{1+\sigma} \frac{\partial^2}{\partial y \partial z} \left(\hat{xx} + \hat{yy} + \hat{zz} \right) = - \left[\frac{\partial Z}{\partial y} + \frac{\partial Y}{\partial z} \right] ,$$

$$\text{where} \quad \nabla^2 = \left[\frac{\partial^2}{\partial x^2} + \frac{\partial^2}{\partial y^2} + \frac{\partial^2}{\partial z^2} \right]$$

and σ is Poisson's ratio.

The other four Beltrami-Michell compatibility equations are obtained by the cyclic transposition of co-ordinates. Equations for evaluating the displacement (U, V, W) may be formulated in terms of integrals of functions of strain, since strain components were originally defined as partial differentials of displacement.

The theory of elasticity for infinitesimal strains is based on a generalized form of Hooke's Law, and assumes that each of the six components of strain is a homogeneous linear function of the components of stress, and vice versa. It can be shown that for a perfectly elastic isotropic material there are just two independent parameters relating stress and strain. If these parameters are taken to be the Lamé elastic parameters λ and ρ, then

$$\hat{xx} = \lambda \Delta + 2\rho e_{xx} \quad , \quad \hat{yy} = \lambda \Delta + 2\rho e_{yy} \quad , \quad \hat{zz} = \lambda \Delta + 2\rho e_{zz} \quad ,$$

$$\hat{yz} = \rho e_{yz} \quad , \quad \hat{zx} = \rho e_{zx} \quad \text{and} \quad \hat{xy} = \rho e_{xy} .$$

If these equations are solved for strains in terms of stresses, then

$$e_{xx} = \frac{1}{E}\left\{\hat{x}\hat{x} - \sigma(\hat{y}\hat{y}+\hat{z}\hat{z})\right\} \quad , \quad e_{yy} = \frac{1}{E}\left\{\hat{y}\hat{y} - \sigma(\hat{z}\hat{z}+\hat{x}\hat{x})\right\} \quad , \quad e_{zz} = \frac{1}{E}\left\{\hat{z}\hat{z} - \sigma(\hat{x}\hat{x}+\hat{y}\hat{y})\right\} \ ,$$

$$e_{yz} = \frac{2(1+\sigma)}{E}\,\hat{y}\hat{z} \quad , \quad e_{zx} = \frac{2(1+\sigma)}{E}\,\hat{z}\hat{x} \quad \text{and} \quad e_{xy} = \frac{2(1+\sigma)}{E}\,\hat{x}\hat{y} \ ,$$

$$\text{where } E = \frac{\mu(3\lambda+2\mu)}{\lambda+\mu} \quad , \quad \sigma = \frac{\lambda}{2(\lambda+\mu)} \ .$$

The quantity E is "Young's modulus", the number σ is "Poisson's ratio", the quantity μ is the "rigidity" and the quantity $\lambda + \frac{2}{3}\mu$ is the "modulus of compression".

A simplifying approximation that is sometimes made is to assume the material to be incompressible by letting Δ tend to zero and λ tend to infinity in such a way that $\lambda\Delta$ has a finite limit. This corresponds to the limiting value of Poisson's ratio equal to a half.

The stresses representing a unique and valid solution of an elastostatic problem must satisfy the following three requirements:-

(1) the boundary values of the problem,

(2) the equations of equilibrium,

and (3) the Beltrami-Michell compatibility equations.

The exact solution of the three dimensional, elastostatic problem is usually only practicable for simple models with some symmetry. Consequently, it is often necessary to consider two dimensional approximations, and in the present work the "plane strain" assumption will be used. It should be noted that the mathematics of the "generalized plane stress" problem, which is applicable to the treatment of thin plates, differs from that of the plane strain problem only in that a different value is given to a constant.

For the plane strain problem, assume

$$\hat{xx} = \hat{xx}(x,y) \quad , \quad \hat{yy} = \hat{yy}(x,y) \quad , \quad \hat{zz} = \sigma(\hat{xx}+\hat{yy}) \ ,$$

$$\hat{xy} = \hat{xy}(x,y) \quad , \quad \hat{yz} = 0 \qquad \text{and} \quad \hat{zx} = 0 \ .$$

It can be seen from the stress-strain relations that e_{zz} is zero.

For such a two dimensional stress system, the two principal stresses with principal directions lying in the x-y plane are given by

$$PP_{11} = \frac{\hat{xx}+\hat{yy}}{2} + \left\{\left(\frac{\hat{xx}-\hat{yy}}{2}\right)^2 + \hat{xy}^2\right\}^{\frac{1}{2}} \qquad \ldots\ldots \quad (1.2.1a)$$

$$PP_{22} = \frac{\hat{xx}+\hat{yy}}{2} - \left\{\left(\frac{\hat{xx}-\hat{yy}}{2}\right)^2 + \hat{xy}^2\right\}^{\frac{1}{2}} . \qquad \ldots\ldots \quad (1.2.1b)$$

The third principal stress with its principal direction parallel to the z axis is given by

$$PP_{33} = \hat{zz} = \sigma(\hat{xx}+\hat{yy}) = \sigma(PP_{11}+PP_{22}) . \qquad \ldots\ldots \quad (1.2.1c)$$

The angle Θ between the principal direction of the principal stress pp_{11} and the positive x axis is given by

$$\tan 2\Theta = \frac{2\hat{xy}}{\hat{xx}-\hat{yy}} \quad , \quad \frac{\pi}{2} \geqslant \alpha > -\frac{\pi}{2} . \qquad \ldots\ldots \quad (1.2.2)$$

The equations of equilibrium now reduce to the form

$$\frac{\partial \hat{xx}}{\partial x} + \frac{\partial \hat{xy}}{\partial y} + X = 0 \quad ,$$

$$\frac{\partial \hat{xy}}{\partial x} + \frac{\partial \hat{yy}}{\partial y} + Y = 0 \quad , \qquad \ldots\ldots \quad (1.2.3)$$

where (X, Y, 0) is the body force per unit volume, and the six compatibility equations reduce to the four equations

$$\nabla^2 \hat{xx} + \frac{\partial^2}{\partial x^2}(\hat{xx} + \hat{yy}) = -\frac{\sigma}{1-\sigma}\left(\frac{\partial X}{\partial x} + \frac{\partial Y}{\partial y}\right) - 2\frac{\partial X}{\partial x} \quad , \qquad \ldots\ldots \quad (1.2.4a)$$

$$\nabla^2 \hat{yy} + \frac{\partial^2}{\partial y^2}(\hat{xx} + \hat{yy}) = -\frac{\sigma}{1-\sigma}\left(\frac{\partial X}{\partial x} + \frac{\partial Y}{\partial y}\right) - 2\frac{\partial Y}{\partial y} \quad , \qquad \ldots\ldots \quad (1.2.4b)$$

$$\nabla^2 (\hat{xx} + \hat{yy}) = -\frac{1}{1-\sigma}\left(\frac{\partial X}{\partial x} + \frac{\partial Y}{\partial y}\right) \quad , \qquad \ldots\ldots \quad (1.2.4c)$$

$$\nabla^2 \hat{xy} + \frac{\partial^2}{\partial x \partial y}(\hat{xx} + \hat{yy}) = -\left(\frac{\partial Y}{\partial x} + \frac{\partial X}{\partial y}\right) \quad , \qquad \ldots\ldots \quad (1.2.4d)$$

where now $\nabla^2 = \frac{\partial^2}{\partial x^2} + \frac{\partial^2}{\partial y^2}$.

It can be shown that only three of the above six equations are independent, so that it is sufficient to find a solution that satisfies the equilibrium equations (1.2.3) and one of the compatibility equations, (1.2.4).

Introduce Airy's stress function, ϕ , such that

$$\hat{xx} = \frac{\partial^2 \phi}{\partial y^2} + \Omega \quad , \quad \hat{yy} = \frac{\partial^2 \phi}{\partial x^2} + \Omega \quad , \quad \hat{xy} = -\frac{\partial^2 \phi}{\partial x \partial y} \quad , \qquad \ldots\ldots \quad (1.2.5a)$$

where $\Omega(x,y)$ is a known potential function such that the components of

the body force are given by

$$X = -\frac{\partial \Omega}{\partial x} \quad , \quad Y = -\frac{\partial \Omega}{\partial y} \quad . \qquad (1.2.5b)$$

The equations (1.2.3) are identically satisfied by the definitions of equations (1.2.5) and equation (1.2.4c) is satisfied if

$$\nabla^4 \phi + \frac{1-2\sigma}{1-\sigma} \nabla^2 \Omega = 0 \qquad (1.2.6)$$

$$\text{where } \nabla^4 = \left(\frac{\partial^4}{\partial x^4} + 2 \frac{\partial^4}{\partial x^2 \partial y^2} + \frac{\partial^4}{\partial y^4} \right) .$$

Thus the problem of solving three equations is reduced to solving one equation for Airy's stress function. In particular, equation (1.2.6) reduces to the "biharmonic equation"

$$\nabla^4 \phi = 0 \qquad (1.2.7)$$

in the absence of body forces.

It seems that two general techniques have emerged for the solution of advanced two dimensional problems. The approach described by Muskhelishvili (1953), Sokolnikoff (1956), Green and Zerna (1954) and others using two potential functions of a complex variable stems from the fact that the general expression for Airy's stress function which satisfies the biharmonic equation may be expressed in terms of two such functions. This approach simplifies the formulae for the transformation of stress and strain under an orthogonal transformation of co-ordinates and allows regions with complicated

boundaries to be studied by the use of conformal representation.

The second technique using integral transforms is described by Sneddon (1951). The effect of applying an integral transform to the biharmonic equation is to exclude temporarily a chosen independent variable and to leave for solution an ordinary differential equation of the fourth order in one less variable. The solution of this equation is a function of the remaining variable and a parameter, and when the solution has been obtained it is "inverted" to recover the second variable. The complex Fourier transform is used for the plane strain problem and the Hankel transform is used for axially symmetric stress distributions. According to Sneddon, the integral transform method has the advantage of being more suited to extension to three dimensional problems.

Consider now the theory of concentrated forces acting at a point. Love shows (§ 144) that the plane strain equilibrium equations in the absence of body forces expressed in terms of the dilatation Δ and the rotation ϖ are

$$(\lambda+2\mu)\frac{\partial \Delta}{\partial x} - 2\mu \frac{\partial \varpi}{\partial y} = 0 \quad , \quad (\lambda+2\mu)\frac{\partial \Delta}{\partial y} + 2\mu \frac{\partial \varpi}{\partial x} = 0 \quad ,$$

and hence that $((\lambda+2\mu)\Delta + i\,2\mu\varpi)$ is a function of the complex variable $(x + iy)$ obeying the Cauchy-Riemann equations. If one introduces a function $(\xi + i\eta)$ of $(x + iy)$ equal to the integral of the above function with respect to $(x + iy)$, then the displacements U and V may be expressed in terms of ξ and η and an arbitrary plane harmonic function. In order to investigate the problem of point forces, Love (§ 147, 148) considers solutions which tend to become infinite at specific points. Such points cannot be in the material of the body but may be in cavities within the body. The simplest form of singularity

at the origin,

$$(\lambda+2\mu)\Delta + i\,2\mu\,\varpi = \frac{A}{x+iy} \quad ,$$

defines ($\xi+i\eta$) equal to the logarithmic function, and the arbitrary harmonic function in the expressions for U and V has to be selected to remove the term containing the multi-valued argument. Hence equations for the displacements and therefore also the stress components are derived, and the resultant of the stresses acting on the surface of the circular cavity may be shown to be equivalent to a point force of known finite magnitude.

The problem of a concentrated force acting within a semi-infinite half-space requires a solution that gives the necessary boundary conditions at the free surface and also has a singularity at the point of application of the type shown by Love to represent a concentrated force. The present discussion will be restricted to the case of forces acting in a direction normal to the free surface.

Sneddon(1944) considers an equilibrium system of two equal and opposite "image" point forces acting in an infinite medium. This configuration makes the shear stress at the "surface" zero, and an additional solution is found such that the total shear and normal stresses at the "surface" are zero, so that the physical model may now be divided along the "surface" without altering the stresses. Sneddon also gives the result, obtained by integration, for a force acting along a finite line parallel to the free surface. This result is given in Appendix I.

The solution of the problem using complex potential methods is given by Green and Zerna (§ 8.8) and the method is indicated by Muskhelishvili (§ 112, 1 working in the other half-plane. The approach here is different from that of

Sneddon. From the start the material is assumed to occupy only one half-plane, so that the two complex potential functions are only defined in this half-plane. The definition of one of the potential functions is extended to the other half-plane in such a way that using the theory of complex integration and, in particular, the Plemelj formulae, the necessary free surface boundary conditions can be enforced, and the general expressions for the stress components be accordingly transformed.

The problem of an internal point force applied in a direction normal to the free surface of a three dimensional semi-infinite body was solved first by Mindlin (1936) and later by Dean, Parsons and Sneddon (1944). The latter authors also considered the case of a force uniformly distributed over the area of a circle of radius a at depth h lying in a plane parallel to the surface of a semi-infinite body. The surface stress components are tabulated for a range of values of h/a, assuming the medium to be incompressible, and for Poisson's ratio equal to $\frac{1}{4}$ and $\frac{1}{2}$ (incompressible medium) for the case $h/a = 0.2$. These are thought to be the most significant stresses because, for the two dimensional line force analogue, the maximum stress differences occur at the free surface. It is found that the effect on the surface stresses of the assumption of incompressibility does not significantly alter the shape of the surface stress distribution but alters the magnitude by a factor that may be readily calculated. Sneddon (1944) gives further results for stresses in the planes $z = h$ $(r > a)$ and $z = \frac{h}{2}$ for an incompressible medium. The treatment by Sneddon of the plane strain solution for a line force is an approximation to this three dimensional problem. The function $\frac{\pi a^2 \hat{z}\hat{r}}{F}$ is compared to the corresponding plane strain function $\frac{2a \hat{x}\hat{y}}{F}$ and is shown to be similar in form and magnitude. It is also concluded that the assumption that the medium is incompressible does not affect the physics of the problem in any significant manner.

(iii) The application of the theory of elasticity to crustal processes

The deformation of the crust of the Earth cannot be fully described by any rheological model. The principal difficulties apart from the mathematical complexity arise from uncertainties in the behaviour of materials at great confining pressures and over long periods of time. Two simple rheological models that give useful theories of deformation are the infinitesimal theory of elasticity, which is defined by assuming that displacements are always small and that Hooke's Law is obeyed, and the hydrodynamic theory of viscous fluids, which assumes that a fluid cannot resist transverse shearing but that a resisting force acts with a magnitude proportional to the rate of shear. A further model is the perfectly plastic solid whose behaviour is elastic for stresses below some "yield stress", but which can sustain no stress greater than this. Another model for materials possessing a yield point is the Bingham body which behaves as an elastic body for stresses less than the yield point, and for greater stresses gives a steadily increasing strain. There are many properties of deformation that linear models such as these fail to explain. In the present context the most important of these is probably "steady state creep", which can over long time intervals produce slow steady deformation under load even for stresses in the elastic range. The rate of this creep increases rapidly with both the magnitude of the stresses and the temperature (Jaeger, 1962). Another non-linear process is discussed by Orowan (1965) who points out that the mantle is usually believed to be substantially crystalline, and that crystalline materials show no viscosity but only plasticity with transient creep in the low temperature range, and a characteristic non-Newtonian viscosity at higher temperatures. For many materials the gradual transition between the two temperature ranges takes place around one-half of the absolute melting temperature. This typical non-Newtonian viscosity of crystalline matter was recognized, and separated from transient creep, by Andrade (1911). Transient

creep is the process whereby, in the plastic range, strain is not taken up instantaneously but is approached asymptotically. Andradean viscosity is closer to ideal plasticity than to Newtonian viscosity, for if the shear stress sinks below the creep limit, the strain rate vanishes, but if it rises above the limit, the flow rate increases rapidly in a quasi-exponential manner. Gravimetric evidence also indicates that crustal processes cannot be explained by a viscous flow mechanism in the upper mantle which would tend always to produce exact isostasy, but are not inconsistent with what would be expected if the rocks at great depth have a non-zero strength and flow is negligible unless the stress-difference exceeds the strength (Jeffreys, 1962, p. 347). Thus a model is built up of a relatively strong lithosphere deforming elastically or behaving as a series of separate blocks overlying an asthenosphere in which Non-Newtonian flow occurs. Criteria for fracture will be applied to the crust and yield criteria will be applied at depth in the mantle. The application of the theory of elasticity to the crust is therefore valid so long as brittle failure or flow do not occur in the vicinity. If they do occur there will be stress re-adjustment and the static model will no longer be applicable. However, it is the purpose of such studies to determine the likelihood of such processes occurring.

The supplementary stress system due to some structural situation under study has to be added to the "natural state" of stress in the uniform crust due to gravity. Any supplementary or natural state stress distribution must satisfy the boundary condition that, at the free surface y equals zero,

$$\hat{yy} = \hat{xy} = \hat{zy} = 0$$

One possible natural state is to suppose that rock pressure is essentially that due to the weight of the overburden with the lateral pressures adjusting themselves

according to Poisson's ratio of the material. If it is assumed that there is no horizontal displacement, then the principal stresses at a depth y below the surface are equal to the Cartesian components given by

$$\hat{yy} = -\rho g y \ , \quad \hat{xx} = \hat{zz} = \frac{\sigma}{1-\sigma} \hat{yy} \ . \qquad \ldots \quad (1.3.1)$$

This system has the feature that the stress-difference increases rapidly with depth, and if the magnitude of the stress-difference is a valid criterion, flow will occur. An alternative assumption is that because of such flow or because of steady state creep, the stresses at any depth will tend to become hydrostatic so that at a depth y they are given by

$$\hat{xx} = \hat{yy} = \hat{zz} = -\rho g y \ . \qquad \ldots \quad (1.3.2)$$

Equation (1.3.2) is not a plane strain solution, but nevertheless is a valid solution of the general equations of equilibrium and of compatibility. The corresponding plane strain system is

$$\hat{xx} = \hat{yy} = -\rho g y \ , \quad \hat{xy} = 0 \ , \quad \hat{zz} = -2\sigma \rho g y \ ,$$

which is only identical to equation (1.3.2) for liquids, ($\sigma = \frac{1}{2}$). The difference between the states of stress represented by equations (1.3.1) and (1.3.2) is not fundamental in the sense that it may be represented by a superposed horizontal stress of the form

$$\hat{xx} = \hat{zz} = \frac{1-2\sigma}{1-\sigma} \rho g y \ , \quad \hat{yy} = 0 \ ,$$

which again is a valid solution of the equations of elasticity.

Many writers follow Anderson (1951) and regard the hydrostatic assumption of equation (1.3.2) as the standard reference state and refer to increase or relief of stress relative to it. Field measurements of stresses in mine shafts tend not to clarify the problem of the natural state because of the uncertainties of the effects of irregular terrain, tectonic influences and of the mine itself. Jaeger (1962) concludes that the results given by Talobre (1957) give some support to the hydrostatic assumption. Murrell (1965) reports the work of Hast (1958) who has shown that the stresses in the groundrock around mining excavations in Scandanavia are related to the tectonic structure of the region. Kehle (1964) has advanced the theory of the determination of tectonic stresses from the analysis of hydraulic well fracture data and gives five examples where the tectonic stresses in apparently orogenically inactive continental areas are in a relaxed state which approximates to a hydrostatic pressure. However, this method is still the subject of controversy (Gretener, 1965). The assumption of a hydrostatic natural state does give a workable model that permits the relatively simple treatment of stress distributions within the Earth. In particular, the stress-difference and the orientation of the principal directions are independent of the hydrostatic pressure.

The approach to crustal problems indicated above implies that the anomaly giving rise to the supplementary stress system is not erased by steady state creep. This is only a re-statement of the fact that for stress-differences less than the strength, the apparent influence of flow on geological processes is negligible, and also that large anomalous crustal loads are known to exist for long periods of time.

Before discussing the stress distributions obtained in crustal models, the

criteria for interpreting these systems will be considered. Brittle materials such as rocks suffer "shear fracture" under compression and "brittle fracture" under tension. However, brittle materials tend to become ductile under high confining pressures. Orowan (1960) concluded that the mechanism of seismic faulting must be based on some such plastic phenomenon, and a great deal of experimental work has been done on the brittle-ductile transition.

The simplest criterion for fracture that goes some way towards explaining experimental observations is the Coulomb-Hopkins Law that failure occurs when the maximum shear stress reaches some definite value which is called the shear strength of the material. The main faults in this criterion are that it implies that the tensile and compressive strengths are equal and that failure should occur across a plane inclined at 45° to the direction of the greatest principal stress. Navier modified this criterion to overcome these two difficulties by assuming that the shear strength is increased by a constant multiple, μ , of the normal pressure across the plane of fracture. The constant μ is called the "coefficient of interna l friction". This modification yields the rule that failure takes place when

$$PP_{11}\left\{\mu+(\mu^2+1)^{\frac{1}{2}}\right\}+PP_{33}\left\{\mu-(\mu^2+1)^{\frac{1}{2}}\right\}=2S_o \quad , \qquad (1.3.3)$$

where So is the shear strength and $pp_{11} \geqslant pp_{22} \geqslant pp_{33}$, across two planes whose normals are at an angle γ to the pp_{11} principal direction which is given by

$$\tan 2\gamma=\frac{1}{\mu} . \qquad (1.3.4)$$

Thus the planes of fracture pass through the axis of the intermediate principal stress and make an angle $\pm \left(\frac{\pi}{4}+\frac{\phi}{2}\right)$ with the greatest principal stress

where ϕ equals (arctan μ) and is the "angle of internal friction". In the present work the function equal to So in the above equation will be called the Coulomb-Navier fracture function", since failure will occur when it equals the shear strength. This theory gives a reasonably accurate quantitative account of the behaviour of rocks under compression and below the yield point. Laboratory experiments on rocks at moderate confining pressure and room temperature give values of So ranging usually between 100 and 300 bars and values of ϕ between 30° and 55° (Jaeger, 1962, p. 173). The shear strength So increases with increasing confining pressure and decreases with increasing temperature. However, under tensile stresses failure generally occurs by brittle fracture with the plane of fracture normal to the direction of tension. According to the Griffith theory of brittle fracture (Griffith, 1920) it is supposed that the material contains a large number of randomly orientated, incipient cracks and that failure occurs when the highest local stress at the longest crack of the most dangerous orientation is equal to some critical stress dependent on the properties of the material according to a simple theory of crack formation. In this theory the crack is likened to an elongated ellipse and the approximation is made that the radius of curvature of the ellipse at the end of the major axis is of the order of the intermolecular spacing. This theory which fits quantitatively with experimental results gives the criterion for failure

$$\begin{aligned} p_{11} &= T_o \quad , \text{ if } \quad 3p_{11} + p_{22} > 0 \quad , \\ (p_{11} - p_{22})^2 + 8T_o(p_{11} + p_{22}) &= 0 \quad , \text{ if } \quad 3p_{11} + p_{22} < 0 \quad , \end{aligned} \qquad (1.3.5)$$

where To is the tensile strength in uniaxial tension.

Jaeger (1962, p. 75) quotes tensile strengths of rocks in the range from 20 to

60 bars. The above criterion is expressed in terms of pp_{11} and pp_{22} because its derivation uses a plane two-dimensional model for a crack. Sack (1946) extended the model to three dimensions with axial symmetry by considering the tensile strength of a brittle body containing circular cracks. McLintock and Walsh (1962), Brace (1960) and Murrell (1964a) have considered the form of the criterion under general plane two dimensional conditions of stress. Murrell (1964b) adopted a reasonable hypothesis in order to extend the criterion to triaxial stress systems and tested the results experimentally (Murrell, 1965).

Mohr's theory of fracture takes a generalized form in which it is only assumed that at failure across a plane the normal and shear stresses across the plane are connected by some functional relationship characteristic of the material. The "Mohr envelope" is the envelope of Mohr circles corresponding to all conditions at which fracture takes place. The Coulomb-Navier criterion corresponds to a Mohr envelope made up of a pair of intersecting straight lines and the Griffith criterion for fracture under tension to a parabolic envelope.

The mechanics of a fluid filled porous solid was considered by Hubbert and Rubey (1959) who discussed its application to overthrust faulting. In discussion in 1960 they defended their model against criticism from Laubscher (1960). The influence of fluid pressure on both the Coulomb-Navier and the Griffith criteria is to reduce the effective principal stresses by the magnitude of the pore pressure (Jaeger, 1962, p. 166).

In order to formulate the equations of a rheological model to study ductile materials a generalized yield criterion is required. Such a criterion is applicable to the processes of flow occurring at depth in the mantle. The simplest criterion is that yield occurs when the maximum shearing stress (or the stress-difference) reaches a critical value. This law which is analogous

to the Coulomb-Hopkins Law for the fracture of brittle materials is called Tresca's criterion. The von Mises criterion may be introduced either from the concept that any yield criterion that is to be independent of the mean normal stress must be expressible in terms of invariants of the stress deviation or from the criterion that yield takes place when the elastic strain energy of distortion reaches a value characteristic of the material. The invariant equal to

$$\frac{1}{6}\left\{(\hat{y}\hat{y}-\hat{z}\hat{z})^2+(\hat{z}\hat{z}-\hat{x}\hat{x})^2+(\hat{x}\hat{x}-\hat{y}\hat{y})^2\right\}+\hat{y}\hat{z}^2+\hat{z}\hat{x}^2+\hat{x}\hat{y}^2 \qquad \ldots \quad (1.3.6)$$

will in the present work be known as the "von Mises function". Failure occurs when this function equals one third of the square of the yield stress in uniaxial tension or compression. The results of experimental work on yield stresses tend to support the von Mises criterion rather than Tresca's criterion.

Consider the application of these theories of fracture and flow to the features of crustal and mantle dynamics. Anderson (1905, 1951) used the Coulomb-Navier criterion to explain the three major types of fault. It is assumed that one principal stress is nearly vertical and always compressive and that the natural state is approximately hydrostatic. It is then feasible to distinguish the three cases in which the compressive vertical stress is the greatest, intermediate or least principal stress in magnitude and which give rise to normal, transcurrent or thrust faults respectively. The dips of thrust and normal faults (Hubbert, 1951) and the orientation of transcurrent faults (Moody and Hill, 1956) measured in the field give values of the angle of internal friction agreeing with laboratory measurements. Hubbert also performed experiments to demonstrate these mechanism of faulting. Vertical dykes are tensile in origin, at least in the sense that they occur under conditions when

the magnitude of the horizontal stress is considerably less than the magnitude of the vertical compression. It is generally supposed that they are opened by the magma pressure so the theory of fluid pressure in a Griffith crack may be applied. The formation of large scale joint systems is considered by Price (1959) who concludes that they are post tectonic phenomena which develop as a result of uplift.

It is now necessary to consider the interpretation of two dimensional plane strain stress distributions which might be supposed to exist in the crust in terms of these processes. It will be assumed that the calculated supplementary stress system is superimposed upon a hydrostatic natural state so that the "isostatics", which are the orthogonal system of curves whose directions at any point are the directions of the principal axes, are unaltered by the natural state. Then, assuming it is known which family of curves correspond to the greatest principal stress, a set of curves may be plotted using the Coulomb-Navier theory for a specified value of the angle of internal friction ϕ , which, if the Coulomb-Navier fracture function was large enough, would represent the possible fault planes. Then the Coulomb-Navier fracture function could be plotted and contoured for the same value of the angle, ϕ . This approach has the disadvantage that although the variation of the potential fault surfaces with the value of ϕ is easily visualized, the variation of the Coulomb-Navier fracture function is much more complicated. Also, this function is not independent of the hydrostatic pressure except in the special case where ϕ is zero. Such potential fault surfaces are of course based on the original stress distributions and no allowance is made for the alteration of stress due to fracture. Anderson (1942) considered a model for the relief of stress by a transcurrent fault and found that pronounced changes in both the intensity and magnitude of stress occur in the immediate neighbourhood

of the fault but that they diminish rapidly with distance.

Assuming a hydrostatic natural state and the absence of any tectonic stress, the principal directions at depth can deviate considerably from the horizontal and vertical, and if this occurs then the interpretation of failure in terms of, for example, normal faulting is meaningless. However, consider the effect of a horizontal tectonic tension

$$\hat{x}x = C_x \quad , \quad \hat{y}y = 0 \quad , \quad \hat{z}z = \sigma C_x \qquad \ldots \quad (1.3.7)$$

where the magnitude of the tectonic stress is much greater than the components of the supplementary stress system. There does now exist at depth a vertical principal direction and the corresponding principal stress is the greatest compression, so that failure will be by normal faulting. Similarly, for a horizontal tectonic compression, the compression of least magnitude has a vertical principal direction and failure is by thrust faulting.

At shallow depths where one principal direction must tend towards the vertical, the justification of the hydrostatic natural state hypothesis becomes less likely, and, indeed, absolute tensions as opposed to tensional relief of the hydrostatic state can occur. In this circumstance the Griffith criterion is applicable. The simple model used to represent a tectonic tension breaks down at the free surface, where the natural state does not contribute, in the sense that it gives a large absolute tension which, if it did in fact exist, would certainly cause brittle fracture.

Two useful yield criteria for plastic solids are the magnitudes of the "stress-difference" and the von Mises function, which have already been discussed. The stress-difference is defined to be the positive difference between the

greatest and least of the three principal stresses. In the presence of a horizontal crustal tension, a large value of the stress-difference in the elastic crust indicates that the supplementary stress system tends to reinforce the tectonic stress and increase the likelihood of normal faulting. Conversely, a low value of the stress-difference in the crust would indicate the decreased likelihood of normal faulting. Similarly, in the presence of a horizontal crustal compression, a large stress-difference indicates an increased likelihood of thrust faulting, and a low stress-difference indicates that thrust faults would tend to be inhibited.

In general the numerical results obtained in Chapter 3 will be interpreted using this stress-difference technique, although the use of some of the other criteria will be demonstrated.

Finally, the published work relating to the application of the theory of elasticity to crustal processes will be reviewed.

If studies of stresses in spheres due to their own gravity are excluded, three elastic models have been used to consider stress distributions in the crust of the Earth (Jeffreys, 1962). It should be noted that, unless the mode of formation is considered, stresses in spheres under their own gravity cannot satisfy the requirement of zero initial stress implicit in the theory of elasticity. The first model is that of a sphere with a load expressed by surface harmonics. The second is the plane strain solution for a semi-infinite elastic half-space with surface loads. Since this model neglects the curvature of the Earth, its application is restricted to features with a maximum horizontal scale of some hundreds of kilometres. Other restrictive assumptions are those of homogeneity and isotropy. Solutions for various surface loads of this model have been used to estimate the maximum stress-difference that must occur in the crust in order to support the topography,

and thereby give a minimum estimate of the strength at the corresponding depth. Non-elastic solutions, in which the relationship between the stresses and the displacements are relaxed, have been considered, but give very similar results. It is found that stress-differences equal to about half the surface load will occur somewhere. The third elastic model, which is particularly relevant to the question of isostasy, is that of a surface layer resting on a substratum of negligible strength. In the case of a horizontal feature large compared to the thickness of the layer, it is found that the stress-difference may be up to ten times the surface load, and also that isostatic compensation for loads of less than several hundreds of kilometres in extent is poorer than is indicated in practice by gravity measurements. However, a non-elastic solution of this problem may be obtained in which not only is the isostatic compensation improved but also the greatest stress-difference is reduced and is about equal to the load. When investigating isostasy using the floating crust model with allowance for the curvature of the Earth, Jeffreys (p. 206) found that the condition that mass per unit area is uniform did not quite correspond to the distribution of stress that gives the smallest stress-difference. In considering the results of the present work, which of course uses the half-space model, we will find that isostatic compensation greatly decreases the stress-difference below the level of compensation, but tends to increase it above this level. Vening Meinesz (1939, 1941) modified the Airy theory of local isostatic compensation to permit regional compensation by considering the elastic deformation of a "floating" crust. The stress required for the elastic buckling of the crust is far greater than the strength of the crust, so that elastic buckling would not be expected to occur. He also introduced a theory of plastic deformation of the crust leading to downward buckling, and used this theory to explain the occurrence of the negative gravity anomalies associated with island arcs.

Bott (1965), using the half-space model with a uniform surface load of finite lateral extent, considers the effect of a superimposed uniform horizontal tension and shows that under regional tension the maximum stress-difference is increased beneath the load and reduced beneath the adjacent regions. This is interpreted in the manner discussed earlier to indicate that normal faulting and other tensile features are enhanced at depth in regions of positive isostatic anomaly and inhibited in regions of negative anomaly. It is suggested that the tectonic and igneous history of the Midland Valley of Scotland offers some confirmation of this hypothesis. Hafner (1951) considered the two dimensional stress distribution within a block in static equilibrium subject to various boundary forces, and plotted isostatics and planes of potential shear for equal to 30°. He uses an empirical form of the Coulomb-Navier criterion in which some allowance is made for the increase of the shear strength So with confining pressure. The results of this study are confirmed by the model experiments of Hubbert (1951). Sandford (1959) considered analytically the elastic response of a homogeneous rock layer which is 5 kilometres thick to three types of displacement applied along its lower edge. The displacement field, isostatics and distortional strain-energy density (i.e. von Mises function) diagrams are presented, and the modes of failure predicted analytically are largely confirmed by model experiments.

In a recent paper Durney (1965) considered the plane strain model of the homogeneous half-space with harmonic surface loads and anomalous internal density distribution of the form

$$\rho(x,y) = \rho_{\circ}\, e^{py} \cos kx$$

where, in his notation, the material is situated in the negative y half-space.

A linear increase in density with depth decreases the significance of "induced body forces" due to increases in density under deformation. This secondary density contrast which Durney calculates for his examples of stress in a homogeneous half-space is therefore an overestimate, and because this induced density contrast is numerically much less than the primary density anomaly, it has no significant effect on the stress distribution in the two dimensional model.

Durney finds that a one dimensional model with a surface load and also the two dimensional model with a harmonic surface load in the special case of the wavelength tending to infinity both give very large, or even infinite, surface displacements. Also, the one dimensional model gives finite stresses at infinite depth. He attributes these effects to the need to add material to the half-space to maintain the boundary conditions as the boundary deforms under the imposed load. The author of the present work wrote to Durney, (21 March, 1966), expressing concern about this dynamic interpretation of a solution of the elastostatic equations and demonstrating that, for a simple model, these large displacements and non-zero stresses at infinity could be exactly explained by the fact that the system of forces to which the model was subjected did not preserve its equilibrium. Consequently, the equations of elasticity, which are derived from the equations of equilibrium and not from the equations of motion, are invalid. It is necessary to allow for the additional effects of the simplest force distribution necessary to preserve equilibrium.

The reply, (4th April), dealt only with the case of the harmonic load, and the interpretation of infinite displacements in the case of k equal to zero was agreed. The point was made that for the case of a "Gaussian" mountain the removal of the Fourier components for small k was not arbitrary, but was such that the total surface force was reduced to zero and equilibrium was maintained.

Durney's general results for harmonic loads and density anomalies are, of

course, not affected by these problems. He discusses Gaussian mountain profiles and density distributions and, in general terms, their application to isostasy. He shows that if the horizontal dimension, D, of a density deficiency is much larger than its vertical dimension, ($\frac{1}{p}$), an equilibrium situation exists formed by the density deficiency and a mountain above it such that stresses are small for depths large compared to $\frac{1}{p}$. In a numerical example, ($\frac{1}{p}$ = 20 km., D = 400 km.), the stresses at a depth of a hundred kilometres are said to be less than a tenth of those due to the density deficiency alone. In this case the compensation is "local" in the sense that the topography directly reflects the mass deficiency beneath. As an illustration of the general results the magnitudes of the stress components are plotted with depth for a density excess of the form

$$\rho_0 \left(e^{py} - e^{qy}\right) \cos kx \quad , \qquad \ldots \qquad (1.3.8)$$

where p and q equal $\frac{1}{300}$ km^{-1} and $\frac{1}{200}$ km^{-1} respectively and ρ_0 equals 0.35 gm/cc, for three different values of $\frac{1}{k}$ equal to 100, 250 and 400 kilometres. The induced density anomalies are calcula ted and shown to be insignificant.

In a second paper (to be published) entitled "Equilibrium configurations between density and topographic surface irregularities in a purely elastic Earth model", Durney derives the shape of the mountain in equilibrium with a density deficiency by specifying that the vertical displacement due to both the mountain and the density deficiency vanish at the "surface". He considers a Gaussian lateral distribution of density but a "square pulse" distribution with depth, as in the present study. This model yields regional mass compensation (as opposed to local mass compensation) and it is found that the height of the "mountain"

decreases as the depth of the density deficiency increases. He also considers one model of local mass compensation occurring within the half-space.

CHAPTER 2

A MODEL FOR CALCULATING STRESS SYSTEMS IN AN ELASTIC CRUST OF VARYING DENSITY

(1) The initial equations

The model used for this work involves the double integration of the plane strain solution for a concentrated force acting at a point in a semi-infinite elastic half-plane in order to simulate the effect under gravity of a density anomaly existing over a rectangular area of the cross section, (see figure 1). Throughout this work the anomalous body forces will be assumed to be balanced analytically by concentrated forces at great depth so that the equilibrium of the half-space is not affected.

In ignorance of the work of Sneddon using Fourier transforms, the problem was approached using complex potential functions (see(ii) of Chapter 1). The derivation of the point force result is indicated by Muskhelishvili, (1953, § 112, 113), and is given in full by Green and Zerna, (1954) in paragraph 8.8.

If the x axis is taken to represent the free surface and the y axis to be positive into the half-space (see figure 1), then the Cartesian stress components at a point z(x,y) due to a concentrated force P equal to iY acting at a point Zo (u,v) may be shown to be given by

$$\hat{x}\hat{x} - \hat{y}\hat{y} + 2i\,\hat{x}\hat{y} = \frac{-iY}{\pi(1+\kappa)}\left\{\frac{\kappa}{\bar{z}-\bar{z}_o} - \frac{\kappa}{\bar{z}-z_o} - \frac{z-z_o}{(\bar{z}-\bar{z}_o)^2} + \frac{(3+\kappa)\bar{z} - (2+\kappa)z - \bar{z}_o}{(\bar{z}-z_o)^2} - 2\frac{(\bar{z}-z)(\bar{z}-\bar{z}_o)}{(\bar{z}-z_o)^3}\right\} \quad \ldots (2.1.1)$$

and

$$\hat{x}\hat{x} + \hat{y}\hat{y} = \frac{iY}{\pi(1+\kappa)}\left\{\frac{-1}{z-z_o} - \frac{\kappa}{z-\bar{z}_o} - \frac{2iv}{(z-\bar{z}_o)^2} + \frac{1}{\bar{z}-\bar{z}_o} + \frac{\kappa}{\bar{z}-z_o} - \frac{2iv}{(\bar{z}-z_o)^2}\right\}, \quad \ldots (2.1.2)$$

where, for a plane strain solution, $k = 3 - 4\sigma$.

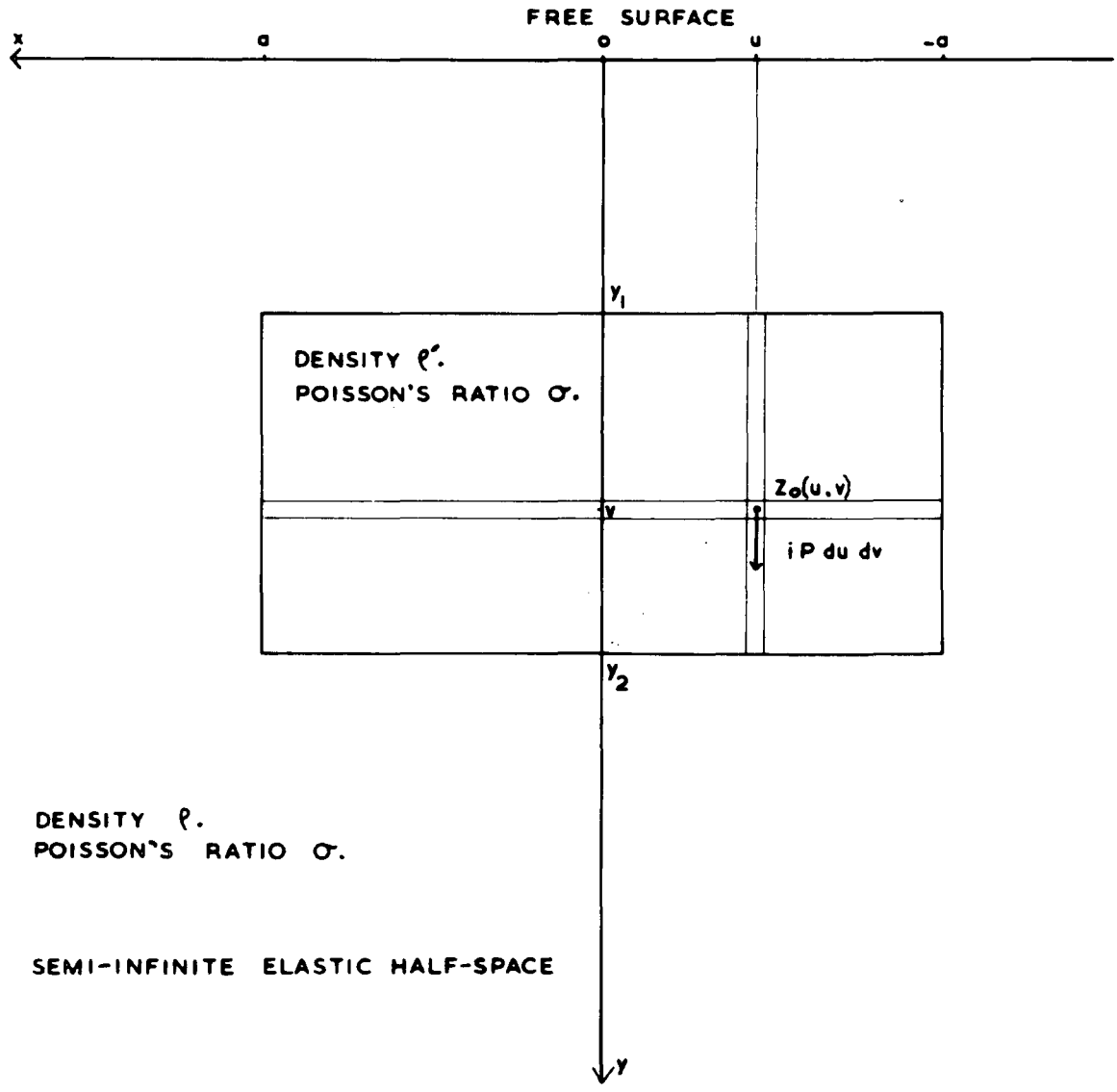

A CROSS SECTION OF THE PLANE MODEL.

Figure 1

Note that $\hat{xx}$, $\hat{yy}$ and $\hat{xy}$ all tend to zero in the special case of $\frac{V}{x}$, $\frac{V}{y}$ and $\frac{V}{u}$ all tending to infinity. Referring to diagram (1) of figure 2, this means that if the point force required for equilibrium is considered to be applied at very great depth, then the point force does not contribute to the stress components in the region of the density anomaly.

(ii) The first integration

The next stage was to replace Y in equations (2.1.1) and (2.1.2) by the infinitesimal element L du where L is the magnitude per unit length of the line force in the positive y direction, and integrate with respect to U between the limits + a to - a, so obtaining the result for a line force acting along a finite line in the cross section. This line is parallel to the free surface and of length 2a. The results were obtained in the following forms

$$\hat{xx}-\hat{yy}+2i\,\hat{xy}=\frac{-iL}{\pi(1+K)}\left[(1-K)\left\{\log(\bar{z}-\bar{z}_o)-\log(\bar{z}-z_o)\right\}+2iv\left\{\frac{1}{\bar{z}-\bar{z}_o}+\frac{1}{\bar{z}-z_o}\right\}+(\bar{z}-z)\left\{\frac{1}{\bar{z}-\bar{z}_o}+\frac{K}{\bar{z}-z_o}-\frac{2iv}{(\bar{z}-z_o)^2}\right\}\right]_{u=-a}^{u=+a} \quad \ldots (2.2.$$

and

$$\hat{xx}+\hat{yy}=\frac{iL}{\pi(1+K)}\left[\log\frac{z-z_o}{\bar{z}-\bar{z}_o}+K\log\frac{z-\bar{z}_o}{\bar{z}-z_o}-2iv\left\{\frac{1}{z-\bar{z}_o}+\frac{1}{\bar{z}-z_o}\right\}\right]_{u=-a}^{u=+a}. \qquad (2.2.2)$$

Separating the real and imaginary parts of equation (2.2.1), remembering that (arc tan $\frac{V}{x}$) is an odd function of y, gives

$$\hat{xx}-\hat{yy}=\frac{L}{\pi(K+1)}\left[(K-1)\left\{\arctan\frac{y-v}{x-u}-\arctan\frac{y+v}{x-u}\right\}-\frac{2(y-v)(x-u)}{(x-u)^2+(y-v)^2}-\frac{2(Ky-v)(x-u)}{(x-u)^2+(y+v)^2}-\frac{8yv(x-u)(y+v)}{\left\{(x-u)^2+(y+v)^2\right\}^2}\right]_{u=-a}^{u=+a} \quad \ldots (2.2$$

and $\hat{xy}=\frac{L}{2\pi(K+1)}\left[\frac{1}{2}(K-1)\left\{\log\left[(x-u)^2+(y-v)^2\right]-\log\left[(x-u)^2+(y+v)^2\right]\right\}-\frac{2(y-v)^2}{(x-u)^2+(y-v)^2}+4yv\frac{(x-u)^2-(y+v)^2}{\left\{(x-u)^2+(y+v)^2\right\}^2}\right.$

$$\left.-\frac{2(Ky-v)(y+v)}{(x-u)^2+(y+v)^2}\right]_{u=-a}^{u=+a} \quad \ldots (2.2.$$

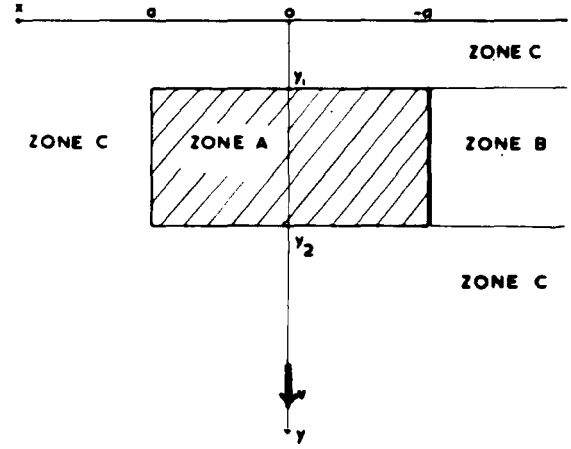

BODY FORCE P per unit area.

POINT FORCE $-2aP(y_2-y_1)$.

DIAGRAM 1 – THE RECTANGULAR MODEL.

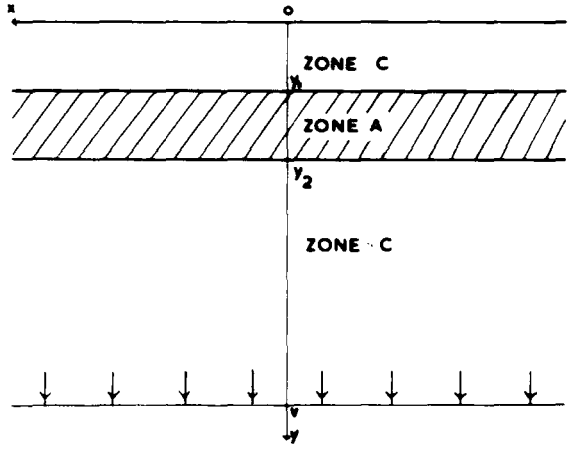

BODY FORCE P per unit area.

LINE FORCE $-P(Y_2-Y_1)$ per unit length.

DIAGRAM 2 – THE PLANE SUBSTRATUM.

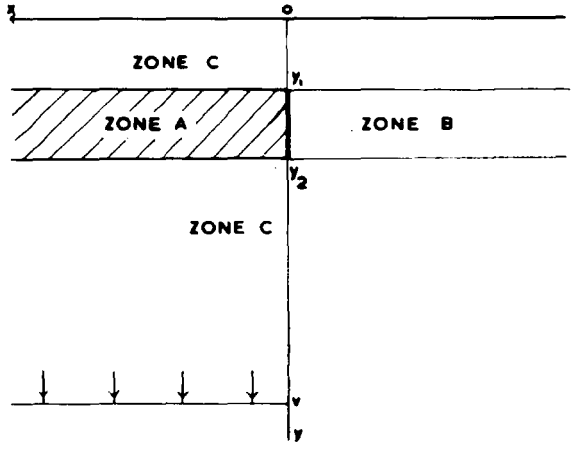

BODY FORCE P per unit area.

LINE FORCE $-P(Y_2-Y_1)$ per unit length.

DIAGRAM 3 – THE SEMI-INFINITE PLANE SUBSTRATUM

EQUILIBRIUM MODELS WITH ZONING.

Figure 2

Equation (2.2.2) gives

$$\hat{xx} + \hat{yy} = \frac{2L}{\pi(K+1)} \left[- \arctan \frac{y-v}{x-u} - K \arctan \frac{y+v}{x-u} + \frac{2v(x-u)}{(x-u)^2+(y+v)^2} \right]_{u=-a}^{u=+a} \quad . \quad . \quad . \quad (2.2.5)$$

It is shown in Appendix I that equations (2.2.3), (2.2.4.) and(2.2.5) agree with the results obtained by Sneddon (1944).

The standard case of a normal surface load may be considered by putting V equal to zero in equations (2.2.3), (2.2.4) and (2.2.5) as follows

$$\hat{xx} - \hat{yy} = \frac{L}{\pi} 2y \left\{ \frac{x+a}{(x+a)^2+y^2} - \frac{x-a}{(x-a)^2+y^2} \right\} ,$$

$$\hat{xy} = \frac{L}{\pi} y^2 \left\{ \frac{1}{(x+a)^2+y^2} - \frac{1}{(x-a)^2+y^2} \right\}$$

and $$\hat{xx} + \hat{yy} = \frac{2L}{\pi} \left\{ \arctan \frac{y}{x+a} - \arctan \frac{y}{x-a} \right\} .$$

These equations are commonly expressed in the forms

$$\hat{xx} = \frac{L}{\pi} \left\{ \arctan \frac{y}{x+a} - \arctan \frac{y}{x-a} - \frac{2ay(x^2-a^2-y^2)}{\{(x+a)^2+y^2\}.\{(x-a)^2+y^2\}} \right\} , \quad . \quad . \quad (2.2.6a)$$

$$\hat{yy} = \frac{L}{\pi} \left\{ \arctan \frac{y}{x+a} - \arctan \frac{y}{x-a} + \frac{2ay(x^2-a^2-y^2)}{\{(x+a)^2+y^2\}.\{(x-a)^2+y^2\}} \right\} \quad . \quad . \quad (2.2.6b)$$

and $$\hat{xy} = - \frac{L}{\pi} \frac{4axy^2}{\{(x+a)^2+y^2\}.\{(x-a)^2+y^2\}} \quad . \quad . \quad . \quad (2.2.6c)$$

Before proceeding to the second integration it is necessary to examine equations (2.2.3), (2.2.4) and (2.2.5) in order to determine whether for any values of Z(x,y) equations (2.2.1) and (2.2.2) are invalid. Clearly the stresses cannot be evaluated at the two end points of the line force, where $|x| = a$ and $y = V$.

Also, log z has a branch point at the origin, and the principal value of log z is that such that $|\vartheta(\log z)| < \pi$, which corresponds to a cut along the negative real axis. (Jeffreys and Jeffreys, 1946, p. 332). This cut makes the inverse tangent of $(\frac{y}{x})$ an odd function in y. Thus, the term arc tan $\frac{y - V}{x - a}$ is indeterminate if $y = V$ and $x - a \leq 0$, and the results for a line force along $y = V, |x| \leq a$, are not applicable at points (x, y) along the semi-infinite line, $y = V$ and $-\infty \leq x \leq +\infty$.

(iii) <u>The second integration</u>

In order to simulate the effect of a body force of magnitude P units per unit of cross sectional area acting in the positive y direction over the area $|x| \leq a$, $y1 \leq y \leq y2$, substitute the infinitesimal element P dv for L in equations (2.2.1) and (2.2.2) and integrate with respect to V between the limits V = y1 and V = y2. It has been shown in the previous paragraph that the stress due to a line force cannot be evaluated at all points in the half plane, and because of this it is necessary for the second integration to divide the cross-section into three zones denoted by A, B and C, (see diagram (1) of figure 2).

Consider a point z (x, y) in zone C defined by $y > y2$ <u>or</u> $y < y1$ <u>or</u> $x > a$. For such a point the stress distribution at z due to a line force along $y = V$, $|x| \leq a$, may be determined for any value of v in the range $y1 \leq v \leq y2$, and thus equations (2.2.1) and (2.2.2) with P dv substituted for L may be integrated directly with respect to v between these limits. Taking real and imaginary parts of the resulting equations and introducing the notation

$$R^2 = (x-u)^2 + (y+v)^2 \qquad r^2 = (x-u)^2 + (y-v)^2$$

$$\tan\theta = \frac{y+v}{x-u} \qquad \tan\phi = \frac{y-v}{x-u}$$

gives

$$\hat{x}x - \hat{y}y = \frac{P}{\pi(\kappa+1)}\left[\left[\tfrac{1}{2}(\kappa+1)(x-u)\log(R^2r^2) - (\kappa-1)(y-v)\phi - \left\{(3\kappa+5)y+(\kappa-1)v\right\}\theta + \frac{4yv(x-u)}{R^2}\right]_{u=-a}^{u=+a}\right]_{v=y_1}^{v=y_2} \quad (2.3.1)$$

$$\hat{x}y = -\frac{P}{2\pi(\kappa+1)}\left[\left[\tfrac{1}{2}(\kappa-1)(y-v)\log(r^2) + \tfrac{1}{2}\left\{(3\kappa+5)y+(\kappa-1)v\right\}\log(R^2) + (\kappa+1)(x-u)(\theta+\phi) - \frac{4yv(y+v)}{R^2}\right]_{u=-a}^{u=+a}\right]_{v=y_1}^{v=y_2} \quad (2.3.2)$$

and

$$\hat{x}\hat{x} + \hat{y}\hat{y} = \frac{2P}{\pi(\kappa+1)}\left[\left[\tfrac{1}{2}(\kappa+2)(x-u)\log(R^2) - \tfrac{1}{2}(x-u)\log(r^2) + (y-v)\phi - \left\{(\kappa+2)y+\kappa v\right\}\theta\right]_{u=-a}^{u=+a}\right]_{v=y_1}^{v=y_2} \quad (2.3.3)$$

Solving equations (2.3.1) and (2.3.3) gives

$$\hat{x}\hat{x} = \frac{P}{2\pi(\kappa+1)}\left[\left[\tfrac{1}{2}(3\kappa+5)(x-u)\log(R^2) + \tfrac{1}{2}(\kappa-1)(x-u)\log(r^2) - \left\{(5\kappa+9)y+(3\kappa-1)v\right\}\theta + (3-\kappa)(y-v)\phi + \frac{4yv(x-u)}{R^2}\right]_{u=-a}^{u=+a}\right]_{v=y_1}^{v=y_2} \quad (2.3.$$

and

$$\hat{y}\hat{y} = \frac{P}{2\pi(\kappa+1)}\left[\left[\tfrac{1}{2}(\kappa+3)(x-u)\log\left(\frac{R^2}{r^2}\right) + (\kappa+1)(y-v)(\theta+\phi) - \frac{4yv(x-u)}{R^2}\right]_{u=-a}^{u=+a}\right]_{v=y_1}^{v=y_2} \quad (2.3.$$

Thus expressions have been derived for $\hat{x}x$, $\hat{y}y$ and $\hat{x}y$ at a point (x,y) in the infinite zone C.

Now consider the cases of Z (x,y) in zones A or B. Remembering that the results for a line force acting along $y = V, |x| \leq a$, are not applicable at z

on the semi-infinite line $y = V, -\infty < x < a$, it follows that for Z in zones A or B it is necessary to replace the integral with respect to v by the sum of two integrals between the limits v = y1 to $v = y - \delta$ and $v = y + \delta$ to v = y2, where δ is positive and tends to zero. This procedure excludes the theoretically indeterminate effect of the force acting along a particular line, but the body force acting along a particular line is zero so that this omission has no effect. An equivalent viewpoint is that integration across the discontinuity in the angle ϕ is avoided by this process. Terms other than those in ϕ are continuous and are therefore not affected by this infinitesimal break in the integration path.

In fact it is found by letting δ tend to zero that $\hat{xx}$ and $\hat{yy}$ given by equations (2.3.4) and (2.3.5) are directly valid in zones A and B. This comes about because whenever ϕ is indeterminate it is multiplied by a zero factor, so effectively removing the discontinuity. Thus equations (2.3.4) and (2.3.5) are the required expressions for $\hat{xx}$ and $\hat{yy}$ for z in any of the three zones, and are continuous and may be evaluated throughout the positive half-plane except at the corners of zone A, $|x| = a$, y = y1 or y = y2., where the logarithmic terms have poles.

Divide the expression for $\hat{xy}$ given by equation (2.3.2.) into two components such that

$$\hat{xy} = \hat{xy}_1 + \hat{xy}_2 \quad \ldots\ldots\ldots (2.3.6)$$

where, for all z ,

$$\hat{xy}_1 = \frac{-P}{2\pi(\kappa+1)} \left[\left[\frac{1}{2}(\kappa-1)(y-v)\log(r^2) + \frac{1}{2}\left\{(3\kappa+5)y + (\kappa-1)v\right\}\log(R^2) + (\kappa+1)(x-u)\Theta - \frac{4yv(y+v)}{R^2} \right]_{u=-a}^{u=+a} \right]_{v=y_1}^{v=y_2} \quad (2.3$$

$$\text{and } \hat{xy}_2 = \lim_{\delta \to 0} \left\{ -\frac{P}{2\pi} \left[\left[(x-u)\phi \right]_{v=y_1}^{v=y-\delta} + \left[(x-u)\phi \right]_{v=y+\delta}^{v=y_2} \right]_{u=-a}^{u=+a} \right\} . \quad (2.3.$$

The component $\hat{xy}_1$ has poles at the four corners of zone A, but is otherwise continuous.

Equation (2.3.8) may be evaluated for Z in any of the three zones. For Z in zone A, (defined by $|x| \leqslant a$ and $y_2 \geqslant y \geqslant y_1$),

$$\hat{xy}_2 = \frac{P}{2\pi}\left[(x-a)\arctan\frac{y-v}{-(x-a)} + (x+a)\arctan\frac{y-v}{x+a}\right]_{v=y_1}^{v=y_2} \quad . \qquad (2.3.9)$$

for Z in zone B,(defined by $x < -a$ and $y2 \geqslant y \geqslant y1$),

$$\hat{xy}_2 = \frac{P}{2\pi}\left[\left[(x-u)\arctan\frac{y-v}{-(x-u)}\right]_{u=-a}^{u=+a}\right]_{v=y_1}^{v=y_2} \qquad (2.3.10)$$

and for Z in zone C, (defined by $x > a$ or $y > y2$ or $y < y1$),

$$\hat{xy}_2 = -\frac{P}{2\pi}\left[\left[(x-u)\phi\right]_{v=y_1}^{v=y_2}\right]_{u=-a}^{u=+a} \quad . \qquad (2.3.11)$$

The expression for $\hat{xy}2$ given by equation (2.3.11) is, of course, identical with the term in ϕ in equation (2.3.2).

It can be demonstrated that $\hat{xy}2$ as defined by equations (2.3.9), (2.3.10) and (2.3.11) is a continuous function throughout the half-plane.

In the circumstance $y = y1 = 0$, $x - u < 0$ the angle ϕ is analytically indeterminate but may be given the value $(+\pi)$ since there is no question of the integration path crossing the discontinuity.

To summarize, the stress components may be evaluated throughout the x - y half-plane except at the four points $|x| = a$, $y = y1$ or $y = y2$. The components $\hat{xx}$, $\hat{yy}$ and $\hat{xy}_1$ are given for all other values of z by equations (2.3.4), (2.3.5) and (2.3.7) respectively, and $\hat{xy}_2$ is defined for all z by equations (2.3.9), (2.3.10) or (2.3.11).

(iv) The symmetry of the general result

Consider firstly the symmetry of the general result with respect to x in order to check that $\hat{xx}$ and $\hat{yy}$ have even and $\hat{xy}$ has odd symmetry with respect to x.

The general form of the expressions for the stress components is

$$\hat{pq}(x,y) = \Big[\Big[f(v, x-u) \Big]_{u=-a}^{u=+a}\Big]_{v=y_1}^{v=y_2} , \qquad (2.4.1)$$

$$\text{so} \quad \hat{pq}(-x,y) = \Big[\Big[f(v, -x-u) \Big]_{u=-a}^{u=+a}\Big]_{v=y_1}^{v=y_2}$$

$$= -\Big[\Big[f(v, -(x-u)) \Big]_{u=-a}^{u=+a}\Big]_{v=y_1}^{v=y_2} . \qquad (2.4.2)$$

It follows from equations (2.4.1) and (2.4.2) that the symmetry of $\hat{pq}$ with respect to x is the opposite of that of the function f with respect to (x - u).

By inspection, the logarithmic and algebraic terms (i.e. all terms excluding the inverse tangent terms) within the double brackets of equations (2.3.4) and (2.3.5) for $\hat{xx}$ and $\hat{yy}$ are odd functions of (x - u), and the corresponding terms in equation (2.3.7) for $\hat{xy}_1$ are even functions of (x - u). Therefore the contributions of these terms to $\hat{xx}$ and $\hat{yy}$ are even functions of x, and the contribution to $\hat{xy}_1$ is an odd function of x.

Now consider the contributions of the remaining inverse tangent terms which are of the form

$$\hat{pq}(x,y) = \Big[\Big[F_1(v, x-u) \arctan\tfrac{y+v}{x-u} + F_2(v, x-u) \arctan\tfrac{y-v}{x-u} \Big]_{u=-a}^{u=+a}\Big]_{v=y_1}^{v=y_2} . \qquad (2.4.3)$$

Using the relationship $\arctan \dfrac{y}{-x} = (\text{sign of } y) \times \pi - \arctan \dfrac{y}{x}$, an analysis of $\hat{pq}(-x,y)$ where F_1 and F_2 have the forms occurring in equations (2.3.4), and (2.3.5) and (2.3.7), shows that, for such F_1 and F_2,

$$\hat{pq}(-x,y) = \left[\left[F_1(v,-(x-u)) \arctan\frac{y+v}{x-u} + F_2(v,-(x-u)) \arctan\frac{y-v}{x-u} \right]_{u=-a}^{u=+a} \right]_{v=y_1}^{v=y_2} \quad \ldots \quad (2.4.$$

Thus, for these terms, the symmetry of $\hat{pq}(x,y)$ in x is the same as that of the coefficients of the inverse tangent terms in $(x - u)$. It follows from inspection of equations (2.3.4), (2.3.5) and (2.3.7) that it has now been proved that $\hat{xx}$ and $\hat{yy}$ are even functions of x and that $\hat{xy}_1$ is an odd function of x.

It only remains to prove that $\hat{xy}_2$ is an odd function in x. This is easily done by using equations (2.3.9), (2.3.10) and (2.3.11) to prove the following three identities

(1) for $y < y_1$ or $y > y_2$, $(\hat{xy}_2(x,y))_{\text{Zone C}} = -(\hat{xy}_2(-x,y))_{\text{Zone C}}$

(2) for $y_1 \leq y \leq y_2$ and $|x| \leq a$, $(\hat{xy}_2(x,y))_{\text{Zone A}} = -(\hat{xy}_2(-x,y))_{\text{Zone A}}$

and (3) for $y_1 \leq y \leq y_2$ and $x > a$, $(\hat{xy}_2(x,y))_{\text{Zone C}} = -(\hat{xy}_2(-x,y))_{\text{Zone B}}$.

Hence it can be shown that the general result satisfies the fundamental requirements with respect to symmetry in x.

(v) The stresses at infinity

A further fundamental requirement is that the stress components $\hat{xx}$, $\hat{yy}$ and $\hat{xy}$ should, for finite a and y_2, tend to zero as $|x|$ or y tend to infinity. By considering the expressions within the double brackets of equations (2.3.4), (2.3.5), (2.3.7), (2.3.9), (2.3.10) and (2.3.11) term by term for the three cases, $x \to \infty$, $y \to \infty$ and $y = cx \to \infty$, (where c is a positive constant), it can be simply shown that the terms inside the brackets tend either to zero or a function independent of the limits which yields zero on expansion of the brackets.

It follows from consideration of the physical model that the general result should contract to the point force result given by equations (2.1.1) and (2.1.2)

for the case U equals zero if a tends to zero, y_1 and y_2 each tend to v, and P behaves in such a manner that $2a\,(y_2 - y_1)\,P$ tends to a constant Y, which is the magnitude of the equivalent point force. When this arduous task is carried out it is found that the general result does satisfy this check. The process used is of course basically a double differentiation carried out from first principles, but it has the advantage that it can be thought of purely in terms of the physical model rather than the mathematical model.

(vi) The equations of equilibrium

In order to prove the validity and uniqueness of the general solution it is necessary to show that the stress components satisfy the equations of equilibrium and the equations of compatibility. For the plane problem, the equations of equilibrium reduce to equations (1.2.3), which are

$$\frac{\partial}{\partial x}(\hat{xx}) + \frac{\partial}{\partial y}(\hat{yx}) + X = 0 \qquad (2.6.1)$$

and

$$\frac{\partial}{\partial x}(\hat{xy}) + \frac{\partial}{\partial y}(\hat{yy}) + Y = 0 \qquad (2.6.2)$$

It must be remembered that in the original point force model X and Y were zero, but now there is a simulated body force in zone A so that X is zero for all Z, and Y is zero in zones B and C but equal to P in zone A.

Remembering that $(\hat{yx})$ equals $(\hat{xy})$, differentiate and add equations (2.3.4) and (2.3.7), giving, for all (x,y),

$$\frac{\partial}{\partial x}(\hat{xx}) + \frac{\partial}{\partial y}(\hat{xy}_1) = \frac{P}{2\pi(\kappa+1)}\left[\left[\frac{1}{2}(3\kappa+5)\left\{\log(R^2) + \frac{2(x-u)^2}{R^2}\right\} + \frac{1}{2}(\kappa-1)\left\{\log(T^2) + \frac{2(x-u)^2}{T^2}\right\}\right.\right.$$

$$\left. + 4yv\frac{(y+v)^2-(x-u)^2}{R^4} + \left\{(5\kappa+9)y + (3\kappa-1)v\right\}\frac{y+v}{R^2} - (3-\kappa)(y-v)\frac{y-v}{T^2}\right.$$

P.T.O.

$$-\tfrac{1}{2}(\kappa-1)\left\{\log(r^2)+\frac{2(y-v)}{r^2}\right\}-\tfrac{1}{2}(3\kappa+5)\left\{\log(R^2)+\frac{2y(y+v)}{R^2}\right\}$$

$$-(\kappa-1)\frac{v(y+v)}{R^2}-(\kappa+1)\frac{(x-u)^2}{R^2}+4v\left\{\frac{2y+v}{R^2}-\frac{2y(y+v)^2}{R^4}\right\}\Bigg]_{u=-a}^{u=+a}\Bigg]_{v=y_1}^{v=y_2},$$

which, since constants within the brackets cancel on expansion, can be reduced to the form

$$\frac{\partial}{\partial x}(\hat{xx})+\frac{\partial}{\partial y}(\hat{xy}_1)=\frac{P}{2\pi}\left[\left[\frac{(x-u)^2}{r^2}\right]_{u=-a}^{u=+a}\right]_{v=y_1}^{v=y_2}. \qquad (2.6.3)$$

Subtract equation (2.6.3) from equation (2.6.1) and put X equal to zero for all (x,y), giving, for all (x,y),

$$\frac{\partial}{\partial y}(\hat{xy}_2)=-\frac{P}{2\pi}\left[\left[\frac{(x-u)^2}{r^2}\right]_{u=-a}^{u=+a}\right]_{v=y_1}^{v=y_2}. \qquad (2.6.4)$$

If the expressions for $\hat{xy}_2$ as given by equations (2.3.9), (2.3.10) and (2.3.11) for (x,y) in zones A, B and C are examined in turn, it may easily be shown that they all satisfy equation (2.6.4) and that therefore the general results satisfy equation (2.6.1).

Similarly, differentiating and adding equations (2.3.7) and (2.3.5) gives, for all (x,y),

$$\frac{\partial}{\partial x}(\hat{xy}_1)+\frac{\partial}{\partial y}(\hat{yy})=\frac{P}{2\pi(\kappa+1)}\left[\left[-\tfrac{1}{2}(\kappa-1)(y-v)\frac{2(x-u)}{r^2}-\tfrac{1}{2}\left\{(3\kappa+5)y+(\kappa-1)v\right\}\frac{2(x-u)}{R^2}-(\kappa+1)\left\{-\frac{(x-u)(y+v)}{R^2}+\Theta\right\}\right.\right.$$

$$-4yv(y+v)\frac{2(x-u)}{R^4}+\tfrac{1}{2}(\kappa+3)(x-u)\left\{\frac{2(y+v)}{R^2}-\frac{2(y-v)}{r^2}\right\}-4v(x-u)\left\{\frac{R^2-2y(y+v)}{R^4}\right\}$$

$$\left.\left.+(\kappa+1)(y-v)(x-u)\left\{\frac{1}{R^2}+\frac{1}{r^2}\right\}+(\kappa+1)(\Theta+\phi)\right]_{u=-a}^{u=+a}\right]_{v=y_1}^{v=y_2},$$

which reduces to

$$\frac{\partial}{\partial x}(x\hat{y}_1) + \frac{\partial}{\partial y}(y\hat{y}) = \frac{P}{2\pi}\left[\left[-\frac{(x-u)(y-v)}{r^2} + \phi\right]_{u=-a}^{u=+a}\right]_{v=y_1}^{v=y_2} \quad . \qquad (2.6.5)$$

Subtracting equation (2.6.5) from equation (2.6.2) gives

$$\frac{\partial}{\partial x}(x\hat{y}_2) + Y = -\frac{P}{2\pi}\left[\left[-\frac{(x-u)(y-v)}{r^2} + \phi\right]_{u=-a}^{u=+a}\right]_{v=y_1}^{v=y_2} \quad . \qquad (2.6.6)$$

It may readily be shown from equations (2.3.9), (2.3.10) and (2.3.11) that equation (2.6.6) is satisfied for (x,y) in zones B and C where Y equals zero and also for (x,y) in zone A where Y is put equal to P.

Thus the general results are seen to satisfy the equations of equilibrium.

(vii) The equations of compatibility

If stress components are to represent a valid solution of the elastic problem they must satisfy the equations of compatibility (see (ii) of Chapter 1). Assuming a plane strain solution and that $\frac{\partial Y}{\partial x} = \frac{\partial Y}{\partial y} = 0$ everywhere, the equations of compatibility reduce in number to four of which only one is independent of the other three and the equations of equilibrium. The present model is such that although changes in the body forces occur at the boundaries of zone A, it is not possible to specify co-ordinates at which the differentials of Y are not equal to zero.

Consequently the equations of compatibility are proved to be satisfied if it is shown, for example, that

$$\left(\frac{\partial^2}{\partial x^2} + \frac{\partial^2}{\partial y^2}\right)(x\hat{x} + y\hat{y}) = 0 \quad , \qquad (2.7.1)$$

which is equation (1.2.4c).

It follows from equation (2.3.3) that for (x,y) in zones A, B or C,

$$x\hat{x} + y\hat{y} = \frac{2P}{\pi(\kappa+1)} \left[\left[F \right]_{u=-a}^{u=+a} \right]_{v=y_1}^{v=y_2} ,$$

where $F = \left\{ \frac{1}{2}(\kappa+2)(x-u)\log(R^2) - \frac{1}{2}(x-u)\log(T^2) + (y-v)\phi - \left\{ (\kappa+2)y + \kappa v \right\} \Theta \right\}$ . . . . . (2.7.2)

Then,

$$\frac{\partial^2 F}{\partial x^2} = \left\{ \frac{1}{2}(\kappa+2)\left\{ \frac{2(x-u)}{R^2} + 2\,\frac{R^2 \cdot 2(x-u) - 2(x-u)^3}{R^4} \right\} - \frac{1}{2}\left\{ \frac{2(x-u)}{T^2} + 2\,\frac{T^2 \cdot 2(x-u) - 2(x-u)^3}{T^4} \right\} \right.$$

$$\left. + (y-v)^2\,\frac{2(x-u)}{T^4} - (y+v)\left\{ (\kappa+2)y + \kappa v \right\}\frac{2(x-u)}{R^4} \right\} \qquad (2.7.3)$$

and

$$\frac{\partial^2 F}{\partial y^2} = \left\{ -2(x-u)v\,\frac{2(y+v)}{R^4} + \frac{x-u}{T^2} - (\kappa+2)\,\frac{x-u}{R^2} \right\} . \qquad (2.7.4)$$

It follows from equations (2.7.3) and (2.7.4) that

$$\left(\frac{\partial^2}{\partial x^2} + \frac{\partial^2}{\partial y^2} \right) F = 0$$

and therefore that equation (2.7.1) and all the equations of compatibility are satisfied by the general result.

(viii) <u>The stresses at the free surface</u>

Consider the stress system at the free surface by putting y equal to zero in equations (2.3.4), (2.3.5), (2.3.7), (2.3.9), (2.3.10) and (2.3.11). Making use of the fact that $(\arctan \frac{y}{x})$ is an odd function of y, it follows that, excluding the two points ($|x| = a$, $y = 0$) in the special case where y_1

equals zero, then

$$(\hat{xx})_{y=0} = \frac{P}{2\pi(\kappa+1)} \left[\left[2(\kappa+1)(x-u)\log\{(x-u)^2+v^2\} - 4(\kappa-1)v \arctan\frac{v}{x-u} \right]_{u=-a}^{u=+a} \right]_{v=y_1}^{v=y_2} \quad \ldots \quad (2.8.1)$$

$$\text{and} \quad (\hat{yy})_{y=0} = (\hat{xy})_{y=0} = 0 .$$

Thus the inherent boundary conditions at a free surface are satisfied.

(ix) The plane substratum

Consider the case of an infinite, plane, horizontal substratum by letting the dimension a tend to infinity in the general results. The corresponding simplest equilibrium system is shown in diagram 2 of figure 2. It is necessary to maintain the equilibrium of the half-space by a line force applied along a line at great depth and of infinite length. Unlike the point force or line force of finite length used to maintain equilibrium in the general case, this line force distribution of infinite length does not have a negligible effect near the surface, and the associated stress system must be regarded as part of the main solution, since equilibrium is a primary requirement.

Consider first this supplementary stress system by letting a and v in equations (2.2.2), (2.2.3) and (2.2.4) tend to infinity in such a way that $\frac{a}{v}$ also tends to infinity. The only terms that are significant as a tends to infinity and the expressions are expanded are those in which the limit is a function of V of such a type that the terms do not cancel. This is true whether the "limit" of the term be finite or infinite. Thus only the inverse tangent terms prove to be significant as a tends to infinity.

Assuming $y < V$ and putting $L = -P(y_2 - y_1)$ into equations (2.2.2), (22.3) and (2.2.4) gives, as a tends to infinity, the supplementary stress

system defined by

$$\hat{xx} = P\frac{2(\kappa-1)}{\kappa+1}(y_2-y_1) \quad , \quad \hat{yy} = \hat{xy} = 0 . \qquad (2.9.1)$$

Now let a tend to infinity in the main results. Since $\arctan \dfrac{y \pm v}{x + a}$ tends to zero as a tends to infinity for all $(y \pm v)$, it follows from equations (2.3.4) and (2.3.5) that

$$\hat{xx} \to \frac{P}{2\pi(\kappa+1)}\left[(3-\kappa)(y-v)\arctan\frac{y-v}{x-a} - \left\{(5\kappa+9)y+(3\kappa-1)v\right\}\arctan\frac{y+v}{x-a}\right]_{v=y_1}^{v=y_2}$$

and $$\hat{yy} \to \frac{P}{2\pi(\kappa+1)}\left[(\kappa+1)(y-v)\left\{\arctan\frac{y+v}{x-a} + \arctan\frac{y-v}{x-a}\right\}\right]_{v=y_1}^{v=y_2} .$$

The limits of these equations as a tends to infinity are functions of y, so that the three ranges of y must be considered in turn. The results obtained are

$$\text{for } y < y_1 < y_2 \quad , \quad \hat{xx} = -P\frac{2(\kappa-1)}{\kappa+1}(y_2-y_1) \quad , \quad \hat{yy} = 0 \quad ,$$

$$\text{for } y_1 \le y \le y_2 \quad , \quad \hat{xx} = \frac{-P}{\kappa+1}\left\{(3-\kappa)y + 2(\kappa-1)y_2 - (\kappa+1)y_1\right\}, \quad \hat{yy} = -P(y-y_1) \quad ,$$

$$\text{and for } y_1 < y_2 < y \quad , \quad \hat{xx} = -P(y_2-y_1) \quad , \quad \hat{yy} = -P(y_2-y_1) \quad . \qquad (2.9$$

The stress component $\hat{xy}$ defined by equations (2.3.6), (2.3.7), (2.3.9) and (2.3.11) may be treated similarly except that both limits of u have to be considered since when the inverse tangent tends to zero, it is multiplied by a term tending to infinity. The result obtained is

for $y < y_1 < y_2$ (zone C) , $\hat{xy} = 0$,

for $y_1 \leq y \leq y_2$ (zone A) , $\hat{xy} = 0$,

and for $y_1 < y_2 < y$ (zone C) , $\hat{xy} = 0$ . . . . . (2.9.3)

Add the stress system given by equations (2.9.1), (2.9.2) and (2.9.3) to find the following final results for the case of the plane substratum,

for $y < y_1 < y_2$, $\hat{xx} = 0$, $\hat{yy} = 0$, $\hat{xy} = 0$,

for $y_1 \leq y \leq y_2$, $\hat{xx} = -P\frac{3-k}{k+1}(y-y_1)$, $\hat{yy} = -P(y-y_1)$, $\hat{xy} = 0$,

and for $y_1 < y_2 < y$, $\hat{xx} = -P\frac{3-k}{k+1}(y_2-y_1)$, $\hat{yy} = -P(y_2-y_1)$, $\hat{xy} = 0$ . . . (2.9.4)

A further special case is that of the homogeneous half-space in equilibrium. This may be considered by putting y_1 equal to zero in equations (2.9.4) for the case $y_1 \leq y \leq y_2$.

Thus, $\hat{xx} = -P\frac{3-k}{k+1}y$, $\hat{yy} = -Py$, $\hat{xy} = 0$, . . . (2.9.5)

which is, of course, the expected result. Note that the plane strain solutions for the substratum and half-space are complete solutions in that the physical assumptions in the x and z directions are identical and

$$\hat{zz} = \sigma(\hat{xx} + \hat{yy}) = \hat{xx} .$$

(x) The terminated substratum

A further case of interest is that of the terminated, semi-infinite substratum

shown in diagram 3 of figure 2. The results for this case may be regarded as an alternative expression of the general result since a finite rectangular density anomaly may be built up by adding two terminated substrata. This is illustrated by figure 4.

The method of obtaining this result from the earlier general result is to move the origin to -a, so that $(x - u)_{u = a}$ is replaced by $(x - 2a)$ and $(x - u)_{u = -a}$ is replaced by x, and then let a tend to infinity.

Consider first the stress system due to the line force required for equilibrium. Applying the above procedure to equations (2.2.2), (2.2.3) and (2.2.4), and assuming that v also tends to infinity, but in such a way that $\frac{a}{v}$ tends to infinity, it can be shown that for finite x and y,

$$\hat{xx} = -\frac{\kappa-1}{\kappa+1} L , \quad \hat{yy} = \hat{xy} = 0 . \qquad (2.10.1)$$

If this process is now applied to the general results given by equations (2.3.4), (2.3.5), (2.3.7), (2.3.9), (2.3.10) and (2.3.11) it is found that

$$\hat{xx} = \frac{P}{2\pi(\kappa+1)} \Bigg[-\tfrac{1}{2}(3\kappa+5)x \log\{x^2+(y+v)^2\} - \tfrac{1}{2}(\kappa-1)x \log\{x^2+(y-v)^2\}$$
$$- \{(5\kappa+9)y + (3\kappa-1)v\} \arctan\frac{y+v}{-x} + (3-\kappa)(y-v)\arctan\frac{y-v}{-x} - \frac{4yvx}{x^2+(y+v)^2} \Bigg]_{v=y_1}^{v=y_2} , \qquad (2.10.2)$$

$$\hat{yy} = \frac{P}{2\pi(\kappa+1)} \Bigg[-\tfrac{1}{2}(\kappa+3)x \log\frac{x^2+(y+v)^2}{x^2+(y-v)^2} + (\kappa+1)(y-v)\left\{\arctan\frac{y+v}{-x} + \arctan\frac{y-v}{-x}\right\} + \frac{4yvx}{x^2+(y+v)^2} \Bigg]_{v=y_1}^{v=y_2} , \qquad (2.10.3)$$

$$\hat{xy} = \frac{-P}{2\pi(\kappa+1)} \Bigg[-\tfrac{1}{2}(\kappa-1)(y-v)\log\{x^2+(y-v)^2\} - \tfrac{1}{2}\{(3\kappa+5)y + (\kappa-1)v\}\log\{x^2+(y+v)^2\}$$
$$+ (\kappa+1)\left\{v - x\arctan\frac{y+v}{x}\right\} + \frac{4yv(y+v)}{x^2+(y+v)^2} \Bigg]_{v=y_1}^{v=y_2} , \qquad (2.10.4)$$

for z in zones A or C,

$$\hat{xy}_2 = \frac{P}{2\pi}\left[v + x \arctan\frac{y-v}{x} \right]_{v=y_1}^{v=y_2} , \qquad (2.10.5)$$

and for z in zone B,

$$\hat{xy}_2 = \frac{P}{2\pi}\left[v - x \arctan\frac{y-v}{-x} \right]_{v=y_1}^{v=y_2} . \qquad (2.10.6)$$

On adding the supplementary system given by equation (2.10.1), with L equal to $-P(y_2 - y_1)$, only equation (2.10.2) is modified and becomes

$$\hat{xx} = \frac{P}{2\pi(\kappa+1)}\left[-\tfrac{1}{2}(3\kappa+5)x \log\{x^2+(y+v)^2\} - \tfrac{1}{2}(\kappa-1)x \log\{x^2+(y-v)^2\} - \{(5\kappa+9)y + (3\kappa-1)v\} \arctan\frac{y+v}{-x} \right.$$
$$\left. + (3-\kappa)(y-v) \arctan\frac{y-v}{-x} - \frac{4yvx}{x^2+(y+v)^2} + 2\pi(\kappa-1)v \right]_{v=y_1}^{v=y_2} . \qquad (2.10.7)$$

Thus the full solution for the case of the terminated semi-infinite substratum is given by equations (2.10.7), (2.10.3), (2.3.6), (2.10.4), (2.10.5) and (2.10.6).

In order to find expressions for the surface stresses in the case of the terminated substratum, put y equal to zero in these equations. Then,

$$(\hat{xx})_{y=0} = \frac{-P}{\pi(\kappa+1)}\left[(\kappa+1)x \log(x^2+v^2) + (\kappa-1)v\left\{ \arctan\frac{v}{-x} - \arctan\frac{v}{x} \right\} \right]_{v=y_1}^{v=y_2} , \qquad (2.10.8)$$

and $(\hat{yy})_{y=0} = (\hat{xy})_{y=0} = 0$.

(xi) Summary

Plane strain solutions have been derived for the stress components at points within an otherwise homogeneous elastic half-space in which there are various rectangular zones of the cross section with a contrasting density. These zones are defined by planes parallel or normal to the free surface.

It is emphasized that the solution has been obtained to a static problem.

CHAPTER 3

SOME NUMERICAL RESULTS AND THEIR INTERPRETATION

(i) General considerations

The results of Chapter 2 are to be applied to geological models, and therefore only the plane strain solution will be used. The work of Dean, Parsons and Sneddon (1944) and of Sneddon (1944), which was described in Chapter 1, suggests that the effects of this approximation are unlikely to be serious. The stress field is a function of only one elastic parameter, namely Poisson's ratio. It has been shown numerically from equation (2.8.1) that the stress distribution over the free surface for a wide range of models is not unduly sensitive to changes in the value of Poisson's ratio. A similar conclusion was reached with respect to their own model by Dean, Parsons and Sneddon. In the numerical work described in this chapter Poisson's ratio is equal to 0.25, except for the simulation of the results obtained by Durney, where his value of 0.28 is used. Similarly, the acceleration due to gravity is put equal to 1000 cm/sec^2 in this special case but is otherwise taken as 981 cm/sec^2.

The values of the stress components given by the results of Chapter 2 are directly proportional to the density contrast, the acceleration due to gravity and the linear scale of the model. Thus, when considering only the form, (and not the magnitude), of the stress field, models may be scaled so that one dimension is always constant. If this is done, then there are generally two independent dimensional parameters required to specify the shape and location of a single mass anomaly.

The method of applying the expressions derived in the previous chapter is to evaluate the state of stress at a series of grid points over the area of the cross section of the model. If the model is symmetrical, then only half of the

cross section need be considered. As indicated in Chapter 1, the function most generally evaluated and contoured will be the positive stress-difference of the three principal stresses. The main problems that will be considered numerically are the general variation of stress at the free surface, two models representing a mass anomaly within the crust and presented here as models of a granite batholith either outcropping at the free surface (first model) or existing at considerable depth (second model), and a set of models representing the Airy isostatic compensation of a surface load such as a large mountain chain. The granite batholith models are defined by (y2 - y1) equal to eight kilometres, 'a' equal to eleven kilometres, the density contrast equal to -0.1 gm/cc, and y1 equal to zero (first model) or to eight kilometres (second model). The compensated mountain chain model is made up of a uniform surface load, which represents a mountain with a width of 600 kilometres, an average height of 3 kilometres and a density of 2.8 gm/cc, and which is compensated by a rectangular mass deficit of equal magnitude defined by y1 equal to 30 kilometres, y2 equal to 51 kilometres, 'a' equal to 300 kilometres and a density contrast of -0.4 gm/cc.

The stress-difference used for the numerical calculations is defined as the positive stress-difference of the three principal stresses. This is contrary to the practice of many authors who consider the difference of the two principal stresses in the x - y plane. This two dimensional definition corresponds to the function determined by photoelastic results. There are two reasons for using the three principal stresses in the present problem. Firstly, the plane strain assumption assigns a value to all three principal stresses, and therefore it is necessary to include all three stresses in the definition in order to be consistent with the implications of this initial assumption. Secondly, the definition involving all three principal stresses has physical significance,

because it is a measure of the approximation of the stress to the hydrostatic state. Jeffreys (1962) uses this definition of the stress-difference while discussing harmonic surface loading of an elastic half-space when at small depths his pp_{22}, ($\equiv \hat{zz}$), is an extreme stress.

(ii) The half-space stress computer programme

A computer programme has been written in the Algolprogramming language which calculates the state of stress at any point in a half-space of specified density due to any number of rectangular density anomalies, infinite or semi-infinite plane substrata and uniform surface loads. The position of each of these components along the horizontal x - axis is variable, and tectonic stresses may be allowed for according to equation (1.3.7).

The programme and its specification are given in appendices 2 and 3 respectively. The programme consists of a series of "procedures" (sub-routines) corresponding to the different model components and stress functions that may be required, and a main part which reads the model parameters from data tapes, calls up the required procedures, and controls the form of the output.

The following is a brief description of the procedures.

INVTAN This procedure evaluates inverse tangents in the range $+\pi$ to $-\pi$. Unusual precautions are necessary since the procedure operates upon identifiers of type real, which are often the small difference between two large numbers, and therefore liable to significant error, which might prove critical in evaluating a discontinuous function such as the inverse tangent. The numerical constants used in this procedure imply that when the programme is used to study geological models, the unit of length should be of the same order of magnitude as the centimetre.

INSIDE and RECTANGLE These procedures calculate the Cartesian stress components $\hat{xx}$, $\hat{yy}$ and $\hat{xy}$, given by equations (2.3.4), (2.3.5), (2.3.7), (2.3.9), (2.3.10) and (2.3.11), at a given point (x,y) for a rectangular density anomaly.

INSURECT and SURECT These procedures calculate $\hat{xx}$ given by equation (2.8.1) at a given point (x,o) at the free surface for a rectangular density anomaly.

SUBSTRATUM This procedure calculates $\hat{xx}$ and $\hat{yy}$ given by equations (2.9.4) at a given point (x,y) for a plane substratum model.

SURFACE This procedure calculates $\hat{xx}$, $\hat{yy}$ and $\hat{xy}$ given by equations (2.2.6) at a given point (x,y) due to a uniform surface load.

INNER and TERMINATED These procedures calculate $\hat{xx}$, $\hat{yy}$ and $\hat{xy}$, given by equations (2.10.7), (2.10.3), (2.3.6), (2.10.4), (2.10.5) and (2.10.6), at a given point (x,y) for a semi-infinite substratum model.

SURTERM This procedure calculates $\hat{xx}$ given by equation (2.10.8) at a given point (x,o) at the free surface for a semi-infinite substratum model.

PRINCIPAL STRESSES This procedure calculates the three principal stresses of the plane strain solution from the values of $\hat{xx}$, $\hat{yy}$ and $\hat{xy}$ according to equations (1.2.1), and prints out these three principal stresses, the angle Θ given by equation (1.2.2), and the positive stress-difference of the three principal stresses.

MISES This procedure calculates the von Mises function given by equation (1.3.6) from $\hat{xx}$, $\hat{yy}$ and $\hat{xy}$, assuming a plane strain solution.

CLASSIFY In order to reduce the considerable labour of examining the results, this procedure may be used to classify the state of stress at a point (x,y) given in terms of the principal stresses in the following

manner:-

(a) A 'g', 'i' or 'l' is printed according to whether the third principal stress, $\hat{z}z$, is algebraically the greatest, intermediate or least principal stress.

(b) An 'a', 'b', 'c' or 'd' is printed according to whether three, two, one or zero principal stresses are less than zero, (i.e. compressional).

(c) If the sum of three principal stresses is less than zero, then print 'cn' and the values of the Coulomb-Navier fracture function, which is the value of So given by equation (1.3.3), for the cases $\phi = 30^{\circ}$ and $\phi = 55^{\circ}$. Otherwise, if $3pp_{11} + pp_{22} > 0$ print 'ga', else print 'gb', and then the value of the tensile strength necessary for failure according to the Griffith theory of equation (1.3.5). In the programme which has been used for production work and which is given in appendix 2, this part of this procedure is not strictly correct in that the Griffith criterion is evaluated in terms of the greatest and least principal stresses instead of pp_{11} and pp_{22}. The significance of this distinction is indicated in Chapter 1. However, in all the cases that it has been used, zz has been the intermediate principal stress.

In the main programme parameters such as the density and Poisson's ratio of the half-space, the acceleration due to gravity, tectonic stress systems represented by equation (1.3.7), the programme control integers which determine the sequence of the calculations, and the parameters of the mass anomaly models are read from data tapes. The values of(x,y) are either read directly from data tapes or defined by a grid. The common case of the supplementary stress for a

hydrostatic natural state is treated by putting the half-space density equal to zero. A flow diagram of this programme and details of the data tape format are included in appendix 3.

The reasons for writing the programme with so many distinct special cases were to check the consistency of the different equations derived in Chapter 2 and to save computer time during production runs. This saving of computer time was of course reduced by the extra time taken to compile the programme during testing. Numerical calculations using the results of Chapter 2 were first carried out in 1963 using a Pegasus Autocode programme which was thoroughly tested by comparing the results with hand calculations. The programme described here, which was written in 1966 using the much simpler Algol language, was fully tested and found to be self consistent (e.g. simulation of a rectangle by two semi-infinite plane substrata) and also to give identical results to the Autocode programme. New results such as SURFACE, MISES or CLASSIFY were tested by hand calculations.

The accuracy of the calculation is limited by the number of significant figures used for constants such as π . The accuracy of about 1 in 10^4 is clearly more than adequate for the type of problem considered, and the error is insignificant in comparison to the effects of the various approximations implied in the model.

(iii) The stresses at the free surface

The discussion of the state of stress at the free surface of the elastic half-space due to internal density anomalies is simplified by the facts that the principal directions are orientated parallel and normal to the free surface and that only one principal stress, (equal to $\hat{xx}$), is not zero. Also, in the absence of tectonic stresses, the surface stress is independent of the assumed natural state at depth.

The variation of surface stress over a semi-infinite terminated substratum with a density contrast of + 0.1 gm/cc and thickness of one kilometre is shown in figure 3 for different depths (y1) to the upper surface. The magnitude of the surface stress is zero directly above the end of the anomalous mass, (x = 0), and increases steadily as |x| increases, reaching a maximum value when |x| equals 1.25 - 1.5 times y2, (y2 is the depth of the lower surface of the anomaly). The magnitude of the surface stress decreases only slightly for further increases in |x| . The magnitude of the maximum surface stress is largely independent of the depth of burial, and is equal to about 4.10^6 dyne/cm^2, (i.e. 4 bars). The use of these curves for interpretation tends to be misleading because of the infinite extent of the model. The importance of these results is the understanding that they give of the variation of surface stress over a rectangular density anomaly of finite lateral extent. The relationship between the two cases is demonstrated in figure 4. The distribution of surface stress due to a rectangular density contrast of + 0.1 gm/cc, with a thickness of one kilometre and various widths, is shown in figures 5, 6, 7 and 8. The surface stress is greatest and compressional over a positive density anomaly, and tends to be tensile outside the limits of the anomaly. Except for the case of anomalous bodies with a width, 2a, much greater than the depth to the lower boundary, y2, the maximum surface stress amplitude occurs over the centre of the body. In the exceptional case, it occurs over the limits of the body, but the value over the centre is still high.

The surface stress over the centre of a finite anomaly of width 2a equals twice that over the corresponding terminated substratum at x equal to a. Thus, for fixed thickness (y2 - y1), the central surface stress increases steadily as 'a' increases from zero to about $1\frac{1}{4}$ times y2, and then decreases slightly for further increases in 'a'. For a positive density anomaly of 0.1 gm/cc, with a

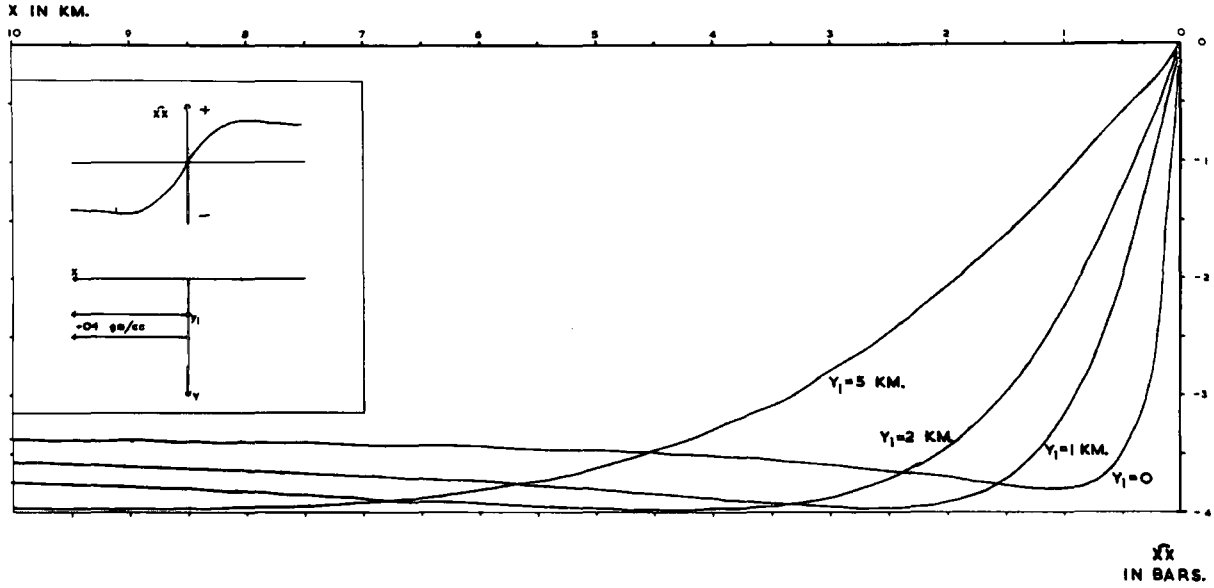

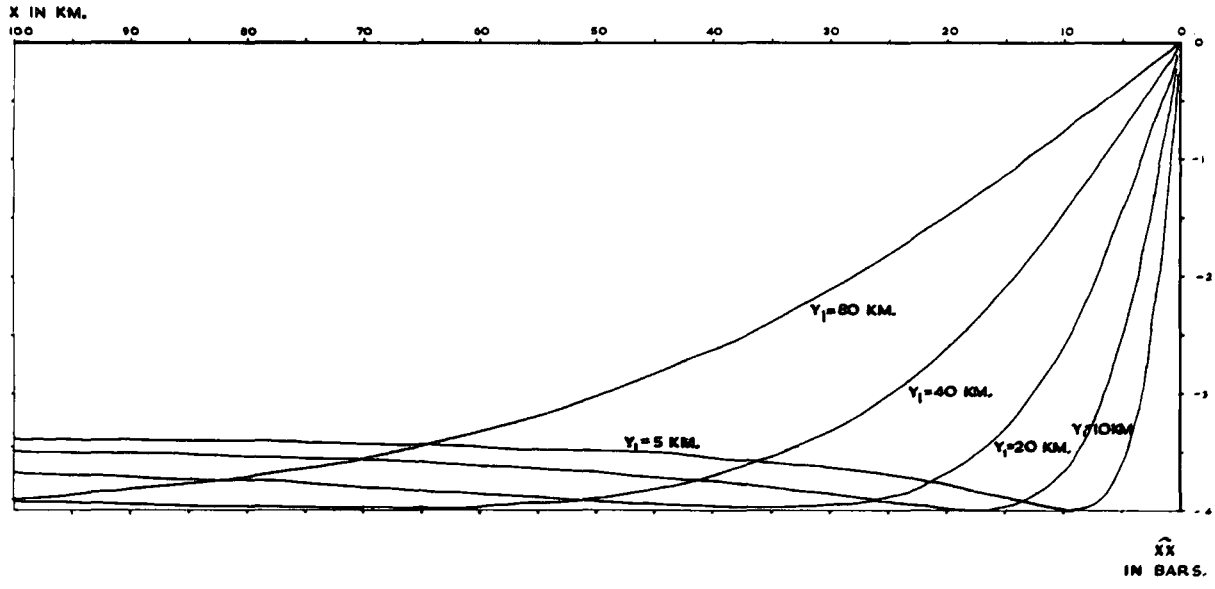

THE SURFACE STRESS OVER A SEMI-INFINITE PLANE SUBSTRATUM OF DENSITY CONTRAST +0·1 gm/cc AND THICKNESS 1·0 KILOMETRES AT DIFFERENT DEPTHS.

Figure 3

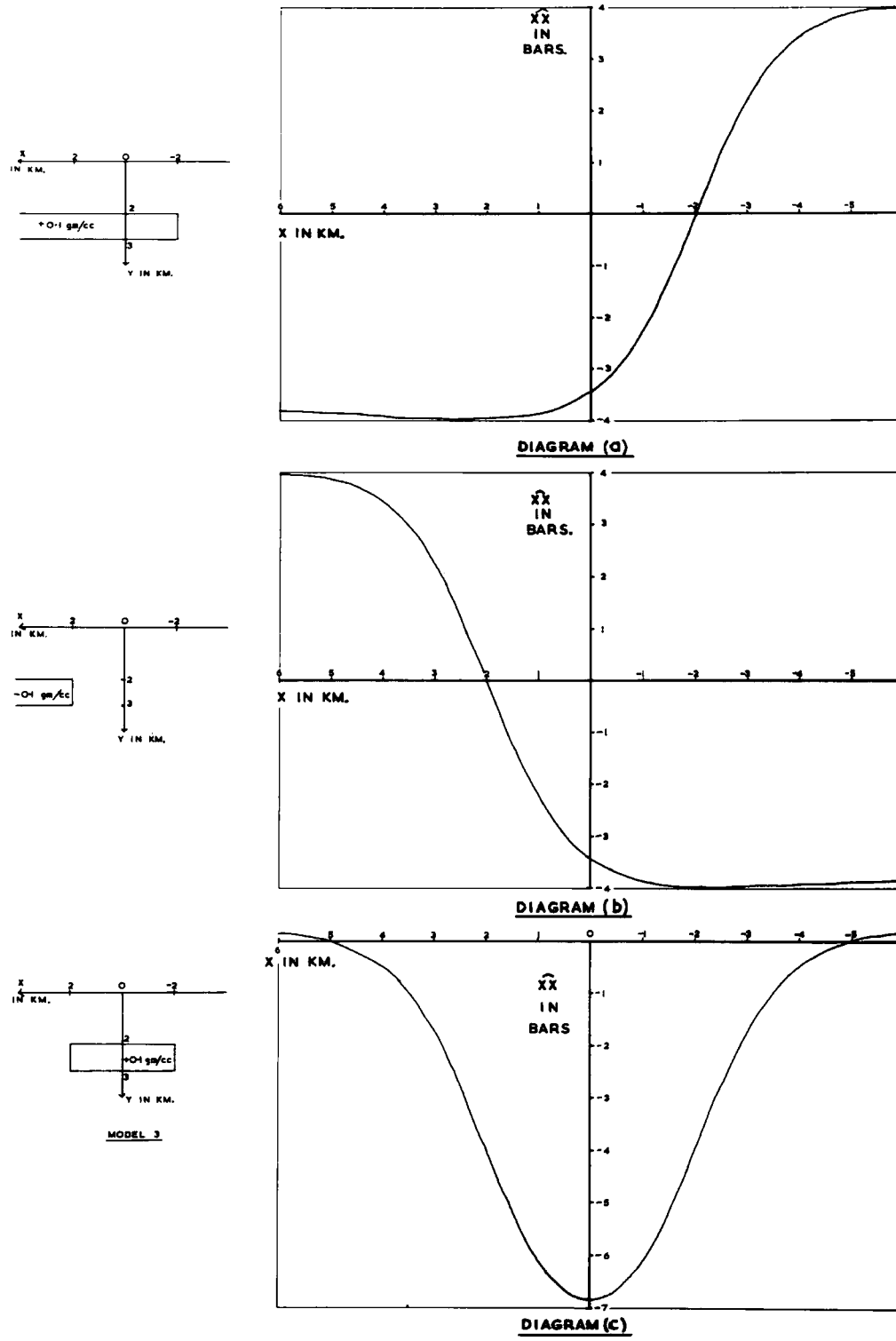

THE CALCULATION OF THE SURFACE STRESS OVER A RECTANGULAR ANOMALY FROM THE SEMI-INFINITE SUBSTRATUM RESULT.

Figure 4

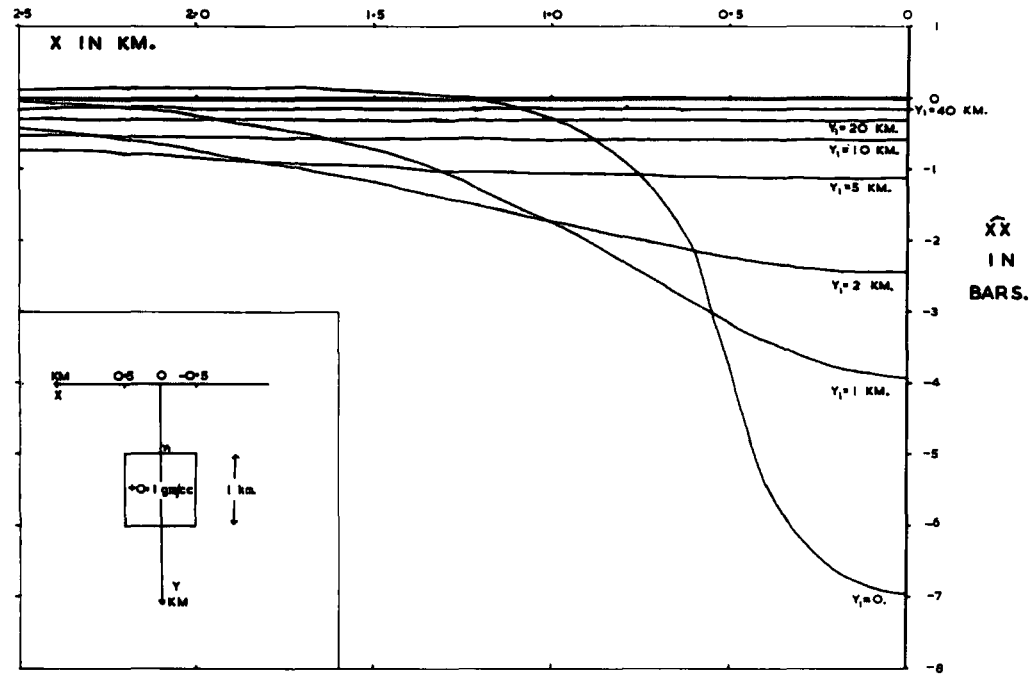

MODEL 1 , a=0·5 KM.

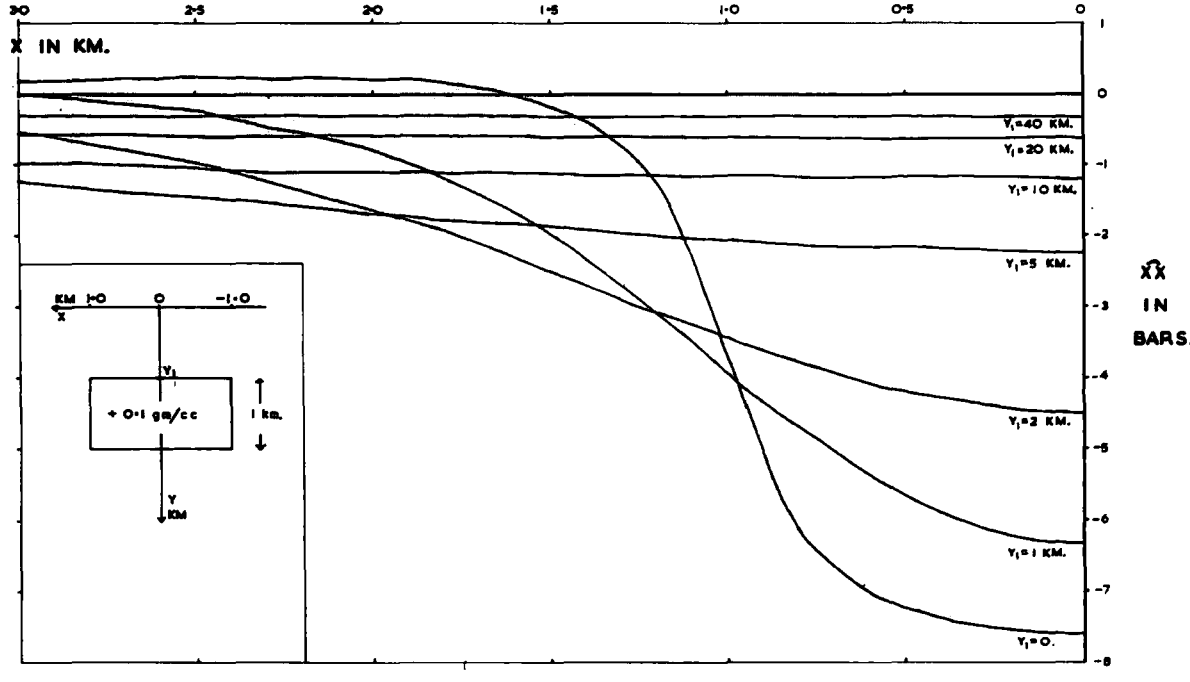

MODEL 2 , a=1·0 KM.

THE SURFACE STRESS DUE TO A RECTANGULAR DENSITY ANOMALY – SHEET 1

Figure 5

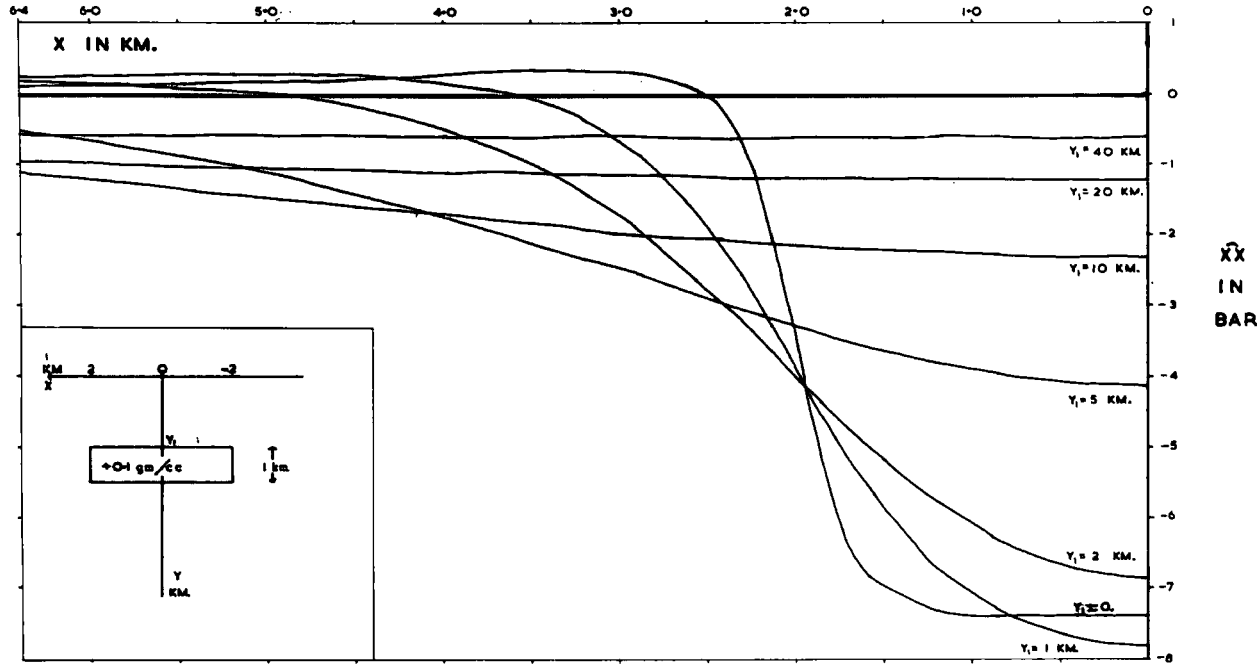

MODEL 3 , a=2 KM.

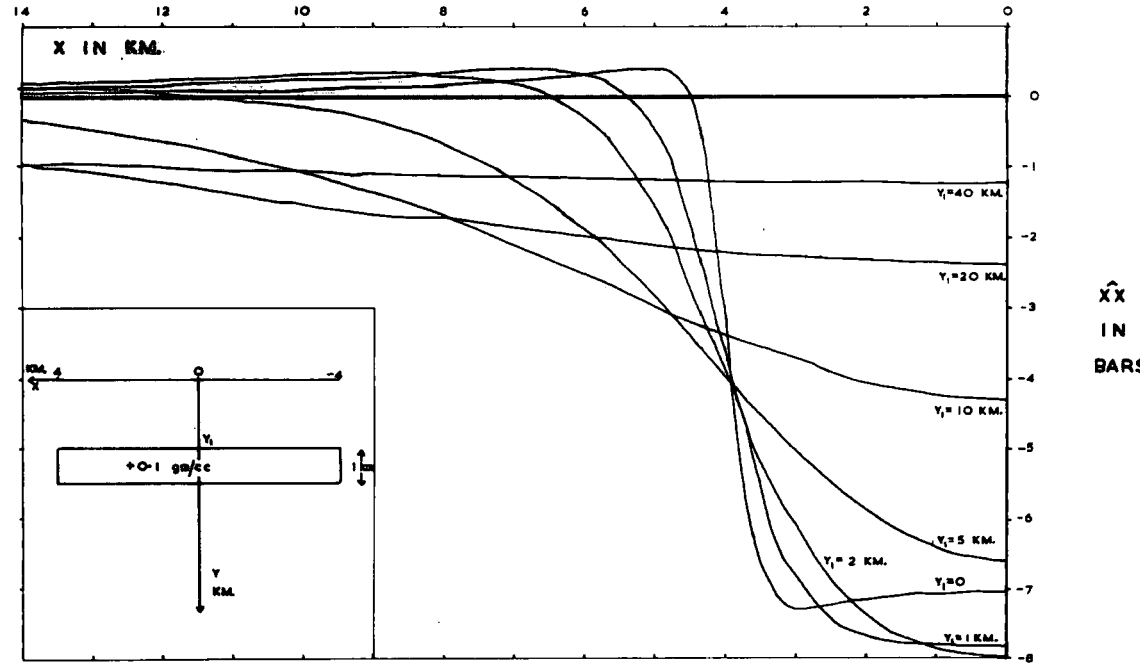

MODEL 4 a=4 KM.

THE SURFACE STRESS DUE TO A RECTANGULAR DENSITY ANOMALY —SHEET II

Figure 6

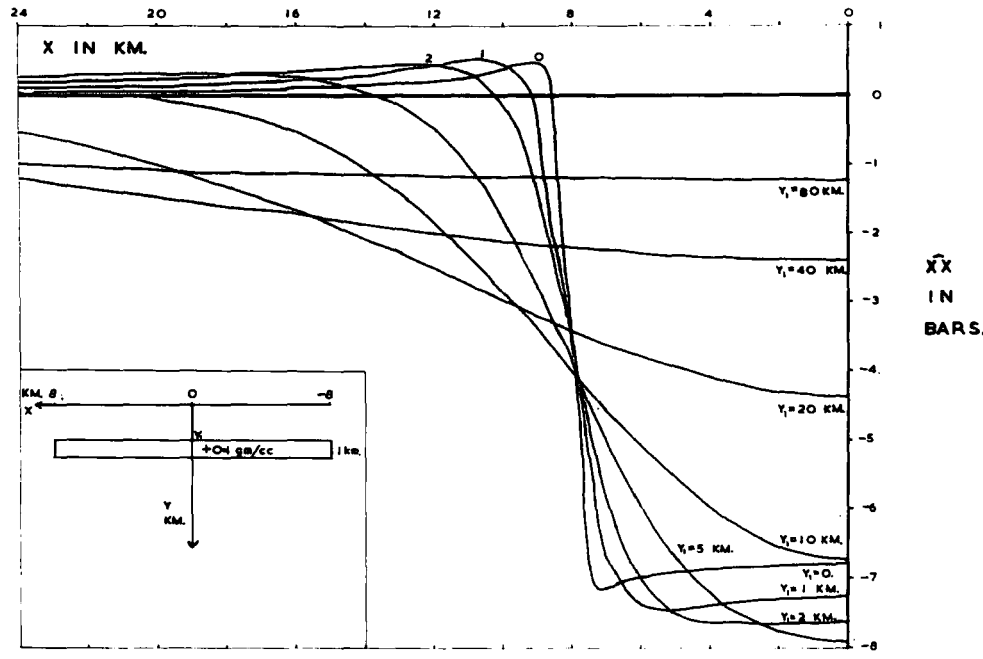

MODEL 5, a=8 KM.

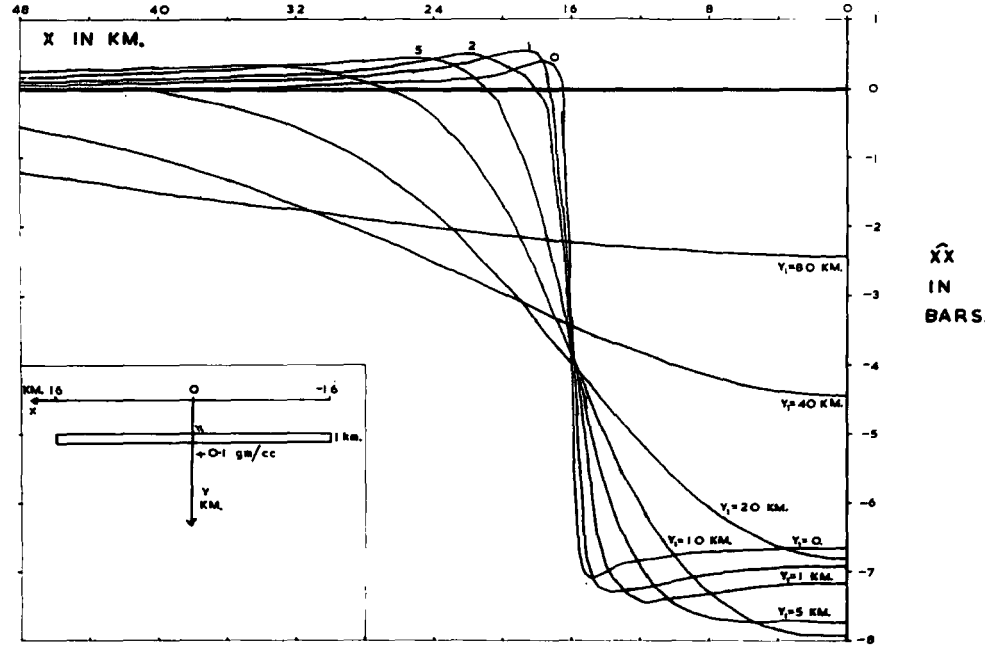

MODEL 6, a=16 KM.

THE SURFACE STRESS DUE TO A RECTANGULAR DENSITY ANOMALY – SHEET III

Figure 7

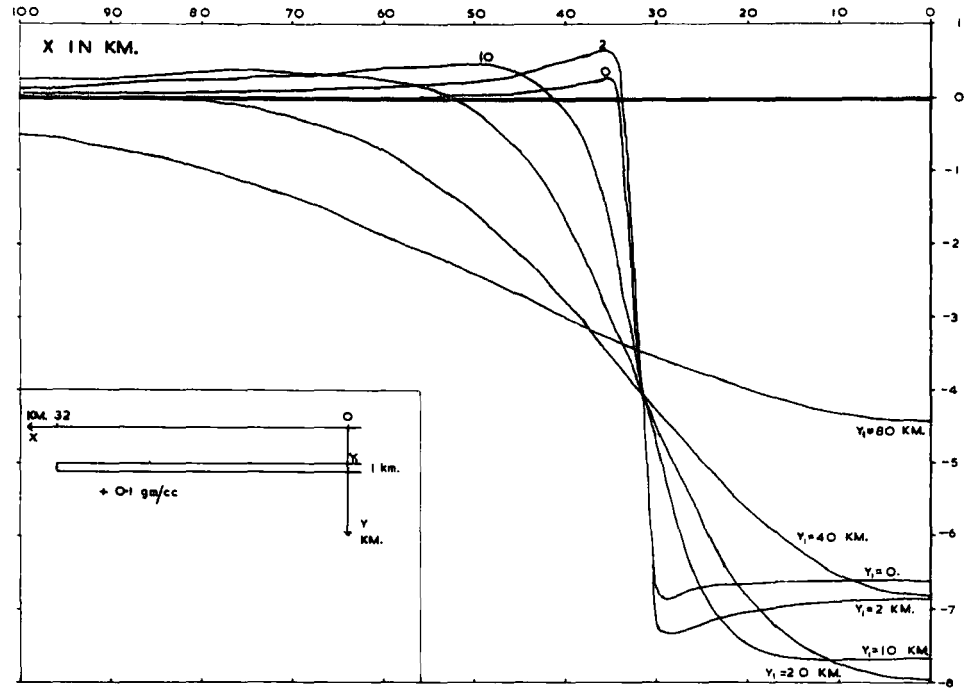

MODEL 7, a=32 KM.

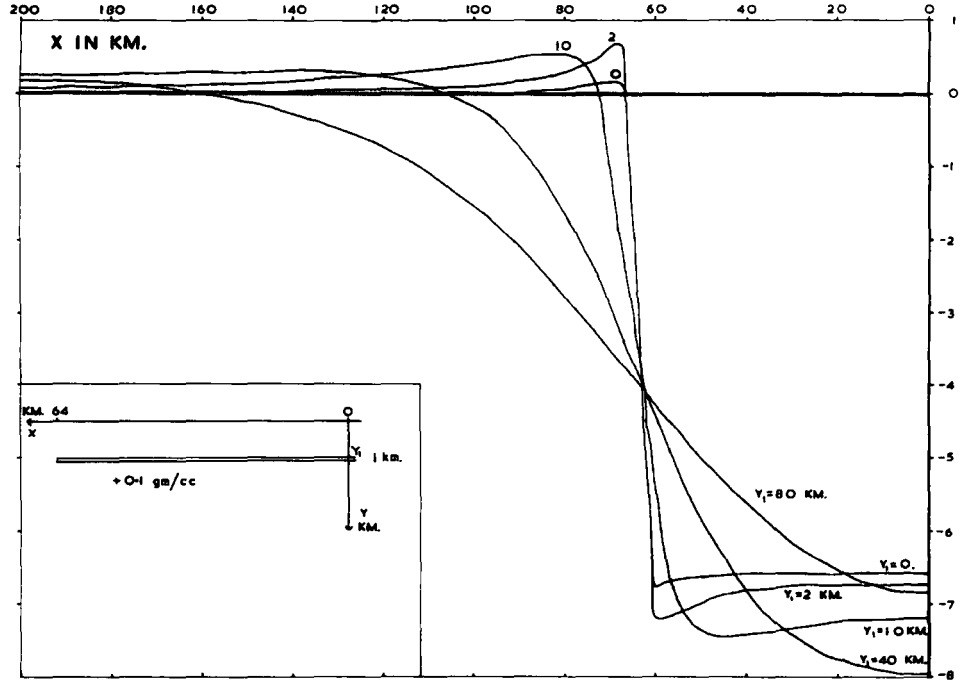

MODEL 8, a=64 KM.

THE SURFACE STRESS DUE TO A RECTANGULAR DENSITY ANOMALY – SHEET IV

Figure 8

thickness of one kilometre, the surface stress of greatest magnitude, (corresponding to an optimum value of 'a'), is equal to about -8 bars.

The surface stress over an anomalous mass of general thickness may be considered by summing the effects of the constituent one kilometre layers. In particular, if 'a' is greater than about $1\frac{1}{2}$ times y2, each layer makes an equal contribution to the maximum surface stress of approximately -8 bars per 0.1 gm/cc positive density contrast per kilometre thickness. The magnitude of the surface stress at the secondary maxima or minima lying outside the limits of the anomaly is at least an order of magnitude less than the value over the centre of the anomalous body, and is greatest for a body at or near the surface.

Before considering the interpretation of the surface stress results, two comparisons will be made with available similar results.

Taking $\hat{rr}$ or $\hat{\theta\theta}$ of Dean, Parsons and Sneddon (1944) to be analagous to $\hat{xx}$, then, from their figures 5 and 6, (where $\sigma = \frac{1}{4}$ and $\frac{h}{a} = 0.2$), their results give

$$\hat{xx} = 0.55 \times F ,$$

where F is the force per unit area of the circle of radius a and depth h, acting towards the free surface.

Putting $F = -g\rho\,(y2 - y1)$

$= -10^7$ dyne/cm^2 per 0.1 gm/cc per kilometre thickness,

then $\hat{xx} = -5.5$ bars.

Considering the great difference in the two models, this value is consistent with the value of -8 bars obtained in the current work.

A second opportunity for comparison is given in the second unpublished paper by Durney, where the density excess

$$\rho_o \, \eta(200 \text{ km}, 400 \text{ km}) \, e^{-\left(\frac{x}{D}\right)^2} ,$$

for D = 100 km, $\rho_o = 3.5 \cdot 10^{-2}$ gm/cc, and $\eta(1,d) = 1$ for $d \geqslant y \geqslant 1$ and zero otherwise,

is said to give a surface compression at the centre of about 185 bars. This distribution may be crudely simulated by model I of figure 5, with a linear scaling factor of 200 and a correction factor of $\frac{\sqrt{\pi}}{2}$ for an equal total mass anomaly.

Thus from figure 5,

$$\hat{xx} = -3.9 \times 200 \times 0.35 \times 0.886 \text{ bars}$$

$$= -242 \text{ bars.}$$

The discrepancy in magnitude is not unexpected in view of the significantly different lateral mass distribution and the different value of Poisson's ratio used by Durney.

The application of these theoretical results to the surface of the Earth in the absence of tectonic stresses naturally concentrates on the surface tensions produced by a structure of anomalously low density, because much lower stress magnitudes are required to initiate failure under tension than under compression. For example, a density anomaly of - 0.1 gm/cc and thickness 5 kilometres could, according to this theory, give a surface tension of 40 bars, which is the approximate tensile strength of granite (Jaeger, 1962). Thus, according to this theory, significant tensions can occur at the surface of an inhomogeneous crust without the occurrence of regional tectonic stresses. However, it seems unlikely that the existence of the stresses due to density anomalies could be proved in the field, since this would require the elimination of effects due to the mode of origin of the density anomaly and due to other consequences of external tectonic stresses.

The justification for assuming a hydrostatic natural state of stress becomes

uncertain near the free surface. The state of stress at shallow depths was investigated using various failure criteria for the first granite batholith model and a half-space of density 2.7 gm/cc. The results are demonstrated in figure 9. The first point is that, in spite of the overburden, the main stress is tensile to a depth of about 150 metres. This indicates that tensile phenomena caused by this effect could appear at the surface as quite major features. The Griffith theory is the appropriate criterion in this tensile zone. The second point, which relates to the use of failure criteria, is that the trends of the contours of the stress-difference and the von Mises function are similar, (i.e. the two criteria are approximately consistent,) but that the trends of the Coulomb-Navier fracture functions for the angle of internal friction, ϕ , equal to 30° and 50° are entirely different. Note also that this natural state yields an increasing positive stress-difference, (ϕ = o), with depth and an increasingly negative Coulomb-Navier fracture function with depth for ϕ equal to 55°. For Poisson's ratio equal to 0.25, this natural state does not contribute to the fracture function if ϕ equals 30°.

The effect on the surface stress of a uniform tectonic stress represented by equation (1.3.7) is to move the zero stress axis of the surface stress diagram, but to leave the shape of the distribution unaltered. Under conditions of increasing crustal compression, failure at the free surface will first occur at the location where the anomalous surface stress has its greatest compressional value, and similarly, under conditions of increasing crustal tension, failure will occur where the supplementary surface stress has a maximum tensile value. This approach assumes that failure will not occur elsewhere in the model for a tectonic stress of lower magnitude.

Thus the following trends for failure <u>at the free surface</u> are indicated. For a positive density anomaly, failure under crustal compression will generally

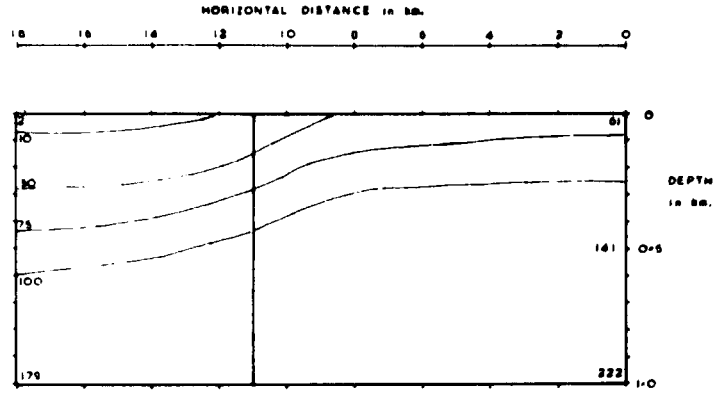

(a) THE STRESS-DIFFERENCE $(i.e. \phi = 0)$ IN BARS

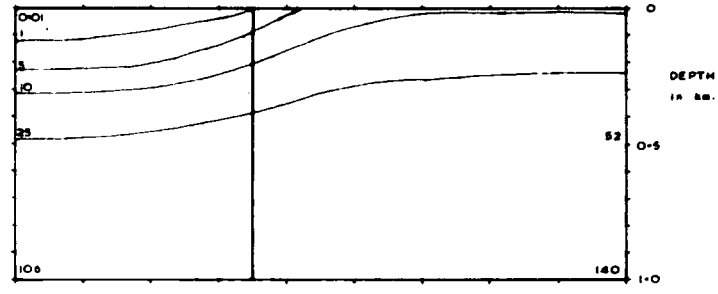

(b) THE VON MISES FUNCTION IN $(BARS)^2 \times 10^{14}$

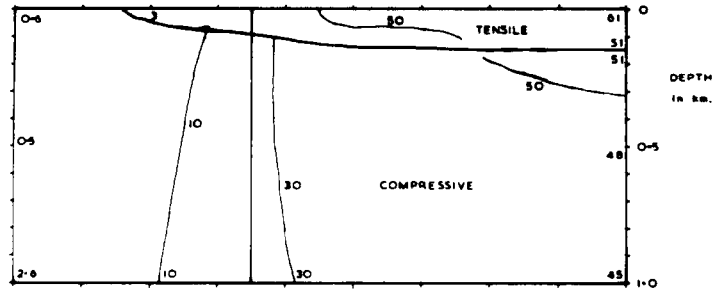

(c) THE GRIFFITH AND COULOMB-NAVIER $[\phi = 30^\circ]$ FUNCTIONS IN BARS

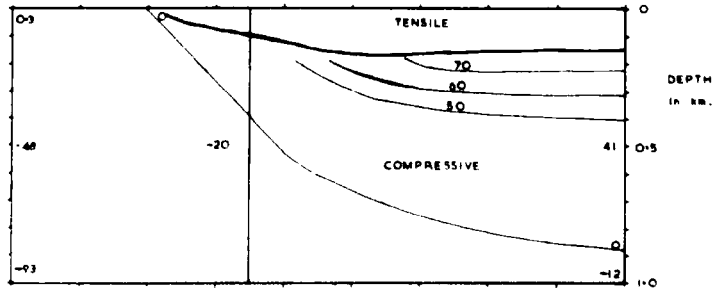

(d) THE GRIFFITH AND COULOMB-NAVIER $[\phi = 55^\circ]$ FUNCTIONS IN BARS

THE FAILURE CRITERIA FOR A GRANITE MODEL AND HALF-SPACE

Figure 9

occur above the anomaly, and failure under crustal tension will generally occur outside the limits of the anomaly. For a negative density anomaly, the reverse is true.

(iv) The stresses due to a uniform surface load

In diagrams (a) of figures (16), (17) and (18), the stress-difference within an elastic half-space due to a uniform surface load is considered for models corresponding to cases of no tectonic stress, tectonic tension and tectonic compression. The uniform crustal load is a large feature corresponding to a mountain range with an average height of 3 kilometres, a width of 600 kilometres and a density of 2.8 gm/cc, and the assumed tectonic stresses are of the same order of magnitude as the stresses due to the surface load. The case of a crustal tension has been considered by Bott (1965), and although his results appear slightly different because here the stress-difference is defined as the maximum positive difference between the three principal stresses, it still follows from the results that normal faulting is most likely to occur beneath the load and is least likely to occur in the adjacent regions. Diagram (a) of figure (18) shows that for the case of a crustal compression large stress-differences occur throughout the diagram and particularly beneath the extremities of the surface load. One could speculate that this large stress-difference beneath the limits of the surface load, which is a feature of the uniform surface load result for depths much less than the width of the load, might favour the onset of local isostatic compensation by permitting the crustal block bounded by these regions of likely failure to sink under the surface load. Comparison of diagrams (a) and (c) of figures (16), (17) and (18) show that the effect of any isostatic compensation according to the Airy hypothesis, (see section (vi) of this chapter), has the effect above the level of compensation of tending to exaggerate the features of the stress-distribution due to the surface load alone.

(v) The stresses due to an internal density anomaly.

Three different models for a rectangular density anomaly within an elastic half-space model of the crust will be considered, and each will be examined under conditions of crustal tension and crustal compression represented by equation (1.3.7). General conclusions will be drawn from these models, but the first two models are particularly selected to represent granite batholiths occurring within the crust and the third model is designed for use in the discussion of the isostatic compensation of surface loads. The parameters of these three models are given in the table below.

	a, in km.	y1, in km.	y2, in km.	density contrast in gm/cc	figure numbers
First granite model	11	0	8	-0.1	10, 11, 12.
Second granite model	11	8	16	-0.1	13, 14, 15.
Mountain root model	300	30	51	-0.4	16B, 17B, 18B.

TABLE (3.5.1) - The parameters of the rectangular density anomaly models

However, before these models are discussed, a calculation will be described which aimed to compare the results of chapter 2 with those of Durney (1965). Durney considers the density distribution

$$\rho_0 \left(e^{-py} - e^{-qy}\right) \cos kx \ ,$$

where p equals $\frac{1}{300}$ km^{-1}, q equals $\frac{1}{200}$ km^{-1}, ρ_0 equals 0.35 gm/cc and $\frac{1}{k}$ equals 100, 250 or 400 km.

The functions $T_1(y)$, $T_2(y)$ and $T_3(y)$ defined by

$$T_{xx} = T_1(y) \cos kx \ , \ T_{xy} = T_2(y) \sin kx \ , \ T_{yy} = T_3(y) \cos kx$$

are plotted for the three values of k. A simulation using the same values of

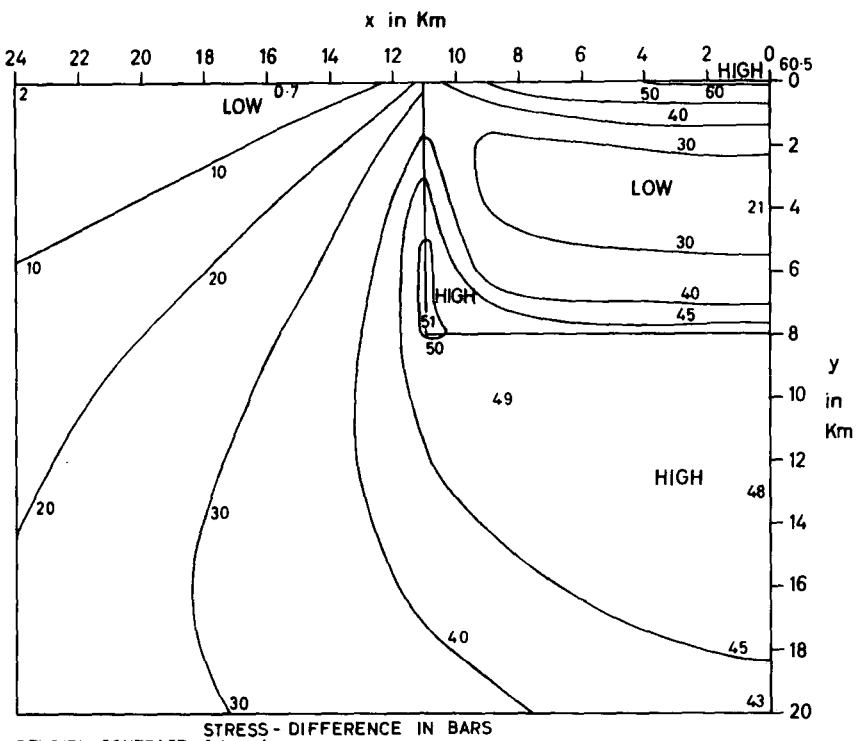

THE STRESS - DIFFERENCE

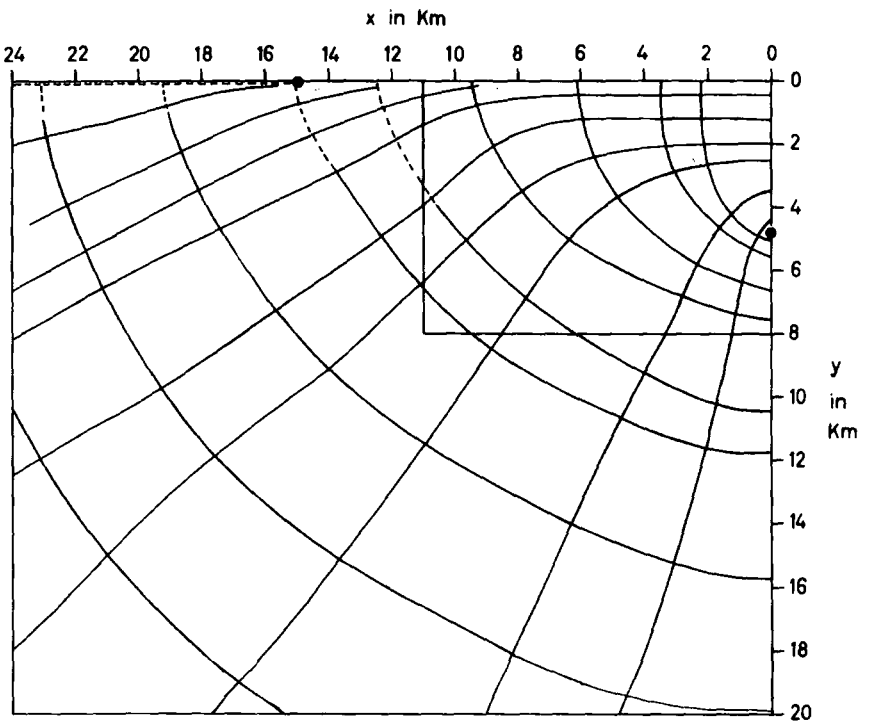

THE ISOSTATIC CURVES

THE FIRST GRANITE MODEL IN AN UNSTRESSED CRUST

Figure 10

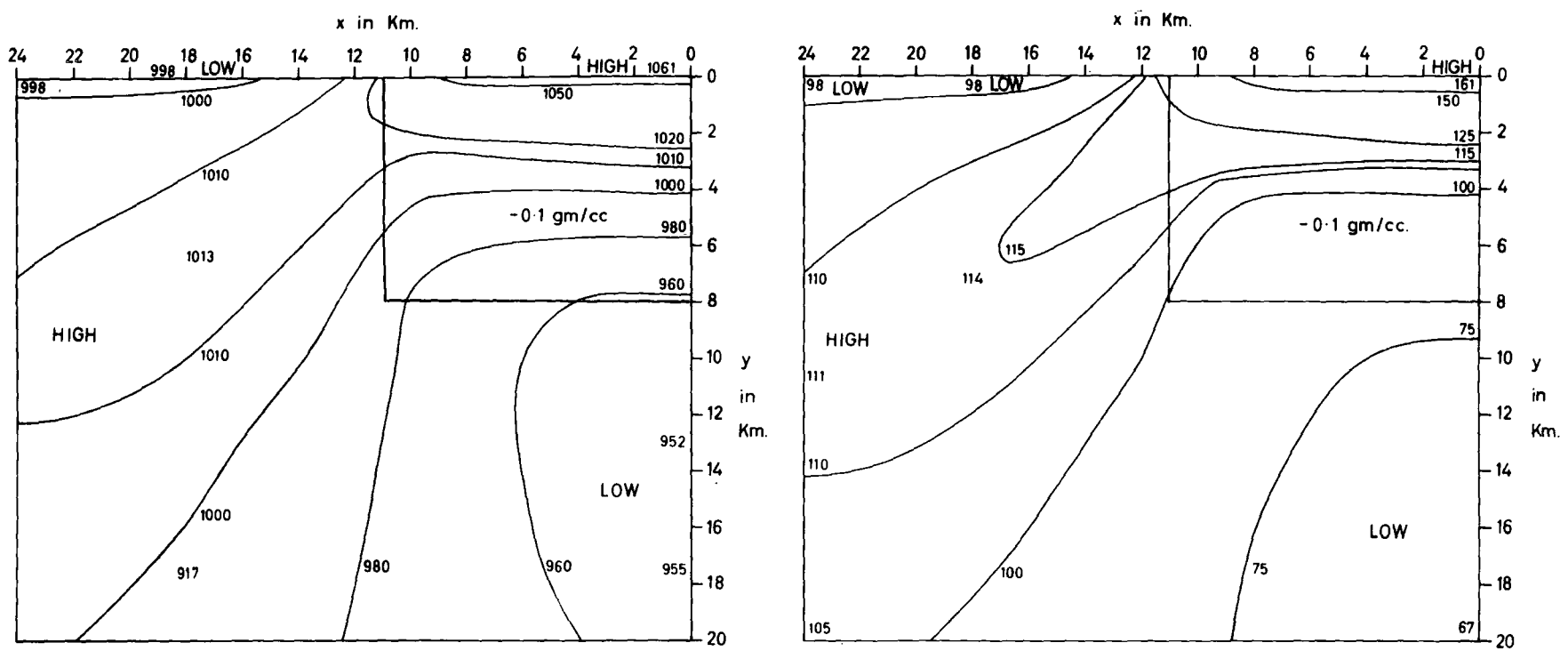

STRESS-DIFFERENCE IN BARS

CRUSTAL TENSION 1000 BARS

CRUSTAL TENSION 100 BARS

THE STRESS-DIFFERENCE FOR THE FIRST GRANITE MODEL UNDER CRUSTAL TENSION

Figure 11

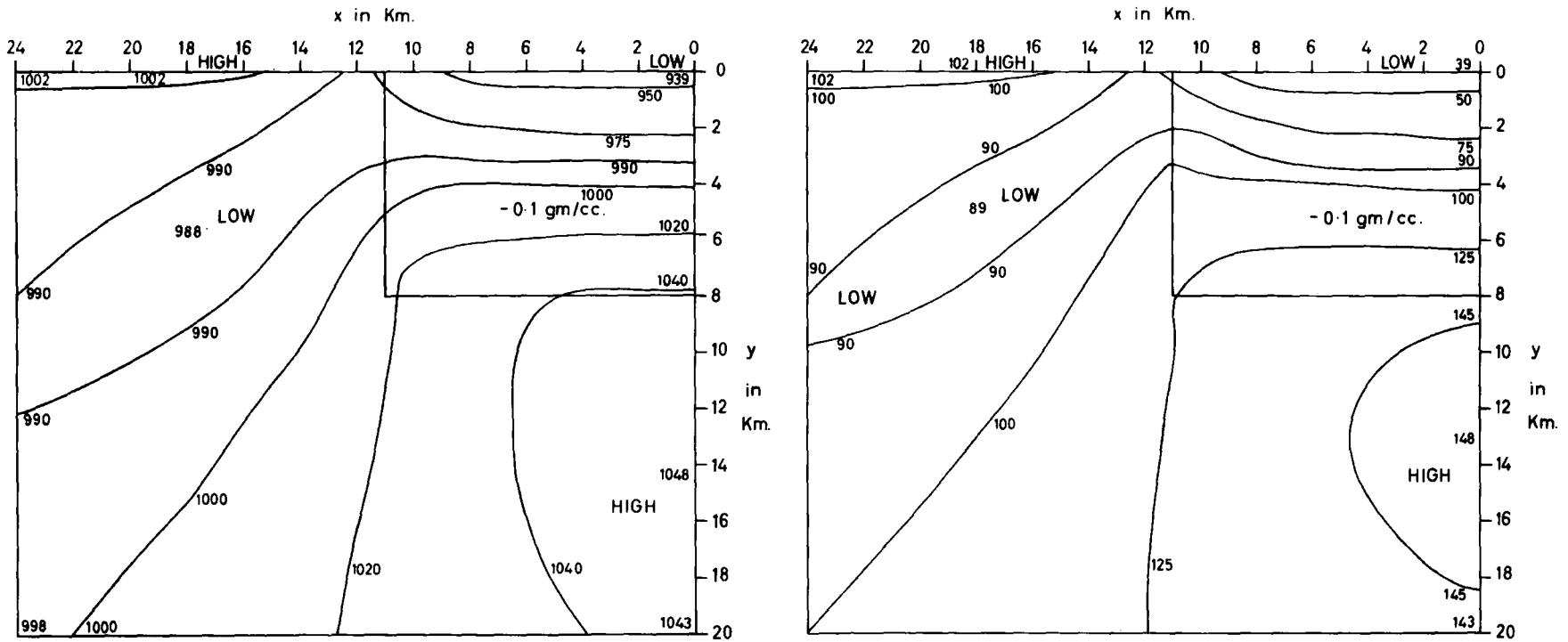

STRESS - DIFFERENCE IN BARS

CRUSTAL COMPRESSION 1000 BARS

CRUSTAL COMPRESSION 100 BARS

THE STRESS - DIFFERENCE FOR THE FIRST GRANITE MODEL UNDER CRUSTAL COMPRESSION

Figure 12

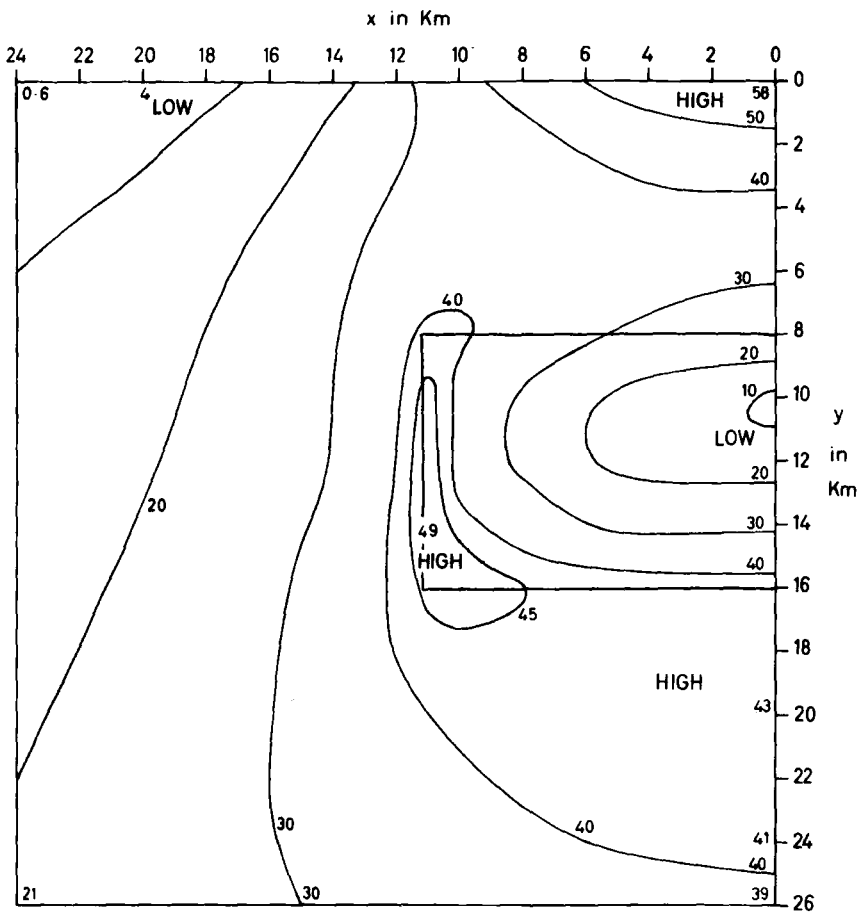

DENSITY CONTRAST — 0·1 gm/cc
POISSONS RATIO 0·25
g 981 cm/sec^2

THE STRESS - DIFFERENCE IN BARS

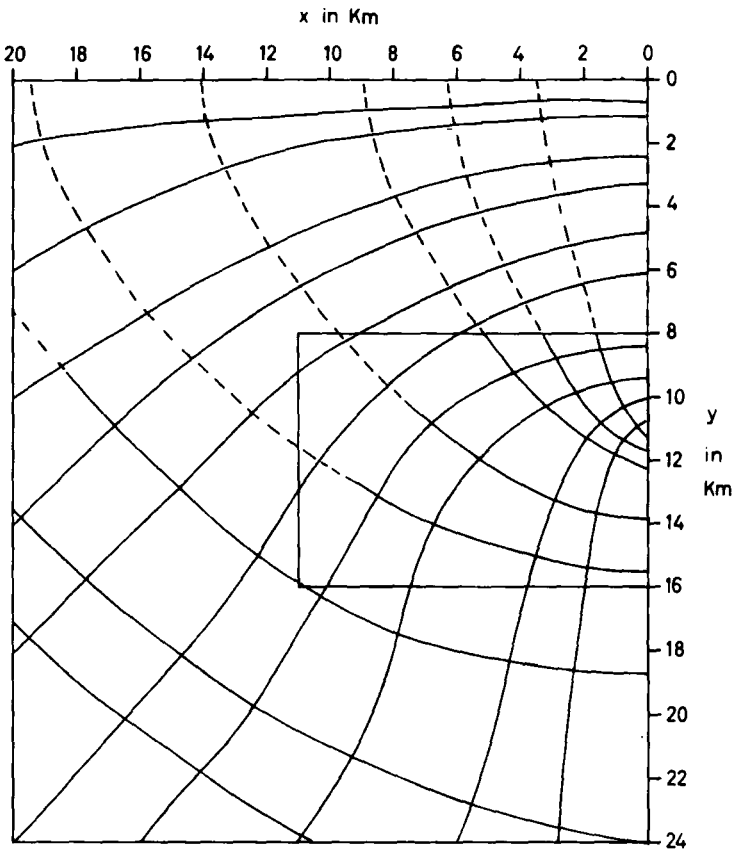

—— TENSILE PRINCIPAL STRESS
– – – COMPRESSIVE PRINCIPAL STRESS

THE ISOSTATIC CURVES

THE SECOND GRANITE MODEL IN AN UNSTRESSED CRUST

Figure 13

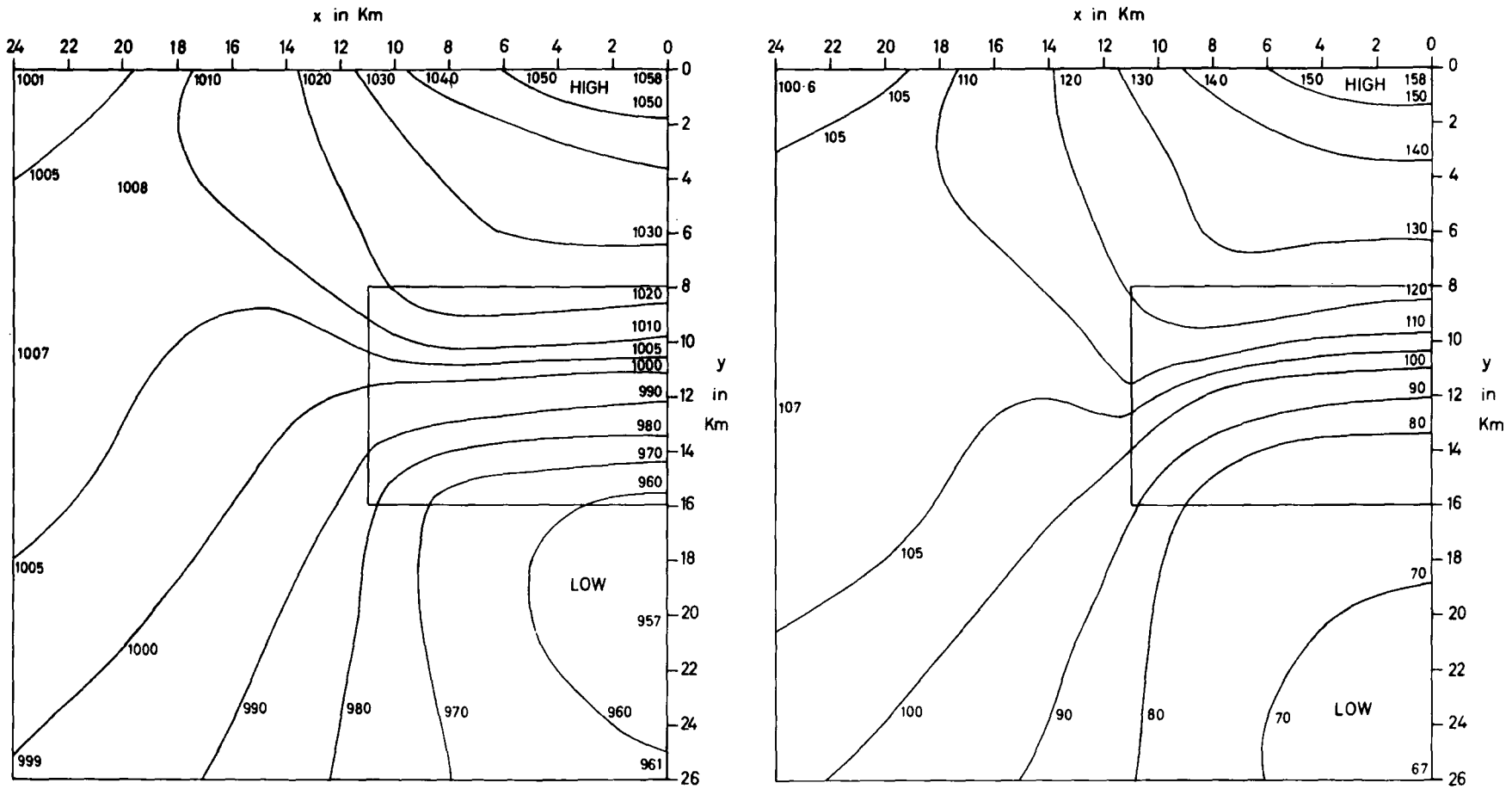

STRESS - DIFFERENCE IN BARS

CRUSTAL TENSION 1000 BARS

CRUSTAL TENSION 100 BARS

THE STRESS - DIFFERENCE FOR THE SECOND GRANITE MODEL UNDER CRUSTAL TENSION

Figure 14

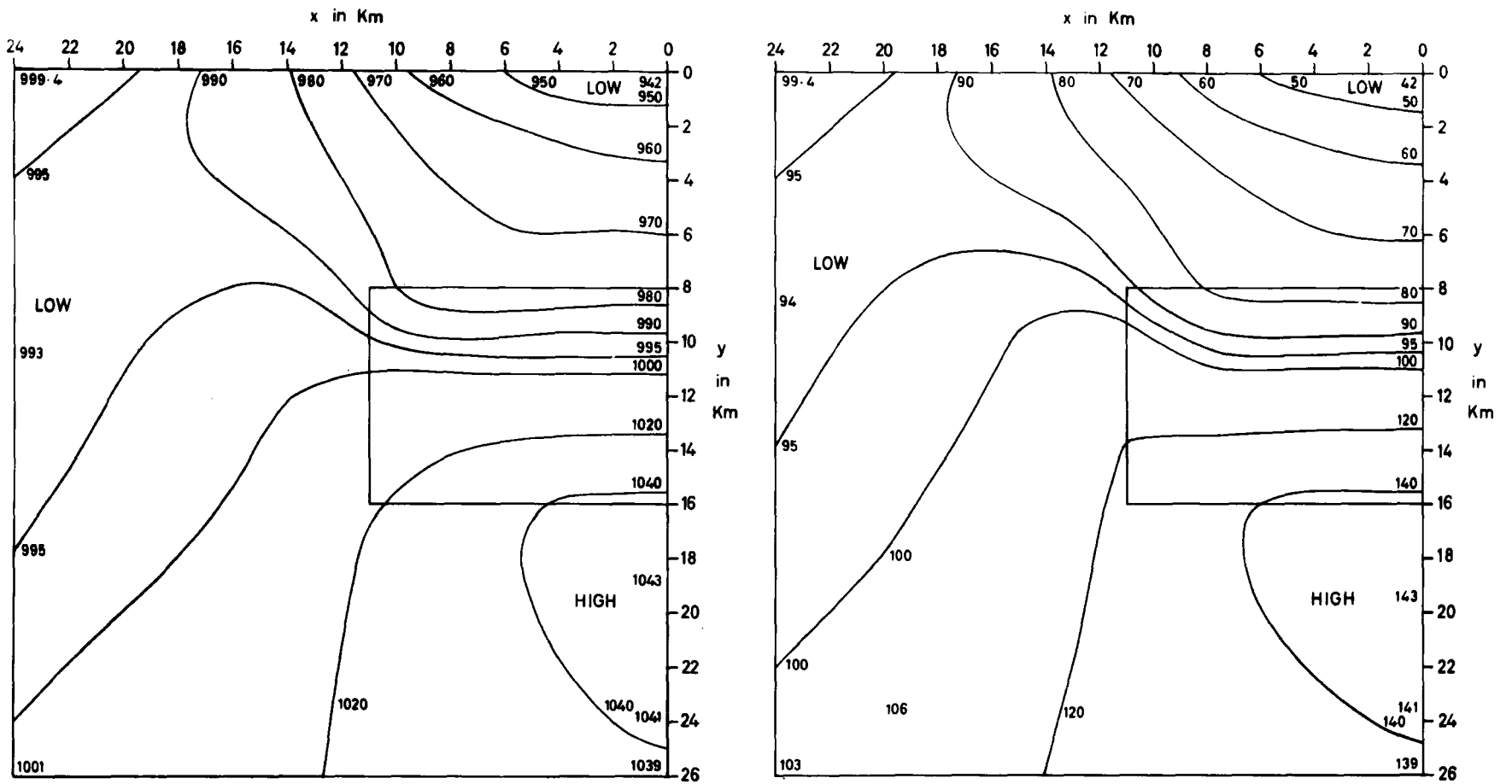

STRESS-DIFFERENCE IN BARS

CRUSTAL COMPRESSION 1000 BARS

CRUSTAL COMPRESSION 1000 BARS

THE STRESS-DIFFERENCE FOR THE SECOND GRANITE MODEL UNDER CRUSTAL COMPRESSION

Figure 15

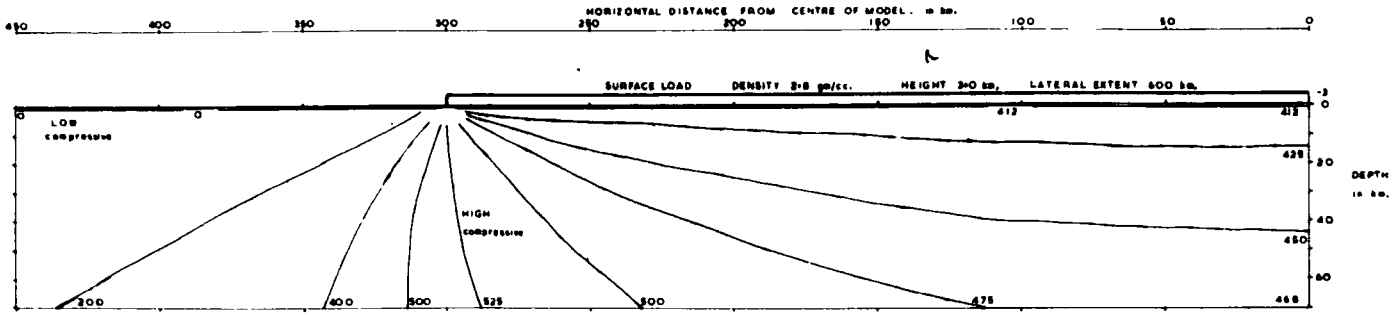

(a) SURFACE LOAD ONLY

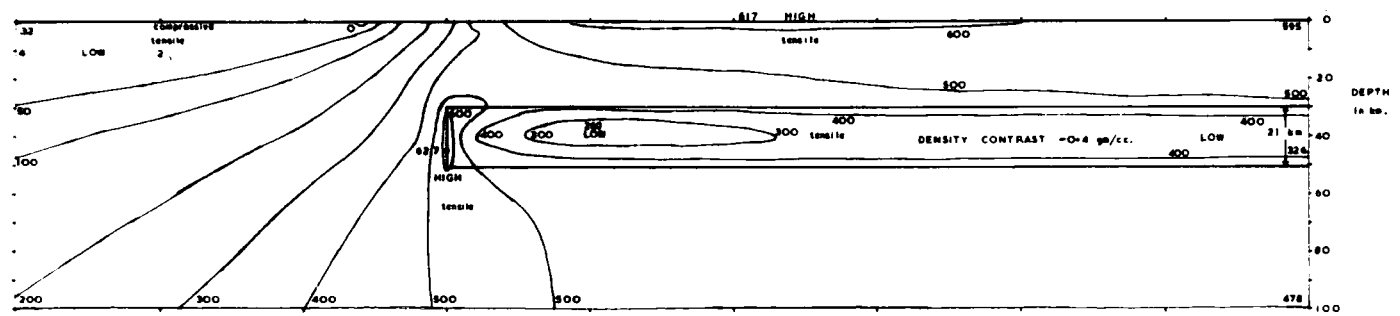

(b) INTERNAL DENSITY LOW ONLY

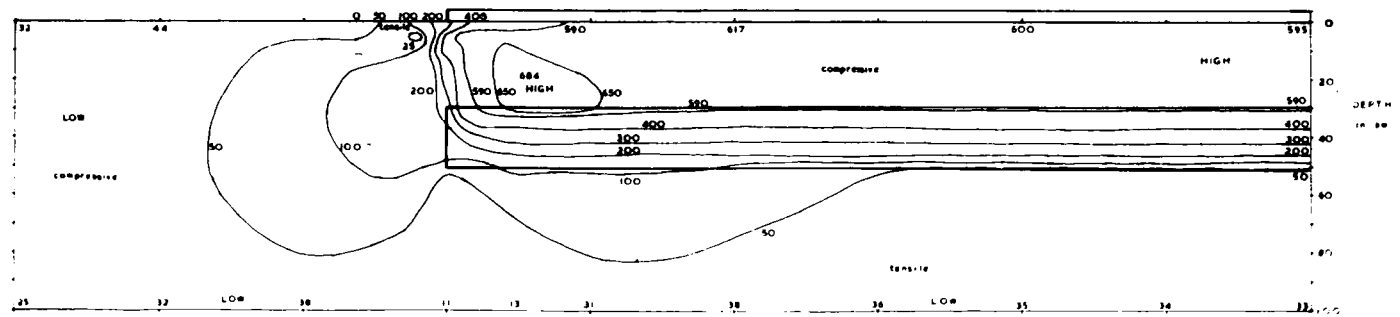

(c) COMBINED MODEL WITH MASS COMPENSATION

THE STRESS-DIFFERENCE IN BARS FOR THE MOUNTAIN RANGE MODEL IN AN UNSTRESSED CRUST

Figure 16

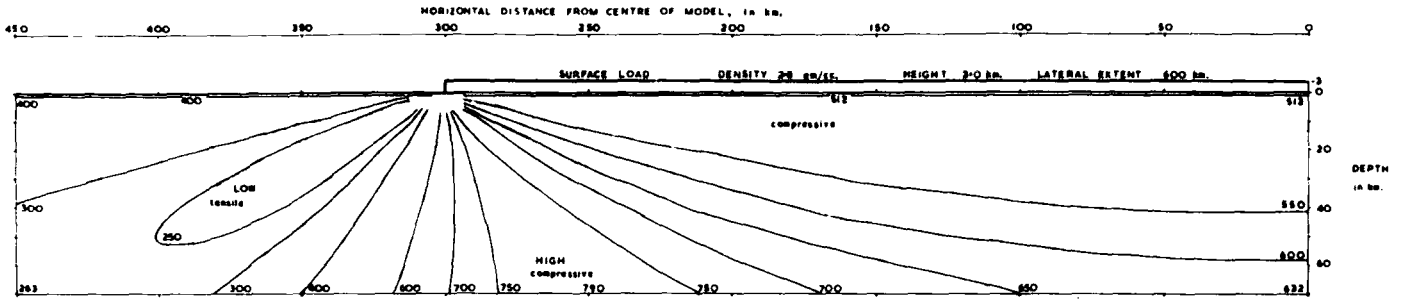

(a) SURFACE LOAD ONLY

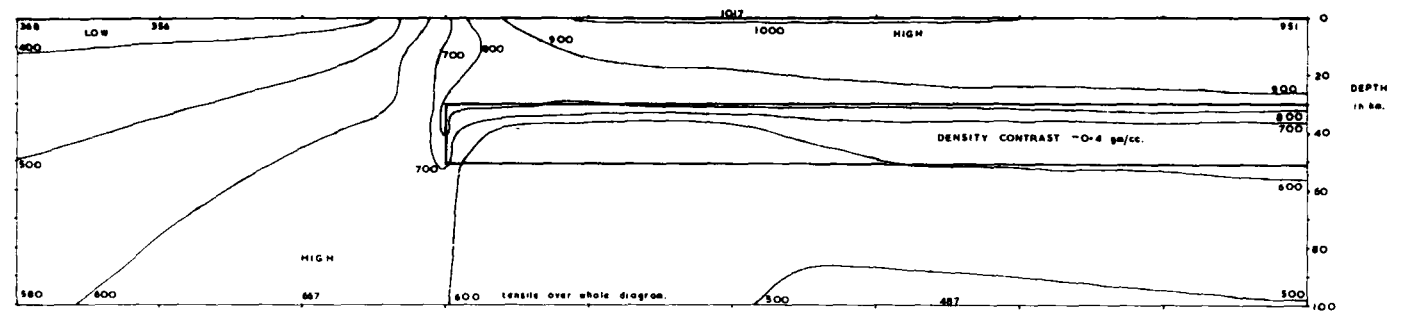

(b) INTERNAL DENSITY LOW ONLY

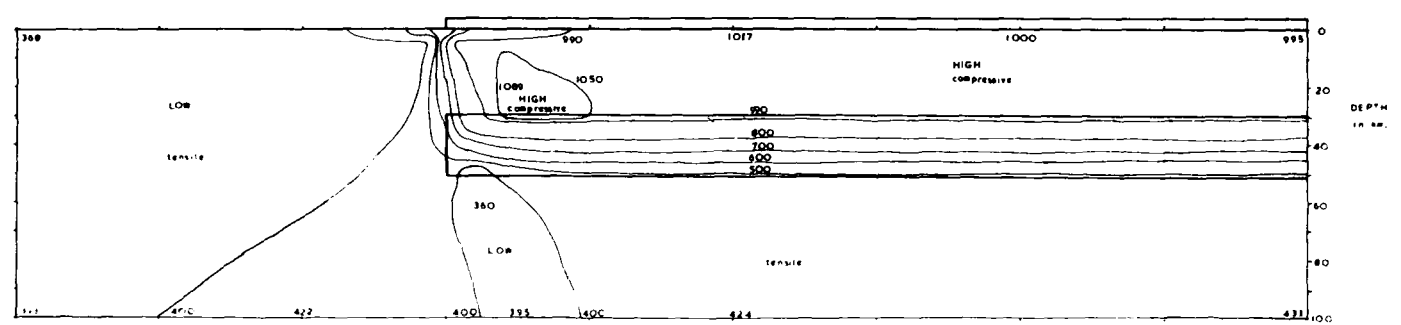

(c) COMBINED MODEL WITH MASS COMPENSATION

THE STRESS-DIFFERENCE IN BARS FOR THE MOUNTAIN RANGE MODEL WITH A CRUSTAL TENSION OF 400 BARS

Figure 17

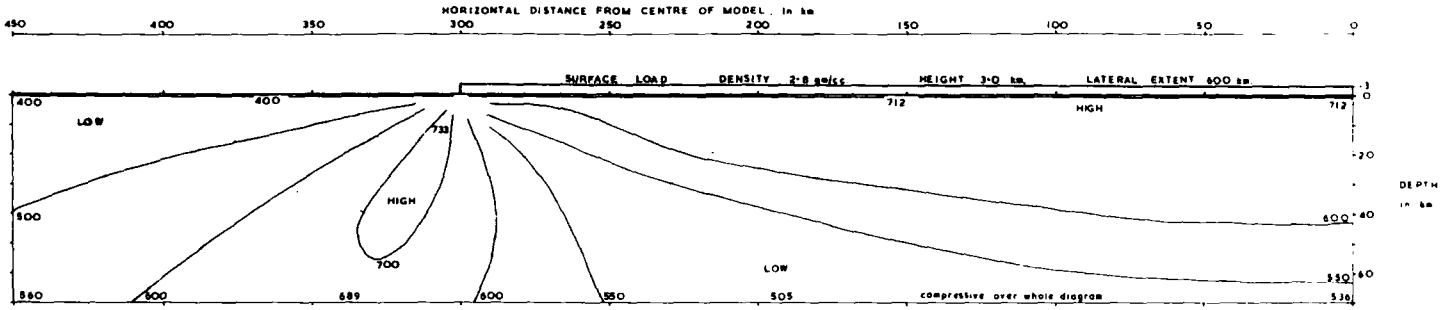

(a) SURFACE LOAD ONLY

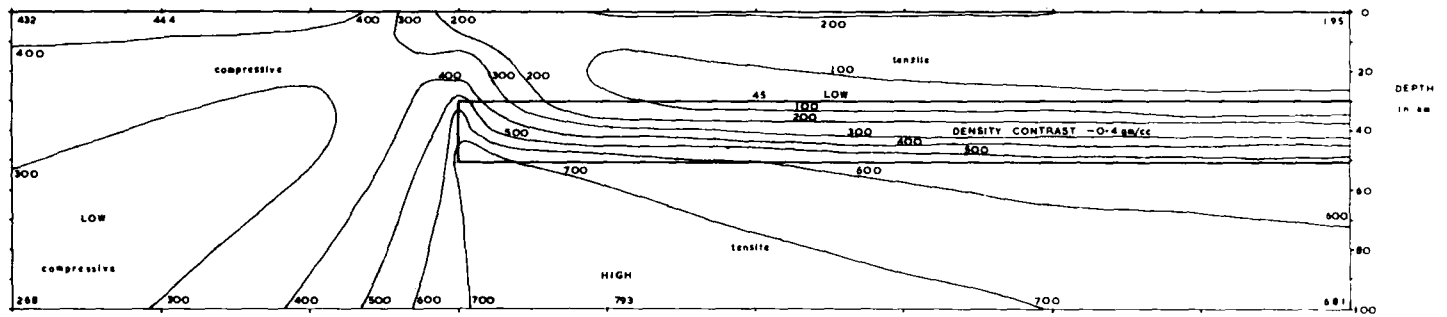

(b) INTERNAL DENSITY LOW ONLY

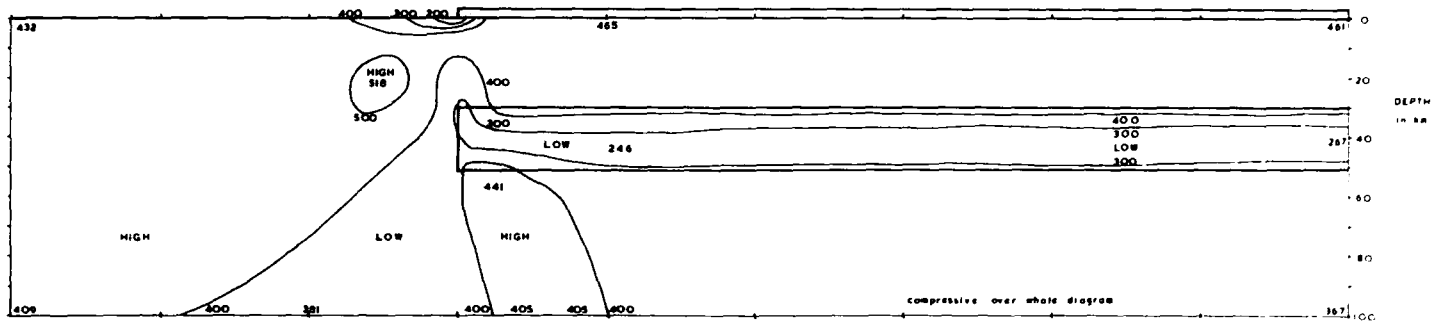

(c) COMBINED MODEL WITH MASS COMPENSATION

THE STRESS-DIFFERENCE IN BARS FOR THE MOUNTAIN RANGE MODEL WITH A CRUSTAL COMPRESSION OF 400 BARS

Figure 18

Poisson's ratio and the acceleration due to gravity was carried out for the case of k equal to $\frac{1}{250}$ km^{-1} using six rectangular anomalous blocks of identical total mass per wavelength of x. This simulation is demonstrated in figure (19). The functions $\hat{xx}$ (o,y), $\hat{xy}$ ($\frac{\pi}{2k}$, y) and $\hat{yy}$ (o,y) are anologous to $T_1(y)$, $T_2(y)$ and $T_3(y)$ respectively, and are illustrated for this one value of k. If these curves are compared with those of Durney's paper, $\hat{yy}$ and $\hat{xy}$ show good agreement over the range of y considered, but $\hat{xx}$, which shows good agreement at the free surface, is too large at the maximum occurring at a depth of about 800 kilometres, (490 bars instead of about 250 bars). This discrepancy, which is not so significant if it is related to the free surface value of -1680 bars, can be attributed to the effect of the large step in the simulated density function occurring at a depth of 500 kilometres. In general, the agreement between the results is unexpectedly good when the method of simulation is considered.

Consider the contours of equal stress-difference for the three models of a low density anomaly in the crust which is free from tectonic stresses. Figures (10) and (13) include the isostatic curves for the two granite models. These curves represent the orientation of the principal directions, and are drawn to indicate whether the principal stress whose principal direction is parallel to the curve is compressional or tensile. They also indicate the orientation of possible fault planes according to equation (1.3.4). It can be seen that the stress-difference is large at the free surface above the density anomaly and at the side contact and below the anomaly. It is low at the centre of the anomalous body and near the surface outside the limits of the body. This is true whatever the sign of the density contrast. For a mass deficit, (negative density contrast), the average stress is tensile except very near the free surface outside the limits of the body. The converse is true for a mass excess, (positive density contrast).

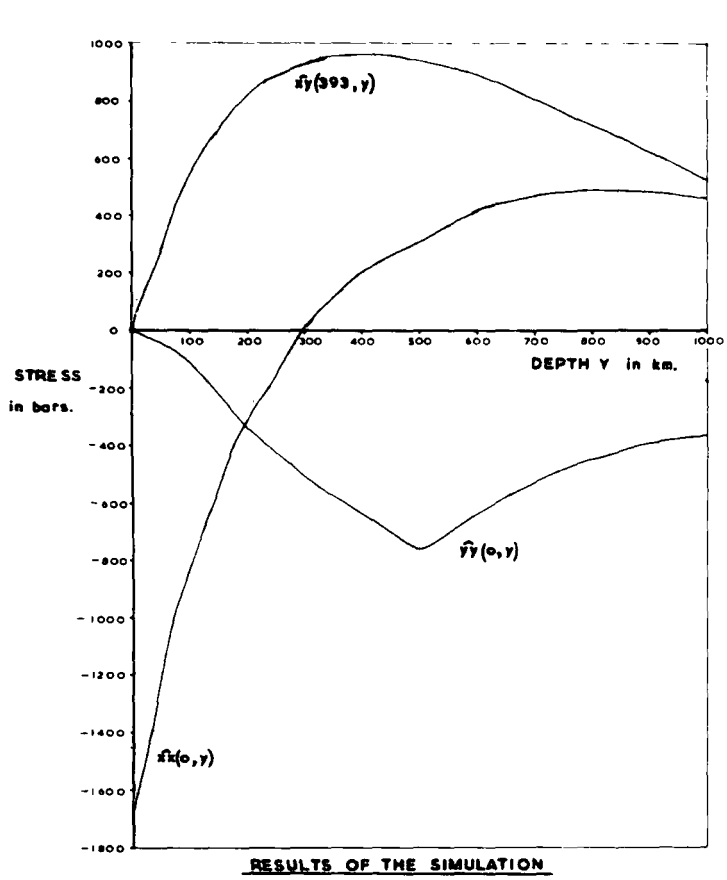

RESULTS OF THE SIMULATION

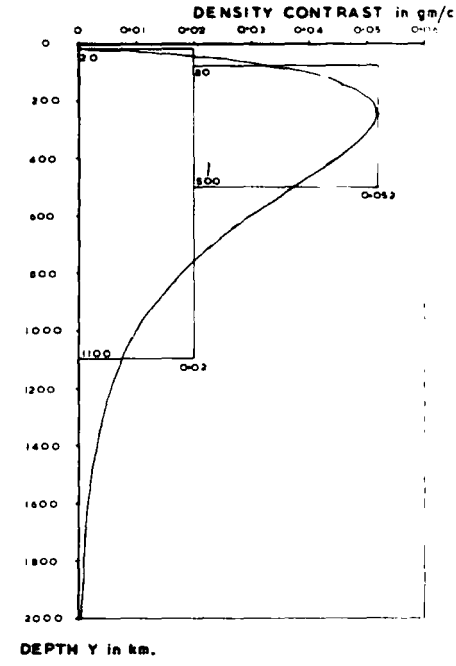

APPROXIMATION OF DENSITY FUNCTION $\rho(Y)$

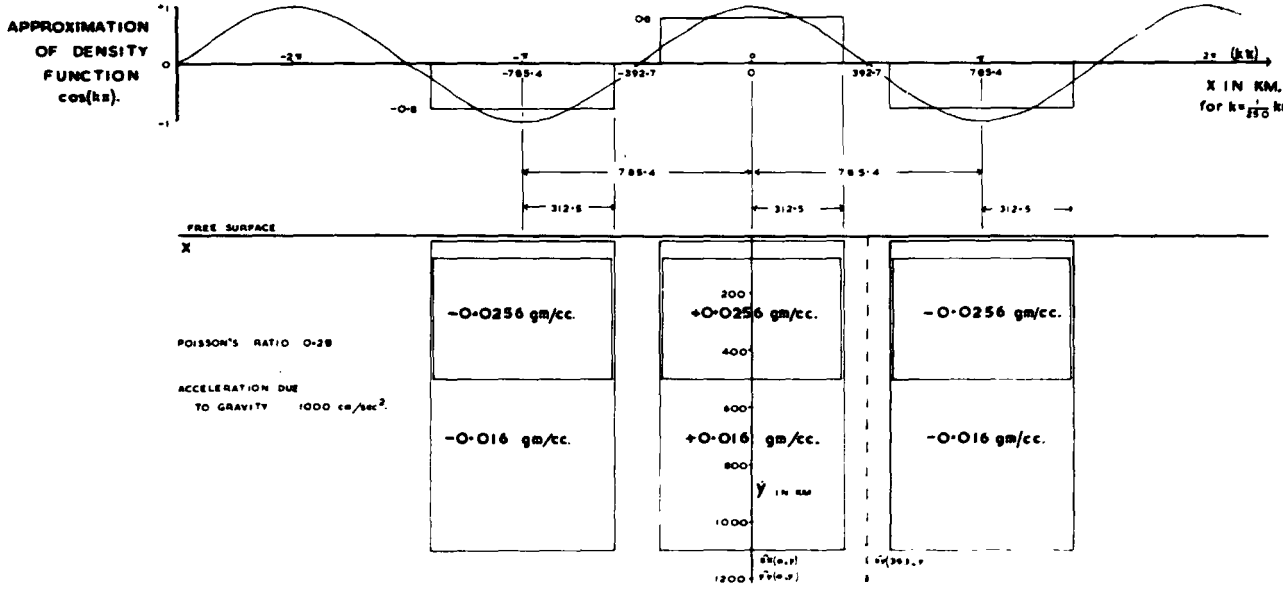

THE MODEL USED FOR THE SIMULATION

THE SIMULATION OF DURNEY'S NUMERICAL RESULTS FOR k EQUALS $\frac{1}{250}$ km.⁻¹

Figure 19

The maximum stress-difference for the two granite models occurs at the free surface. The maximum value in the mountain root model occurs at the side contact of the mass deficit, but is only very slightly larger than the maximum stress-difference at the surface. The interpretation of surface stresses has been discussed in section (iii) of this chapter.

General conclusions about the influence of density anomalies in an inhomogeneous elastic crust on tectonic stresses will be derived from consideration of the two granite models only. This is because the mountain root model is complicated by the fact that the stresses due to the mass anomaly are of the same order of magnitude as the assumed tectonic stresses. However, the stress-difference follows the same general pattern as will be deduced from the granite models. This would be more evident if the mountain root model were extended to a depth comparable to its width. The general conclusions derived from figures (11), (12), (14) and (15) of the granite models are as follows:-

for a density low and a crustal compression
or a density high and a crustal tension,
the stress-difference is increased below the density anomaly and is decreased above and to the side of the anomaly,
and for a density low and a crustal tension
or a density high and a crustal compression,
the converse is true;
that is, the stress-difference is increased above and to the side of the density anomaly and is decreased below the density anomaly.

It will be recalled that, according to the principles outlined in section(iii) of chapter 1, a large-stress difference under a crustal tension tends to increase

the likelihood of normal faulting, and a large stress-difference under a crustal compression tends to increase the likelihood of thrust faulting. If one considers only faulting occurring above or within the upper half of the density anomaly, it may be postulated that in a region of uniform topography, the likelihood of normal faulting is increased in an area of anomalously low gravity and the likelihood of thrust faulting is increased in an area of high gravity. Of course, these two different types of failure would not occur at the same time, but under conditions of regional crustal tension and compression respectively. Conversely, if one considers processes in the lower half of the anomalous region or below, normal faulting is most likely in regions of high gravity and thrust faulting in regions of low gravity anomaly.

It is worth repeating here the opinion expressed during the discussion of the interpretation of surface stresses, derived using the present relatively simple model, that the mechanisms of crustal processes are so various and relatively complex that it is very unlikely that one can isolate an effect such as those discussed above and prove its occurrence in the field. At the best, one can use some reasonable theory to explain trends of behaviour which are consistent with the field data. However, the uncertainties of geological science are such that this consistency is in no way a proof of the theory.

The second case considered above corresponds to that treated by Bott (1965), since the distributed load was simulated by a surface load, and the entire half-space was necessarily below the anomaly. He cites the tectonic and igneous history of the Midland Valley of Scotland as a possible example of this mechanism, and attributes the normal faulting and dyke-intrusion of late Palaeozoic and early Mesozoic age to a positive gravity anomaly due to either a thinner or a denser crust. It is postulated that the high regional Bouguer anomaly over the

north-eastern Irish Sea similarly corresponds to a load on the underlying mantle and enhances the likelihood of normal faulting therein, leading to the formation of sedimentary basins. Subsidence is supposed to be initiated by local flow in the upper mantle due to the uplift of nearby mountains in response to erosion (Bott, 1964b).

The present work emphasizes the point that this theory requires that the initiation of normal faults and dykes occur below the mass anomaly and therefore near the bottom of the crust or in the upper mantle. The state of stress above the anomaly is such as to inhibit the origination of these tensile features. However, once the initial breakdown has occurred at depth beneath the load, the state of stress is greatly modified and the current model is invalid. In particular, large stress-differences will occur above the region of yield, and faults or dykes may propagate to the surface.

(vi) A model with mass compensation

Consider the mountain range model for an unstressed crust as shown in figure (16). Diagrams (a) and (b) represent respectively a uniform surface load and an internal mass deficit of equal magnitude situated at the base of the crust. In both cases it can be seen that the stress-differences are still large at depths of a hundred kilometres. In diagram (c) the two models are combined to give simple local mass compensation at depth. This corresponds to a form of Airy-Heiskanen isostatic compensation, (Heiskanen and Vening Meinesz, 1958), with a non-standard value of the density contrast and ignoring the effect of curvature of the Earth. It is immediately apparent from diagram (c) of figure (16) that the stress-differences below the level of compensation are an order of magnitude smaller than those at the same location in diagrams (a) or (b), and that large stress-differences occur in the layer between the two compensating mass anomalies.

The diagrams of figures (16), (17) and (18) also indicate whether the average principal stress is tensile or compressional. The average principal stress is compressional in the layer between the two compensating mass anomalies.

It is seen from figures (17) and (18) that the effect of a crustal stress (represented by equation (1.3.7)) on the compensated model is to give approximately the tectonic background stress-difference below the level of compensation and to the side of the anomalous region. In the case of a crustal tension large stress-differences occur above the compensating mass deficit, but, for a crustal compression, these values are not much greater than the background level. In both instances the average stress in this region is compressional.

Two features of these diagrams which may seem unexpected are the facts that, firstly, the 'surface' stress-difference is the same in diagrams (b) and (c) of figures (16) and (17), (the same is true of figure (18) for $x > 300$ km.), and, secondly, the largest stress-difference in the layer between the mass anomalies occurs for a tectonic tension, even though the average stress in this zone is compressional.

The first feature is a consequence of the fact that the solution of the uniform surface load problem gives $\hat{xx} = \hat{yy} = L$ at $y = 0$, so that, for Poisson's ratio equal to $\frac{1}{4}$, the corresponding stress-difference is $\frac{1}{2}L$. Thus, when the surface load is added to diagram (b), $\hat{xx}$ and $\hat{yy}$ are changed equally, so that, if zz is the intermediate principal stress, the stress-difference is unaltered. The second feature is a consequence of the fact that the stresses occurring in this large scale crustal model are larger than the assumed tectonic stress magnitude of 400 bars. The dominant principal stress in the layer above the compensating mass deficit is a near-vertical compression of sufficient magnitude to keep the average stress compressional. The effect of a horizontal tension represented by equation (1.3.7) is therefore to increase the stress-difference, and the effect of a horizontal compression is to decrease it.

(vii) Conclusions

The exact solutions of chapter 2 for a two-dimensional, elastostatic model of an isotropic half-space with homogeneous elastic properties but inhomogeneous density have been used for numerical calculations of the supplementary stress systems due to the variations of the density. The elastostatic stress fields have been described for models corresponding to certain geological situations, and the results have been used to discuss some of the non-elastic, dynamic processes that are thought to occur in the crust of the Earth and the upper mantle. Consequently, the approach to the interpretation has been cautious.

It has been shown that density anomalies in the crust can induce stresses of sufficient magnitude to have a significant effect on the tectonics of the region. It seems from the models examined that, in the absence of superposed tectonic stresses, the stress-difference never attains a value that is significantly greater than the maximum stress at the free surface. Data has been presented which enables the surface stress to be estimated in the vicinity of any uniform, rectangular density contrast. This rectangular density contrast must be defined by planes which are parallel or normal to the free surface. The stress at the free surface can be as large as - 8 bars for a density anomaly of + 0.1 gm/cc magnitude and one kilometre thickness. Because the tensile strength of rocks is much less than their strength under compression, the most important case is the surface stress existing above a mass of anomalously low density.

In the absence of tectonic stresses, the stress-difference is small at the centre of an anomalous body, and is larger above and below the body and at the side contact. The effect of a superposed tectonic stress is either to make the stress-difference larger above the anomalous mass and smaller below, or vice

versa. For example, a tectonic tension enhances the likelihood of the initiation of tensile features above a mass deficiency or below a mass excess.

A model of Airy isostatic compensation of a surface load in the absence of tectonic stresses shows that the stress-difference is greatly reduced below the compensating mass deficiency, but that the maximum stress-difference within the crust is increased by isostatic compensation.

REFERENCES

Anderson, E.M. 1905. The dynamics of faulting. Trans. Edin. Geol. Soc., 8, 387-402.

Anderson, E.M. 1951. The dynamics of faulting and dyke formation with applications to Britain, 2nd Ed., 206 pp. Oliver and Boyd, London.

Andrade, E.N. da C. 1911. On the viscous flow in metals, and allied phenomena. Proc. R. Soc. A, 84, 1 - 12.

Bott, M.H.P. 1964a. Gravity measurements in the north-eastern part of the Irish Sea. Quart. J. geol. Soc. Lond., 120, 369-396.

Bott, M.H.P. 1964b. Formation of sedimentary basins by ductile flow of isostatic origin in the upper mantle. Nature, Lond., 201, 1082-10

Bott, M.H.P. 1965. The deep structure of the northern Irish Sea - a problem of crustal dynamics. Colston Papers, 17, 179-201.

Brace, W.F. 1960. An extension of the Griffith theory of fracture to rocks. J. geophys. Res., 65, 3477-3480.

Dean, W.R., Parsons, H.W. and Sneddon, I.N. 1944. A type of stress distribution on the surface of a semi-infinite elastic solid. Proc. Cambridge Phil. Soc., 40, 5-19.

Durney, B. 1965. Stresses induced in a purely elastic earth model under various tectonic loads. Geophys. J.R. astr. Soc., 10, 163-173.

Durney, B. 1966. Equilibrium configurations between density and topographic surface irregularities in a purely elastic earth model. J. geophys. Res., 71, 3029-3032.

Green, A.E. and Zerna, W. 1954. Theoretical Elasticity, 437 pp. Oxford.

Gretener, P.E. 1965. Can the state of stress be determined from hydraulic fracturing data? J. geophys. Res., 70, 6205-6212.

Griffith, A.A. 1920. The phenomena of rupture and flow in solids. Phil. Trans. R. Soc. A, 221, 163-197.

Hafner, W. 1951. Stress distributions and faulting. Bull. Geol. Soc. Amer., 62, 373-398.

Hast, N. 1958. The measurement of rock pressures in mines. Årsb. Sver. geol. Unders., 52, Stockholm.

Heiskanen, W.A. and Vening Meinesz, F.A. 1958. The Earth and its gravity field, 470 pp. McGraw-Hill Book Company.

Hubbert, M.K. 1951. Mechanical basis for certain familiar geologic structures. Bull. Geol. Soc. Amer., 62, 355-372.

Hubbert, M.K. and Rubey, W.W. 1959. The role of fluid pressure in mechanics of overthrust faulting : I- Mechanics of fluid-filled porous solids and its application to overthrust faulting. Bull. Geol. Soc. Amer., 70, 115-166.

Hubbert, M.K. and Rubey, W.W. 1960. Role of fluid pressure in mechanics of overthrust faulting. Bull. Geol. Soc. Amer., 71, 617-628.

Jaeger, J.C. 1962. Elasticity, fracture and flow with engineering and geological applications, 2nd Ed., 212 pp. Methuen, London.

Jeffreys, H. and Jeffreys, B.S. 1946. Methods of mathematical physics, 679 pp. Cambridge.

Jeffreys, H. 1962. The Earth, 4th Ed., 438 pp. Cambridge.

Kehle, R.O. 1964. The determination of tectonic stresses through analysis of hydraulic well fracture. J. geophys. Res., 69, 259-273.

Laubscher, H.P. 1960. Role of fluid pressure in mechanics of overthrust faulting. Bull. Geol. Soc. Amer., 71, 611-616.

Love, A.E.H. 1927. A treatise on the mathematical theory of elasticity. 4th Ed., 643 pp. Cambridge.

Mindlin, R.D. 1936. Force at a point in the interior of a semi-infinite solid. Physics, 7, 195-202.

McLintock, F.A. and Walsh, J.B. 1962. Proc. 4th U.S. National Congress of Applied Mechanics (Berkeley, California), 2, 1015. American Society of Mechanical Engineers, New York.

Moody, J.D. and Hill, M.J. 1956. Wrench-fault tectonics. Bull. Geol. Soc. Amer., 67, 1207-1246.

Murrell, S.A.F. 1964a. The theory of the propagation of elliptical Griffith cracks under various conditions of plane strain or plane stress: Part I. Br. J. appl. Phys., 15, 1195-1210.

Murrell, S.A.F. 1964b. The theory of the propagation of elliptical Griffith cracks under various conditions of plane strain or plane stress: Parts II and III. Br. J. appl. Phys., 15, 1211-1223.

Murrell, S.A.F. 1965. The effect of triaxial stress systems on the strength of rocks at atmospheric temperatures. Geophys. J.R. astr. Soc., 10, 231-281.

Muskhelishvili, N.I. 1953. Some basic problems of the mathematical theory of elasticity, 704 pp. P. Noordhoff.

Orowan, E. 1960. Mechanism of seismic faulting. Mem. Geol. Soc. Am., 79, 323-345.

Orowan, E. 1965. Convection in a non-Newtonian mantle, continental drift, and mountain building. Phil. Trans. R. Soc. A, 258, 284-313.

Price, N.J. 1959. Mechanics of jointing in rocks. Geol. Mag., 96, 149-167.

Sack, R.A. 1946. Extension of Griffith's theory to three dimensions. Proc. Phys. Soc. Lond., 58, 729-736.

Sandford, A.R. 1959. Analytical and experimental study of simple geological structures. Bull. Geol. Soc. Amer., 70, 10-52.

Sneddon, I.N. 1944. The stress distribution due to a force in the interior of a semi-infinite elastic medium. Proc. Cambridge Phil. Soc., 40, 229-238.

Sneddon, I.N. 1951. Fourier transforms, 542 pp. McGraw-Hill Book Company.

Sokolnikoff, I.S. 1956. Mathematical theory of elasticity, 2nd Ed., 476 pp. McGraw-Hill Book Company.

Talobre, J. 1957. La Mécanique des Roches, Dunod.

Vening Meinesz, F.A. 1939. Tables fondamentales pour la réduction isostatique régionale. Bull. géod., No. 63.

Vening Meinesz, F.A. 1941. Tables for regional and local isostatic reduction (Airy system) for gravity values. Publ. Neth. Geod. Comm., Waltman, Delft, 1941.

APPENDIX I

The plane strain solution for a line force within a half-space

The purpose of this appendix is to quote the results obtained by Sneddon (1944) for the components of stress at the point (x,y) in the interior of a semi-infinite elastic medium defined by $x > 0$ due to the action of a force of magnitude F distributed uniformly over the strip $x = h$, $-a \leqslant y \leqslant a$, and in the direction of the negative x direction, and to show that Sneddon's result is identical to equations (2.2.3), (2.2.4) and (2.2.5) obtained by integrating the point force result derived from complex potential theory before Sneddon's paper was found.

Introducing the notation

$$r_1^2 = (x-h)^2 + (y-a)^2 \quad , \quad r_2^2 = (x-h)^2 + (y+a)^2 \quad , \quad \tan\theta_1 = \frac{y-a}{x-h} \quad , \quad \tan\theta_2 = \frac{y+a}{x-h} \quad ,$$

$$R_1^2 = (x+h)^2 + (y-a)^2 \quad , \quad R_2^2 = (x+h)^2 + (y+a)^2 \quad , \quad \tan\phi_1 = \frac{y-a}{x+h} \quad , \quad \tan\phi_2 = \frac{y+a}{x+h} \quad ,$$

then Sneddon's results are

$$\hat{xy} = \frac{F}{8\pi a(1-\sigma)}\left[(1-2\sigma)\log\frac{r_2 R_1}{r_1 R_2} + (x-h)^2\left(\frac{1}{r_2^2} - \frac{1}{r_2^2}\right) + 4xh(x+h)^2\left(\frac{1}{R_1^4} - \frac{1}{R_2^4}\right) + \left\{(3-4\sigma)x^2 - 4\sigma hx - h^2\right\}\left(\frac{1}{R_1^2} - \frac{1}{R_2^2}\right)\right] \quad , \qquad (A1.$$

$$\hat{xx} + \hat{yy} = \frac{F}{4\pi a(1-\sigma)}\left[\theta_2 - \theta_1 + (3-4\sigma)(\phi_2 - \phi_1) + \frac{h}{h+x}\left(\sin 2\phi_2 - \sin 2\phi_1\right)\right] \quad , \qquad (A1.2)$$

$$\hat{xx} - \hat{yy} = \frac{F}{4\pi a(1-\sigma)}\left[(1-2\sigma)(\theta_2 - \theta_1 - \phi_2 + \phi_1) + \tfrac{1}{2}\left(\sin 2\theta_2 - \sin 2\theta_1\right) + \frac{(3-4\sigma)x^2 + 4(1-\sigma)hx - h^2}{2(h+x)^2}\left(\sin 2\phi_2 - \sin 2\phi_1\right)\right.$$

$$\left. + \frac{hx}{2(h+x)^2}\left(\sin 4\phi_2 - \sin 4\phi_1\right)\right] \quad . \qquad (A1.3)$$

The notation of equations (2.2.3), (2.2.4) and (2.2.5) may be converted to that of Sneddon by substituting (-y) for x, x for y, h for v and $(\frac{-F}{2a})$ for L. Putting also $(3 - 4\sigma)$ for K into equation (2.2.3) and transforming both sides of the equation gives

$$\hat{y}y - \hat{x}x = \frac{-F}{8a\pi(1-\sigma)}\left[2(1-2\sigma)\left\{\arctan\frac{x-h}{-y-u} - \arctan\frac{x+h}{-y-u}\right\} - \frac{2(x-h)(-y-u)}{(-y-u)^2+(x-h)^2} - \frac{2\{(3-4\sigma)x-h\}(-y-u)}{(-y-u)^2+(x+h)^2}\right.$$

$$\left. - \frac{8xh(-y-u)(x+h)}{\{(-y-u)^2+(x+h)^2\}^2}\right]_{u=-a}^{u=+a},$$

so $$x\hat{x} - y\hat{y} = \frac{F}{4\pi a(1-\sigma)}\left[(1-2\sigma)\left\{\arctan\frac{y+u}{x-h} - \arctan\frac{y+u}{x+h}\right\} + \frac{(x-h)(y+u)}{(y+u)^2+(x-h)^2} + \frac{(3-4\sigma)x-h}{x+h}\cdot\frac{(x+h)(y+u)}{(y+u)^2+(x+h)^2}\right.$$

$$\left. + \frac{4hx}{(x+h)^2}\cdot\frac{(y+u)(x+h)^3}{\{(y+u)^2+(x+h)^2\}^2}\right]_{u=-a}^{u=+a}$$

$$= \frac{F}{4\pi a(1-\sigma)}\left\{(1-2\sigma)(\theta_2 - \phi_2 - \theta_1 + \phi_1) + \sin\theta_2\cos\theta_2 - \sin\theta_1\cos\theta_1 + \frac{(3-4\sigma)x-h}{x+h}(\sin\phi_2\cos\phi_2 - \sin\phi_1\cos\phi_1)\right.$$

$$\left. + \frac{4hx}{(x+h)^2}(\cos^3\phi_2\sin\phi_2 - \cos^3\phi_1\sin\phi_1)\right\}.$$

Since $\sin 4x \equiv 8\sin x\cos^3 x - 4\sin x\cos x$, it follows that

$$x\hat{x} - y\hat{y} = \frac{F}{4\pi a(1-\sigma)}\left\{(1-2\sigma)(\theta_2 - \phi_2 - \theta_1 + \phi_1) + \tfrac{1}{2}(\sin 2\theta_2 - \sin 2\theta_1) + \left\{\frac{(3-4\sigma)x-h}{x+h} + \frac{2hx}{(x+h)^2}\right\}\tfrac{1}{2}(\sin 2\phi_2 - \sin 2\phi_1)\right.$$

$$\left. + \frac{hx}{2(x+h)^2}(\sin 4\phi_2 - \sin 4\phi_1)\right\},$$

which can be seen to reduce to the form of equation (A1.3). Similarly transform equation (2.2.4), remembering that $x\hat{y}$ transforms to $-y\hat{x}$.

Thus

$$\hat{y}x = x\hat{y} = \frac{F}{4a\pi.4(1-\sigma)}\left\{(1-2\sigma)\log\left(\frac{\tau_2^2 R_1^2}{R_2^2 \tau_1^2}\right) - 2(x-h)^2\left(\frac{1}{\tau_2^2} - \frac{1}{\tau_1^2}\right) - 2\left\{(3-4\sigma)x-h\right\}(x+h)\left(\frac{1}{R_2^2} - \frac{1}{R_1^2}\right)\right.$$

$$\left. + 4hx\left\{\frac{R_2^2 - 2(x+h)^2}{R_2^4} - \frac{R_1^2 - 2(x+h)^2}{R_1^4}\right\}\right\},$$

which reduces to equation (A1.1).

Finally, transforming equation (2.2.5) gives

$$\hat{y}y + \hat{x}z = \frac{-F}{4\pi a(1-\sigma)}\left\{-\arctan\frac{x-h}{-y-a} + \arctan\frac{x-h}{-y+a} - (3-4\sigma)\left\{\arctan\frac{x+h}{-y-a} - \arctan\frac{x+h}{-y+a}\right\}\right.$$

$$\left. + 2h\left\{\frac{(-y-a)}{(y+a)^2+(x+h)^2} - \frac{(-y+a)}{(y-a)^2+(x+h)^2}\right\}\right\}$$

$$= \frac{F}{4\pi a(1-\sigma)}\left\{\arctan\frac{y+a}{x-h} - \arctan\frac{y-a}{x-h} + (3-4\sigma)\left\{\arctan\frac{y+a}{x+h} - \arctan\frac{y-a}{x+h}\right\}\right.$$

$$\left. + \frac{2h}{x+h}\left\{\frac{(x+h)(y+a)}{(y+a)^2+(x+h)^2} - \frac{(x+h)(y-a)}{(y-a)^2+(x+h)^2}\right\}\right\},$$

which is equivalent to equation (A1.2).

APPENDIX 2

The half-space stress computer programme

A. Lucas Halfspace stress programme;

```
begin real pr, density, k, scale, con1, con2, con3,con4, con5,
           con6, con7, gravity, x, y, xx, yy, xy, sxx, syy, sxy,
           pp1, pp2, pp3;
      integer n1,n2,n3,n4,n5,p,q,px,qy,check,l1,l2,l3,l4,l5,l6,l7,
               l8,l9,l10,l11,pxstart,pxend,pxstep,qystart,qyend,qystep;

real procedure invtan(x,y);
        real x,y;
comment the numerical constants herein are particular to this problem
        overflow and underflow error  indicate possible inaccuracy;

begin  checks(£enter invtan?);
       if abs(y)>10^20 then begin print ££13?y overflow error?,x,y;
                                  invtan:=sign(y)*1.57079;
                            end
       else if abs(x)≤1 then  begin
               if abs(y)≤1 then begin print££13?invtan indeterminate?;
                                      invtan:=0;
                                       end
             else  if  abs(y)≤1000 then begin
                                    print££13?y underflow error?,x,y;
                                    invtan:=sign(y)*1.57079;
                                     end
              else invtan:=sign(y)*1.57079;
              end
     else if x<0 then  begin
                 if y≥0 and y≤1 then begin
                      invtan:=3.14159;
                       if x>-1000 then print££13?x underflow error+?,
                                                          x,y;
                      end
              else if  abs(y)≤1 then begin
                        invtan:=-3.14159;
                       if x>-1000 then print££13?x underflow error-?,
                                                          x,y;
                        end
              else  invtan:=sign(y)*3.14159+arctan(y/x);
              end
    else invtan:=arctan(y/x);
checks(£exit invtan?);

end of procedure;
```

```
procedure inside(a,u,v,sx,y,y1,y2,inxx,inyy,inxy1,inxy2);
          value u,v;
          real a,u,v,sx,y,y1,y2,inxx,inyy,inxy1,inxy2;
          comment inner procedure of procedure rectangle;
begin real xlessu,ylessv,bigr2,litr2,theta,epsi,lgbr2,lglr2,ff;

        xlessu:=sx-u;
        ylessv:=y-v;
        bigr2:=xlessu↑2+(y+v)↑2;
        litr2:=xlessu↑2+(y-v)↑2;
        theta:=invtan(xlessu,y+v);
        epsi:=invtan(xlessu,y-v);
        lgbr2:=ln(bigr2);
        lglr2:=ln(litr2);
        ff:=4*y*v*xlessu/bigr2;
        inxx:=con1*xlessu*lgbr2+con2*xlessu*lglr2-(con3*y+con4*v)
              *theta+con5*ylessv*epsi+ff;

        inyy:=con6*xlessu*(lgbr2-lglr2)+con7*ylessv*(theta+epsi)-ff;
        inxy1:=con2*ylessv*lglr2+(con1*y+con2*v)*lgbr2
           +con7*xlessu*theta-4*y*v*(y+v)/bigr2;
      if sx+a<0 and y2>y and y>y1 then
           inxy2:=-xlessu*invtan(-xlessu,ylessv)*con7
      else if y>y2 or y<y1 or sx>a then
           inxy2:=xlessu*epsi*con7
      else if u>0 then
           inxy2:=-(xlessu*invtan(-xlessu,ylessv)
                 +(sx+u)*invtan(sx+u,ylessv))*con7
      else inxy2:=0; comment zones in order b,c,a,dummya;
end of procedure;

procedure rectangle(a,y1,y2,sx,y,dcon);
      value a,y1,y2,sx,dcon;
      real a,y1,y2,sx,y,dcon;
begin real inxx,inyy,inxy1,inxy2,ff;
      inside(a,a,y2,sx,y,y1,y2,inxx,inyy,inxy1,inxy2);
      xx:=inxx;
      yy:=inyy;
      xy:=inxy1+inxy2;
      inside(a,-a,y2,sx,y,y1,y2,inxx,inyy,inxy1,inxy2);
      xx:=xx-inxx;
      yy:=yy-inyy;
      xy:=xy-inxy1-inxy2;
      inside(a,a,y1,sx,y,y1,y2,inxx,inyy,inxy1,inxy2);
      xx:=xx-inxx;
      yy:=yy-inyy;
      xy:=xy-inxy1-inxy2;
      inside(a,-a,y1,sx,y,y1,y2,inxx,inyy,inxy1,inxy2);
      xx:=xx+inxx;
      yy:=yy+inyy;
      xy:=xy+inxy1+inxy2;
      ff:=dcon*gravity/(con7*6.2832);
      xx:=ff*xx;
      yy:=ff*yy;
      xy:=-ff*xy;
end of procedure;
```

```
procedure insurect(sx,u,v,inxx); value u,v;
          real sx,u,v,inxx;
          comment inner procedure for surface stresses for rectangle;
   begin real xlessu;
                xlessu:=sx-u;
                inxx:=2*con7*xlessu*ln(xlessu↑2+v↑2)-8*con2*v*invtan
               (xlessu,v);
    end of procedure;


procedure surect(a,y2,y1,sx,dcon);
          value a,y2,y1,sx,dcon;
          real a,y2,y1,sx,dcon;
          comment surface stress for rectangle;
   begin real inxx;
          insurect(sx,a,y2,inxx);
          xx:=inxx;
         insurect(sx,-a,y2,inxx);
         xx:=xx-inxx;
         insurect(sx,a,y1,inxx);
         xx:=xx-inxx;
         insurect(sx,-a,y1,inxx);
         xx:=xx+inxx;
         xx:=dcon*gravity*xx/(con7*6.2832);
   end of procedure;


procedure substratum(y,y1,y2,dcon);
          value y1,y2,dcon;
          real y,y1,y2,dcon;
          begin real ff,fff;
                  ff:=-dcon*gravity;
                fff:=ff*con5/con7;
        if y≤y1 then xx:=yy:=0
        else if y≤y2 then
             begin xx:=fff*(y-y1);
                   yy:=ff*(y-y1);
             end
        else begin xx:=fff*(y2-y1);
                   yy:=ff*(y2-y1);
              end;
 end of procedure;
```

```
procedure surface(a,sx,load);
          value a,sx,load;
          real a,sx,load;
          comment uniform vertical load over part of free surface;
          begin if abs(y)<1 and abs(sx)<a then
                 begin xx:=yy:=-load*gravity;
                       xy:=0;
                end
                else if abs(y)<1 then xx:=yy:=xy:=0
                else begin real theta,epsi,bigr2,litr2,ff,fff;
                           theta:=invtan(sx+a,y);
                           epsi:=invtan(sx-a,y);
                           bigr2:=(sx+a)↑2+y↑2;
                           litr2:=(sx-a)↑2+y↑2;
                              ff:=load*gravity/3.14159;
                             fff:=2*a*y*(sx↑2-a↑2-y↑2)/(bigr2*litr2);
                              xx:=ff*(theta-epsi-fff);
                              yy:=ff*(theta-epsi+fff);
                              xy:=-4*ff*a*sx*y↑2/(bigr2*litr2);
                           end of inner block;
                     end of procedure;

procedure inner(v,sx,y1,y2,inxx,inyy,inxy);
      real v,sx,y1,y2,inxx,inyy,inxy;
      comment inner procedure of procedure terminated;

begin real yplusv,ylessv,
           bigr2,litr2,lgbr,lglr,theta,epsi,ff,theta1,epsi1;
      yplusv:=y+v;
      ylessv:=y-v;
      bigr2:=sx↑2+yplusv↑2;
      litr2:=sx↑2+ylessv↑2;
      lgbr:=ln(bigr2);
      lglr:=ln(litr2);
      theta:=invtan(-sx,yplusv);
      epsi:=invtan(-sx,ylessv);
      theta1:=invtan(sx,yplusv);
      epsi1:=invtan(sx,ylessv);
      ff:=4*y*v*sx/bigr2;
   inxx:=-con1*sx*lgbr-con2*sx*lglr
      -(con3*y+con4*v)*theta+con5*ylessv*epsi
      -ff+12.56636*con2*v;
   inyy:=-con6*sx*(lgbr-lglr)+con7*ylessv*(theta+epsi)+ff;
   if sx<0 and y≥y1 and y≤y2 then
      ff:=-sx*epsi
   else ff:=+sx*epsi1;
   inxy:=-con2*ylessv*lglr-(con1*y+con2*v)*lgbr
      +con7*(v-sx*theta1)+4*y*v*yplusv/bigr2-con7*(v+ff);
end of procedure;
```

```
procedure terminated(sx,y1,y2,dcon);
      value sx,y1,y2,dcon;
      real sx,y1,y2,dcon;
      comment terminated substratum for nonzeroy;

begin real inxx,inyy,inxy,ff;
      inner(y2,sx,y1,y2,inxx,inyy,inxy);
      xx:=inxx;
      yy:=inyy;
      xy:=inxy;
      inner(y1,sx,y1,y2,inxx,inyy,inxy);
      xx:=xx-inxx;
      yy:=yy-inyy;
      xy:=xy-inxy;
      ff:=dcon*gravity/(con7*6.2832);
      xx:=ff*xx;
      yy:=ff*yy;
      xy:=-ff*xy;
end of procedure;

procedure surterm(sx,y1,y2,dcon);
      value sx,y1,y2,dcon;
      real sx,y1,y2,dcon;
      comment surface stress for terminated substratum;

      begin yy:=xy:=0;
      xx:=-dcon*gravity*(con7*sx*(ln(sx↑2+y2↑2)-ln(sx↑2+y1↑2))
      +2*con2*(y2*(invtan(-sx,y2)-invtan(sx,y2))-y1*(invtan(-sx,y1)-
      invtan(sx,y1))))/(con7*3.14159);
end of procedure;

procedure principal stresses(xx,yy,xy,pp1,pp2,pp3);
      real xx,yy,xy,pp1,pp2,pp3;
      comment calculates and prints principal stresses for plane strain
            model;
      begin real great,least,dif,ff1,ff2,theta;
            ff1:=(xx+yy)/2;
            ff2:=sqrt((xx-yy)↑2/4+xy↑2);
                              pp1:=ff1+ff2;
            pp2:=ff1-ff2;
            pp3:=(pp1+pp2)*pr;

          if pp1>pp2 then begin great:=pp1;
                                least:=pp2;end
                        else begin  great:=pp2;least:=pp1; end;
          if pp3>great then great:=pp3
               else  if pp3<least then least:=pp3;
           dif:=great-least;
            theta:=invtan(xx-yy,2*xy)*28.65;
            print ££11?ps?,pp1,pp2,pp3,theta,dif;
end of procedure;
```

```
procedure mises(xx,yy,xy);
      real xx,yy,xy;
      begin real zz,function;
            zz:=pr*(xx+yy);
      function:=((yy-zz)↑2+(zz-xx)↑2+(xx-yy)↑2)/6+xy;
            print ££1¶? von mises criterion?, function;
end of procedure;

procedure classify(pp1,pp2,pp3);
      real pp1,pp2,pp3;
begin real greatest,inter,least,sum,par1,ff,par2;
      switch qqq:=q1,q2,q3,q4;
      if pp1>pp2 then begin greatest:=pp1;
            least:=pp2; end
            else begin greatest:=pp2;
                  least:=pp1; end;

      if pp3>greatest then begin inter:=greatest;
            greatest:=pp3; end
      else if pp3>least then inter:=pp3
      else begin inter:=least;
            least:=pp3; end;
      sum:=pp1+pp2+pp3; ff:=greatest-least; print ff;
      if pp3=least then print ££1¶?1?
      else if pp3=inter then print ££1¶?i?
      else print ££1¶?g?;
      if greatest<0 then begin print £a?;
            goto q1; end
      else if inter<0 then begin print £b?;
            goto q3; end
      else if least<0 then begin print £c?;
            goto q3; end
      else begin print £d?;
            goto q2; end;
      q3:  if sum<0 then goto q1 else goto q2;
      q1:   par1:=(greatest*1.732-least*0.578)/2;
            par2:=(greatest*3.172-least*0.316)/2;
            print £cn?,par1,par2;
            goto q4;
      q2:   if 3*greatest+least>0 then print £ga?,greatest

      else begin par1:=-(greatest-least)↑2/(8*(greatest+least));
            print £gb?,par1;
      end;

      q4:  end of procedure;
```

```
   scaled(4);sameline;
read n1,n2,n3,n4,n5;
begin array a1,x1,y11,y12,dcon1[0:n1],
            y21,y22,dcon2[0:n2],
            a3,x3,htxdens[0:n3],
            x4,y41,y42,dcon4[0:n4],
           cx[0:n5];
      switch ss:=p1,p2,p3,p4,p5,p6,p7;
      wait;
      read pr,density,gravity,scale;
      wait;
      if n1≠0 then begin for p:=1 step 1 until n1 do
                          begin read con1,con2,con3,con4,dcon1[p];
                                a1[p]:=con1*scale;
                                x1[p]:=con2*scale;
                               y11[p]:=con3*scale;
                                y12[p]:=con4*scale;
                          end; wait;end;
     if n2≠0 then begin for p:=1 step 1 until n2 do
                          begin read con1,con2,dcon2[p];
                                y21[p]:=con1*scale;
                               y22[p]:=con2*scale;
                           end; wait; end;
    if n3≠0 then begin for p:=1 step 1 until n3 do
                         begin read con1,con2,con3;
                               a3[p]:=con1*scale;
                                x3[p]:=con2*scale;
                               htxdens[p]:=con3*scale;
                         end; wait; end;
    if n4≠0 then begin for p:=1 step 1 until n4 do
                         begin read con1,con2,con3,dcon4[p];
                              x4[p]:=con1*scale;
                                y41[p]:=con2*scale;
                                y42[p]:=con3*scale;
                         end; wait; end;
if n5≠0 then for p:=1 step 1 until n5 do read cx[p];
k:=3-4*pr;
con1:=(3*k+5)/2;
con2:=(k-1)/2;
con3:=5*k+9;
con4:=3*k-1;
con5:=3-k;
con6:=(k+3)/2;
con7:=k+1;
wait;
p2:read l1,l2,l3,l4,l5,l6,l7,l8,l9,l10,l11;
   wait;
   if l1=1 then goto p1;
   read pxstart,pxend,pxstep,qystart,qyend, qystep;
   check:=(pxend-pxstart)/pxstep;
   if pxend≠pxstart+check*pxstep then
       begin print ££13? px step error?;
             wait;
             goto p2;
       end;
```

```
      check:=(qyend-qystart)/qystep;
      if qyend≠qystart+check*qystep then
          begin print ££13? qy step error?;
                wait;
                goto p2; end;
      px:=pxstart-pxstep;
      qy:=qystart;


p1: if l1=1 then begin read x,y;
                         x:=x*scale;
                         y:=y*scale;
                       if y<0 then begin wait; goto p2; end;
                  end
    else begin if px=pxend and qy=qyend then
                 begin print ££13? end of x,y scan?;
                       wait; goto p2;
                 end;

                   if px=pxend then
                       begin px:=pxstart;
                             qy:=qy+qystep;
                       end
                   else px:=px+pxstep;
                         x:=px*scale;
                         y:=qy*scale;
end;
print ££12??,x,y;
sxx:=syy:=sxy:=0;
if n1=0 then goto p3;
for p:=1 step 1 until n1 do
begin if y<1 then
      begin surect(a1[p],y12[p],y11[p],x-x1[p],dcon1[p]);
            yy:=xy:=0;
      end
else rectangle(a1[p],y11[p],y12[p],x-x1[p],y,dcon1[p]);

       sxx:=sxx+xx;
       syy:=syy+yy;
       sxy:=sxy+xy;
      if l2≠1 then print ££11??,p,xx,yy,xy;
       principal(xx,yy,xy,pp1,pp2,pp3);
end;
p3:if n2=0 then goto p4;
   for p:=1 step 1 until n2 do
       begin substratum(y,y21[p],y22[p],dcon2[p]);
        sxx:=sxx+xx;
        syy:=syy+yy;
     if l3≠1 then print ££11? sub?,xx,yy;
       end;
```

```
p4:if n3=0 then goto p5;
for p:=1 step 1 until n3 do
    begin surface(a3[p],x-x3[p],htxdens[p]);
          sxx:=sxx+xx;
          syy:=syy+yy;
          sxy:=sxy+xy;
          if 14≠1 then print ££11? surface?, xx,yy,xy;
    end;


p5: if n4=0 then goto p6;
    for p:=1 step 1 until n4 do
    begin if abs(y)<1 then
            surterm(x-x4[p],y41[p],y42[p],dcon4 p])
    else terminated(x-x4[p],y41[p],y42[p],dcon4[p]);
          sxx:=sxx+xx;
          syy:=syy+yy;
          sxy:=sxy+xy;
         if 15≠1 then print ££11? term?,xx,yy,xy;
   end;

p6: if 18≠1 then mises(sxx,syy,sxy);
    if 16≠1 then print ££11s4??,sxx,syy,sxy;
    sxx:=sxx-density*gravity*con5*y/con7;
    syy:=syy-density*gravity*y;


   if 17≠1 then print ££11?17?,sxx,syy,sxy;
   if 19≠1 then mises(sxx,syy,sxy);
   principal(sxx,syy,sxy,pp1,pp2,pp3);
   if 110≠1 then classify(pp1,pp2,pp3);
   if n5=0 then goto p1;
   for p:=1 step 1 until n5 do
       begin xx:=sxx+cx[p];
             if 19≠1 then mises(xx,syy,sxy);
                 principal(xx,syy,sxy,pp1,pp2,pp3);
             if 111≠1 then classify(pp1,pp2,pp3);
       end;


    goto p1;
  end of inner block;
end of programme;
```

APPENDIX 3

The specification of the half-space stress programme

This is a detailed description of the use of an Algol computer programme (Appendix 2) which evaluates the algebraic expressions derived in Chapter 2. This programme, which has been run on an Elliott 803 computer, has already been described in section (ii) of Chapter 3.

(i) Data input

This programme calculates the plane strain state of stress at points (x,y), in the positive y elastic half-space, which has a specified density and Poisson's ratio, (identifiers "density" and "PR"). The state of stress is made up of additional components due to

n1 rectangular density anomalies, each defined by (a1, x1, y11, y12, dcon 1),

n2 plane substrata, each defined by (y21, y22, d con 2),

n3 uniform surface loads, each defined by (a3, x3, htxdens),

n4 semi-infinite substrata, each defined by (x4, y41, y42, d con 4),

and one of n5 tectonic stresses, each defined by (Cx).

The definitions of most of these parameters follow immediately from a comparison with the notation of Chapter 2 and, in particular, figure 2. The parameters x1, x3 and x4 are the values of x at the centre of symmetry of the component of the model, which corresponded to x equal to zero in Chapter 2. The parameters d con 1, d con 2 and d con 4 are density contrasts; the parameter htxdens is a surface load which is represented as the product of a density and a height, for multiplication by the acceleration due to gravity occurs in the procedure SURFACE; the parameter Cx is the horizontal tectonic stress component. Two other parameters which have to be given values are "gravity", which is the acceleration due to gravity, and "scale", which is a factor by which all linear dimensions (including 'htxdens') are multiplied at the time of input.

The values of x and y may either be read in pairs from a data tape, in which case they are of type real, or be defined by a rectangular grid which is itself defined by six integer parameters, (px start, px end, px step, qystart, qy end, qy step), whose names clearly indicate their functions. Both (x,y) and these six parameters are scaled by the factor 'scale'. A set of values (x,y) must be ended by a negative value of y, and each new set of (x,y) or x - y grid parameters must be preceded by a set of control parameters. If it is required to define a line rather than a rectangular grid, then either PX STEP or QY STEP has an arbitrary value. This value must not be zero.

The input and output functions of the programme are controlled by the eleven integers l1 to l11, which have the following functions,

if l1 $\neq$ 1, use x - y grid; otherwise read (x,y),

if l2 $\neq$ 1, print xx, yy, xy for each rectangular anomaly,

if l3 $\neq$ 1, print xx, yy, xy for each substratum,

if l4 $\neq$ 1, print xx, yy, xy for each surface load,

if l5 $\neq$ 1, print xx, yy, xy for each terminated substratum,

if l6 $\neq$ 1, print xx, yy, xy for total supplementary stress system,

if l7 $\neq$ 1, print total stress system (no tectonic stress),

if l8 $\neq$ 1, print MISES for total supplementary stress,

if l9 $\neq$ 1, print MISES for total stress system (with and without tectonic stres

if l10 $\neq$ 1, CLASSIFY total stress system (no tectonic stress),

and if l11 $\neq$ 1, CLASSIFY total stress systems with tectonic stresses.

In addition to these optional forms of output, there is also output of PRINCIPAL STRESSES for each rectangular anomaly and for the total stress system (without tectonic stress and with each tectonic stress in turn).

The programme has been run using data expressed in c.g.s. units. This is not

a fundamental requirement of the programme, because no dimensional parameters are assigned fixed values within the programme, but if other units are used it may be necessary to change the values of the arbitrary constants used in the INVTAN procedure. Similar precautions might be necessary if models of smaller linear scale than geological features are to be considered. In practice it would be simpler to change the units in such a way as to make the linear dimension between grid points and the values of the stress components greater than a thousand. Note also that since x and y are of type real, the condition 'y = 0' is always replaced in the main programme by 'abs(y) < 1'. The most common c.g.s. data tape-format has been with 'scale' equal to 10^5, so that all linear dimensions (including 'htxdens') are punched in units of kilometres. If it is required to use a x - y grid where x or y are not integer numbers of kilometres, the value of 'scale' must be reduced because the grid coordinate parameters must be of type integer.

(ii) Running the programme

Programmed 'data waits' occur between each read instruction, so permitting the easy use of separate data tapes. A 'data wait' also occurs at the end of a x - y grid or of a set of (x,y) read from adata tape. The end of such a set must be indicated by a negative value of y. An entirely new model represented by a complete set of data tapes may be considered by 'manually restarting' the programme, or a new set of coordinates (x,y) for the same model may be considered by reading in a set of control integers and a corresponding coordinate data tape by continuing the calculation. Continuation after a 'data wait' is effected by changing the most significant F2 bit on the computer keyboard.

A 'data wait', accompanied by an Algol compiler LOG ERROR message, occurs if (x,y) is located at a corner of the rectangular model (or at an equivalent singularity of another model). The INVTAN procedure avoids a compiler TAN ERROR

in these circumstances, but a programme message INVTAN INDETERMINATE is also printed. The calculation should be continued, and it appears from comparison with results at points adjacent to the corner that the calculated stress is probably acceptable.

Warning messages (PX STEP ERROR or QY STEP ERROR) and a 'data wait' are generated if the x - y grid parameters are not consistent. The programme may then be restarted with a new model or a further set of (x,y) in the manner described above. A message END OF X,Y SCAN occurs immediately before the 'data wait' at the finish of the calculations for a complete x - y grid.

The INVTAN procedure was written to eliminate the possibility of stoppages due to 'floating point overflow' which is caused when a real identifier is given a magnitude greater than 5.8×10^{76}. If $|y|$ is greater than 10^{20}, the message OVERFLOW ERROR is printed. If $|x|$ is less than one and y is greater than one, then the inverse tangent is given the appropriate value $\pm \frac{\pi}{2}$, and a Y UNDERFLOW message followed by the values of x and y is printed if $|y|$ is less than 10^{3}, in order to warn of the possible inaccuracy of this value of the inverse tangent. If $|x| \leq 1$ and $|y| \leq 1$ the message INVTAN INDETERMINATE is printed. In the region, $|y| < 1$, $x < 0$, of the discontinuity of the inverse tangent function, INVTAN is again assigned a value, because the general formula breaks down if y is equal to zero. An X UNDERFLOW MESSAGE indicates possible inaccuracy of this assigned value.

The approximate time taken to calculate the stress components at one point (x,y) using this programme on an Elliot 803 B computer and generating a minimum of output, (i.e. 12 to 111 equal to one), is

$$(5\tfrac{1}{2} + 9.\, n1 + n3 + 4.\, n4 + 3.\, n5) \text{ seconds.}$$

The time taken to evaluate the plane substrata contributions is not significant.

If the five integers n1 to n5 are each set to one, the minimum computing time is $22\frac{1}{2}$ seconds for each (x,y); if all possible output is generated, (i.e. l2 to l11 equal to zero), the corresponding running time is 42 seconds. For a production run such as the compensated mountain chain model, for which more than 220 grid points were used, the five minutes taken to read in the 'dumped' version of the programme and the model parameters are relatively insignificant.

(iii) Data tape format

model parameters

n1 n2 n3 n4 n5

PR (Poisson's ratio) DENSITY (Half-space) GRAVITY SCALE

n1 sets of (a1, x1, y11, y12, d con 1)

n2 sets of (y21, y22, dcon 2)

n3 sets of (a3, x3, htxdens)

n4 sets of (x4, y41, y42, d con 4)

n5 values of Cx

x - y parameters

	I1	I2	I3	I4	I5	I6	I7	I8	I9	I10	I11
either	(I1 = 1)	x_1	y_1	x_2	y_2	.....	x_s	y_s	0		-1
or	(I1 ≠ 1)	PX START	PX END	PX STEP	QY START	QY END	QY STEP				

Note that further sets of x - y parameters may follow without repeating the model parameters.

(iv) Sample date tape

The following is a sample data tape for the compensated mountain chain model with a hydrostatic natural state and tectonic stresses of 400 bars and -400 bars.

```
  1     0     1     0     2
0.25    0    981    @ 5
300     0     30    51   -•4
300     0     8.4
4 @ 8          - 4 @ 8
0  1  1  1  1  1  1  1  1  1  1
0  450  50  100  0  -10
1  1  1  1  1  1  1  1  1  1  1
300    5  300  15  300  20  0  -1
```

Note:- @ n represents x 10^n .

(v) Stress programme flow diagram

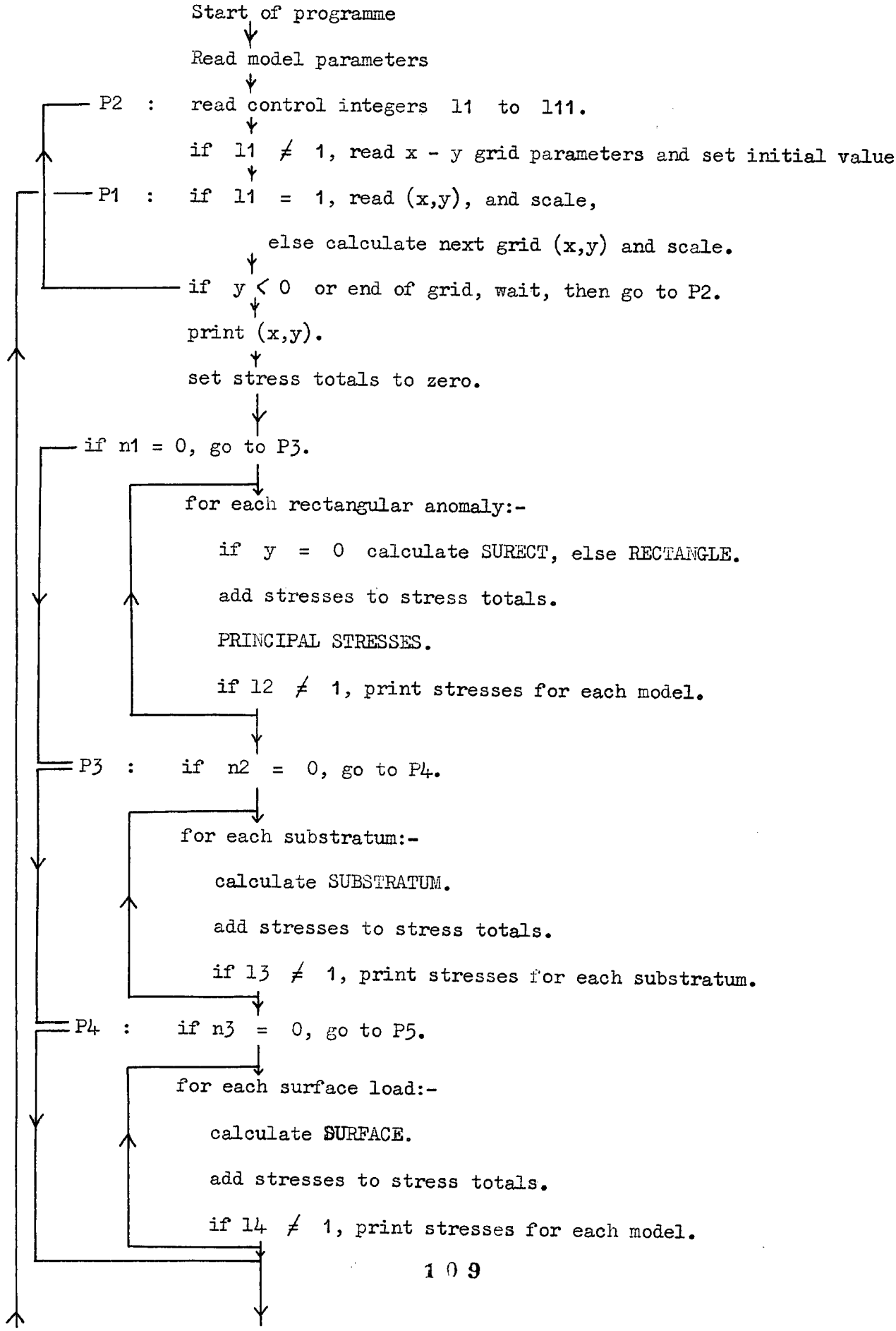

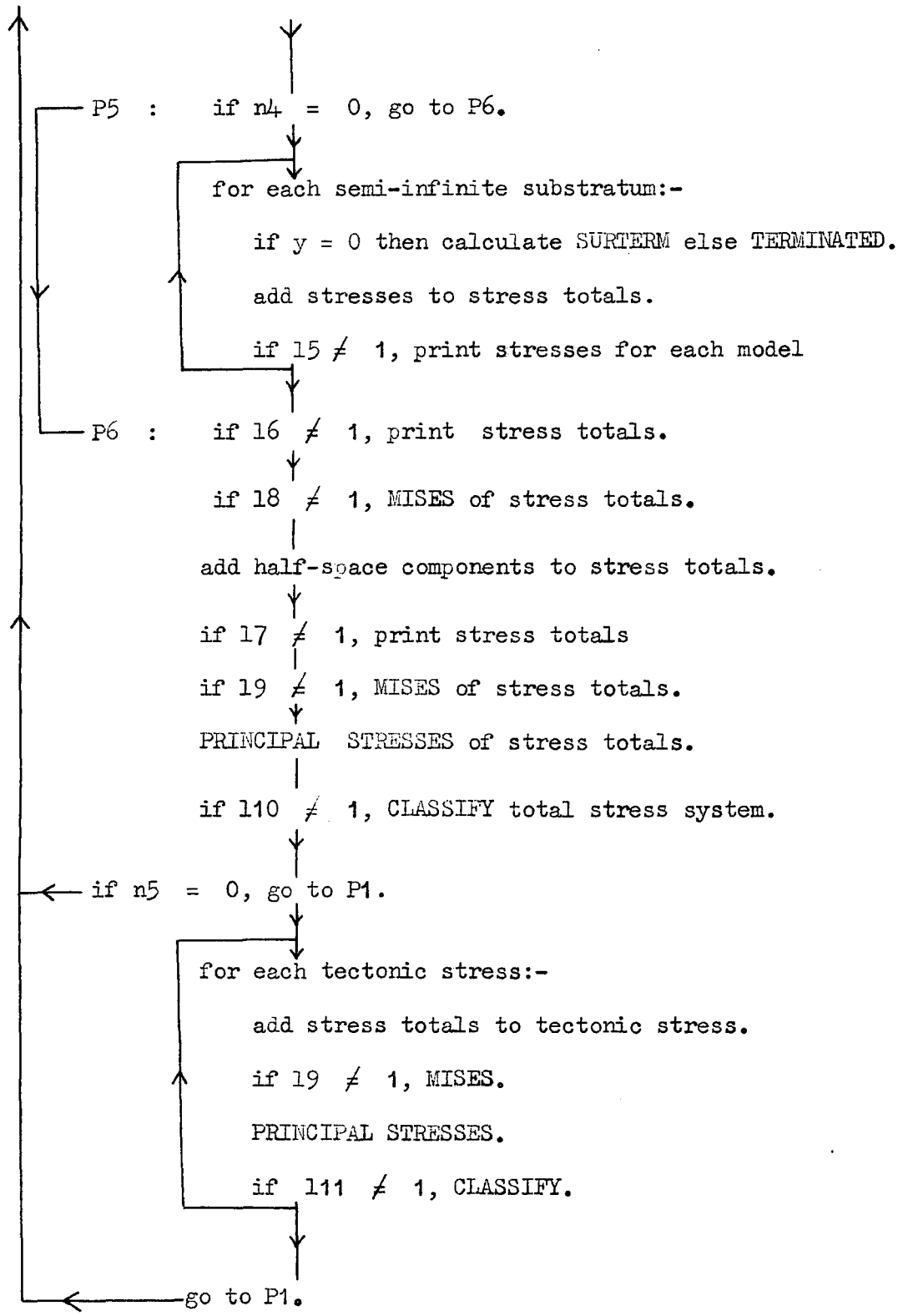
P5 : if n4 = 0, go to P6.
for each semi-infinite substratum:-
if y = 0 then calculate SURTERM else TERMINATED.
add stresses to stress totals.
if 15 ≠ 1, print stresses for each model
P6 : if 16 ≠ 1, print stress totals.
if 18 ≠ 1, MISES of stress totals.
add half-space components to stress totals.
if 17 ≠ 1, print stress totals
if 19 ≠ 1, MISES of stress totals.
PRINCIPAL STRESSES of stress totals.
if 110 ≠ 1, CLASSIFY total stress system.
if n5 = 0, go to P1.
for each tectonic stress:-
add stress totals to tectonic stress.
if 19 ≠ 1, MISES.
PRINCIPAL STRESSES.
if 111 ≠ 1, CLASSIFY.
go to P1.